

**Characterization of a PUF protein in *Dictyostelium*
*discoideum***

**Thesis submitted to
Jawaharlal Nehru University
for the award of the Degree of
DOCTOR OF PHILOSOPHY**

KARAN SINGH RAJPUT



**School of Life Sciences
Jawaharlal Nehru University
New Delhi-110067**

INDIA

2019

SCHOOL OF LIFE SCIENCES
JAWAHARLAL NEHRU UNIVERSITY
NEW DELHI-110067

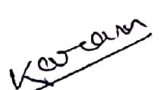


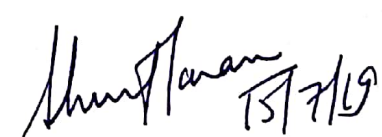
Dated: 15/7/2019

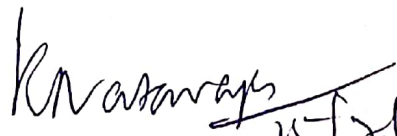
CERTIFICATE

This is to certify that the research work embodied in this thesis entitled “**Characterization of a PUF protein in *Dictyostelium discoideum***” submitted for the award of Degree of **Doctor of Philosophy** has been carried out by **Mr. Karan Singh Rajput** under the supervision of **Prof. Shweta Saran** in the school of Life Sciences, Jawaharlal Nehru University, New Delhi, India.

This work is original and has not been submitted so far, in part or in full for any degree or diploma of any other university.


Karan Singh Rajput
(Candidate)


Prof. Shweta Saran
(Supervisor)


Prof. K. Natarajan
(Dean, SLS, JNU)

ACKNOWLEDGMENT

First and foremost, I would like to thank almighty God for giving me the strength, and opportunity to undertake this research study and complete it satisfactorily. Without his blessings, this achievement would not have been possible.

I would like to pay my sincere gratitude to my supervisor Prof. Shweta Saran for the support, her patience, motivation and immense knowledge. She helped me throughout my PhD work and thesis writing and I am deeply indebted to her for being so supportive during my tough times.

I am grateful to the present and past Dean of the department, Prof. B. N. Mallik, Prof. B. C. Tripathy, Prof. S. K. Goswami and Prof. K. Natarajan for providing adequate facilities in the department. I am indebted to my doctoral committee Prof. Alok Bhattacharya, Prof. P.C. Rath and Dr. Niti Puri for their invaluable suggestions and guidance.

I am also thankful to Prof. Nalini Shrivastava, Prof. Y. K. Jaiswal, Prof. G. B. K. S. Prashad and Dr. Purnima Kishore for their immense knowledge and guidance during my M.Sc and it is because of them that I was in JNU.

I would like to acknowledge CIF staff, staff members of AIREF, School administration and faculty Staff and JNU administration staff for their kind support. A special mention of Dr. Sarika, Miss Jyoti and Mrs Tripti Panwar for helping in FACS and microscopy.

I would like to acknowledge Council for Scientific and Industrial Research for the financial support during the course of my Ph.D.

I am really thankful and grateful for all my seniors, Dr. Pynskhem, Dr. Himanshu Mishra, Dr. Rakhee, Dr. Abhishek, Dr. Rafia, Dr. Rakesh, Dr. Ranajana, Dr. Punita, Dr. Priyanka, Dr. Neha, Dr. Eba, Mrs. Pooja, Mr. Mukul for their valuable guidance and suggestions for improving my research work. I would also like to acknowledge my lovely juniors B. Bhanu, Madhu, Afrozi, Tasneem, Chanchal and Anuranjan and trainees Abhineet, Bidisha, Barnani, Almas, Ishita for all their assistance in experiments. I specially thank Dr. Rakesh, Madhu and Chanchal for their help during my PhD work. I appreciate all of them for maintaining healthy and joyous environment in lab and their helpful nature. I also would like to thank technical staff of the lab, Bijender ji, Bittu ji and Hemant ji, for their kind help and support.

Special words of gratitude for my friends for being a part of my journey in PhD, I would like to thank my SLS PhD 2013 batchmates Anamika, Anupriya, Deepika, Priya, Dhakaram, Farah, Graham, Manoj, Neha, Shivani. Shabnam, T. Shivani, Raghunandan, Sanya, Sumiran, Vijendra, Ramesh, Ved and others.... I cherish the moments we spent together during initial phase specially with Ved, Vijendra and Ramesh, and it was always a pleasure to hang out with them. Especially the SLS boys gang who are a bunch of fun people, helped me to release my anxiety and stress. Our late night India gate trips will always remain in the memory.

Friends are the pearl in the ocean; they fill your life with happy memories. I would like to express my gratitude to my school friends, Shiva and Manish, college friends Pooran, Kamal, Prabhash, Jitendra and Amit. I would also like to thank my friends in JNU Ved, Ramesh and Vijendra were the first few people I came across in JNU and has always been with me since that time and share a special bond with them. I am grateful to Bhanu, Rangati, Swati, Preeti, Garima and Chandra for being my gang and sharing all my secrets with them has helped me in all my circumstances. You all are my extended family. Especially I would like to mention Nalini who has been like my backbone and supported me throughout during my good and bad times. This journey would not have been possible without her. Samant has been a good friend and the most newly added member of our group as the husband of "Nalini seth". I would like to specially mention Bhanu as a person with pure heart and great sence of humour, I am really lucky to have him as a friend and my roommate, he is the best roommate one could ever have. I also would like to mention Mrinalini didi and Vinay jijaji for their love and affection. I am thankful to them for giving two precious gems Mahu and Pihu, their laughter brighten ups my life.

Last but not the least I would highly like to acknowledge my Parents, for their love care and support. They have struggled a lot but never made me go through any tough situations, and always inspired me to do better in life. I am indebted to my mother for her unconditional love and she is the one who has taught me how to be strong in tough situation and to hustle and not back down in front of problems. My father always encouraged me and it was his hard work made me the person I am today or will be in the future. My Chacha ji has always been the pillar of support for me as well as my family. He has been my idol and I aspire to be as responsible and humble as him. My elder brothers and sister in laws have always supported me and I am grateful for their love and affection. I would like to thank my cute nephews and nieces for their unconditional love. I also would like to thank my loving younger brothers and sisters for their support.

This thesis would not have been possible without the joint effort of all the people involved, I also would like to acknowledge people who contributed directly or indirectly and has been the part of my PhD journey.

Karan Singh Rajput

TABLE OF CONTENTS

Abstract	a-d
Chapter 1: A comprehensive review on <i>Dictyostelium</i> and PUF	
1.1 Introduction	1
1.2 Phylogenetic position of <i>D. discoideum</i>	1
1.3 Advantages of using <i>D. discoideum</i> as a model system	1-3
1.4 Life cycle of <i>D. discoideum</i>	3
1.4.1 The vegetative (unicellular) phase	3-4
1.4.2 The development/asexual (multicellular) phase	4-8
1.5 Cell signaling during <i>D. discoideum</i> development	9-11
1.6 PUF (Pumilio and FBF)	11
1.6.1 Introduction	11-12
1.6.2 PUF protein structure and its RNA-binding mechanism	12-14
1.6.3 PUF proteins and their functions in different organisms	14-18
1.6.4 Mechanisms of RNA repression	18-20
1.7 Work done so far in <i>D. discoideum</i>	20-21
1.8 Objectives of the present study	21-22
Chapter 2: Characterization of <i>PUFB</i> in <i>Dictyostelium discoideum</i>	
2.1 Introduction	23-27
2.2 Objectives of the present study	27
2.3 Materials and methods	28
2.3.1 Homology search, domain analyses and phylogenetic analyses	28
2.3.2 <i>in silico</i> analysis of the promoters of 5 <i>PUF</i> genes	28
2.3.3 Structure deduction and Molecular Dynamics (MD) simulation protocol	29
2.3.4 Culture of <i>Dictyostelium</i> cells	29
2.3.5 Growth and development of <i>D. discoideum</i> cells	29-30
2.3.6 Temporal <i>DdPUFB</i> mRNA expression pattern analysis using semi-quantitative RT PCR	30-31
2.3.7 Spatial expression analysis of <i>DdPUFB</i> mRNA by <i>in situ</i> hybridization in	31-34

	multicellular structures developed	
2.3.8	Bacterial transformation	34
2.3.9	Statistical analyses	34
2.4	Results and discussion	35
2.4.1	Phylogenetic analysis of PUF proteins	35-40
2.4.2	<i>In silico</i> analysis of the 5 <i>PUF</i> promoters	40-43
2.4.3	Structure modeling and Molecular Dynamics simulations of the 5 <i>PUF</i> proteins	43-51
2.4.4	Temporal mRNA expression pattern of <i>PUFB</i> by RT-PCR	51-52
2.4.5	Spatial mRNA expression pattern analysis of <i>PUFB</i> by <i>in situ</i> hybridization	52-53
2.5	Conclusions	53-54

Chapter 3: Role of *PUFB* in growth and development of *Dictyostelium discoideum*

3.1	Introduction	55-57
3.2	Objectives of the present study	57-58
3.3	Materials and methods	58
3.3.1	Materials used in the study	58
3.3.2	Transformation of <i>D. discoideum</i> Ax2 cells	58
3.3.3	Construct preparation and confirmation of <i>PUFB</i> overexpressing strain	58-59
3.3.4	Subcellular localization of the <i>PUFB</i> -eYFP fusion protein by confocal microscopy	59-60
3.3.5	Construct preparation and confirmation of <i>PUFB</i> knockout (<i>PUFB</i> ⁻) strain	60-61
3.3.6	Confirmation of <i>PUFB</i> mutant strains through mRNA level measurement	62
3.3.7	Cell proliferation analysis	62-63
3.3.8	Analysis of development	63
3.3.9	Morphological analyses of multicellular structures formed during development	63
3.3.10	Spore viability assay	63-64

3.3.11	Cell cycle and cell size analysis	64
3.3.12	Endocytosis and exocytosis assay	64-65
3.3.13	Measurement of mRNA levels for developmental genes	65
3.3.14	cAMP level measurement	65-66
3.4	Results and discussion	66
3.3.1	Preparation of <i>PUFB</i> overexpressing strain [<i>act15/PUFB-eYFP/Ax2</i>]	66
3.3.2	Subcellular localization of PUFB-eYFP fusion protein	67
3.3.3	Preparation of the <i>PUFB</i> knockout construct	67-69
3.3.4	Preparation and validation knockout (<i>PUFB</i> ⁻) strain by PCR	69-70
3.3.5	Confirmation of <i>PUFB</i> overexpressor (<i>PUFB</i> ^{OE}) and knockout strain (<i>PUFB</i> ⁻) by mRNA levels	70-71
3.3.6	Comparative cell proliferation and growth profile studies of Ax2, <i>PUFB</i> ⁻ and <i>PUFB</i> ^{OE} strains	71-72
3.3.7	Cell cycle analysis of <i>PUFB</i> mutants	72-73
3.3.8	Endocytosis and exocytosis studies in <i>PUFB</i> mutants	73-75
3.3.9	Comparative developmental profile study of Ax2, <i>PUFB</i> ⁻ and <i>PUFB</i> ^{OE}	75-77
3.3.10	Morphological analysis of the fruiting bodies in Ax2 and <i>PUFB</i> mutants	78
3.3.11	mRNA expression of genes involved in aggregate formation	79-81
3.3.12	Expression levels of spore coat proteins and spore viability in <i>PUFB</i> mutants	81-82
3.3.13	<i>PUFB</i> mutants show reduced cAMP signaling	82-83
3.3.14	Expression level of genes involved in the cAMP signaling	84-85
3.5	Conclusions	85-86

Chapter 4: Role of *PUFB* in cell type differentiation, spatial patterning, cell lineage tracing and autophagy

4.1	Introduction	87-88
4.3.1	Cell death and autophagy in <i>Dictyostelium</i>	89-91
4.2	Objectives	91
4.3	Materials and Methods	91
4.3.1	Storage of <i>Dictyostelium</i> spores	91

4.3.2	mRNA expression analysis of cell-type specific marker using semi-quantitative RT-PCR	91-92
4.3.3	β - galactosidase staining in multicellular structure for cell type patterning studies	92-93
4.3.4	Development of chimeras of Ax2 cells tagged with GFP and <i>PUFB</i> ⁻ cells tagged with RFP	93
4.3.5	Spore count from fruiting bodies developed from the chimeras	93
4.3.6	mRNA levels of autophagy-related genes in wild type Ax2 and <i>PUFB</i> ⁻ cells	93-94
4.3.7	Analysis of autophagic flux using <i>RFP-GFP-Atg8</i> assay	94
4.4	Results and discussion	95
4.3.1	Cell-type differentiation and patterning in <i>PUFB</i> ⁻	95-101
4.3.2	Cell lineage tracing by chimera formation of GFP marked Ax2 cells and RFP marked <i>PUFB</i> ⁻ cells	101-104
4.3.3	Contribution of <i>PUFB</i> ⁻ cells in spore formation in the chimeras developed	104-105
4.3.4	Expression of autophagy-related genes in Ax2 and <i>PUFB</i> ⁻ cells	105-106
4.3.5	<i>PUFB</i> knockout leads to suppression of autophagy and autophagic flux in <i>Dictyostelium</i>	106-109
4.5	Conclusions	109-110
	Summary and Conclusions	111-114
	Bibliography	115-128
	Appendix A	
	<ul style="list-style-type: none"> • Media, chemicals and reagents • Vector maps 	
	Appendix B	
	<ul style="list-style-type: none"> • Conferences • Publications 	
	Plagiarism report	

Abstract

PUF (Pumilio and FBF) proteins are the RNA binding proteins having highly conserved domain called PUF domain which regulate diverse eukaryotic processes like organelle biogenesis, oogenesis, neuron function, stem cell maintenance, and memory formation, anterior-posterior patterning of early embryo of *Drosophila*, maintenance of germline stem cells and germline switch from spermatogenesis to oogenesis in case of *C. elegans*, etc. They are known to be post-transcriptional regulators. By interacting with the cis-regulatory element present at the 3'UTR of mRNA, PUF protein promotes the degradation or translation repression of the target mRNA. It recruits or makes interaction with protein cofactors and other regulatory machinery leads to translation repression or degradation. crystal structure of PUF-RNA complex reveals that PUF protein can attain different structural confirmation to recognize sequence and bind to target RNA.

Dictyostelium is a soil-living social amoeba present in two life forms i.e. unicellular and multicellular. This enables us to study growth and development independent of each other. In absence of nutrition, *Dictyostelium* cells start chemotactic movement in response to cAMP and aggregate to form multicellular structures which undergo developmental changes to form mound, slug and finally culminates into the terminally differentiated fruiting body consisting of the stalk (dead vacuolated cells) and sorus (spores). This is a very useful model organism for studying many fundamental processes like chemotaxis, pattern formation, endocytic vesicle traffic, cell adhesion, autophagy-associated cell death, etc. Since PUF proteins are also involved in the differentiation and patterning of many organisms, we were interested to know the role of PUF protein in *Dictyostelium discoideum*. *Dictyostelium* has been considered as a very good model system for the study of growth, development and differentiation. It serves as a preferable model organism for our study to understand the role of PUF. Therefore we laid down following objectives

- To carry out *in silico* analysis for the identification of genes encoding PUF proteins in *D. discoideum* and characterization of one selected gene. It involves phylogenetic analysis, molecular modeling of PUF protein to determine its 3-D structure. Spatio-temporal expression pattern would also be analyzed.

- To carry out the functional analysis of the identified PUF protein during growth, development and differentiation of this organism. This would be accomplished by creating both overexpressor and knock out mutant strains where all the above parameters would be analyzed.
- To explore the role of *PUF* in cell-type differentiation, spatial patterning and cell lineage tracing. Further we explored the role of PUF in autophagy.

Dictyostelium genome encodes 5 *PUF* genes named as *PUFA*, *PUFB*, *PUFC*, *PUFD* and *PUFE*. Bioinformatic analysis revealed that *PUFA*, *PUFB* and *PUFC* showed more closeness to yeast and plant PUF proteins while *PUFA* also showed similarity to human PUF. But *PUFC* and *PUFE* are distantly related to PUF proteins of other organisms. Three highly conserved motifs in the promoter region of all the 5 *PUF* was found, which could act as binding sites for different transcription factors. Tertiary structure modeling of all the 5 DdPUF protein suggests that they consist mainly of alpha-helix. *PUFA*, *PUFB* and *PUFD* showed the presence of eight repeats in their PUF domain while *PUFC* and *PUFE* have six domains only. It has been studied that *PUFA* plays an important role during growth to development transition in *Dictyostelium*. Based on the better structural and stereochemical quality and also the presence of eight repeats in their PUF domain as suggested by the structural modeling data we chose *PUFB* to work upon further and also, it shows more similarity to yeast and plants PUF. mRNA expression pattern of *PUFB* was found to be high during early and later stages of development suggesting that it may have a role in cell division, growth to development transition and terminal differentiation of cell types. Prestalk specific localization of *PUFB* mRNA as inferred from Whole-mount *in situ* hybridization analysis suggested it might have a role in autophagic cell death and stalk cell differentiation.

To study the functional aspects of *PUFB* during growth, development and differentiation of *Dictyostelium* two mutant strains (*PUFB*⁻ and *PUFB*^{OE}) were created and its role in cell proliferation, development and differentiation was analyzed. *PUFB*⁻ strain showed slightly higher proliferation rate and Cell cycle analysis showed that this could be possibly by suppressing G1 arrest and initiating the G1-S transition. *PUFB*^{OE}

showed decreased proliferation rate and defects in the exocytosis rate of *PUFB^{OE}* suggesting the possible cause of decrease in cell proliferation and cell growth.

Next, we observed the role of PUFB in the multicellular development of *Dictyostelium*. Delay in the early stages of development of both the mutants was observed. *PUFB^{OE}* formed small sized, less number of aggregate with asynchronous development leading to the formation of small sized fruiting body. Their fruiting body had smaller stalk and large sori, with reduced stalk/spore ratio and displaying reduced spore viability as compared to wild type. While *PUFB⁻* formed less number of aggregate of relatively large size which form fruiting body having long stalk and small sorus with reduced spore viability. Small-sized aggregates formed by *PUFB^{OE}* could be due to increased expression of *Countin* and *csA*, a cell adhesion molecule and lower expression of *cadA*. While in case of *PUFB⁻*, *Countin* and *csA* expression was low and higher expression of *cadA* leading to relatively large-sized aggregates. Levels of cAMP were low in both the mutant strains suggesting the defects in cAMP signaling. The decrease in the mRNA level of *acaA* and *carA* in both the mutant strain further confirmed this result. Thus we can conclude that PUFB plays a crucial role during growth and development of this organism.

Next, the role of PUFB in cell-type differentiation, patterning and cell-type specific marker expression studies was explored during the development of Ax2 and *PUFB⁻*. There was increased expression of prestalk-specific gene *ecmA* and reduced expression of prespore gene in *PUFB⁻* as compared to the wild type. Also the staining region of some prestalk marker were increased and mislocalized while there was decrease in the staining region of prespore marker in *PUFB⁻* as compared to the wild type. There was misregulated prestalk cell-type patterning due to disturbed prestalk/prespore ratio, which results in the formation of fruiting bodies with long stalk and small sori due to reduced prespore region. Our results suggest that PUFB is not only involved in the growth and development of *Dictyostelium* but also in the cell-type differentiation, proper proportioning of prestalk/prespore ratio and patterning during multicellular development in *Dictyostelium*.

To know the role of PUFB in cell lineage tracing, chimera studies were performed. When wild type Ax2 cells tagged with GFP and *PUFB⁻* cells tagged with RFP

in different proportions, *PUFB*⁻ cells tend to distribute themselves in the prespore region of the multicellular structure and thus contributed majorly in the spore formation in the chimeric mixtures with wild type.

Further, the role of PUFB in autophagy was analyzed by monitoring the autophagic flux using RFP-GFP-Atg8/LC3 (early autophagosome marker). As compared to the wild type significantly lower number of yellow or red puncta per cell was observed during starvation in *PUFB*⁻. Also the mRNA expression level of autophagy-related genes in the *PUFB*⁻ was reduced suggesting the regulatory role of PUFB during starvation-induced autophagy and is required for normal development in *Dictyostelium*.

Hence our study demonstrated that PUFB suppresses cell proliferation and growth, and also regulate aggregation size by modulating the early developmental gene expression and cAMP signaling. It is involved in the regulation of development, differentiation and cell type patterning by maintaining the boundary between prestalk and prespore region. It also plays a crucial role in the starvation-induced autophagy.

1.1 INTRODUCTION

Dictyostelium discoideum was first isolated and identified by Kenneth Raper in the year 1935 from the deciduous forest soil and decaying leaves of North Carolina, USA. In the natural habitat, *D. discoideum* cells feed on bacteria and yeast by chemotaxis tracking and multiply mitotically (Raper, 1935). *D. discoideum* is a valuable model system to study differentiation, development, phagocytosis, chemotaxis and signal transduction. The genome of Ax2 strain of *D. discoideum* has been completely sequenced and has nearly 12,500 protein coding genes (Eichinger et al., 2005).

1.2 Phylogenetic position of *D. discoideum*

D. discoideum, a social amoeba has a life cycle that encompasses both unicellular and multicellular forms. On the basis of proteome-based studies, it has been confirmed that *Dictyostelium* resides in the amoeboid group (protist). It is an eukaryote, forms a separate branch from fungi, plants and animals. It occupies a strategic phylogenetic position and appeared after the divergence of plant and animal. It is present on the animal branch (Figure 1.1) (Eichinger et al., 2005).

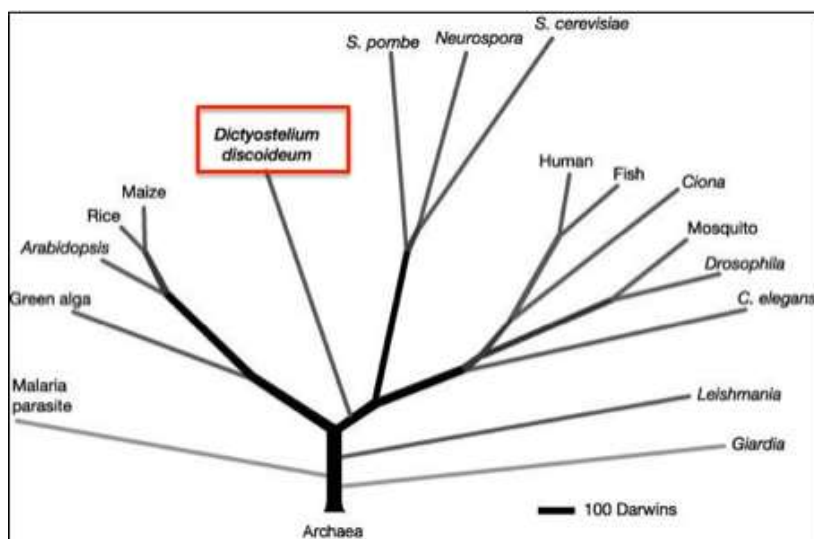


Figure 1.1: Phylogenetic tree exhibiting evolutionary relationship for *D. discoideum*. The phylogenetic analysis shows *D. discoideum* diverged after the animal-plant split and before fungi and yeast (reproduced from Eichinger et al., 2005).

1.3 Advantages of using *D. discoideum* as a model system

The social amoeba, *D. discoideum* (hereafter referred as *Dictyostelium*) is an attractive eukaryotic microbe having the capability of shifting from unicellular to multicellular forms. It is a simple yet powerful model organism for eukaryotic cell

biology, developmental biology and molecular mechanisms of disease as it shows higher level of complexity than the yeast but simpler than animals and plants (Kreppel and Kimmel, 2002). Some of the important characteristics of this model organism are listed below:

- It has a simple and short life cycle having both vegetative (unicellular) and developmental (multicellular) stages. The unicellular stage can be maintained till there is enough of food where it can divide asexually by mitotic divisions and shows a generation time of nearly 10-12 h. Once food is depleted or starvation is set in, the unicellular amoebae comes to form multicellular structures which ultimately forms a fruiting body in approximately 24 h. The fruiting body has two terminally differentiated cells: the stalk (made up of dead vacuolated cells) and spores (viable cells). Interestingly both the forms can be maintained independent of each other.
- *Dictyostelium* can be grown both in rich liquid medium as well as in association with bacteria. Isolation of cellular products for further analyses using biochemical as well as proteomic approaches can be performed.
- The haploid genome of nearly 34 Mb has been completely sequenced (available online at www.dictybase.org) and is divided into 6 chromosomes. Therefore, to establish a direct link between functions and genes reverse genetic methods can be employed (Eichinger et al., 2005).
- Genetic manipulations like preparation of knockout by homologous recombination, preparation of overexpressors, knockdown by antisense RNA or RNAi are well established and relatively easy to perform (Kuhlmann et al., 2006)
- Multicellularity in this organism is initiated by a complex cAMP signaling pathway, which also acts as a chemoattractant. Thus, chemotaxis and phagocytosis are well established and can be extrapolated to study the macrophages, which share similarity with them.
- This organism shows developmental cell death, which is caspase-independent and is accompanied by autophagic cell death. It is now declared by NIH as a model system to answer questions regarding autophagy, something similar to what *C. elegans* gave for apoptosis (Roisin-Bouffay et al., 2004).
- Due to its phylogenetic position, *Dictyostelium* possess homologs of many eukaryotic genes which are even absent in yeast. It has emerged as a promising

eukaryotic host for the ectopic expression of recombinant eukaryotic proteins (Arya et al., 2008).

- Due to the ease of handling of *Dictyostelium* cells and the lack of any cell wall (being transparent) helps in the utilization of enzymatic, fluorescent, antigenic protein tags and *in-situ* hybridization (Gerisch and Muller-Taubenberger, 2003; Maeda *et al.*, 2003).
- As these cells show controlled cell movement and cell differentiation, generation of pattern during multicellular development allows the analysis of pattern formation (Kimmel and Firtel, 2004; Williams, 2006; Weijer, 2009).

1.4 Life cycle of *D. discoideum*

Dictyostelium is a facultative multicellular organism having a very short life cycle and comprising of both unicellular and multicellular forms. Unicellular amoeba shows vegetative growth by feeding upon bacteria and divides mitotically by binary fission. In the absence of food, it enters multicellular developmental pathway to form spore-harboring structure called fruiting body. The life cycle can be divided into the following stages (Schaap, 2011) (Figure 1.2).

1.4.1 The vegetative (unicellular) phase

Dictyostelium cells exist as a unicellular haploid amoeba/ myxamoeba that via phagocytosis feed on bacteria and grow vegetatively through mitotic divisions (binary fission). *Dictyostelium* cells are approximately 10 to 20 microns in diameter. The cell is defined by a plasma membrane showing numerous pseudopods and food vacuoles. Cell wall and flagella are absent hence, they are non-motile in nature (Raper, 1935; Gezelius and Rånby, 1957; George et al., 1972). Presence of toxic agents cause physiological and morphological changes to the cells, which include the change in gene expression of a number of genes to increase resistance against toxins and the cells are called as aspidocytes (Serafimidis et al., 2007).

Pre-starvation factor (PSF) is secreted by vegetative cells whose function is to monitor cell density in proportion to the available nutrients (Rathi et al., 1991). PSF is a glycoprotein of 87 kDa molecular mass and is sensitive to heat and proteases. Presence of bacteria as food source inhibits the accumulation of PSF. High levels of PSF induces the

expression of genes required for aggregation. Along with the depletion of food supply PSF production declines and the level of conditioned medium factor (CMF), another cell density sensing factor begins to increase. PSF leads to the induction of gene expression of *yakA* and *discoidin-I*.

1.4.2 *The development/asexual (multicellular) phase*

Starvation is the major factor that triggers the vegetative unicellular cells towards multicellular development and leads to the expression of a variety of new genes, which are responsible for chemotaxis both towards folic acid (factors from bacteria) and cAMP. Each and every amoeba can sense the cAMP, respond by releasing cAMP and leads to the signal amplification and relay. Following starvation, production of PSF declines and the accumulation of another cell density sensing factor CMF (conditioned medium factor) begins (Clarke and Gomer, 1995). As cell density of the starving cells is increased, accumulation of CMF regulates the cAMP signal relay to initiate cell aggregation. Under normal conditions each aggregate is formed by $\sim 10^5$ amoebae (Yuen et al., 1995).

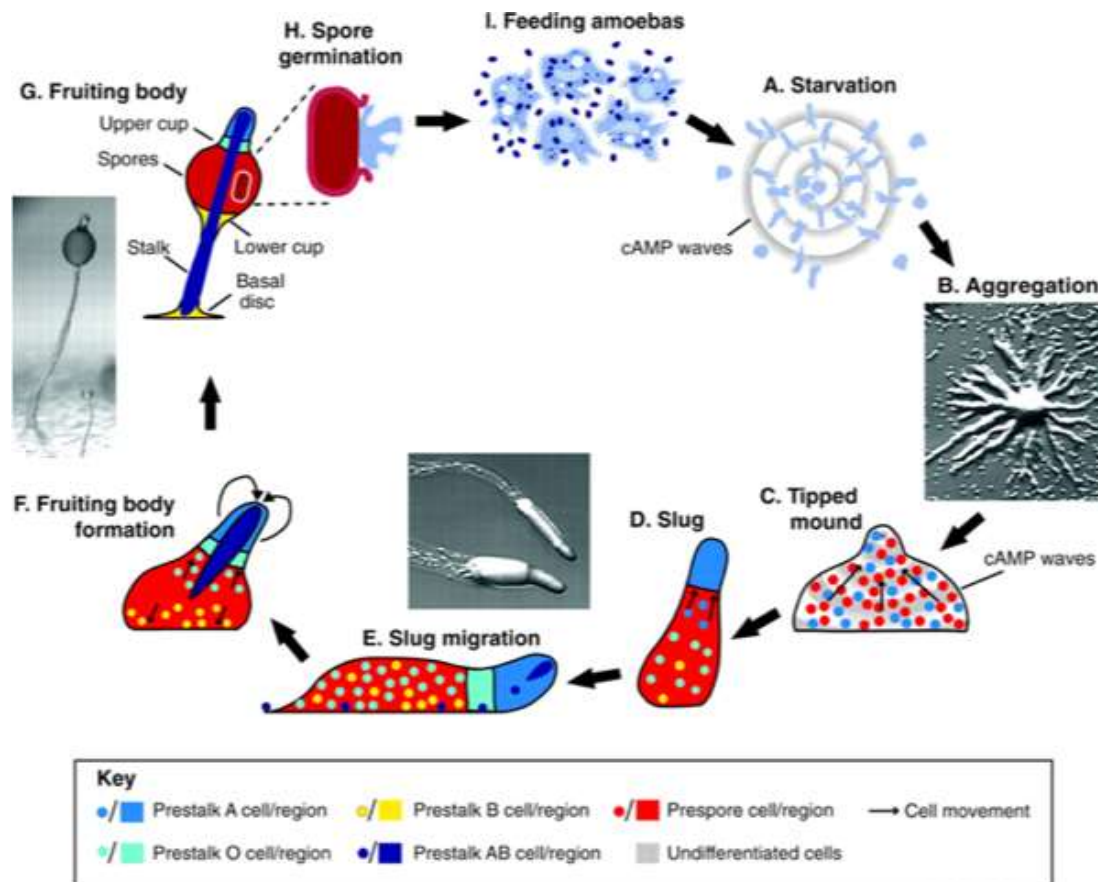


Figure 1.2: Life cycle of *Dictyostelium discoideum*. (A) Starved *Dictyostelium* cells secrete cyclic adenosine monophosphate (cAMP) pulses. (B) These cells migrate to common collecting points via chemotactic aggregation and develop into mounds. The anterior region of the mound produces cAMP and in response to that cells move upwards (C) and form the tipped mound. At this stage, cells begin to differentiate into prespore and prestalk cells. (D) After this, the slug is formed in which further differentiation leads to the formation of prestalk A, B, AB and O cells. (E) The slug can now migrate over the surface to show a clear-cut pattern formation with prestalk cells in the anterior and prespore cells in the posterior region. (F) A massive cell movement occurs before terminal differentiation occurs where the prespore forms spore cells to be located in the anterior end and posterior end has a stalk. (G) Finally, these cell-types culminate into fruiting body that consists of a stalk and a spore head. (H) As favourable condition arises (availability of nutrient), spores germinate which (I) divide mitotically to increase in numbers and continues the vegetative phase. (Adapted from Schaap, 2011).

Another component in this signaling system involves the gene *srsA* (Sasaki et al., 2008). Within few minutes of starvation, *srsA* is induced and is repressed within 2 h. In *yakA* null cells, expression of *srsA* is not altered suggesting that it functions independent of *yakA*. Disruption or overexpression of *srsA* cause reduction in the expression of *acaA* and *carA* resulting in a delay in development along with the formation of aberrant structures, suggesting that certain critical levels of the proteins was crucial for the regulation of early development (Sasaki et al., 2008). *yakA* plays an important role in the initiation of development as *yakA* null strains fails to aggregate. In the wild type cells, induction of *carA* and *acaA* occurs within first 2 h of starvation but in case of *yakA* null cells these are not expressed. This mutant is unable to synthesize or respond to cAMP. *yakA* regulates the transition from growth-to-development (Souza et al., 1998).

Aggregation

Under nutrient depleted condition, vegetative cells undergo physiological changes that lead to the induction of multicellular developmental. The amoeboid cell then produces, secretes and also responds to cAMP. In response to cAMP millions (10, 000-1, 00, 000) of highly polarized chemotactic amoeba undergo head to tail streaming to a common point to form a multicellular structure called loose aggregate (Raper, 1935; Bonner and Savage, 1947; (Raper, 1935; Bonner and Savage, 1947; Bonner, 1952; Konijn et al., 1967). Loose aggregates are a flat, adherent mass of cells with indistinct borders (Raper, 1935) aggregation is controlled by two important molecular mechanisms i.e. cAMP mediated signaling and chemotaxis in response to cAMP (Kimmel and Parent,

2003; Manahan et al., 2004). Mostly undifferentiated cells are present in loose aggregates and very few cells start expressing cell-type specific gene markers.

In loose aggregate majority of the pstA cells (anterior-most part of prestalk cells) appear at the periphery while other prestalk specific cells are randomly distributed (Williams et al., 1989; Early et al., 1993; Early et al., 1995; Jermyn et al., 1996). At the loose aggregate stage, a slimy surface of polysaccharides and proteins starts forming which is completed by the late aggregation stage (George et al., 1972; Farnsworth and Loomis, 1975; Freeze and Loomis, 1977). It holds the mass of cells together in the aggregate and help in the formation of mound or tight aggregate.

Cellular movements in the mound stage lead to the formation of distinct prestalk (having prestalk cells) and prespore zones (having prespore cells). Some cells at the tip-organizer secretes cAMP due to which pstA and pstO cells move towards the tip and leads to the formation of tipped-mound (Dormann and Weijer, 2001). Mainly four factors control the size of aggregates formed in *D. discoideum*: number of cells participating, cell-cell adhesion proteins (CadA, CsaA), the counting mechanism and cAMP signal strength (including proteins Adenylyl cyclase A (AcaA), PdsA, cAR-1, PDI) (Jang et al., 2002; Jang and Gomer, 2008). Counting Factor (CF) is released by the starving cells which breakup the aggregation streams into groups of $\sim 10^4$ cells (Tang et al., 2002). High level of CF reduces the cell-cell adhesion and lead to the formation of small-sized aggregates (Jang and Gomer, 2008).

The slug stage

After tipped mound stage, a finger like structure is developed called standing slug, which pulls the mass anteriorly. If the conditions are unfavourable (like cAMP release, ambient light and temperature) it can enter the migratory phase and form migratory slug (Raper, 1940; Bonner, 1952; Newell et al., 1969). Migrating slug has been considered as the best stage to study pattern formation as the two specified prestalk and prespore cells forms a typical pattern where the anterior is composed of prestalk cells and the posterior is composed of prespore (Figure 1.3A). Anterior 15 -20% of the slug is called the prestalk region having prestalk cells while the posterior 80-85% region has prespore cells is called the prespore region. The ratio of these regions remains constant regardless of the size of the slug. Prestalk region can be divided into the following zones: prestalkA region

occupying the anterior-most 10% of slug, prestalkO region is at the boundary of prestalk and prespore cells and in the core region lies the prestalkAB cells (Figure 1.3A). The cells present at these regions are called pstA, pstO and pstAB cells (Williams, 2006). PstA cells express *ecmA* marker gene while pstO cells express low levels of *ecmA* gene. PstB cells express *ecmB* gene. PstAB cells express both *ecmA* and *ecmB* genes (Williams et al., 1989; Gaskell et al., 1992; Early et al., 1993; Early et al., 1995; Yamada et al., 2005). The “tip-organizer” is responsible for maintaining the integrity of the organism and also inhibits the development of other tips in the near vicinity. The tip-organizer directs slug movement by phototaxis and also regulates the timing of entry into culmination (Poff and Loomis Jr, 1973; Rubin and Robertson, 1975; Durston, 1976; Durston and Vork, 1979; Smith and Williams, 1980). The posterior 2/3 region of the slug is occupied by the psp cells and interspersed between them are the anterior-like cells (ALCs), which are similar to pst cells in their properties (Sternfeld and David, 1981, 1982). Rear-guard region is the posterior most region of the slug consisting of pst cells expressing *ecmB* gene.

The culmination stage

The slug stage finally culminates into the fruiting body, which is the final stage in the developmental life cycle of *D. discoideum*. It comprises of three stages: early culminant, mid culminant and late culminant (Figure 1.3B). Fruiting body has two terminally differentiated types of cells: the stalk which are made up of dead and vacuolated cells and spore which are made up of viable cells (Whittingham and Raper, 1960). In early culminant, stalk is formed of thin, translucent and central cell mass consisting of the stalk tube and has extracellular deposition by pstA and pstO cells (Raper, 1940; Raper and Fennell, 1952; MAEDA and TAKEUCHI, 1969; Williams et al., 1989; Sternfeld, 1992). In early culminant prespore region has scattered ALC/pstB cells (*ecmB* expressed by anterior-like cells) which migrate downward and lead to the formation of lower cup region while a distinct subset of ALC/pstA cells which expresses *ecmA* from the distal part of its promoter leads to the formation of upper cup (Figure 1.3B) (Raper and Fennell, 1952; MAEDA and TAKEUCHI, 1969; Ceccarelli et al., 1991; Jermyn and Williams, 1991; Grimson et al., 1996).

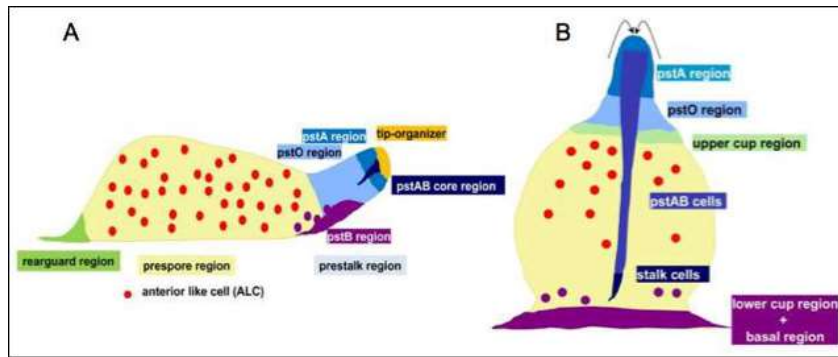


Figure 1.3: Compartmentalization in the multicellular organism. (A) Finer anatomy of the migratory slug of *D. discoideum* shows the presence of prespore and prestalk regions. The localization of different sub-types of prestalk cells was identified by the use of reporter genes. (B) Cell movement during culmination. During the culmination, terminal cell differentiation occurs and is comprised of cellular movements within an early culminant. Firstly, pstB cells migrate towards the stalk tube and are replaced by pstA cells, now called as pstAB cells followed by pstO cells. This proceeds until all prestalk cells are incorporated into the stalk. (Adapted from Schaap, 2011).

During the mid and late culmination stages, the pstAB cells move downwards to the stalk tube away from the prespore region. The pstA and pstO cells follow ‘reverse fountain’ pattern and prestalk differentiation majorly occurs at this stage, which finally differentiate into stalk cells. The pstO cells move upward and differentiate into pstA cells, as pstA cells traverse down into stalk tube it differentiates into the pstAB cells. During late culmination, terminal differentiation of prespore into spore and prestalk into stalk occurs, which ultimately leads to the formation of a fruiting body (Williams, 1995). A basal disc is present at the bottom, which provides support and anchors the fruiting body. A mature fruiting body is made up of a long stalk and a sorus having viable spore cells. Spores are elliptical in shape protected by a rugged spore coat made up of three layer, in which the outer and inner layers are made up of GPS (galactose/N-acetylgalactosamine polysaccharide) and glycoprotein whereas cellulose forms the middle layer (Hohl and Hamamoto, 1969; MAEDA and TAKEUCHI, 1969; West and Erdos, 1990). The length of the stalk is approximately 1.5-3 mm made up of dead vacuolated cells while sorus (viable cells) is lemon shaped and of approximately 125-300 microns in diameter. Because of the presence of spore coat, spores are resistant to the external environmental conditions and can survive for several years without nutrient. Under favourable conditions, spores germinate into amoeba and start dividing by binary fission (Murata and Ohnishi, 1980).

1.5 Cell signaling during *D. discoideum* development

John Bonner in 1947 first time showed that during nutritional stress conditions, *Dictyostelium* cells secrete a chemoattractant which was later identified as cAMP (3'-5'-cyclic adenosine monophosphate), a secondary messenger that is required for the initiation of development and differentiation (Bonner and Savage, 1947; Konijn et al., 1967). The signals and the pathways involved in *Dictyostelium* development are summarized in Figure 1.4 (Schaap, 2016).

When food gets depleted, the growth-to-development transition occurs and the population density of amoeba approaches its peak. Along with cAMP, density sensing factors such as PSF (pre-starvation factor) and CMF (conditioned medium factor) comes into play to initiate development (Grabel and Loomis, 1978). High level of PSF and starvation leads to the induction of YakA expression (Souza et al., 1998) which inhibits the binding of PUFA, a translational repressor to the catalytic subunit of PKA (cAMP-dependent protein kinase) (Souza et al., 1999). Accumulation of PKA-C then mediates the expression of aggregation related genes like *adenylate cyclase (acaA)* and extracellular *cAMP phosphodiesterase (pdsA)* (Schulkes and Schaap, 1995). During growth, AprA and CfaD are secreted which forms a complex of 138 kDa that diminishes cell proliferation (Bakthavatsalam et al., 2008; Bakthavatsalam et al., 2009). Signal transduction mediated by cAR1 is required for the function of CMF which leads to the formation of polyketide MPBD (4-methyl-5-pentylbenzene-1,3-diol) that increase the early genes expression.

CMF that acts as a quorum sensor, also initiates development via the activation of G proteins by cAR1 that cause ACA stimulation that leads to the synthesis of cAMP (Jain and Gomer, 1994). As cAMP bind to cAR1, activation of MAP kinase Erk2 occurs, which inhibits RegA, an internal cAMP phosphodiesterase leads to increase in cAMP concentration (Laub and Loomis, 1998). PdsA, an extracellular cAMP phosphodiesterase and protein kinase, PKA further regulate the high concentration of cAMP (Orlow et al., 1981; Franke and Kessin, 1992; Sugang et al., 1997). Due to the cAMP pulses, GataC (transcription factor) dependent genes like for example *carA*, *acaA*, *gbfA*, *regA*, *pkaR* and the cell adhesion like *csA*, *tgrB1* and *tgrC1* are expressed, which are required during and after aggregation (Cai et al., 2014).

During post-aggregation stage, differentiation of cells into particular cell-types begins. DIF-1 induces the prestalk cell-types *pstA*, *pstO* and *pstB* to differentiate and give rise to upper and lower cups and mainly the basal disc of the fruiting body (Morris et al., 1987; Saito et al., 2008; Yamada et al., 2011). Another polyketide named MPBD (4-methyl-5-pentylbenzene-1,3 diol) mediates terminal differentiation, which inhibits GskA, a protein kinase that enhances the PKA activity thus blocking the release of signal peptide SDF-1 (Anjard et al., 2011). In both prestalk and prespore cells SDF-1 is responsible for terminal differentiation and block DIF-induced stalk cell differentiation via regulating the cAMP levels (Berks and Kay, 1988; Anjard et al., 1998; Anjard et al., 2011) whereas SDF-2 is responsible for terminal differentiation and sporulation induction of prespore cells (Anjard et al., 2009).

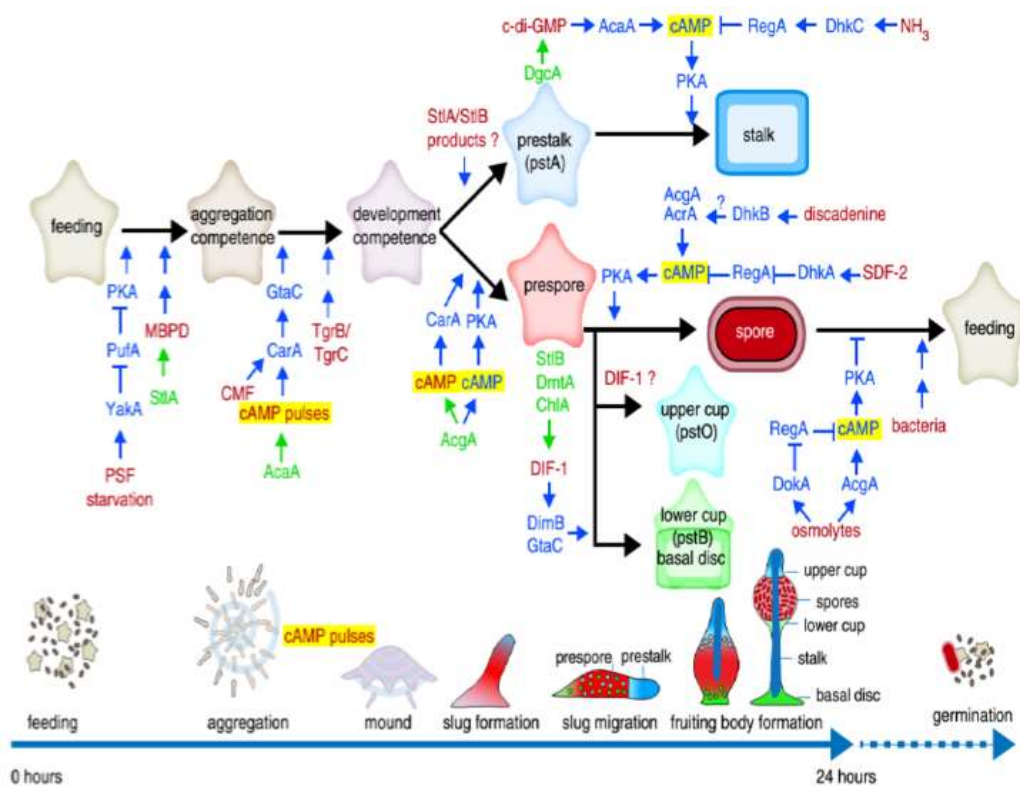


Figure 1.4: Cell signaling during development of *D. discoideum*. Starving amoebae aggregate to form a mound by secreting and relaying cAMP pulses. The tip of the mound moves upwards to form the slug in which cell-type differentiation is initiated. During culmination, prestalk and prespore cells terminally differentiate into stalk and spore cells, respectively. These processes are highly regulated and summarized in above figure for better understanding. The text shown in red colour reveals the secreted and environmental signals that mediate different life cycle transition and cAMP mediated differentiation of *Dictyostelium* (highlighted yellow). Enzyme that lead to synthesis of secreted signals are highlighted by green colour whereas blue text shows the small molecules and proteins mediating the

signal transduction pathway. T-crosses and blue arrows represent inhibitory and stimulatory effects, respectively. Double blue arrows denote that mode of signal transduction are not known. Abbreviations: AcaA (adenylate cyclase A); AcrA (adenylate cyclase R); AcgA (adenylate cyclase G); cAMP (3'-5'-cyclic adenosine monophosphate); cdi- GMP (3',5'-cyclic diguanylic acid); CarA- cAMP receptor 1); ChlA (flavindependent halogenase Chlorination A); PKA (cAMP-dependent protein kinase); RegA (cAMP dependent phosphodiesterase); CMF (conditioned medium factor); Dhk (histidine phosphatase A); DhkB (histidine kinase B); DhkC (histidine kinase C); DgcA (diguanylate cyclase A); NH₃ (ammonia); DIF-1 (differentiation inducing factor 1); DimB (transcription factor DIF insensitive mutant A); DmtA (des-methyl-DIF-1 methyltransferase); DokA (osmosensing histidine phosphatase); GtaC (GATA-binding transcription factor C); MBPD (4-methyl-5-pentylbenzene-1,3-diol); PSF (prestarvation factor); PufA (pumilio RNA binding protein); SDF-2 (spore differentiation factor 2); StlA (polyketide synthase Steely A); StlB (polyketide synthase Steely B); YakA (DYRK family protein kinase); Tgr (transmembrane, IPT, IG, E-set, repeat protein) (Adapted Schaap, 2016).

1.6 PUF (Pumilio and FBF)

1.6.1 Introduction

In most of the eukaryotic organisms, gene expression is regulated at the transcriptional and post-transcriptional levels. To adapt their biological functions like growth and development to the changes in environment, this type of regulation becomes an important strategy in these organisms. Reports suggest that various aspects of RNA processing like RNA splicing, capping, polyadenylation, localization, modification, translation, transport and stability are regulated by different RNA binding proteins (RBPs) (Wickens et al., 2002; Keene, 2007; Glisovic et al., 2008; Abbasi et al., 2010; Ray et al., 2013). Protein structure analyses and their functional characterizations have revealed that the RNA binding proteins (RBPs) have conserved motifs and domains for RNA binding like the K homology (KH) domains, RNA-recognition motifs (RRMs), zinc fingers, DEAD/DEAH boxes [highly conserved motif (Asp-Glu-Ala-Asp) in RNA helicases], pentatricopeptide-repeat (PPR) domains, Pumilio/FPF (Pumilio-fem-3 binding factor, PUF) domains (Wu et al., 2016).

PUF is a large family of RNA binding family present in all eukaryotes. Family got the name PUF from its two founding members: Pumilio from *Drosophila melanogaster* and FBF from *C. elegans* (Murata and Wharton, 1995; Zhang et al., 1997). The numbers of *PUF* genes are variable in different model organisms. They are known to be post-transcriptional regulators where they interact with 3' UTR of their target mRNA through

specific recognition sequence and regulate post-transcriptional processes like RNA decay and translational repression (Wharton and Aggarwal, 2006; Tam et al., 2010). It plays many important roles for example in cell development, stem cell maintenance and differentiation Wickens et al., 2002; Spassov and Jurecic, 2003a).

1.6.2 *PUF protein structure and its RNA-binding mechanism*

All the PUF proteins have an evolutionarily highly conserved domain called PUF domain or Pumilio homology domain (PUM-HD) (Zhang et al., 1997; Wharton et al., 1998) present at the C-terminal of the protein. Human PUM-HD1 crystal structure shows the configuration of an extended crescent shape in which the outer convex surface could possibly be the binding site for different proteins (Figure 1.5A) (Wang et al., 2002). The inner surface, which appears concave-like consists of 8 imperfect repeats of nearly 36 amino acids each having two flanking pseudo repeats. Each repeat consist of 3 α -helices where in the second helix at position number 12, 13 and 16 are most conserved three amino acids. The side chain of amino acid 12 and 16 interact via van der Waals contacts or base-specific hydrogen bonds with the RNA base, while the amino acid side chain present at position 13 makes stacking interactions. In each repeats, specific residues are present which dictate the base recognition (Edwards et al., 2001; Wang et al., 2001; Wang et al., 2002). In general, 8 tandem repeats that are present recognize and bind to 8 RNA bases in an antiparallel fashion i.e. N to C terminal domain of PUF and 3'-5' orientation of RNA (Figure 1.5B) (Wang et al., 2002; Jalal Kiani et al., 2017). The modular arrangement of pumilio domain (PUM-HD) coincides with the modular arrangement of Armadillo repeats of β -catenin and importin- α , suggesting folding pattern like ancestral proteins (Wang et al., 2001).

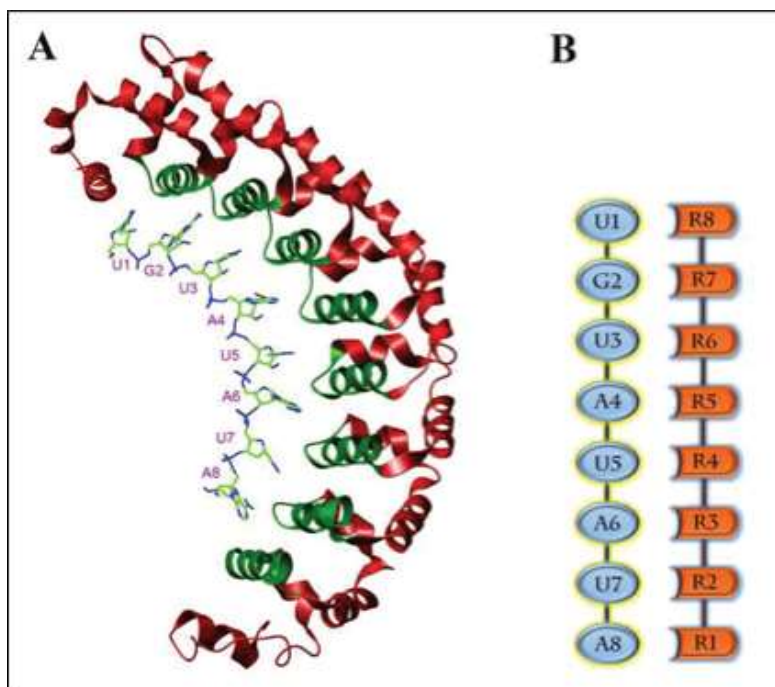


Figure 1.5: **Human PUMILIO-homology domain with Hunchback NRE.** (A) Domain consists of 8 repeats in which each repeat comprises of three α -helices flanked by two pseudo-repeats. Specific amino acid in the second helix of each repeat is shown in green colour dictates the base recognition. (B) Eight repeats of the PUM-HD recognize eight RNA bases specifically in an anti-parallel fashion (adapted from Kiani et al., 2017).

This pattern is also detected in proteins containing penta-tricopeptide repeat (PPR) motif consisting of 2-30 repeats. Each repeats consists of ~ 35 amino acids arranged as two α -helices in hairpin form called as helix-a and helix-b (Yagi et al., 2013; Yin et al., 2013). PUF-A of human and PUF-6 of yeast shows a discrete conformation depicting a L-shaped folding having 11 repeats of PUF that binds to single and double-stranded DNA or RNA in a non-sequence specific manner (Qiu et al., 2014). N-terminal sequence of PUF protein is found not to be so conserved, as it may bear some regulatory regions which could affect the activity of the protein (Spasov and Jurecic, 2003b; Salazar et al., 2010).

PUF protein binds specifically to the conserved RNA sequence UGUR, which is preset on the 3' untranslated regions (UTR) of mRNA (Zamore et al., 1997; Zamore et al., 1999; Crittenden et al., 2002; Jackson et al., 2004; Bernstein et al., 2005). If any mutation is present in these elements it can lead to disruption of protein binding and protein function (Murata and Wharton, 1995; Zhang et al., 1997). An AU-rich sequence is

present downstream of the core UGUR sequence which specify the interaction between PUF and RNA. (Bernstein et al., 2005; Zhu et al., 2009). The consensus recognition sequence found in *Drosophila Pumilio*, *S. cerevisiae* PUF3p, and *Homo sapiens* PUM1 and PUM2 is 5'-UGUANAUA-3' an eight-nucleotide sequence where N can either be A, C or U bases (Gerber et al., 2004; Gerber et al., 2006; Galgano et al., 2008). One repeat of PUF protein recognize one RNA base, this is the general mode of recognition i.e. each Pumilio domain with its eight repeat recognize and bind to eight RNA base of the target RNA. Although there are few exception also to this rule to expand the specificity for the targets (Lu and Hall, 2011). Like in case of budding yeast, in place of 8 bases, consensus sequence of 9 and 10 bases are present in PUF4 and PUF5, respectively. To accommodate these extra bases and to flip out the extra base, PUF protein undergoes distortion from its normal RNA binding concave surface to the flat surface (Gerber et al., 2004; Miller et al., 2008). It is assumed that this extra flip out base may contribute to the interaction with some cofactor that may be responsible for ribonucleoprotein (RNP) complex function and fate of the target RNA. HsPUM1 of human proteins and PUF-5, PUF-6, PUF-7, FBF of *Caenorhabditis elegans* also showed similar pattern of binding specificity (Opperman et al., 2005; Stumpf et al., 2008; Wang et al., 2009; Lu and Hall, 2011). In *Arabidopsis thaliana*, recently a ten-nucleotide binding consensus sequence has been identified for APUM23 having UUGR as core sequence in place of UGUR and has a cytosine present at position eight of nucleotide which shows its preference for PUF repeat 3 (Zhang and Muench, 2015).

1.6.3 *PUF proteins and their functions in different organisms*

Reports have shown that a single PUF protein can recognize a number of RNA targets, suggesting that it can regulate many processes in eukaryotic system including neuron functioning, stem cell control, biogenesis of organelles and developmental patterning. Till now most investigation has been done on *Drosophila melanogaster*, *Caenorhabditis elegans* and *Saccharomyces cerevisiae* while few studies are reported in plants.

In 1987, Lehmann identified a maternal gene *Pumilio*, in the absence of which *hunchback* (*hb*) is expressed uniformly in the posterior of *Drosophila* embryo due to which no abdominal segment developed (Lehmann and Nüsslein-Volhard, 1987). Later in 1995, Murata and Wharton showed that *Pumilio* acts by binding to NRE (Nanos

Response Element) like sequences present on mRNA and recruit Nanos (nos) and inhibit some translation machinery component (Murata and Wharton, 1995). Normally Hunchback protein is expressed at the anterior region during early development in *Drosophila* embryo. However, when *Pumilio* is mutated gradient of Pumilio protein is also present in the posterior region which suggest that repression of *hb* mRNA is absent in this region (Tautz, 1988; Barker et al., 1992). This finding was further supported by the fact that in *Pumilio* mutant, the mRNA isolated from the posterior region of embryo was not deadenylated as compared to the wild type suggesting the fact that the mRNA is not repressed translationally (Wreden et al., 1997). This led to the defects in abdominal segmentation (Lehmann and Nüsslein-Volhard, 1987; Barker et al., 1992). Pumilio also regulate some other processes like stem cell proliferation, memory formation and motor neuron functions (Weidmann and Goldstrohm, 2012).

In nematode, *C. elegans*, two sexes are present, males and hermaphrodites. Hermaphrodites produce sperm initially but later on switch to produce oocyte. This switch is controlled by the 3' UTR (untranslated region) of *fem-3* mRNA (Ahringer and Kimble, 1991). Zheng and group (1997) identified that it was the FBF, which binds to the 3' UTR of the *fem-3* mRNA and was responsible for the switch. To regulate spermatogenesis to oogenesis transition, there is requirement of *fem-3* repression and it is achieved post-transcriptionally via the 3' UTR region present in the regulatory region of *fem-3* mRNA (Hodgkin, 1986; Barton et al., 1987; Ahringer and Kimble, 1991). When knock down of *fbf* (*fbf-1* and *fbf-2*) was performed by RNAi it led to an increase in sperm production associated with the oogenesis inhibition and abnormal oocyte production, suggesting that this switch from spermatogenesis to oogenesis is regulated by FBF by repressing *fem-3* (Zhang et al., 1997). Double mutant hermaphrodites of *fbf-1- fbf-2*, defects become even worse as all the germline stem cells undergo meiosis and start spermatogenesis (Crittenden et al., 2002). By the repression of *gld-1*, FBF also promotes self-renewal of germline stem cell which leads to the mitosis at the distal end of the gonad (Crittenden et al., 2002). PUF-3/11 and PUF-5/6/7 are the two groups of PUF/RNA-binding proteins, which play important role in oogenesis of *C. elegans*. In oocyte formation all the PUFs are involved but PUF-3/11 inhibits growth of oocyte whereas PUF-5/6/7 is involved in the organization of oocyte and its formation (Hubstenberger et al., 2012). In *C. elegans*, Notch signaling pathway and PUF RNA binding proteins maintains the pool of Germline stem cells (GSCs) (Wickens et al., 2002;

Bray, 2016). From the niche, GLP-1/Notch signaling is required for the maintenance of GSC and FBF-1 and FBF-2 (collectively FBF) promote GSCs self-renewal by acting as repressors of differentiation RNAs (Crittenden et al., 2002; Kershner et al., 2013). Both *sygl-1* and *lst-1* genes are identified as GSCs regulators that directly target niche signaling (Kershner et al., 2014). A single Nanos-like zinc finger is present in LST-1 which suggests its putative role in post-transcriptional regulation (Kershner et al., 2014). But how this Notch signaling regulates the activity of FBF to maintain self-renewal of stem cell is not understood. But Shin et al. (2017) reported that both SYGL-1 and LST-1 as a cytoplasmic protein present in GSC region. Both SYGL-1 and LST-1 interact with FBF physically and leads to repression of the FBF target RNA within the stem cell pool and thus maintain the stem cell pool.

Salvetti et al. (2005) identified a protein called *Dugesia japonica* (*DjPum*), which is homologous to *Drosophila* Pumilio. It was found to be expressed in stem cells of planaria where it forms the regenerative blastema and also essential for the maintenance of neoblast.

In yeast, HO is an endonuclease responsible for switching mating-types where it causes breaking of double-stranded DNA that initiate recombination. PUF protein Mpt5p removes polyA tail of *HO* mRNA thus leading to stability of *HO* mRNA (Herskowitz, 1988). The PUF3 protein plays an important role in the mitochondrial functions as it binds and regulates mRNAs, which encode for more than 100 proteins that are required (Zhu et al., 2009). In *S. cerevisiae* PUF5p is a broad regulator of RNA, binds to more than thousand RNA targets, which is about 16% transcriptome of yeast. All these RNAs are important in regulation of various aspects of *S. cerevisiae* development like cell wall integrity, embryonic cell cycle, or chromatin structure (Wilinski et al., 2015). Nop9, PUF protein present in *S. cerevisiae*, is an essential small ribosomal subunit biogenesis factor. It recognizes structural features and sequences of 20S pre-rRNA present near the nuclease cleavage site (Nob1) and by inhibiting cleavage leads to the final step, to produce small ribosomal subunit 18S rRNA (Zhang et al., 2016). In *S. cerevisiae*, Mpt5p (also known as PUF5p) can promote temperature tolerance and is also responsible for replicative lifespan increase may be by the involvement of cell wall integrity (CWI) pathway. In case

of Mpt5D mutant lifespan was shortened and this defect was suppressed by the activation of CWI signaling (Stewart et al., 2007).

In other species also there are available reports of PUF proteins. In *Peronophythora litchi*, *PIM90* codes for a PUF protein and shows high expression during sexual and asexual development but during germination of cyst and plant infection its expression is relatively lower. Therefore, sexual and asexual differentiation of *P. litchi* is specifically regulated by *PIM90* (Jiang et al., 2017). In *Plasmodium falciparum*, PfPUF1 is responsible for the differentiation and maintenance of female gametocytes. PfPUF1-disrupted lines showed a sharp decline in gametocytemia (Shrestha et al., 2016). In humans, PUM1 and PUM2 are the two Pumilio proteins, which positively regulates *retinoic acid-inducible gene I (RIG-I)* signaling, that plays an important role during innate immunity. PUM1 and PUM2 overexpression leads to increase in promoter activity of IFN - (an important factor in *retinoic acid-inducible gene I*, which is induced by NDV (Newcastle disease virus) (Narita et al., 2014). Mammalian Pumilio proteins play important roles in ERK signaling (Lee et al., 2007), neuronal activity (Vessey et al., 2006), stress response (Vessey et al., 2006) and also germ cell development (Moore et al., 2003).

In plants, PUF proteins act as post-transcriptional repressors. In *Arabidopsis thaliana* upto 26 PUFs have been identified. *Arabidopsis* PUM5 (APUM5) plays an important role against both abiotic and biotic stress responses. Under salt and drought treatment overexpression of APUM5 showed the hypersensitive phenotypes at vegetative stage and during seedling stage. It was reported that the Pumilio homology domain of APUM5 bind to mRNA of many drought and salt stress-responsive gene at Pumilio RNA binding motif present at 3' UTR (Huh and Paek, 2014). APUM23 was found to regulate morphogenesis in leaf by the regulation of expression of *KANADI (KAN)* genes. GARP family member *KAN* genes, regulate the abaxial identity (Huang et al., 2014). Moreover, in *Arabidopsis* PUF proteins play important roles in many mechanisms like responses to light, nutrients, ABA (abscisic acid) signaling, iron deficiency and osmotic stress (Tam et al., 2010). For example, APUM23 PUF-domain protein constitutively expressed in metabolic tissues was up regulated in presence of sucrose or glucose. APUM23 loss of function in plants lead to the scrunched and serrated leaves, slow growth and also venation show abnormal pattern because of RNA processing (Abbasi et al., 2010). In

Arabidopsis, transcriptome analysis showed that many PUF members like APUM9 and APUM11 in particular, had higher transcript levels during seed imbibition in case of reduced dormancy of mutants. These findings indicate that PUF protein may play an important role in seed dormancy in plants (Machin et al., 1995). Studies suggest that all APUM-1 to APUM-6 could be important for the growth and development of *Arabidopsis* via RNA of target genes like *WUSCHEL*, *CLAVATA-1*, *PINHEAD/ZWILLE* and *FASCIATA-2*, which regulate growth of meristem and maintenance of stem cell (Francischini and Quaggio, 2009; Reichel et al., 2016). Tissues undergoing cell division and rapid proliferations showed high expression of PUF protein APUM24. It is also essential for the rRNA by products removal for fast cell division and early embryogenesis in case of *Arabidopsis*. APUM24 loss of function mutation in plants showed defect in cell patterning (Huh et al., 2013).

1.6.4 Mechanisms of RNA repression

Wickens laboratory initially described the mechanism of PUF protein mediated mRNA repression (Goldstrohm et al., 2006). Yeast PUF5 bind to *Ccr4-Pop2-NOT* mRNA deadenylase complex, specifically at Pop2 subunit of this complex, thereafter recruiting the deadenylase to mRNAs for its repression (Figure 1.6) (Goldstrohm et al., 2006). This PUF5 and *Ccr4-Pop2-NOT* mRNA deadenylase complex act as a cytoplasmic exonuclease, which cleaves the polyA tail and shortens it thus affecting both mRNA stability and translation (PREISS et al., 1998; Amrani et al., 2008; Goldstrohm and Wickens, 2008). According to the closed loop model the 3' and 5' ends of an mRNA are present adjacent to each other (Quenault et al., 2011), which allow the binding of regulators like PUF5 at 3' UTR so that they can act on the 5' end of mRNA effectively as well (Quenault et al., 2011) (Figure 1.6). In fact, the decapping enzyme Dcp1 and the decapping activator and translational repressor Dhh1, interact with the *Ccr4-Pop2-NOT* complex (Coller et al., 2001; Maillet and Collart, 2002) then Pop2–Puf5 interaction lead to the recruitment of this complex to mRNAs (Goldstrohm et al., 2006). Dhh1 and Dcp1 hydrolyze of the 5' cap (decapping) further cause mRNA repression along with the function as translational repressors (Coller and Parker, 2005). When deadenylation is absent then repression by PUF protein is mediated by recruitment of different factors affecting the 5' cap (Chagnovich and Lehmann, 2001; Goldstrohm et al., 2006; Hook et al., 2007). *Ccr4-Pop2-NOT* recruitment is a general

mechanism as *C. elegans* FBF, *Drosophila* Pumilio (Pum), yeast PUFs (PUF3 and PUF4) and human Pum1 also use this Ccr4-Pop2-NOT complex to regulate mRNA repression (Chritton and Wickens, 2010).

Besides Ccr4-Pop2-NOT deadenylase recruitment mechanism, other PUF-dependent repression mechanisms have also been proposed. It includes inhibition of translation initiation factors and interaction with 5' mRNA cap, structural changes in ribonucleoprotein and effect on the elongation and termination of translation process. For instance, the translational inhibitor d4EHP through its cofactor Brain tumor (Brat) can recruit to *Drosophila* Pum mRNAs (Cho et al., 2006). d4EHP inhibits translation by binding to the cap, allowing no space for translation initiation factor eIF4E to bind (Cho et al., 2005). In *Xenopus*, binding of Pum2 to the 5' cap structure leads to the inhibition of eIF4E binding (Cao et al., 2010). In yeast PUF6, *ASH1* mRNA translation is repressed by the interaction with eIF5B/Fun12 (translation initiation factor) which inhibits its function (Deng et al., 2008).

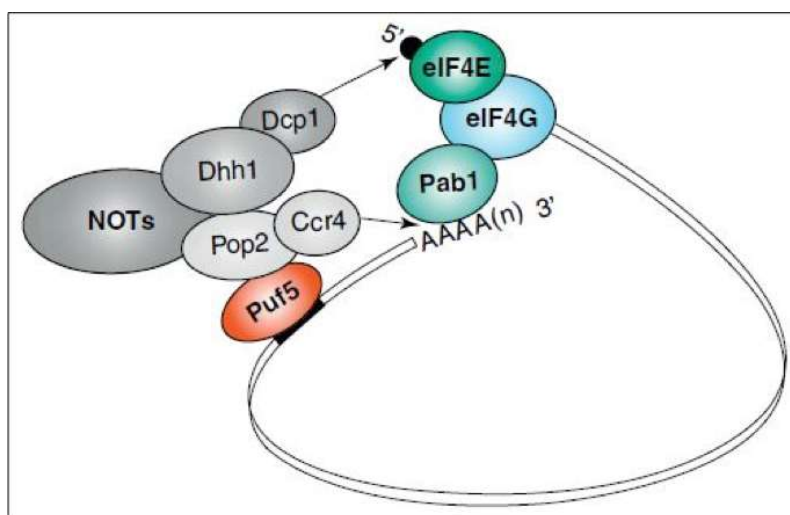


Figure 1.6: **Repression of mRNA by PUF protein.** It is achieved by Ccr4-Pop2-NOT deadenylase complex recruitment. PUF5 recognize and bind to the sequence present at 3' UTR of mRNA and Ccr4-Pop2-NOT mRNA deadenylase complex through Pop2 subunit is recruited. It also recruits decapping factors Dhh1 and Dcp1. Dhh1 and Dcp1 activate the decapping process that leads to translational inhibition. PUF5 recruits different factors, which affect the polyA tail and 5' capping that leads to deadenylation and repress translation (adapted from Quenault et al., 2011).

In case of yeast PUF3, changes in the ribonucleoprotein structure have been suggested as one of the mechanism. Besides *Ccr4-Pop2-NOT* mRNA deadenylase

binding, PUF3 also affect alternative deadenylase Pan2 that causes deadenylation. Although there is no reports of interaction between Pan2 and PUF3, which suggest that PUF3 causes the structural changes in the mRNA and the polyA tail-binding protein Pab1, due to which the polyA tail is exposed to deadenylation (Lee et al., 2010).

1.7 Work done so far in *D. discoideum*

In 1999, Souza et al., identified a protein called PUFA in *D. discoideum*, which codes for a member of Pumilio RNA binding protein family of translational regulators. He showed that *PUFA*⁻ cells develop precociously and overexpress cAMP dependent protein kinase (PKA-C) catalytic subunit, which is required for further development. They showed that PUFA response elements (PRE) are present in the mRNA of PKA-C and binding of PUFA to PREs regulates its translation. PUFA and PKA-C are inversely related to each other. PUFA represses the expression of genes required for the development like *acaA* and it does so by negatively regulating PKA-C via repressing the *PKA-C* mRNA. Function of YakA is required to decrease the PUFA protein and mRNA level.

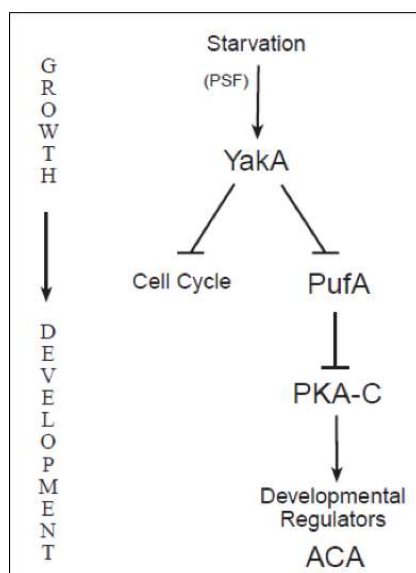


Figure 1.7: A model depicting the function of PUFA and YakA. Lines with bars represent negative regulation while line with arrowheads represent positive regulation. Translation inhibition of PKA-C is regulated by PUFA and this is relieved by YakA inhibition of PUFA. YakA also inhibits cell cycle either by negatively regulating promoters or by positively regulating some cell cycle inhibitor (adapted from Souza et al., 1999).

YakA has a role during growth as it regulates the cell cycle and as nutrient is depleted and starvation begins. YakA is activated or induced which decreases the

expression of vegetative genes. Subsequently repression on PKA-C mRNA by PUFA is also relieved. This leads to the activation of PKA-C, which is required for development initiation and during further development (Loomis, 1998). During the initial 4-6 h, there is around 5 fold increase in the PKA-C mRNA as well as the protein and its activity and this is an essential event for the initiation of development (Leichtling et al., 1984; Mann et al., 1992). They concluded that in response to starvation YakA is activated which represses PUFA expression and the negative control exerted on PKA-C expression is thus relieved and leads to the initiation of development. PUFA protein can also promote continued vegetative divisions. It is required at both initial and later stages of development (terminal morphogenesis into fruiting body) (Souza et al., 1999).

1.8 OBJECTIVES OF THE PRESENT STUDY

PUF proteins are the family of RNA binding proteins whose canonical function is post-transcriptional regulation. From the above literature it is clear that it plays an important role in cell division, differentiation and development. Like in case of *Drosophila* it is required for anterior-posterior patterning, maintenance of germline stem cells (GSCs) in *C. elegans*, normal development in *Arabidopsis thaliana*, aging, mitochondrial function and mating type switching in yeast etc.

Since *Dictyostelium* is a very good model system to study differentiation and development and PUF proteins are also involved in the developmental processes of many organisms. PUFA in *Dictyostelium* plays a very important role in differentiation and development (Souza et al., 1999). Five PUF proteins in *D. discoideum* have been identified which may be involved in cell-type differentiation or in transition from growth to development. Since work on PUFA has already been done so we were interested to determine the role of one of other PUFs in growth, differentiation and development of this organism. Therefore, we have proposed following objectives to accomplish our study:

- To carry out *in silico* analysis for the identification of genes encoding PUF proteins in *D. discoideum* and characterization of one selected gene. It involves phylogenetic analysis, molecular modeling of PUF protein to determine its 3-D structure. Spatio-temporal expression pattern would also be analyzed.

- To carry out the functional analysis of the identified PUF protein during growth, development and differentiation of this organism. This would be accomplished by creating both overexpressor and knock out mutant strains where all the above parameters would be analyzed.
- To explore the role of *PUF* in cell-type differentiation, spatial patterning and cell lineage tracing. Further characterization of the identified PUF protein by finding out its interacting protein partners. Since this could not be achieved we explored the role of PUF in autophagy.

2.1 INTRODUCTION

PUF proteins are the family of RNA binding proteins present in all eukaryotes, mainly involved in the regulation at post-transcriptional level of mRNA. It performs various biological functions like neurogenesis (Ye et al., 2004), morphogenesis (Wharton and Struhl, 1991; Murata and Wharton, 1995) and development of germ cells (Asaoka-Taguchi et al., 1999; Kadyrova et al., 2007) in many eukaryotic organisms. PUF proteins are characterized by the presence of PUF domain, which comprises of 8 PUF repeats present in tandem towards the C-terminal. Each repeat recognizes and binds to specific sequence present at 3' UTR of mRNA NANOS Response Elements (NREs). Each repeat binds to single base of mRNA (Zamore et al., 1997; Zamore et al., 1999). Variable numbers of PUF proteins are present in different organisms like 6 in yeast, 2 in mammals including human, and several paralogs are present in *Arabidopsis thaliana* and *C. elegans*.

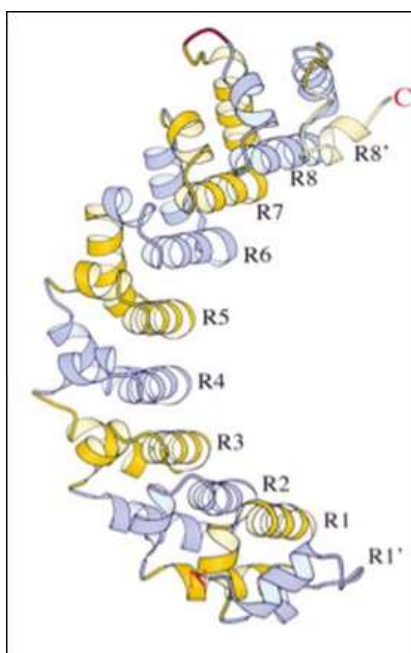


Figure 2.1: Ribbon diagram of human Pumilio1 domain, *HsPUM-HD*. Each repeat has been represented as R1, R2, R3, R4, R5, R6, R7 and R8 comprising of 3 α -helices. Each repeat is shown in alternate blue and yellow colour. N- and C-termini has been shown (adapted from Wang et al., 2001).

Wang et al. (2001) solved the crystal structure of human Pumilio1, PUM-HD at 1.9 Å resolution. They showed that 8 repeats were present in human Pumilio1 and was packed in the form of right-handed superhelix. The side chain distribution of amino acids on outer and inner surfaces of the protein explains that RNA binds to the inner surface

while the outer surface interacts with cofactors to regulate mRNA post-transcriptionally (Wang et al., 2001).

Genome of *Dictyostelium discoideum* harbors 5 *PUF* genes with id, DDB_G0279735, DDB_G0279557, DDB_G0288551, DDB_G0289987 and DDB_G0276255. Out of these DDB_G0279735 has been named as *DdPUFA* and we named the remaining *PUF* genes DDB_G0279557, DDB_G0288551, DDB_G0289987 and DDB_G0276255 as *DdPUFB*, *DdPUFC*, *DdPUFD* and *DdPUFE* respectively. All these are characterized by the presence of PUF (Pumilio) domain. *Dictyostelium PUFA* is located on Chromosome 3 on Crick strand from coordinates 2548824 to 2551966 and is about 3.14 Kb in length encompassing 4 exons interrupted with 3 introns (Figure 2.2 A and B). *Dictyostelium PUFB* is located on Chromosome 3 on Crick strand between coordinates 2250584 to 2253245 and is about 2.66 Kb in length encompassing 3 exons interrupted with 2 introns (Figure 2.2 C and D). *Dictyostelium PUFC* is located on Chromosome 5 on Watson strand from coordinates 1679413 to 1681553 and is about 2.14 Kb in length encompassing 2 exons interrupted with one intron (Figure 2.2 E and F). *Dictyostelium PUFD* is located on Chromosome 5 on Watson strand from coordinates 3515224 to 3518414 and is about 3.19 Kb in length encompassing 2 exons interrupted with one intron (Figure 2.2 G and H). *Dictyostelium PUFE* is located on Chromosome 2 on Crick strand from coordinates 6507776 to 6510379 and is about 2.60 Kb in length encompassing 2 exons interrupted with one intron (Figure 2.2 I and J).

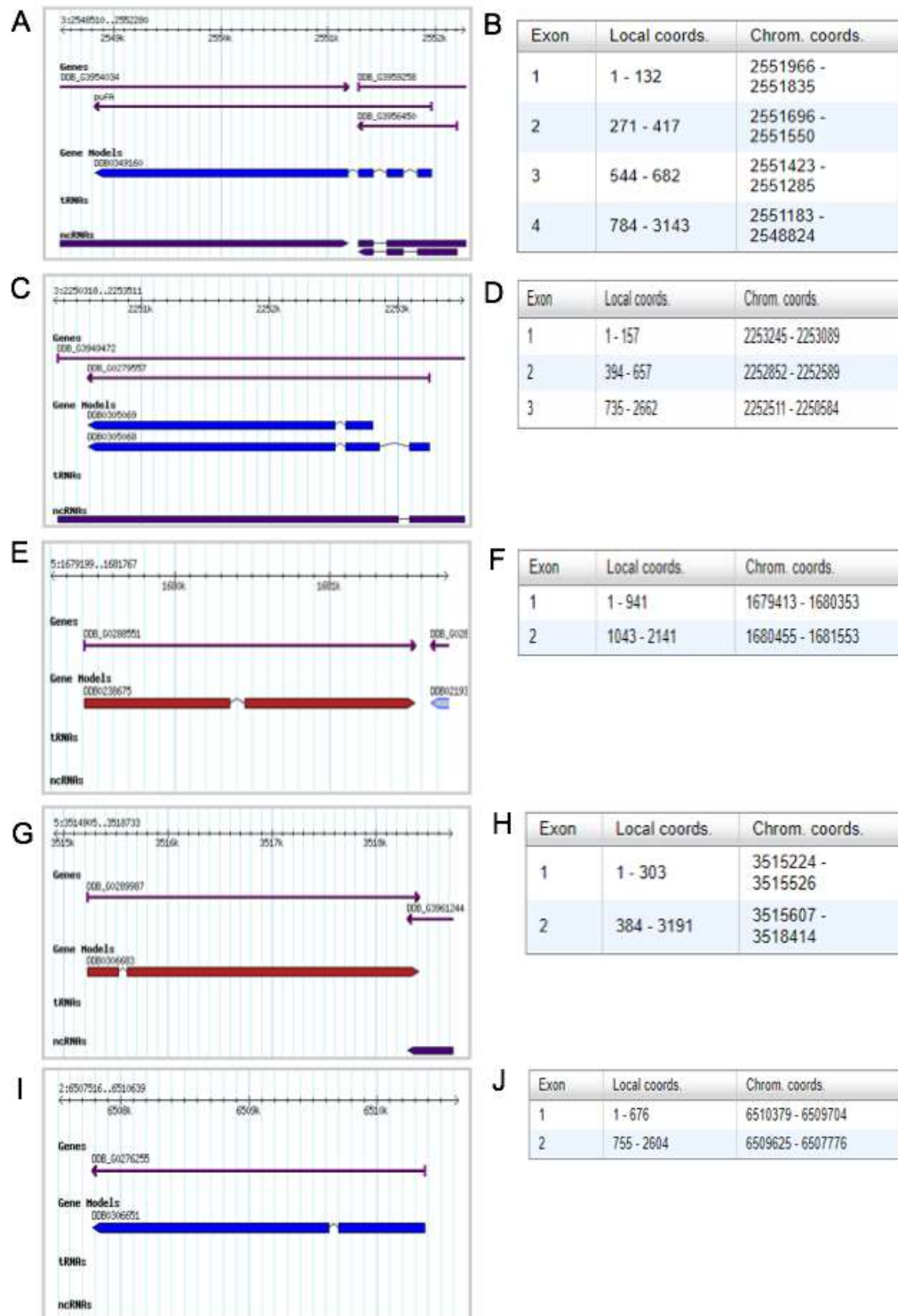


Figure 2.2: Genomic map and exonic positions of 5 *PUF* genes of *Dictyostelium discoideum*. (A) *DdPUFA* located on Chromosome 3 on Crick strand from coordinates 2548824 to 2551966 (B) *DdPUFA* comprises 4 exons and 3 introns. Exons, local and chromosomal coordinates are shown. (C) *DdPUFB* is located on Chromosome 3 on Crick strand from coordinates 2250584 to 2253245 and (D) *DdPUFB* comprises of 3 exons and 2 introns. (E) *DdPUFC* is located on

Chromosome 5 on Watson strand from coordinates 1679413 to 1681553 and (F) *DdPUFC* comprises of 2 exons and 1 intron. (G) *DdPUFD* is located on Chromosome 5 on Watson strand from coordinates 3515224 to 3518414 and (H) *DdPUFD* comprises of 2 exons and 1 intron. (I) *DdPUFE* is located on Chromosome 2 on Crick strand from coordinates 6507776 to 6510379 and (J) *DdPUFE* comprises of 2 exons and 1 intron. [<http://dictybase.org/>].

Domain structure of all the 5 PUFs were predicted from the SMART (Simple Modular Architecture Research tool; <http://SMART.embl-heidelberg.de>) tool, which helps predict and classify domains that are significantly annotated with respect to functional classes, tertiary structures, phyletic distributions and functionally important residues.

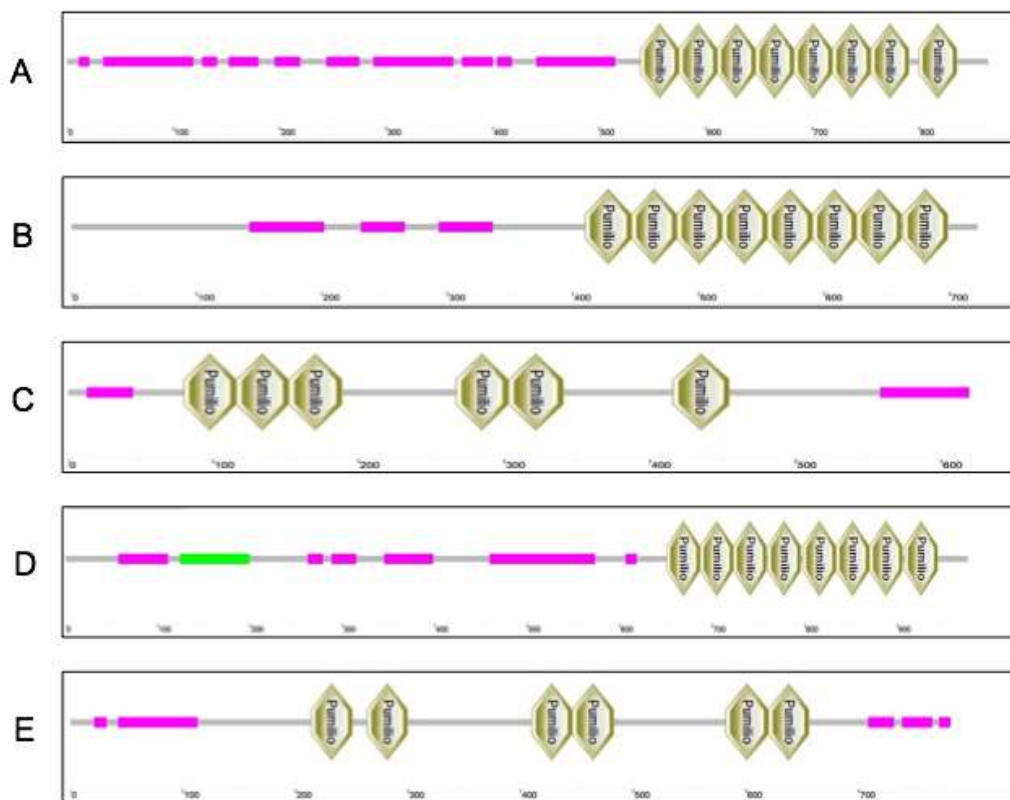


Figure 2.3: Protein domains present in the 5 PUF proteins predicted from SMART program in *D. discoideum*. (A) PUFA comprises of 8 PUF repeats ranging between 539-835 amino acids. (B) 8 PUF repeats present in PUFB ranging between 410-698 amino acids. (C) PUFC comprises of 6 PUF repeats ranging between 80-188, 267-340 and 416-454 amino acids. (D) PUFD shows the presence of 8 PUF repeats ranging between 651-943 amino acids. (E) PUFE shows the presence of 6 PUF repeats ranging between 214-299, 410-482 and 582-655 amino acids (<http://smart.embl-heidelberg.de/>).

The SMART profile of PUFA shows the presence of 8 PUF repeats (domain) present tandemly at the C-terminal from amino acid 539 to 835 (Figure 2.3 A). PUFA protein is 925 amino acids long with a molecular mass of 104.16 kDa. PUFB also shows the presence of 8 domains present tandemly at C-terminal from amino acid 410-698 (Figure 2.3 B). It comprises of 782 amino acids having molecular mass of 85.83 kDa. In case of PUFC, 6 repeats are present which are not arranged tandemly. 3 repeats are present at the N-terminal followed by 2 repeats, which is then followed by a single repeat (Figure 2.3 C). It comprises of 679 amino acids having molecular mass of 77.72 kDa. PUFD shows the presence of 8 domains present tandemly at the C-terminal from amino acid 651-943 (Figure 2.3 D). It comprises of 1036 amino acids having molecular mass of 118.01 kDa. While PUF E shows the presence of 6 domains, which are not present tandemly, rather they are present in a group of two (Figure 2.3 E). It comprises of 841 amino acids having molecular weight of 95.96 kDa.

As discussed in the previous chapter, PUF proteins are involved in many biological processes like cell division, differentiation and development. Like in case of *Drosophila* it is required for anterior-posterior patterning, maintenance of germline stem cells (GSCs) in *C. elegans*, normal development in *Arabidopsis thaliana*, aging, mitochondrial function and mating type switching in yeast etc. PUFA in *Dictyostelium* plays a very important role in differentiation and development. So we were interested to know the role of other PUFs, in particular PUFB of *Dictyostelium*. In this chapter we have carried out bioinformatic analyses of all the 5 PUF proteins, which includes phylogenetic analysis on the basis of sequence homology of PUF proteins in different organisms. Spatial and temporal expression pattern of *PUFB* mRNA was analyzed through semi-quantitative RT-PCR and *in situ* hybridization.

2.2 OBJECTIVES OF THE PRESENT STUDY

- *In silico* analysis for the identification of *Dictyostelium* PUF proteins by performing homology search, sequence alignment and phylogenetic analysis.
- Structural analysis and molecular dynamics simulation of 5 PUF proteins.
- To carry out the spatio-temporal mRNA expression pattern of *PUFB* during development of *Dictyostelium* using semi-quantitative RT-PCR and *in situ* hybridization.

2.3 MATERIALS AND METHODS

2.3.1 Homology search, domain analyses and phylogenetic analyses

Protein sequences of all the 5 PUF proteins were obtained from dictyBase server (www.dictybase.org/). NCBI (National centre for biotechnology information) (<http://blast.ncbi.nlm.nih.gov/Blast.cgi>) server was used to perform protein BLAST. By using BLASTp (Basic local alignment search tool for protein sequences) (<https://blast.ncbi.nlm.nih.gov/Blast.cgi?PROGRAM=blastp>) the percentage homology of individual PUF protein from different species was analyzed. Top scoring hit sequences from various organisms obtained by BLAST were downloaded and multiple sequence alignment was performed using ClustalW 2.0 at the EBI server (<http://www.ebi.ac.uk/tools/clustalw2>). Phylogenetic analysis was performed from the amino acid sequences from approximately 20 organisms ranging from lower to higher eukaryotes with PHYLIP (Phylogeny Inference Package) (Felsenstein, 1993) that help construct the phylogenetic tree with maximum likelihood (Guindon and Gascuel, 2003; Guindon et al., 2005) and neighbour joining (NJ) with replication of 1000 bootstrapp. In PHYLIP, MUSCLE (Edgar, 2004), a-log expectation software (version 3.7) was taken for multiple sequence comparison to perform multiple protein sequence alignment. Consensus tree with bootstrap values was generated using PHYLIP program and TreeDyn was used for visualization and re-rooting of the tree (<http://www.phylogeny.fr>) (Dereeper et al., 2008).

2.3.2 *in silico* analysis of the promoters of 5 PUF genes

About 1000 bp upstream nucleotide sequences from the start codon of all the 5 PUF genes were extracted from the dictyBase server and uploaded in MEME (Bailey et al., 2009) suite. It predicts motifs from MEME (Multiple EM for Motif Elicitation) programme using default parameters. It represents all the motif consensus sequences as sequence logos where the height of each letter is proportional to its frequency and sorted according to the most common residue. Sequence logo is used for determining the relative frequency of the residues and information content in a particular sequence motif (Schneider and Stephens, 1990). Motif sequences were downloaded and sequences with better p-values were used for further processes.

2.3.3 Structure deduction and Molecular Dynamics (MD) simulation protocol

Protein sequences of PUFA (DDB_G0279735), PUFB (DDB_G0279557), PUFC (DDB_G0288551), PUFD (DDB_G0289987) and PUFE (DDB_G0276255) were retrieved from dictyBase (<http://dictybase.org/>). I-TASSER (Iterative Threading/ASSEMBLY/Refinement) program (Roy et al., 2010; Yang and Zhang, 2015) makes use of the primary sequence to predict the secondary structure and help search the PDB library (Protein Data Bank) (Rose et al., 2010) of experimental curated protein structures. Further, using the cluster of 8 threading programs suitable templates were searched. Model quality and B-factors were checked by employing the ResQ program in I-TASSER. C- and the TM- scores are the two criteria, which are used to examine the quality of generated models by I-TASSER. Based on the significance of the threading alignments and the convergence of the I-TASSER simulations, the C-score was calculated. Its value should be in the range of -5 to 2, higher value indicates better quality of model. Structural similarities between the native structure and the predicted model are then measured by the TM score. Value >0.5 indicates protein model with correct global topology. All the predicted 3D models were optimized by molecular dynamics (MD) simulation for nearly 40 ns production run. Simulations were performed in GROMACS 5.0 (Groningen Machine for Chemical Simulation) (Van Der Spoel et al., 2005). Quality assurance was checked by *g_rms*, *g_rmsf*, *g_gyrate* modules of GROMACS. Structural validation of the protein was done by analyzing phi/psi distribution in Ramachandran plot with the help of SAVES (<http://services.mbi.ucla.edu/SAVES/>).

2.3.4 Culture of *Dictyostelium* cells

Fresh spores were germinated and used for all the experiments of growth, development and viability. HL5 media is a rich axenic growth medium, which was used to grow *D. discoideum* cells at 22°C in 90 mm petri plates. For primary culture cells were inoculated from the petri-plates into flasks and incubated at 22°C, under shaken conditions at 120 rpm until the cells reached log phase (density of $2.5\text{-}5 \times 10^6$ cells mL⁻¹).

2.3.5 Growth and development of *D. discoideum* cells

Wild type Ax2 (axenic strain) cells were grown and maintained at 22°C in HL5 media in 90 mm petri-plates. For further experiments, large scale culture was inoculated by diluting cells taken from petri-plates into fresh HL5 media in flasks and was allowed to grow at 22°C under shaken conditions till the log phase was reached. For development,

cells were washed twice with ice-cold 1x KK2 buffer and spotted (15-20 μL) on non-nutrient agar (NNA) plates at a density of 5×10^7 cells mL^{-1} . Plated cells were kept at 4°C for 4-6 h for synchronization followed by incubation at 22°C for development.

2.3.6 Temporal *DdPUFB* mRNA expression pattern analysis using semi-quantitative RT PCR

RNA isolation

Log phase ($3\text{-}5 \times 10^6$ cells mL^{-1}) Ax2 cells were harvested, washed in 1x KK2 buffer and plated on NNA plates at a density of 5×10^7 cells mL^{-1} . Cells were developed synchronously and different developmental stages like vegetative, loose-aggregate, mound, slug, early culminant and late culminant samples were collected at different time points. Samples were collected in chilled 1x KK2, washed twice and lysed in 1.0 mL of TRI reagent (T9424, Sigma-Aldrich) by vortexing. Then, the samples were incubated for 5-10 minutes at room temperature (RT) followed by the addition of 200 μL chloroform, mixed and further incubated for 5 minutes at room temperature. The samples were centrifuged at 12,000 g for 15 minutes at 4°C . The aqueous phase was collected and mixed with equal volume of isopropanol and incubated for 10 minutes at room temperature. The samples were again centrifuged at 12,000 g for 15 minutes at 4°C and the final pellet was washed with 1 mL of 75% ethanol and centrifuged at 12,000 g for 5 minutes at 4°C . The pellet was air-dried and further dissolved in 50 μL diethylpyrocarbonate (DEPC; Sigma-Aldrich) treated water, subsequently treated with RNase free DNase (Qiagen) as per the manufacturer's instructions for 10 minutes at 22°C to remove any traces of genomic DNA. RNA was diluted and quantified using nanodrop spectrophotometer and its purity was checked on 1.5% (w/v) agarose gel in 0.5xTBE running buffer. The RNA samples were stored at -80°C till further use.

cDNA synthesis and PCR

cDNA synthesis was carried using the Verso cDNA synthesis kit (Catalog No. AB1453A, ThermoFisher). Reaction mix (20 μL) was prepared with 1 μg RNA from each sample mixed with 4 μL of 5x cDNA synthesis buffer, 2 μL of dNTP mix, 1 μL of oligo dT, 1 μL of RT enhancer, 1 μL of Verso enzyme mix and nuclease free water to make up the volume to 20 μL . The reaction mixture was incubated at 42°C for 30 minutes to synthesize the cDNA followed by deactivation step at 92°C for 2 minutes. cDNA was then stored at -20°C till further use.

The gene specific primer combinations were used for PCR amplification from cDNA template, which also ensures the purity of the preparation. The primer combinations used for the amplification of *PUFB* gene and *ig7* is shown below in (Table 2.1).

Oligo Name	Primer Sequence (5'--3')	Genomic position	Expected amplicon cDNA size(bp)	Expected amplicon gDNA size(bp)
<i>PufB</i> RT	FP:TAGGTGGTGGTGAATTATTCAACAACA	1481-1507	537	614
	RP:TTGGTGTTGTATTAGTAGATGTTGCTGGTG	2065-2094		
<i>ig7</i> RT	FP: TGAATTGAAGTCTGAGTAAACGG	1795-1815	723	1270
	RP: AGATAGGGACCAAACTGTCTCAC	3065-3042		

Table 2.1: Primer combinations used for the amplification of cDNA for *PUFB* and *rnIA* (*ig7*) genes. Expected amplicon sizes from cDNA and gDNA as templates are mentioned above [FP- Forward primer, RP- Reverse primer, bp- base pair]

PCR amplification for *PUFB* was carried out by initial denaturation at 98°C for 30 seconds followed by 24 cycles amplification of denaturation at 98°C for 45 seconds, primer annealing at 61.5°C for 1 minute and extension at 65°C for 1 minute. PCR amplification for *ig7* was carried out using an initial denaturation for 30 seconds at 98°C followed by amplification which was carried for 24 cycles of denaturation at 98°C for 15 seconds, primer annealing at 52°C for 45 seconds and extension at 68°C for 1 minute.

2.3.7 Spatial expression analysis of *DdPUFB* mRNA by *in situ* hybridization in multicellular structures developed

Genomic DNA isolation

Genomic DNA of *D. discoideum* (Ax2 strain) was isolated according to (Charette and Cosson, 2004) from the log phase cultures. Cells were collected by centrifugation at 3,000 rpm for 5 minutes and washed with 1x KK2. Cells were starved in 1x KK2 for 2 h at 22°C under shaken conditions at a density of approximately 1×10^8 cells mL⁻¹. Upon starvation, cells were centrifuged at 3,000 rpm for 5 minutes and resuspended in DB buffer at a density of approximately 5×10^7 cells mL⁻¹. Cell suspension was then carefully added drop-wise into the microcentrifuge tube containing 1.5 mL of RLB buffer and mixed gently. Hereafter, cells were spun down at 12,000 rpm for 10 minutes at 4°C and cell pellet was resuspended in 1.5 mL of RLB buffer and centrifuged again at 12,000

rpm for 10 minutes at 4°C. The pellet obtained was resuspended in 25 µL of RLB buffer, followed by addition of 200 µL of buffer II containing RNaseA (10 µg mL⁻¹) and incubated at 65°C for 1 h. Further, buffer I containing Proteinase K (0.2 mg mL⁻¹) was added and incubated at 37°C for 30 minutes. Hereafter, 10 µL of 5 M NaCl was added followed by phenol: chloroform (1:1) extraction step. DNA was precipitated with ethanol overnight. Next day, DNA pellet was washed with 70% ethanol, air-dried and finally dissolved in TE buffer. DNA was checked by loading 1-2 µL of it on 1% agarose gel.

in situ construct preparation

The spatial expression pattern of *PUF*B transcript was investigated using *in vitro* transcription of exonic region by cloning in commercially available pBSII SK+ (pBluescript II phagemid) vector. The desired exonic region of 997 bp (genomic position from 2541-3537 bp) was PCR amplified from Ax2 genomic DNA using the specific primer combination (Table 2.2) having restriction sites BamHI and XbaI.

Gene name	Primer sequence (5'...3')	Restriction site	Genomic position	Amplicon Size(bp)
<i>PufB</i> <i>in-situ</i>	FP:TCGCGGATCC <u>AACGTTTACTCTTCAC</u> TTGGTAACATTGGA	<i>Bam</i> HI	2541-2570	997
	RP:CTAGICTAGAGGATCACGAAGTTGGCATATTTATCTTG	<i>Xba</i> I	3510-3537	

Table 2.2: Primer combinations used for the amplification of exonic region of *PUFB* gene. The restrictions sites are underlined. The expected amplicon size is shown.

The amplicon was double digested with BamHI and XbaI enzymes and cloned directly into BamHI/XbaI sites of pBSII SK+ vector at 22°C for 16 h to give a construct as shown in Figure 2.4.

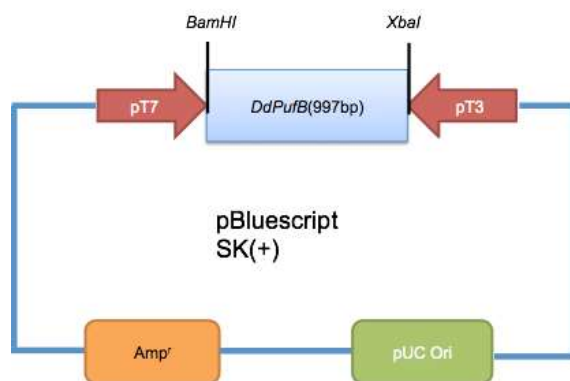


Figure 2.4: Diagrammatic representation of the cloning strategy for *in situ* hybridization of *PUFB* probe in pBSII SK+ vector. Exonic region of *PUFB* gene (~0.997 Kb) was inserted in BamHI/XbaI sites of the multiple cloning sites (mcs) of pBluescript SK+

vector. This vector contains promoters of T3 and T7 RNA polymerases adjacent to the mcs. The construct pBSII SK+ was digested with XbaI to yield template for sense probe by T3 RNA polymerase while digestion with BamHI yield template for antisense probe synthesis by T7 RNA polymerase.

The ligation products were transformed into competent *E. coli* DH5 α cells and the clones were selected on LB-agar with 100 $\mu\text{g mL}^{-1}$ ampicillin. The positive clones were confirmed by appropriate restriction digestions of the construct pBSII SK+ (*PUF*B probe).

Probe preparation

The construct pBSII SK+ was digested with BamHI to yield template for antisense probe synthesis by T3 RNA polymerase; while digestion with XbaI to yield template for sense probe synthesis by T7 RNA polymerase. For probe synthesis 1.0 μg of the linearized construct, 1x digoxigenin RNA labelling mix, 1x transcription buffer, 20U RNase inhibitor, 40U RNA polymerase and DEPC water were used per 20 μL *in vitro* transcription reaction. The reaction mixture was incubated for 2 h at 37°C and further stopped by adding 0.2 M EDTA per reaction. 1.0 μL of the reaction mixture was aliquoted for checking the synthesis on 0.5% TBE agarose gel. The probes were processed for hydrolysis by using 1x carbonate buffer and incubated for 15 minutes at 65°C. The hydrolyzed probes were precipitated using 1/10th volume of 5 M lithium chloride and 2.5 volume absolute ethanol and kept at -80°C for overnight. Hence after, the ethanol was washed off (centrifuged at 10,000 rpm for 20 minutes at 4°C) and pellet was air dried. The pellet was dissolved in 100 μL of DEPEC water and kept for 30 minutes at 37°C. The probe synthesized was checked on 0.5% TBE agarose gel and stored in -80°C until further use.

In situ hybridization

In situ hybridization was done using the commercial available kit from Roche as per the manufacturer's instructions. Ax2 cells were developed ($\sim 1 \times 10^7$ cells mL^{-1}) asynchronously on dialysis membrane and collected with 1x PBS on sterile 24 well tissue culture plates. Different multicellular structures were fixed in 100% methanol and 4% paraformaldehyde. Methanol was removed and structures were kept in 4% paraformaldehyde for 2 h and 30 minutes at room temperature. Structures were washed thrice with 1x PBS and treated with proteinase K (20 $\mu\text{g mL}^{-1}$) in PBS for 50-60 minutes

at 60°C. Further, samples were fixed with 4% paraformaldehyde for 20 minutes at room temperature, washed thrice with 1x PBS and kept in prehybridization buffer for overnight at 50°C. This was followed by hybridization with 0.5 $\mu\text{g mL}^{-1}$ sense or antisense probe for 20 h at 50°C. After washing out the excess probe with 2x SSC, 1x SSC, 0.5x SSC and 0.1x SSC subsequently for 30 minutes at 50°C, structures were treated with 0.2% blocking solution. The structures were treated with 1:1,000 diluted anti-digoxigenin antibody coupled to alkaline phosphatase in PBT containing 0.2% blocking reagent at 4°C overnight. Subsequently, the structures were washed in PBT and phosphatase buffer. Structures were then stained with 340 $\mu\text{g mL}^{-1}$ NBT and 174 $\mu\text{g mL}^{-1}$ BCIP in phosphatase buffer in dark at room temperature till the satisfactory colour was developed. The reaction was stopped with multiple washes of 1xPBS and multicellular structures were photographed under stereomicroscope (Olympus SZ61). Localization of antisense probes was used to determine the spatial expression of *PUFB* in multicellular structures. *In situ* hybridization reaction with sense probe acted as negative control.

2.3.8 Bacterial transformation

Ligation process includes 16 h of incubation at 22°C. The ligation product was mixed with 100 μL of DH5 α competent cells of *E. coli* strain, prepared by TSS method (Chung et al., 1989) by gentle tapping. The cells were then incubated for 20 minutes on ice, followed with a heat shock for 90 seconds at 42°C and then snap cooled on ice for 5 minutes. Cells were then allowed to recover from heat shock by incubation for 1 h at 37°C under shaken conditions. The cells were spread on LB agar plates using glass spreader containing appropriate selection pressure, followed by incubation for 12-16 h at 37°C. The colonies grown were picked and screened for positive transformants by various combinations of restriction digestions.

2.3.9 Statistical analyses

The statistical analyses were performed (mean, standard deviation and standard error) and values were plotted using Microsoft Excel-2013 and GraphPad Prism 6.0. Levels of significance were calculated using Student's t-test and p-values of less than 0.05 were considered as significant.

2.4 RESULTS AND DISCUSSION

2.4.1 Phylogenetic analysis of PUF proteins

Protein sequence of *DdPUFA* (DDB_G0279735), *DdPUFB* (DDB_G0279557), *DdPUFC* (DDB_G0288551), *DdPUFD* (DDB_G0289987) and *DdPUFE* (DDB_G0276255) were taken from dictyBase server and BLASTp tool of NCBI that uses BLOSUM62 with default parameters restricting the target sequence prediction to 1000 was used for sequence alignment of individual PUF protein. Top scoring sequences from BLAST program above a certain threshold represented as e-values (expected value) for all the organisms covering prokaryotes and eukaryotes were selected for multiple sequence alignment. For the phylogenetic analyses, amino acid sequences in fasta format were prepared and multiple sequence alignment (MSA) was performed by using MUSCLE in phylogeny.fr server.

The phylogenetic tree was created in phylogeny.fr server using seqboot with 1000 bootstrapped datasets for protein sequence alignments. The distance between protein sequences can be calculated using Protdist, which uses Jones Taylor Thornton matrix for amino acid substitution. Final tree for individual PUF was predicted from mega software as shown in Figure 2.5 to Figure 2.9

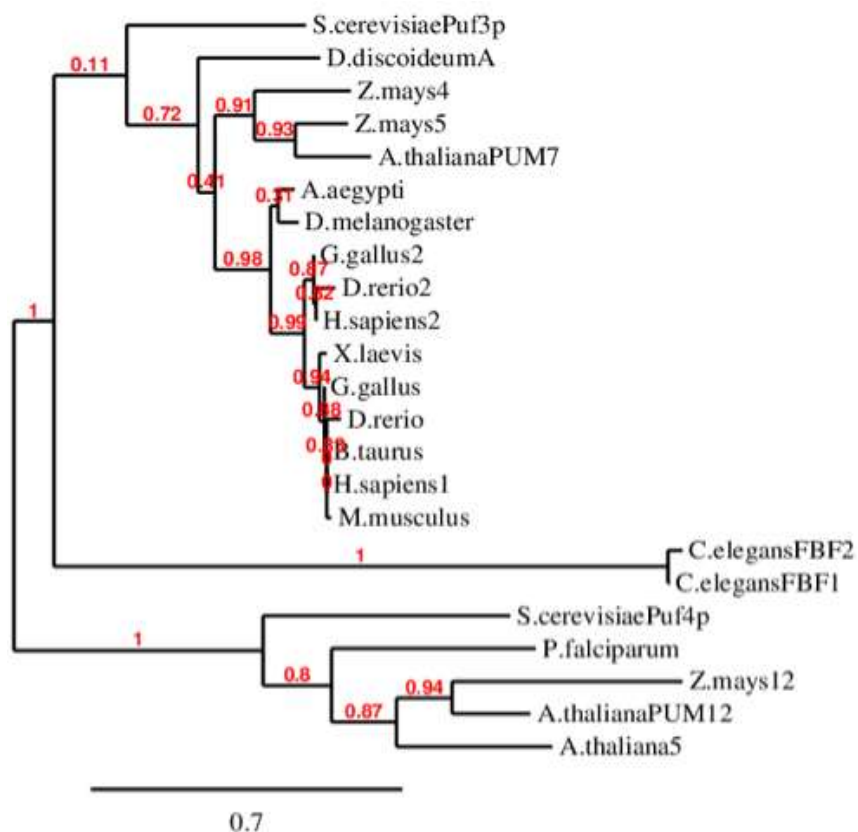


Figure 2.5: Phylogenetic tree of PUFA. A CLUSTALW2 alignment of PUFA full-length protein sequences from different organisms was used to create a bootstrap neighbour-joining (N-J) tree. Organisms used for building the tree were *Dictyostelium discoideum*, *Zea mays*, *Arabidopsis thaliana*, *Saccharomyces cerevisiae*, *Drosophila melanogaster*, *Caenorhabditis elegans*, *Plasmodium falciparum*, *Aedes aegypti*, *Gallus gallus*, *Danio rerio*, *Homo sapien*, *Xenopus laevis*, *Mus musculus* and *Bos Taurus*.

From the phylogenetic tree, PUFA of *D. discoideum* appears closer to plants and yeast. It shows more closeness with some PUF proteins of plants like *Zea mays4*, *Zea mays5*, *Arabidopsis thaliana* PUM7 and yeast PUF protein *Saccharomyces cerevisiae* PUF3p. It is relatively closer to Pumilio of *Drosophila melanogaster* than that of mammals like human, while *Caenorhabditis elegans* PUF proteins, FBF-1 and FBF-2 are present on a separate clade showing *D. discoideum* PUFA is evolutionarily farther to *C. elegans* PUF proteins (Figure 2.5).

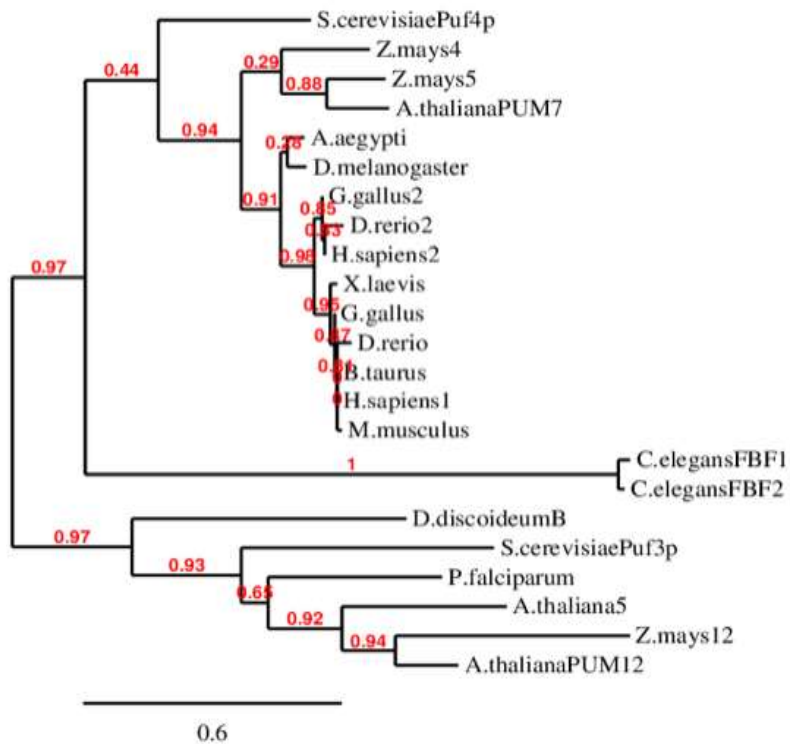


Figure 2.6: Phylogenetic tree of PUF_B. A CLUSTALW2 alignment of PUF_B full-length protein sequences from different organisms was used to create a bootstrap neighbour-joining (N-J) tree. Organisms used for building the tree were *Dictyostelium discoideum*, *Zea mays*, *Arabidopsis thaliana*, *Saccharomyces cerevisiae*, *Drosophila melanogaster*, *Caenorhabditis elegans*, *Plasmodium falciparum*, *Aedes aegypti*, *Gallus gallus*, *Danio rerio*, *Homo sapien*, *Xenopus laevis*, *Mus musculus* and *Bos Taurus*.

Phylogenetic analysis of *Dictyostelium* PUF_B was observed to be evolutionarily closer to the yeast PUF protein, *Saccharomyces cerevisiae* PUF3p, *Plasmodium falciparum* PUF and some PUF proteins from plants like *Arabidopsis thaliana* PUM5, PUM12 and *Zea mays*12. *Dd*PUF_B is observed to be relatively closer to *C. elegans* PUF proteins, FBF-1 and FBF-2 rather than the animals including mammals like humans as they are present on a separate clade (Figure 2.6).

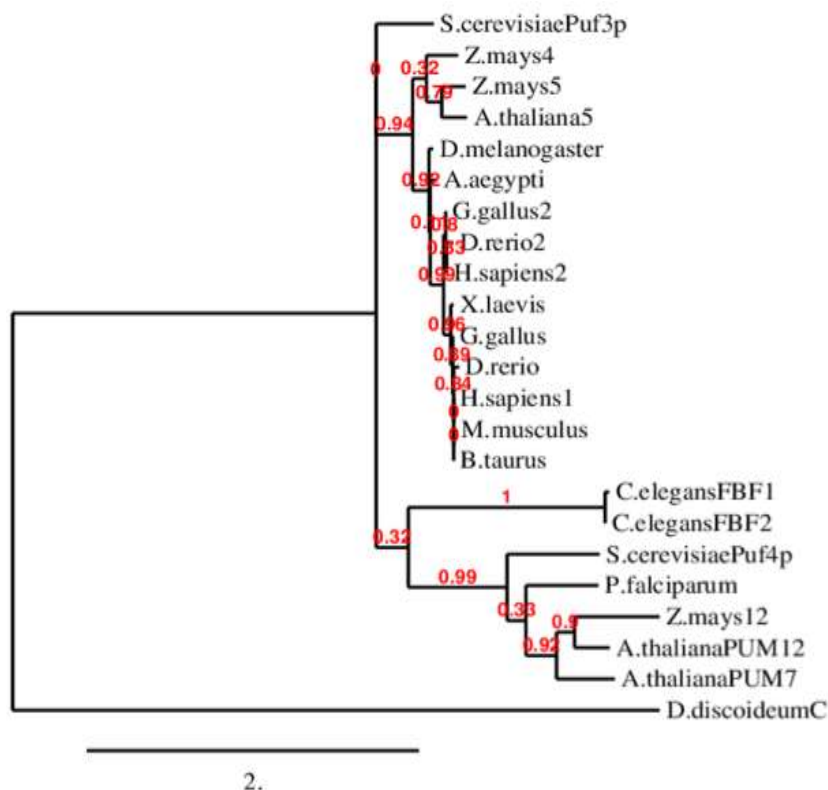


Figure 2.7: **Phylogenetic tree of PUF.** A CLUSTALW2 alignment of PUF full-length protein sequences from different organisms was used to create a bootstrap neighbour-joining (N-J) tree. Organisms used for building the tree were *Dictyostelium discoideum*, *Zea mays*, *Arabidopsis thaliana*, *Saccharomyces cerevisiae*, *Drosophila melanogaster*, *Caenorhabditis elegans*, *Plasmodium falciparum*, *Aedes aegypti*, *Gallus gallus*, *Danio rerio*, *Homo sapiens*, *Xenopus laevis*, *Mus musculus* and *Bos Taurus*.

DdPUFC protein is present on a separate clade than the PUF proteins of plants, animals including mammals, flies, nematodes and yeast. It is present as an out-group, which could be because it has 6 PUF domain/repeats as opposed to 8 PUF domain/repeats that is generally present in most of the PUF proteins (Figure 2.7).

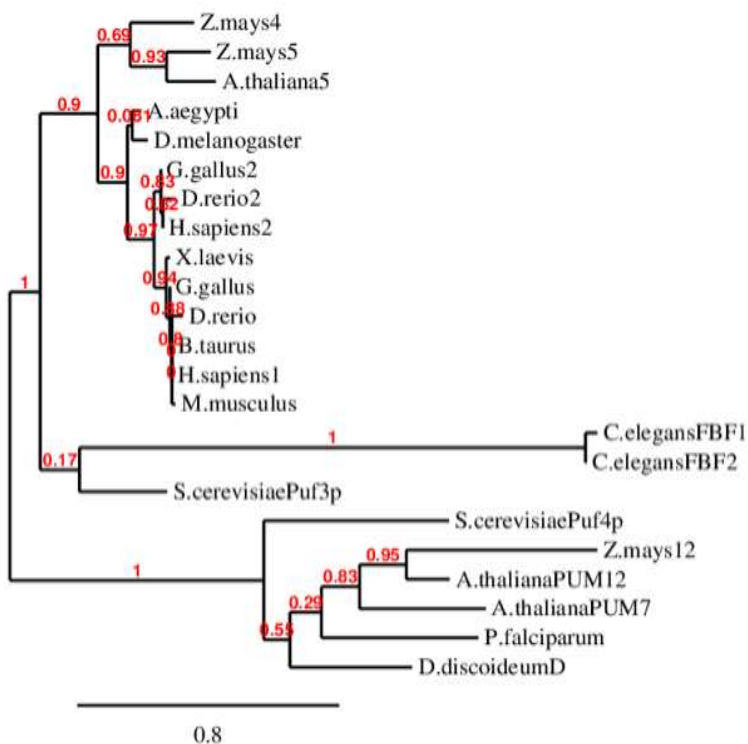


Figure 2.8: Phylogenetic tree of PUF. A CLUSTALW2 alignment of PUF full-length protein sequences from different organisms was used to create a bootstrap neighbour-joining (N-J) tree. Organisms used for building the tree were *Dictyostelium discoideum*, *Zea mays*, *Arabidopsis thaliana*, *Saccharomyces cerevisiae*, *Drosophila melanogaster*, *Caenorhabditis elegans*, *Plasmodium falciparum*, *Aedes aegypti*, *Gallus gallus*, *Danio rerio*, *Homo sapiens*, *Xenopus laevis*, *Mus musculus* and *Bos Taurus*.

From the phylogenetic tree, PUF of *Dictyostelium discoideum* appears closer to the plants and yeast. *DdPUFD* and PUF proteins of animals including mammals like human are present on separate clade. *Plasmodium falciparum* PUF, *Arabidopsis thaliana* PUM7 and PUM12, *Zea mays12* and *Saccharomyces cerevisiae* PUF4p are observed to be relatively closer to *DdPUFC* (Figure2.8).

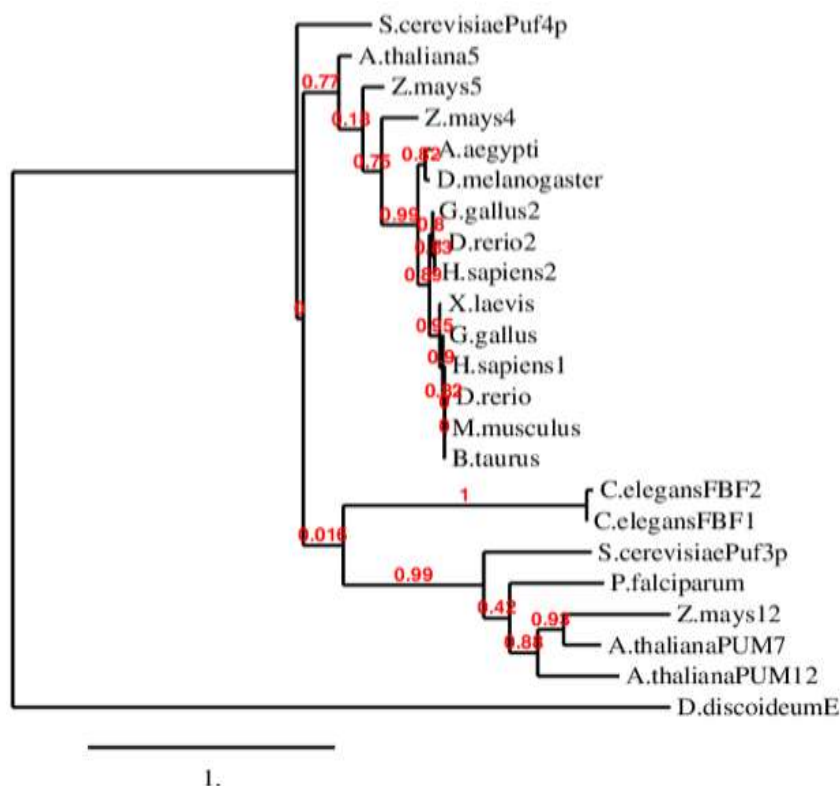


Figure 2.9: Phylogenetic tree of PUFs. A CLUSTALW2 alignment of PUF full-length protein sequences from different organisms was used to create a bootstrap neighbour-joining (N-J) tree. Organisms used for building the tree were *Dictyostelium discoideum*, *Zea mays*, *Arabidopsis thaliana*, *Saccharomyces cerevisiae*, *Drosophila melanogaster*, *Caenorhabditis elegans*, *Plasmodium falciparum*, *Aedes aegypti*, *Gallus gallus*, *Danio rerio*, *Homo sapiens*, *Xenopus laevis*, *Mus musculus* and *Bos Taurus*.

DdPUFE protein is present on a separate clade than the PUF proteins of plants, animals including mammals, flies, nematodes and yeast. It is present as an out-group, this could be because it has 6 PUF domain/repeats as opposed to 8 PUF domain/repeats which is generally present in most of the PUF proteins (Figure 2.9).

2.4.2 *In silico* analysis of the 5 PUF promoters

In silico analysis of promoters of all the 5 *Dictyostelium PUFs* was carried out by predicting the conserved sequence motifs using *PUF* sequences (1000 bp upstream of the start codon was taken).

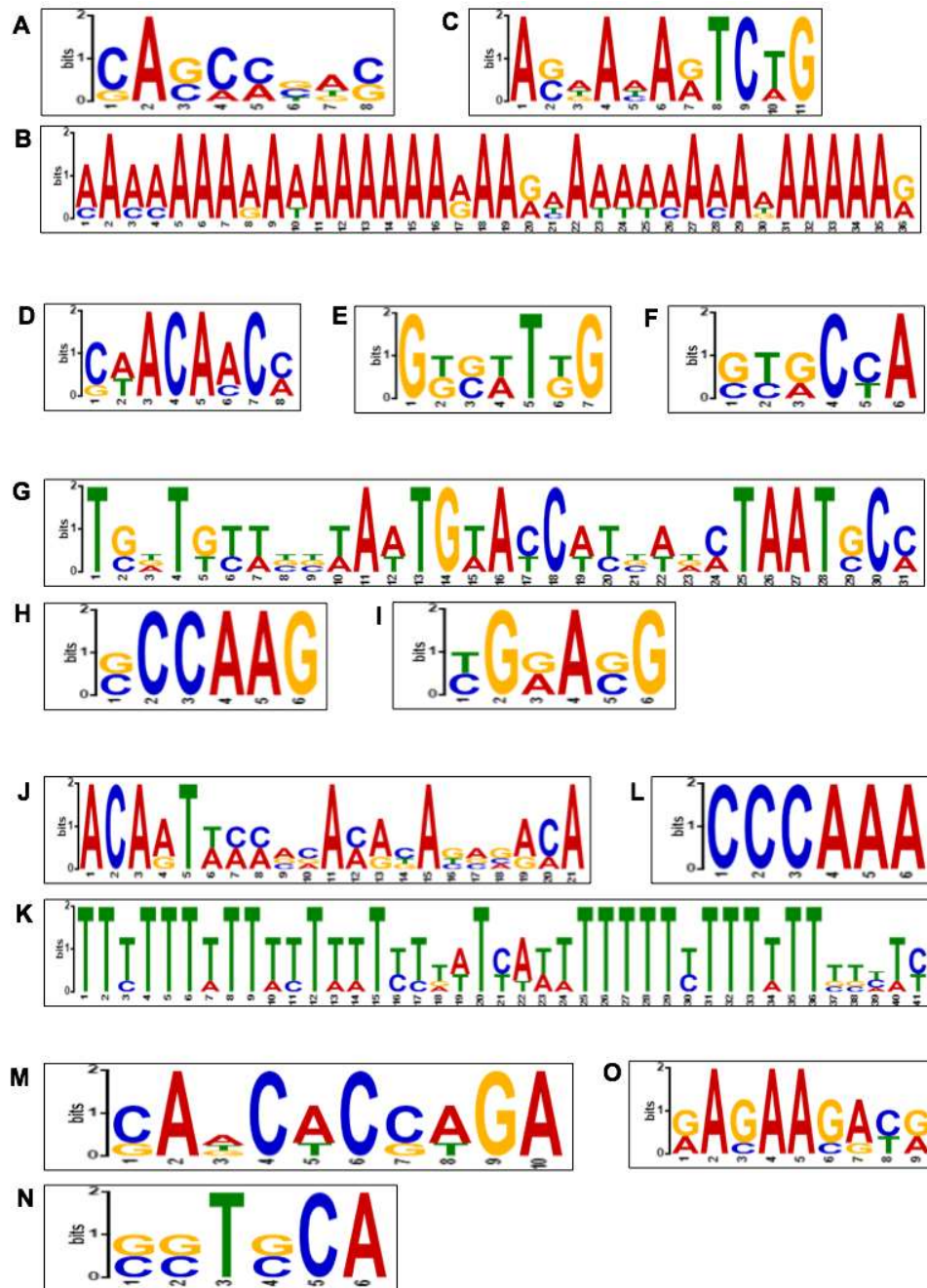


Figure 2.10: Sequence motif analysis of all the 5 *PUF* promoters of *D. discoideum*. Approximately 1000 bp upstream sequence from the start codon of *PUFA*, *PUFB*, *PUFC*, *PUFD* and *PUFE* ORF was used for predicting the conserved motifs in the MEME suite. Motifs with higher p-values were selected and sequence logos are shown as (A) motif 1, (B) motif 2 and (C) motif 3 for *PUFA*. (D) motif 1, (E) motif 2 and (F) motif 3 for *PUFB*. (G) motif 1, (H) motif 2 and (I) motif 3 for *PUFC*. (J) motif 1, (K) motif 2 and (L) motif 3 for *PUFD*. (M) motif 1, (N) motif 2 and (O) motif 3 for *PUFE*.

We observed 3 conserved motifs for *PUFA* having p-values (probability value) as $3.25e-7$, $2.15e-15$ and $3.33e-8$ on sense strand. First motif was the smallest and showed high probability of consensus sequence of A (adenine) at 2nd position with good bit score (Figure 2.10 A) while the second motif was relatively large and showed the consensus sequence of A (adenine) at many positions (Figure 2.10 B). Third motif had a consensus sequence of A (adenine), A (adenine), A (adenine), T (thymine), C (cytosine), G (guanine) at positions 1st, 4th, 6th, 8th, 9th and 11th with better bit score (Figure 2.10 C).

3 conserved motifs for *PUFB* were observed with p-values (probability value) as $5.49e-6$, $2.02e-7$ and $1.74e-6$ on sense strand. First motif showed high probability of consensus sequence of A, C, A, C at position 3rd, 4th, 5th and 7th with good bit score (Figure 2.10 D) while the second motif showed the consensus sequence of G, T, C at positions 1st, 5th, 7th with good bit score (Figure 2.10 E). Third motif is the smallest of all and had a consensus sequence of C and A at positions 4th and 6th with better bit score (Figure 2.10 F).

3 conserved motifs for *PUFC* were observed with p-values (probability value) as $9.16e-17$ on sense strand, $1.23e-5$ on antisense strand and $2.69e-5$ on sense strand. First motif is very large and show high probability of consensus sequence of T, T, A, T, G, A, C, T, A, A, T and C at position 1st, 4th, 11th, 13th, 14th, 16th, 18th, 25th, 26th, 27th, 28th and 30th with good bit score (Figure 2.10 G) while the second motif showed the consensus sequence of C, C, A, A and G at positions 2nd, 3rd, 4th, 5th, 6th with good bit score (Figure 2.10 H). Third motif had a consensus sequence of G, A and G at positions 2nd, 4th and 6th with better bit score (Figure 2.10 I).

We observed 3 conserved motifs for *PUFD* with p-values (probability value) as $3.26e-15$, $1.78e-19$ and $2.02e-5$ on sense strand. First motif is relatively large and show high probability of consensus sequence of A, C, A, T, A, A and A at position 1st, 2nd, 3rd, 5th, 7th, 11th, 15th and 21st with good bit score (Figure 2.10 J) while the second motif is the largest and show the consensus sequence of T at many positions with good bit score (Figure 2.10 K). Third motif is the smallest and had a consensus sequence of C, C, C, A, A and A bases at positions from 1st to 6th with better bit score (Figure 2.10 L).

3 conserved motifs for *PUFE* were observed having the p-values (probability value) as 1.28×10^{-7} , 1.28×10^{-4} and 4.80×10^{-6} on sense strand. First motif showed high probability of consensus sequence A, C, C, G and A at position 2nd, 4th, 6th, 9th and 10th with good bit score (Figure 2.10 M) while the second motif is the smallest of all and show the consensus sequence of T, C and A at positions 3rd, 5th and 6th with good bit score (Figure 2.10 N). Third motif had a consensus sequence of A, A and A at positions 2nd, 4th and 5th with good bit score (Figure 2.10 O). Sequences of the above motifs of each *PUF* can be used for the prediction of the transcription factor bindings to the specific motifs of the *PUF* promoter.

2.4.3 Structure modeling and Molecular Dynamics simulations of the 5 PUF proteins

To understand the structural property of all the 5 PUF proteins (PUFA, PUFB, PUFC, PUFD and PUFE) we took the bioinformatic approach. By using I-TASSER program, tertiary structures were predicted by providing protein sequences, which gave us 5 models, which were sorted on the basis of C-TM scores. We used domain sequences for the structure modeling.

C-scores and TM-scores of PUFA were -3.0 and 0.53, respectively, which indicates better quality and correct global topology. Domains of PUFA were present at the C-terminal side from amino acid 539 to 835. Tertiary structure of PUFA domain consists mainly of α -helices (Figure 2.11 A). 3D structure of PUFA domain mainly consists of 8 repeats where each repeat comprises of 3 α -helices joined together by small loops and turns. 8 repeats are named from R1 to R8, where repeat R8 is present towards the C-terminal. It is second helix of each domain, which interacts with the RNA base. All 8 repeats together form a crescent shape structure.

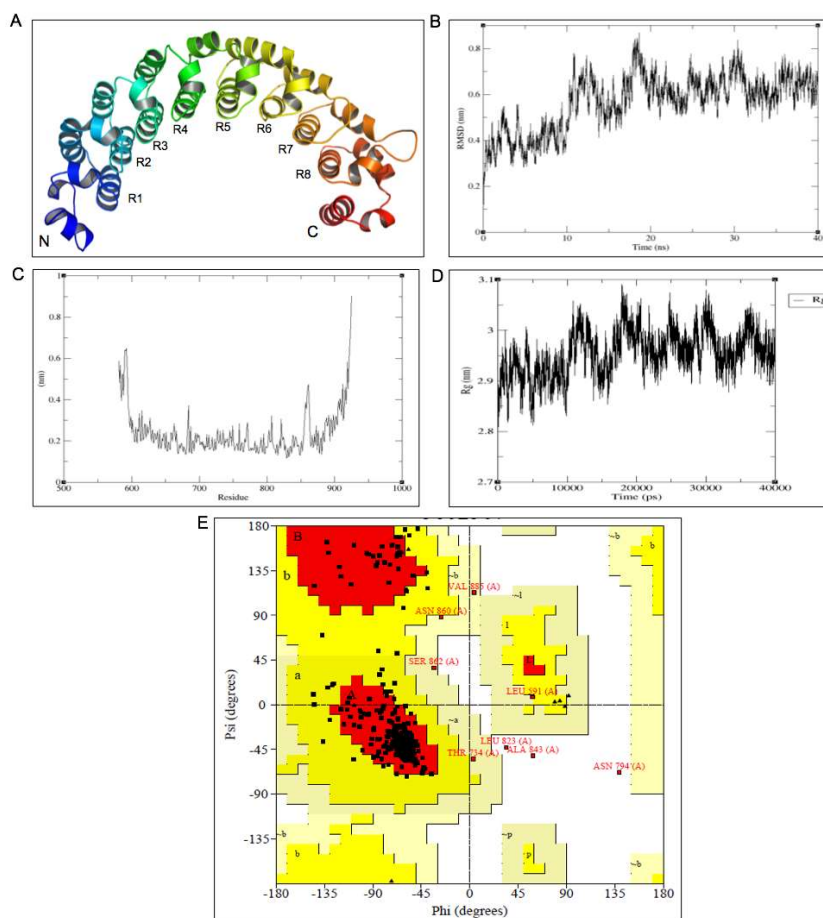


Figure 2.11: **3D structure and MD simulation of PUFA.** (A) Tertiary structure of PUFA. (B) Root mean square deviation (RMSD) of PUFA plotted against time. (C) Root mean square fluctuation (RMSF) of protein residues for *Dd*PUFA and (D) Radius of gyration (Rg) of *Dd*PUFA and (E) Ramachandran plot for structural validation of optimized model of *Dd*PUFA showing 89.2% of the residues are placed in favoured regions.

To refine the tertiary structure of the predicted PUFA model, MD simulations were carried. To statistically validate the predicted model these simulations were run in triplicate. Average values of root mean square deviation (RMSD), root mean square fluctuation (RMSF) and radius of gyration (Rg) were obtained. The RMSD plots showed the convergence achieved at 0.6 nm RMSD for PUFA after 25 ns of simulation confirming the stable behaviour and less deviation from the reference structures (Figure 2.11 B).

The mobility of different parts of protein models was accomplished by examining the RMSF for each residue. In PUFA, fluctuations occurred in the residues around 850-

870 amino acids with the average RMSF value of 0.48 nm (Figure 2.11 C). The globularity and compactness of the structure were evaluated by the radius of gyration (Rg). Radius of gyration achieved stable and steady behaviour after 20000 ps (pico second) simulation time with average value 2.95 nm (Figure 2.11 D). Overall radius of gyration for PUFA protein model was constant and stable suggesting proteins had good compactness.

Stereochemical properties of the model were evaluated through Ramachandran plot. The Ramachandran plot for the optimized *Dd*PUFA (Figure 2.11 E) model showed 89.2% of the residues are placed in favoured regions, 9.8% of the residues are placed in allowed regions and 0.9% of the residues are placed in disallowed regions. Higher proportion of protein residues are present in favoured and allowed regions (>90%) suggest that the model is stereochemically stable.

In case of PUFB, C- and TM-scores were -0.20 and 0.69, respectively, which indicates correct global topology and better quality. PUFB domains are present at the C-terminal side from amino acid 410 to 698. Tertiary structure of domain of PUFB consists mainly of α -helices (Figure 2.12 A). 3D structure of PUFB domain mainly consists of 8 repeats where each repeat comprises of 3 α -helices joined together by small loops and turns. 8 repeats are named from R1 to R8, where repeat R8 is present towards the C-terminal. All 8 repeats together form a crescent shape structure. The RMSD plots showed the convergence achieved at 0.75 nm RMSD for PUFB after 15 ns of simulation confirming the consistent behaviour and less deviation from the reference structures (Figure 2.12 B).

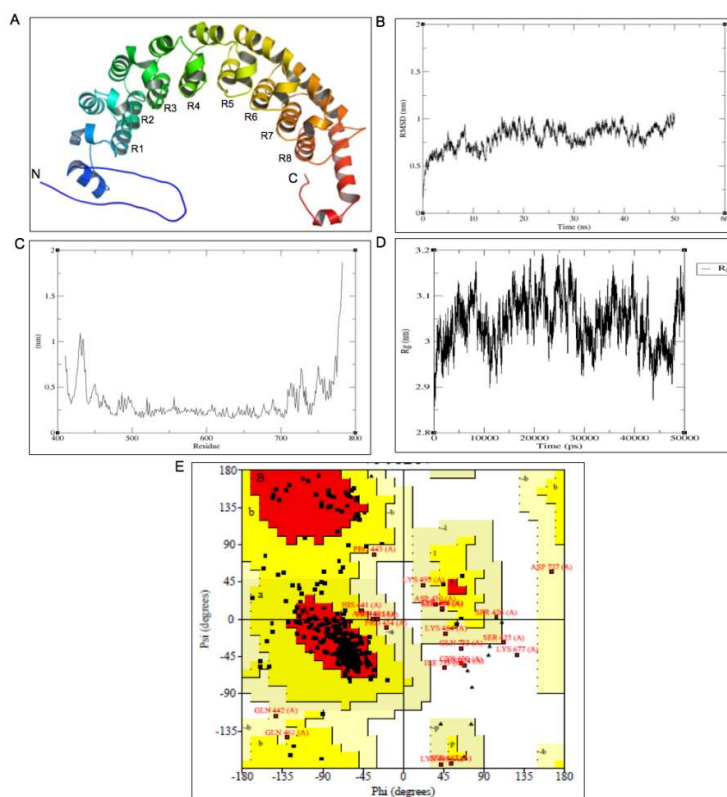


Figure 2.12: **3D structure and MD simulation of PUFB.** (A) Tertiary structure of PUFB. (B) Root mean square deviation (RMSD) of PUFB plotted against time. (C) Root mean square fluctuation (RMSF) of protein residues for *Dd*PUFB. (D) Radius of gyration (R_g) of *Dd*PUFA. (E) Ramachandran plot for structural validation of optimized model of *Dd*PUFB showing 79.2% of the residues are placed in favoured regions.

In PUFB, fluctuations occurred in the residues around 420-430 amino acids with the RMSF value of 1 nm (Figure 2.12 C). While radius of gyration achieved stable and steady behavior after 40000 ps simulation time with average value 3.05 nm (Figure 2.12 D). Overall radius of gyration for the model was slightly unstable.

The Ramachandran plot for the optimized *Dd*PUFB (Figure 2.12 E) model showed 79.2% of the residues are placed in favoured regions, 19% of the residues are placed in allowed regions and 1.8% of the residues are placed in disallowed regions. Higher proportion of protein residues are present in favoured and allowed regions (>90%) which suggest that they are stereochemically stable.

In PUFB, C- and TM-scores were -2.31 and 0.54, respectively indicating better quality with correct global topology. Domain of PUFB was present throughout the protein

length starting from N-terminal side from amino acid 80 to 454. Tertiary structure of domain of PUFC mainly is composed of α -helices (Figure 2.13 A). 3D structure of PUFC domain mainly consists of 6 repeats where each repeat comprises of 3 α -helices joined together by small loops and turns. 6 repeats are named from R1 to R6, where repeat R1 is present near the N-terminal and R6 towards the C-terminal. The RMSD plots showed the convergence achieved at 1 nm RMSD for PUFC after 15 ns of simulation confirming the consistent behaviour and less deviation from the reference structures (Figure 2.13 B). In PUFC, fluctuations occurred in the residues around 40-45 and 60-65 amino acids with the RMSF value of 1.4 and 1.5 nm respectively, both of which lies outside the domain towards C-terminal (Figure 2.13 C). While radius of gyration achieved stable and steady behaviour after 35000 ps simulation time with average value 3.6 nm (Figure 2.13 D). Overall radius of gyration for the model was stable suggesting the proteins had good compactness.

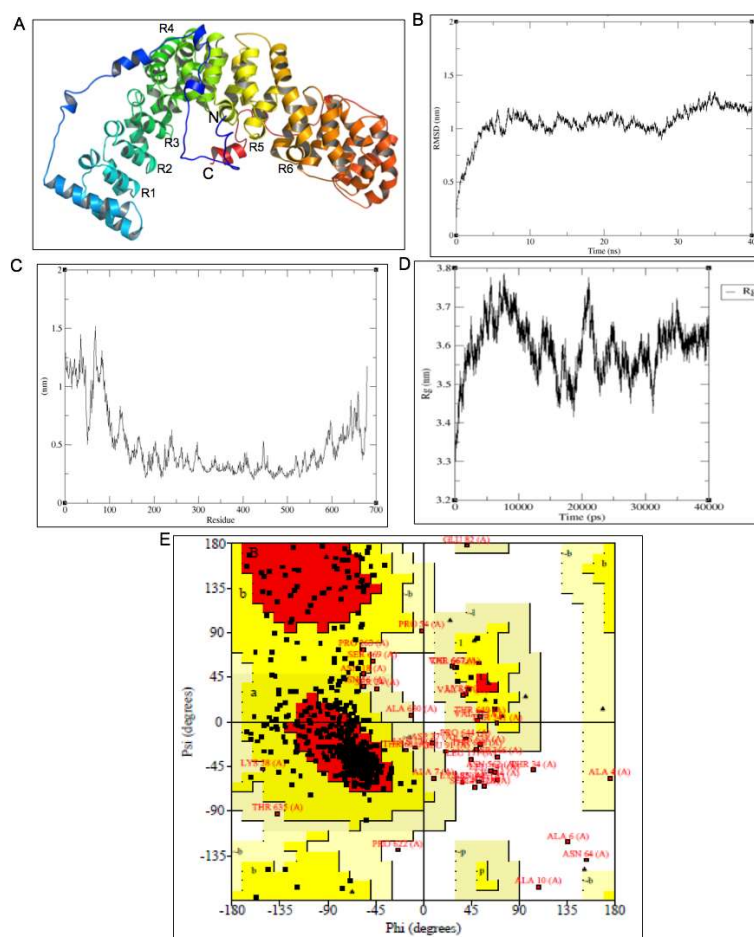


Figure 2.13: 3D structure and MD simulation of PUFC. (A) Tertiary structure of PUFC. (B) Root mean square deviation (RMSD) of PUFC plotted against time. (C) Root mean square fluctuation (RMSF) of protein residues for *Dd*PUFC. (D) Radius of

gyration (R_g) of *Dd*PUFC. (E) Ramachandran plot for structural validation of optimized model of *Dd*PUFC showing 74.4% of the residues are placed in favoured regions.

The Ramachandran plot for the optimized *Dd*PUFC (Figure 2.13 E) model showed 74.4% of the residues are placed in favoured regions, 23.5% of the residues are placed in allowed regions and 2.0% of the residues are placed in disallowed regions. Higher proportion of protein residues are present in favoured and allowed regions (>90%) which suggest that they are stereochemically stable.

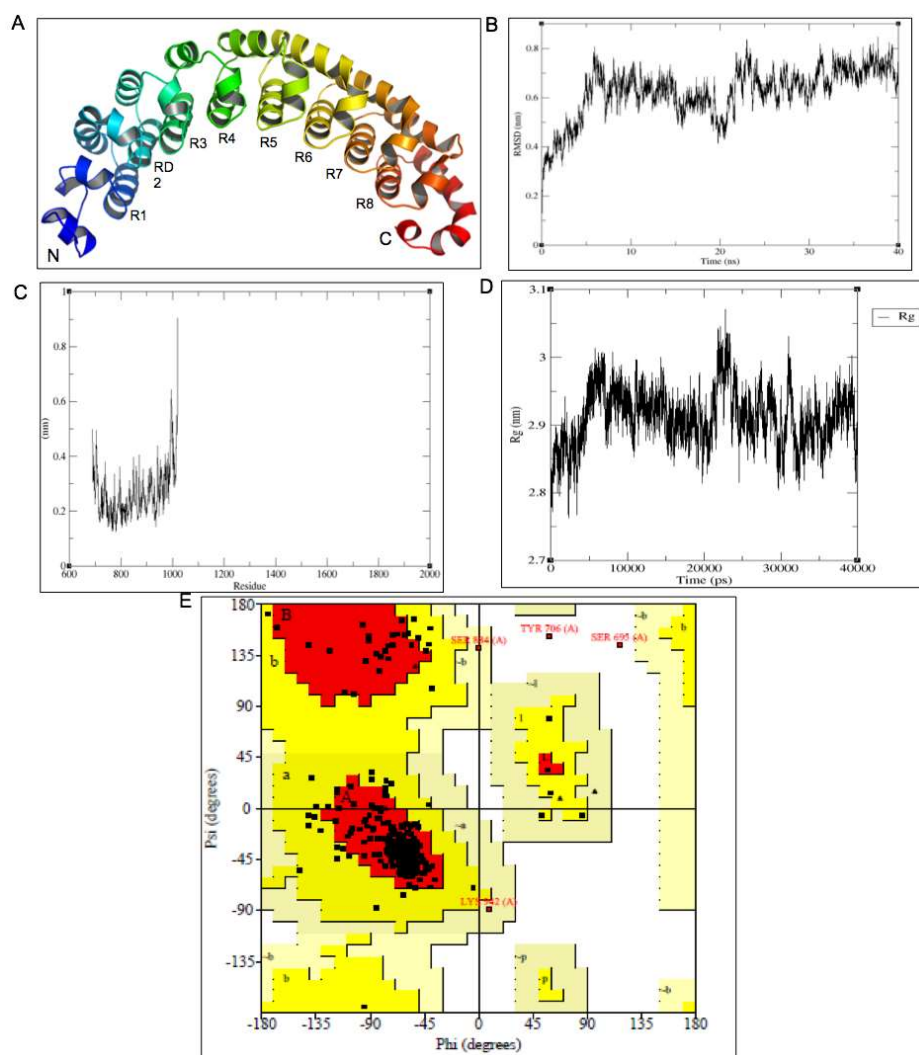


Figure 2.14: 3D structure and MD simulation of PUFd. (A) Tertiary structure of PUFd. (B) Root mean square deviation (RMSD) of PUFd plotted against time. (C) Root mean square fluctuation (RMSF) of protein residues for *Dd*PUFD. (D) Radius of gyration (R_g) of *Dd*PUFD. (E) Ramachandran plot for structural validation of optimized model of *Dd*PUFD showing 87.2% of the residues are placed in favoured regions.

In case of PUF_D, C- and TM-scores were 0.03 and 0.72, respectively, which indicate better quality and correct global topology. Domains of PUF_D are present at the C-terminal side from amino acid 651 to 943. Tertiary structure of domain of PUF_D consists mainly of α -helices (Figure 2.14 A). 3D structure of PUF_D domain mainly consists of 8 repeats where each repeat comprises of 3 α -helices joined together by small loops and turns. 8 repeats are named from R1 to R8, where repeat R8 is present towards the C-terminal and are clustered together. All 8 repeats together form a crescent shape structure. The RMSD plots showed the convergence achieved at 0.7 nm RMSD for PUF_D after 25 ns of simulation confirming the stable behaviour and less deviation from the reference structures (Figure 2.14 B). In PUF_D, there was no fluctuation present in the domain region but was outside the domain, near N and C-terminal which are flanking regions (Figure 2.14 D). The radius of gyration achieved stable and steady behaviour after 25000 ps simulation time with average value 2.92 nm (Figure 2.14 D). Overall radius of gyration for the model was low and stable indicating the proteins had better compactness.

The Ramachandran plot for the optimized *Dd*PUF_D (Figure 2.14 E) model showed 87.2% of the residues are placed in favoured regions, 12.2% of the residues are placed in allowed regions and 0.7% of the residues are placed in disallowed regions. Higher proportion of protein residues are present in favoured and allowed regions (>90%) which suggest that they are stereochemically stable.

In case of PUF_E, C- and TM-scores were -2.95 and 0.58, respectively, which indicate better quality and correct global topology. 6 Domains of PUF_E are present throughout protein length from amino acid 214 to 655 in the cluster of two each separated by loops and coils (also shown in figure 2.3 E). Tertiary structure of domain of PUF_E consists mainly of α -helices. 3D structure of PUF_E domain mainly consists of 6 repeats where each repeat comprises of 3 α -helices joined together by small loops and turns. 6 repeats are named from R1 to R6 (Figure 2.15 A), where repeat R6 is present towards the C-terminal. All 6 repeats together form a crescent shape structure. The RMSD plots showed the convergence achieved at 0.8nm RMSD for PUF_E after 30ns of simulation confirming the consistent behaviour and less deviation from the reference structures (Figure 2.15 B). In PUF_E, no fluctuations occurred in the domain region but only at C-terminal flanking region (Figure 2.15 C).

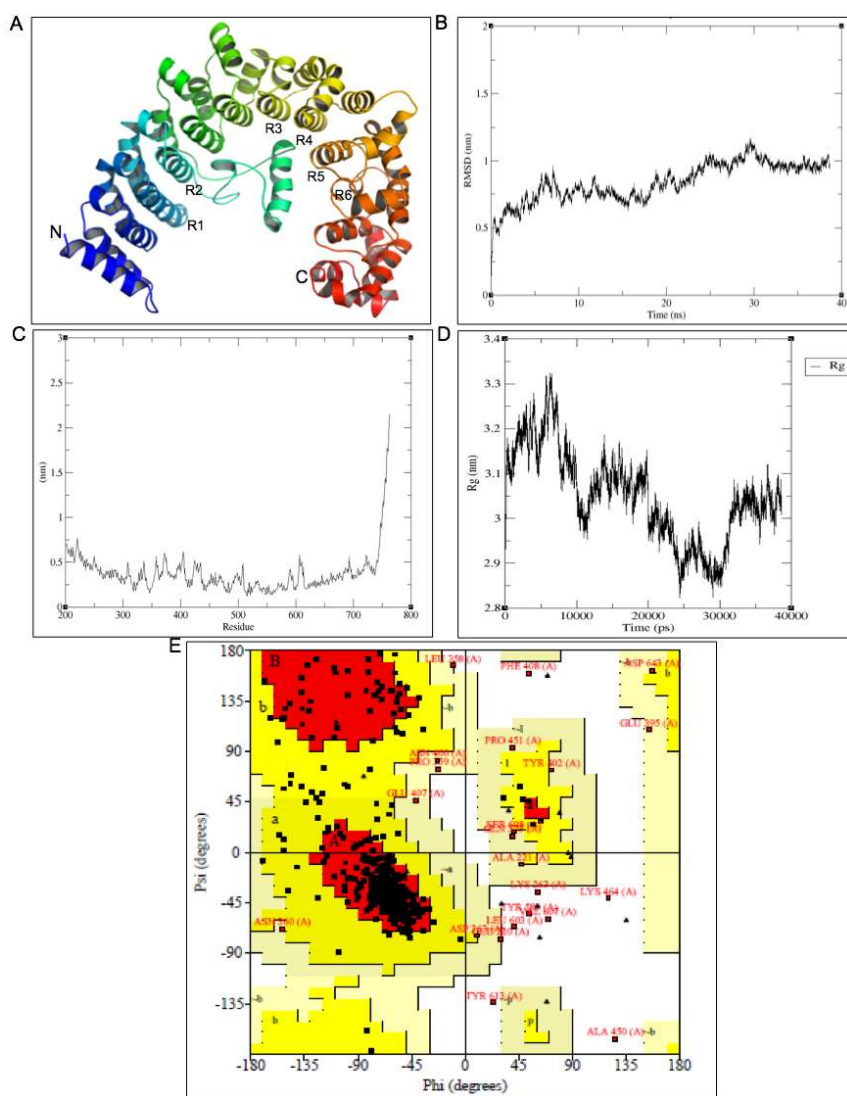


Figure 2.15: 3D structure and MD simulation of PUF6. (A) Tertiary structure of PUF6. (B) Root mean square deviation (RMSD) of PUF6 plotted against time. (C) Root mean square fluctuation (RMSF) of protein residues for *Dd*PUF6. (D) Radius of gyration (Rg) of *Dd*PUF6. (E) Ramachandran plot for structural validation of optimized model of *Dd*PUF6 showing 84.9% of the residues are placed in favoured regions.

While radius of gyration achieved stable and steady behaviour after 25000 ps (picosecond) simulation time with average value 2.92 nm (Figure 2.15 D). Overall radius of gyration for the model was good indicating the proteins had better globularity. The Ramachandran plot for the optimized *Dd*PUF6 (Figure 2.15 E) model showed 84.9% of the residues are placed in favoured regions, 13.5% of the residues are placed in allowed regions and 1.6% of the residues are placed in disallowed regions. Higher proportion of

protein residues are present in favoured and allowed regions (>90%) which suggest that they are stereochemically stable.

2.4.4 Temporal mRNA expression pattern of PUFB by RT-PCR

The temporal mRNA expression pattern of *PUFB* was determined by performing reverse transcriptase PCR (RT-PCR). RNA was isolated from samples collected at different time-points and various developmental stages and cDNA were prepared. The gene specific primer combinations as shown in Table 2.1 were used for the amplification of respective cDNAs. *rnlA* (mitochondrial large subunit rRNA, also referred as *ig7*), a constitutively expressing gene was used as an internal control (Hopper et al., 1993). PCR amplifications at 24 cycles were done for both *PUFB* and *ig7* genes. The expression pattern of both the transcript was quantified by densitometry analysis using AlphaImager software from Alphainotech. The relative expression of *PUFB* transcript as compared to *ig7* transcript was plotted at each plotted at each time point and stage wise.

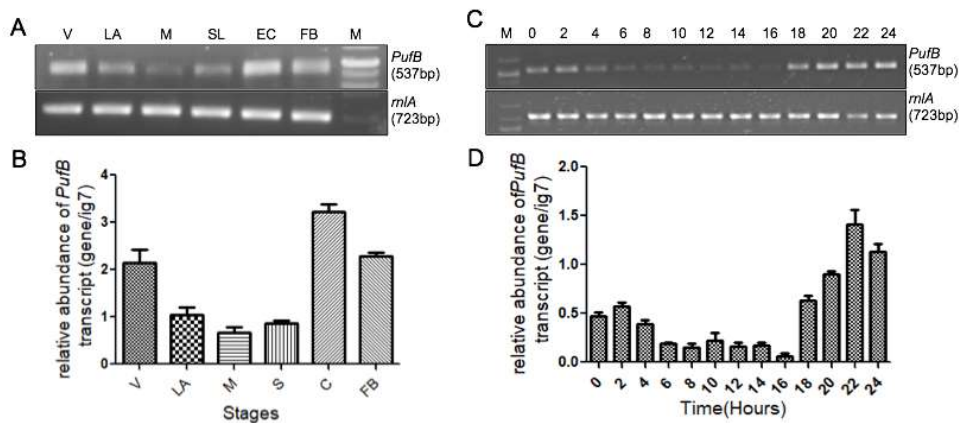


Figure 2.16: Temporal expression pattern of *PUFB* transcript during development. (A) RT-PCR gel picture of *PUFB* and *rnlA* (*ig7*) using cDNA of different development stages; V-vegetative cells, LA-loose aggregate, M-mound, SL-Slug, EC-early culminant and FB-fruited body. (B) Relative abundance of *PUFB* transcript to *rnlA* (*ig7*) transcript at different stages of development. (C) Temporal expression pattern of *PUFB* and *rnlA* (*ig7*) by RT-PCR using cDNA samples at various time-points of development. (D) Relative abundance of *PUFB* to *rnlA* transcript at various time-points [M-DNA marker lane; n=4].

The RT-PCR analysis showed that *PUFB* mRNA was present throughout the growth and development (Figure 2.16). The maximum expression was observed in the early culminant while minimum expression was found in mound and slug stage. Initially its expression is high in vegetative stage then its expression decreases and after slug its

expression reaches maximum in early culminant thereafter expression decreases in fruiting body. mRNA expression pattern suggests that it may be required both during cell proliferation (vegetative stage) as well as during the terminal differentiation.

2.4.5 Spatial mRNA expression pattern analysis of *PUFB* by *in situ* hybridization

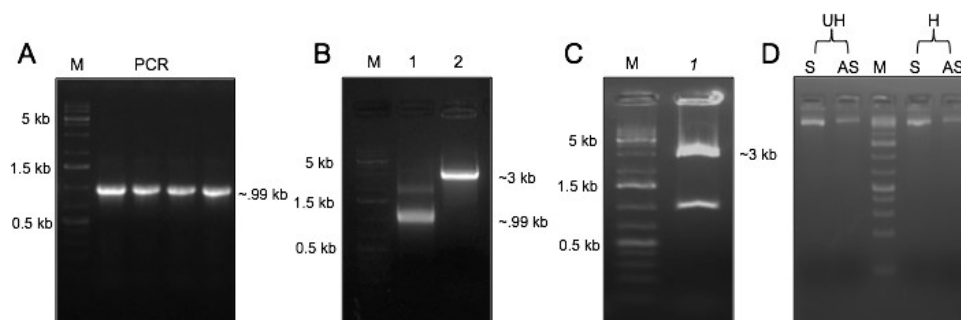


Figure 2.17: Cloning for *in situ* hybridization studies. (A) PCR amplification of ~0.997 Kb genomic region for the preparation of probe. (B) Restriction digestion of *PUFB* PCR product (Lane 1) and pBSII SK+ vector (Lane 2) with BamHI/XbaI. (C) Confirmation of *in situ* positive clone by restriction digestion yielded 3.0 Kb vector backbone and a ~0.997 Kb insert. (D) The unhydrolysed (UH) and hydrolysed (H) product of sense (S) and antisense (AS) probe. [M- DNA marker, PCR- Polymerase Chain Reaction].

Spatial mRNA expression pattern of *PUFB* was analysed by performing whole mount *in situ* hybridization. The exonic region (0.997kb) of *PUFB* was amplified (Figure 2.17 A) followed by restriction digestion (Figure 2.17 B) and cloned in to pBSII SK+ vector (Figure 2.17 C). Linearized vector was used as a template for RNA probes synthesis for in-vitro *invitro* transcription. T3 and T7 promoters were used for antisense and sense probe preparations, respectively. RNA fragments of smaller size were obtained by hydrolysing both anti-sense and sense probes (Figure 2.17 D). Antisense probe was used for hybridization in multicellular structure while sense probe was used as an internal control. To carry out the *in situ* hybridization wild type Ax2 cells were developed on membrane to collect the different stages of *Dictyostelium*. Further these structures were hybridized with probes to examine the expression pattern.

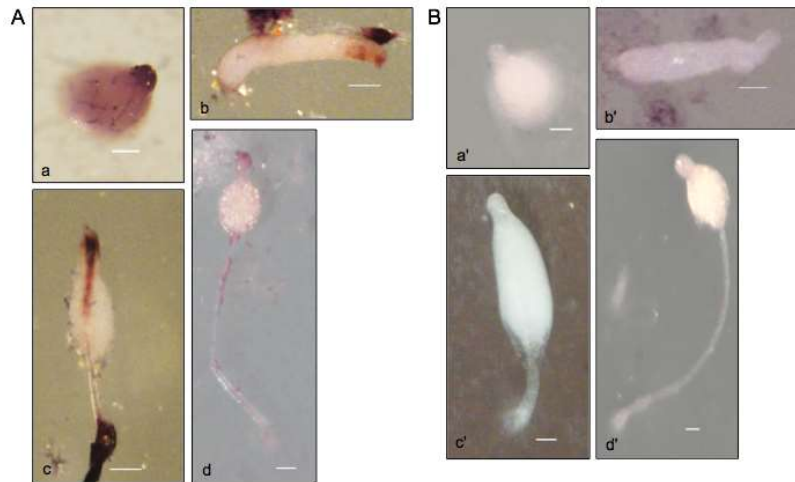


Figure 2.18: Spatial expression patterns of *PUFB* mRNA analysed by *in situ* hybridization in the multicellular structures of *Dictyostelium*. *In situ* hybridization using antisense probe A (a-d) shows the presence of *PUFB* mRNA in the prestalk/stalk cells of multicellular structures while the *in situ* hybridization using sense probe B (a-d) did not show any colour and represents the negative control (a-d) [a- Tipped mound, b-slug, c-early culminants and d-late culminant/FB; n=3].

The results showed that the expression of *PUFB* mRNA was found at the tip of mound (Figure 2.18 Aa). As development proceeded *PUFB* mRNA was clearly visible in the anterior prestalk regions of the slug (Figure 2.18 Ab). Anterior prestalk region comprised of prestalk A, prestalk O and prestalk AB cells. The prestalk A and prestalk O cells then migrate into the initial stalk tube and transform into stalk cells (Jermyn et al., 1989). In early culminant the expression was found in the initial stalk tube which are formed mainly by the pstAB cells and also present at the basal disc (Figure 2.18 Ac). In the late culminant the expression of *PUFB* mRNA remained only in tip and stalk tube. The prestalk specific localization of *PUFB* mRNA suggests it may have role in prestalk differentiation and autophagic cell death. The sense probe did not show any specific staining (Figure 2.18 B).

2.5 CONCLUSIONS

In this chapter, we have traced the phylogenetic position of all the 5 PUF proteins of *Dictyostelium* and found that PUFA shows more homology to plants and yeast. PUFB and PUFD also showed close homology with plants and yeast but they do not show significant similarity to mammals like human. While PUFA show relatively more closeness as compared to PUFB and PUFD protein of *Dictyostelium*. PUFC and PUFE

both are present on separate clade of plants, animals, yeast etc rather they are present as out-group.

Using bioinformatics approaches, 3 highly conserved motifs were observed in the putative promoter region of all 5 *PUF* genes that could act as binding site for different transcription factor. Tertiary structures of all the PUF were constructed using hybrid-modeling approaches. Structural analysis of all the PUF revealed that all the PUF have 8 repeats except PUFC and PUF E, which are having 6 repeats each. Consistent behaviors of RMSD, RMSF and Rg for all the PUF models indicating models have good structural stability. Higher residues present in favoured and allowed region for all the PUF suggesting that they are stereochemically stable.

Work on *DdPUFA* suggests its important role during growth to development transition. Out of the remaining 4 PUF proteins in *Dictyostelium* we choose *DdPUFB* to work upon further. High *PUFB* mRNA expression in initial stages of development suggests that it may have role in cell division and growth to development transition. Its expression is highest in later stages of development implying its role in terminal differentiation of cell types. As inferred from *in situ* hybridization spatial expression of *PUFB* mRNA is expressed in prestalk specific cells suggesting it may have role in autophagic cell death and stalk cell differentiation.

3.1 INTRODUCTION

Pumilio (Pum) of *Drosophila* and Fem-3 binding factor (FBF) of *C. elegans* are the founding members of the family of RNA binding proteins called PUF (Pumilio and FBF) (Wickens et al., 2002). A typical feature of PUF proteins is the presence of 8 repeats present at the C-terminal of the protein forming a domain called PUF domain or Pumilio homology domain (PUM-HD). Alignment of domain present at the C-terminal part of *Drosophila* Pumilio with *Xenopus* and mammalian homologs reveals the PUM-HD architecture (Figure 3.1A). The domain comprises of 8 repeats present tandemly along with N- and C-terminal flanking regions. Each repeat comprises of ~36 amino acids forming three α -helices. Most conserved three amino acids present in the second helix makes the contact with the RNA base (Wang et al., 2002). Crystal structure of Human and *Drosophila* Pumilio revealed that the domain forms an arc-like structure (Edwards et al., 2001; Wang et al., 2001). The RNA interacts with the concave surface and each repeat interacts with the single base of RNA through three conserved amino acid residues present in the second repeat (Figure 3.1B) (Spassov and Jurecic, 2003a). A specific sequence is present at 3' UTR of mRNA called Nanos response element (NRE) which is recognized by the PUF protein and thus regulates the mRNA post-transcriptionally ((Zamore et al., 1999; Wang et al., 2002).

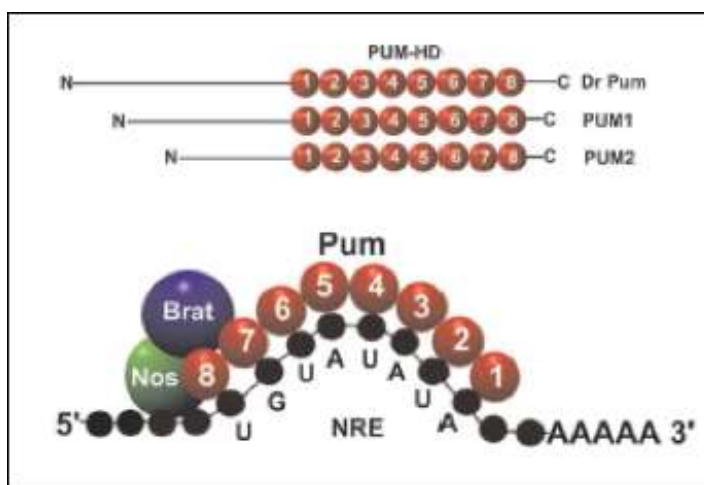


Figure 3.1: Schematic representation of the domain structure of *Drosophila* Pumilio and its human homolog PUM1 and PUM2. (upper panel) 8 conserved RNA binding domains present at the C-terminal while N-terminal region is of varying length and weakly conserved. (lower panel) A schematic representation showing the interaction of fly NRE present at 3'UTR of mRNA with PUM-HD domain. Each repeat interacts with a single base of mRNA in an antiparallel manner. *Nos* and *Brat* recruitment lead to the formation of a quaternary complex with *Pum* and *hb* mRNA, inhibiting the *hb* protein synthesis (adapted from Spassov et al., 2003).

The main function of PUF protein is the post-transcriptional regulation of target mRNA by decay or translational inhibition. Therefore, in most of the cases, it is localized primarily in the cytoplasm of cells (Macdonald, 1992; Zhang et al., 1997; Archer et al., 2009). PUF proteins can regulate various aspects of eukaryotic development like embryogenesis, gametogenesis/gamete maturation, neural development and functions. In *Drosophila*, normally Hunchback (Hb) protein is expressed at the anterior region during early development in *Drosophila* embryo. However, when *Pumilio* is mutated gradient of Pumilio protein is also present in the posterior region, which suggests that repression of *hb* mRNA is absent in this region (Tautz, 1988; Barker et al., 1992). This led to the defects in abdominal segmentation in *pumilio* mutant embryos (Lehmann and Nüsslein-Volhard, 1987; Barker et al., 1992). Pumilio also regulates some other processes like stem cell proliferation, memory formation and motor neuron functions (Weidmann and Goldstrohm, 2012).

In case of *C. elegans*, Notch signaling pathway and *PUF* RNA binding proteins maintain the pool of Germline stem cells (GSCs) (Wickens et al., 2002; Bray, 2016). From the niche, GLP-1/Notch signaling is required for the maintenance of GSC and FBF-1 and FBF-2 (collectively FBF) promote GSCs self-renewal by acting as repressors of differentiation RNAs (Crittenden et al., 2002; Kershner et al., 2013). Both *sygl-1* and *lst-1* genes are identified as GSCs regulators that directly target niche signaling (Kershner et al., 2014). But Shin et al. (2017) reported that both SYGL-1 and LST-1 are present in GSC region as cytoplasmic proteins. Both SYGL-1 and LST-1 interact with FBF physically and lead to repression of the FBF target RNA within the stem cell pool and thus maintain the stem cell pool. Also, to regulate spermatogenesis to oogenesis transition, there is a requirement of *fem-3* repression and it is achieved post-transcriptionally via 3' UTR region present in the regulatory region of *fem-3* mRNA (Hodgkin, 1986; Barton et al., 1987; Ahringer and Kimble, 1991).

In *Arabidopsis thaliana*, PUF proteins are involved in many cellular and developmental processes like abiotic and biotic stress responses such as drought and salt stress-responses and morphogenesis in leaves etc. APUM23 was found to regulate morphogenesis in leaf by the regulation of expression of *KANADI* (*KAN*) genes. GARP family member *KAN* genes, regulate the abaxial identity (Huang et al., 2014). APUM23

loss of function in plants leads to the scrunched and serrated leaves, slow growth and also venation shows abnormal pattern because of RNA processing (Abbasi et al., 2010).

In mice, two *Pumilio* genes *Pum1* and *Pum2* are present. Mice with a single knockout mutation in either of *Pum* are viable and fertile (Xu et al., 2007; Chen et al., 2012; Gennarino et al., 2015; Lin et al., 2018a). It remained unclear whether they can function redundantly to properly regulate the stem cell development during embryogenesis. Recently it was identified that if both *Pum1* and *Pum2* are mutated, it causes gastrulation failure which leads to embryo lethality at E8.5 (Lin et al., 2018b).

As PUF proteins play an important role during the development and morphogenesis of organisms and *Dictyostelium* undergoes multicellular development upon starvation, so we were interested in elucidating its role during growth and development. In this chapter, we have prepared the overexpressor and knockout strains of *PUFB* gene. We observed that it suppresses cell growth and cell proliferation and development of mutant strains are also affected. We have also analyzed the expression of developmentally important genes.

3.2 OBJECTIVES OF THE PRESENT STUDY

- To create *PUFB* mutant strains to modulate the level of PUF in *D. discoideum*.

Mutant strains developed for the present study are:

- Construction of *PUFB* overexpressor (*PUFB^{OE}*) [*act15/PUFB-eYFP/Ax2*] strain of *D. discoideum*: Full length *PUFB* (DDB_G0279557) was expressed as an eYFP-tagged fusion protein with the reporter enhanced yellow fluorescent protein (eYFP) at the C-terminal under the control of constitutive *actin 15* promoter in wild type, Ax2 cells.
- Construction of *PUFB* knockout (*PUFB⁻*) [*PUFB⁻/Ax2*] strain of *D. discoideum*: Knockout strain of *PUFB* was created by gene disruption by insertion of blasticidin resistance (Bsr) cassette between the two *PUFB* homologous fragments followed by homologous recombination. The linearized construct having *PUFB* homologous fragment along with Bsr cassette was then transformed into Ax2 cells.

- To analyse the role of *PUFB* mutant strains during growth and development in their comparison with the wild type Ax2 strain. Morphological analyses of the structures formed during development by *PUFB* mutant strains.
- To analyse the role of *PUFB* in cAMP signaling and cell adhesion.

3.3 MATERIALS AND METHODS

Here we discuss the protocols which are not mentioned earlier in this thesis.

3.3.1 Materials used in the study

The cells were grown in the presence of antibiotics like Geneticin (G418) and Blasticidin S (B) when required. Oligonucleotides used for PCR were synthesized from GCC Biotech, India. For cloning purpose PCR reagents, restriction, ligation enzymes and Gel extraction kits were purchased from Fermentas Life Sciences (Thermo Scientific). Selection markers like Geneticin (G418), Blasticidin S (B) and ampicillin were procured from Sigma Aldrich, USA. The plasmids used in the study are mentioned in the appendix.

3.3.2 Transformation of *D. discoideum* Ax2 cells

Transformation of freshly grown Ax2 cells with DNA was performed according to Gaudet et al., (2007). Approximately 2.5×10^6 cells were taken and washed twice with ice-cold H50 buffer and re-suspended in 100 μ L H50 buffer. Approximately 5-10 μ g plasmid DNA is mixed with the ice-cold cell suspension and poured into the 1 mm chilled electroporation cuvette (Sigma Aldrich USA). The electroporator (Bio-Rad Gene Pulser TM) was set at 0.65-0.70 kV and 25 μ F and the cuvette containing cell suspension and plasmid DNA was pulsed twice with an interval of 10 seconds. After the second pulse, the cells were immediately kept on ice for 5 minutes and then transferred to 90 mm culture plate containing HL5 medium for recovery from the electric pulse. Only after 24 h of incubation at 22°C, appropriate selection marker (antibiotics) was added for the selection of the transformants. Maximum concentration of G418 used was 100 μ g mL⁻¹ and blasticidin S was 10 μ g mL⁻¹.

3.3.3 Construct preparation and confirmation of *PUFB* overexpressing strain

Full length *PUFB* (DDB_G0279557) gene was PCR amplified from the Ax2 genomic DNA (Genomic position 1004-2662) using gene-specific primer set (Table 3.1)

having restriction sites *SacI* at the 5' end and *XhoI* at the 3' end for directional cloning into *act15/acg-eYFP* vector (appendix). The *act15/acg-eYFP* vector contains an *actin15* promoter, reporter enhanced yellow fluorescent protein (eYFP) at the C-terminus, an ampicillin resistance marker for selection in bacteria and a G418 resistance marker for selection in *Dictyostelium*. Plasmids from approximately 6-8 positive colonies were checked by double digestion with *SacI/XhoI*. The positive colonies were then cultured in Luria Broth media and plasmid DNA was isolated using the alkaline lysis method (Bimboim and Doly, 1979). Plasmid DNA (5-10 μg) was then transformed into Ax2 cells by using the electroporation method. They were sequentially selected from 10 $\mu\text{g mL}^{-1}$ and grown till 100 $\mu\text{g mL}^{-1}$ of G418. Single clones of overexpressing cells were isolated and developed on NNA plates to form fruiting bodies. The spores were stored for long-term use in -80°C .

Oligo name	Primer sequence (5'...3')	Restriction site	Genomic position	Amplicon Size(bp)
<i>PUFB^{OE}</i>	FP: ATGCGAGCTCGATCCTAGGTTTTTTTCGCAATGACA	<u>SacI</u>	1004-1030	2662
	RP: ACCGCTCGAGAACTTGAAGTATCTTCTTTTGAATATGAATTAC GTA	<u>XhoI</u>	3627-3659	

Table 3.1: Primer combination used for the amplifying *PUFB* for making overexpressing strain. The restriction sites are underlined and the expected amplicon size is shown.

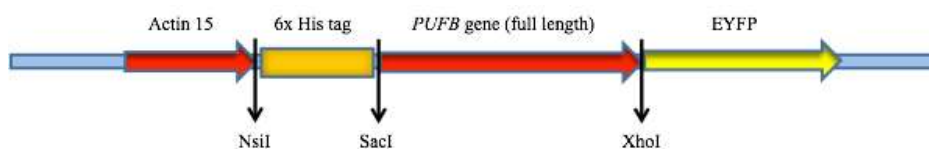


Figure 3.2: Schematic representation of the *PUFB^{OE}* construct. *PUFB* ORF was introduced in *act15/acg-eYFP* vector having an eYFP-tagged gene at the C-terminus and a 6X His tag at the N-terminus. *PUFB* replaced *acg*. The restriction sites used for cloning the *PUFB* gene downstream of *actin15* are shown.

3.3.4 Subcellular localization of the *PUFB*-eYFP fusion protein by confocal microscopy

PUFB^{OE} cells were grown on a sterile coverslip and placed inside 6 well petriplates containing HL5 media. The *PUFB^{OE}* cells have an eYFP reporter for direct visualization under a fluorescent microscope (excitation wavelength of 514 nm and an emission wavelength of 527 nm). Cells were stained with different cellular markers and incubated for 5-10 minutes, washed with 1x KK2 and visualized under Nikon confocal

microscope. For subcellular localization studies, 1 $\mu\text{g mL}^{-1}$ of 4', 6-diamidino-2-phenylindole (DAPI) and 1 $\mu\text{M mL}^{-1}$ of 3, 6-Bis(diethylamino)-9-[2-(4-methylcoumarin-7-yloxy-carbonyl)phenyl] xanthylium chloride Mitored (Rhodamine based dye) were used to stain the cells. DAPI (excitation wavelength of 358 nm; emission wavelength of 461 nm) was used for nuclear staining and cell membrane permeable Rhodamine-based dye, Mitored (excitation of 569 nm; emission of 594 nm) was used for mitochondrial staining. For colocalization studies, cells were then visualized under Nikon confocal microscope at 100X/0.16 objective and subcellular localization was revealed by merging of the images of *PUFB*^{OE} (green) with DAPI (blue), Mitored (red) using Nikon software (NIS-elements).

3.3.5 Construct preparation and confirmation of *PUFB* knockout (*PUFB*⁻) strain

PUFB⁻ (knockout) strain was created by gene disruption method followed by standard homologous recombination. Two knockout fragments (KF1 and KF2) from the 5' and 3' end regions of the gene were PCR amplified from the Ax2 genomic DNA using specific primer sets (Table 3.2) and introduced into the flanking side of the Bsr cassette in pDrive vector by restriction digestion (Figure 3.3). The ligated construct was then transformed in competent *E. coli* DH5 α cells and incubated at 37°C in LB agar plates supplemented with 100 $\mu\text{g mL}^{-1}$ ampicillin. Plasmids from approximately 5-10 positive colonies were checked by double digestion. Linearized plasmid containing KF1-Bsr-KF2 fragment was transformed into Ax2 cells by electroporation. The transformed cells were selected at 10 $\mu\text{g mL}^{-1}$ Blasticidin-S. The validation of the [*PUFB*⁻/Ax2] knockout strain was carried by PCR amplification using different primer combinations (Figure 3.4).

Oligo name	Primer Sequence (5'—3')	Restriction site	Genomic position	Expected Amplicon size(bp)
<i>PUFB</i> KF1	FP: GAAT <u>GCGGCCGCC</u> CACTACAACCCTGCTACAATATCATTCCTTG	NotI	772-801	1050
	RP: CTAGTCTAGAGGTGTAGGTGACATTTGTGATGGTTCA	XbaI	1805-1831	
<i>PUFB</i> KF2	FP:ATCGA <u>CGCGT</u> CAAAGAAATCAACCGACCATCAACCA	MilI	2617-2642	951
	RP:CAGGGGT <u>ACC</u> GAGTATCATTACTGACGTCCAAAGCGG	KpnI	3541-3567	

Table 3.2: Primer combinations used for *PUFB* knockout construct preparation. Primer pairs with restriction sites (underlined) were used for the amplification of first and second fragments (KF1 and KF2) required for creating the knockout construct. The genomic positions of primers and the expected amplicon sizes are mentioned.

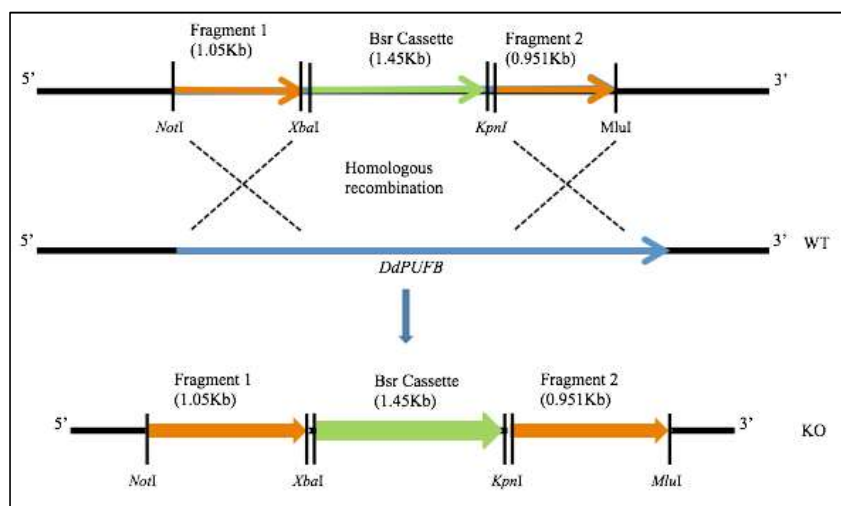


Figure 3.3: Gene disruption strategy for the creation of *PUFB* knockout strain. Transformation of the linearized vector containing 5' and 3' targeting regions (KF1 and KF2) interrupted by the Bsr cassette undergo homologous recombination with the wild type (*Ax2*) *PUFB* gene to create the disruption strain. The sizes and the restrictions sites of the fragments in the construct are also shown.

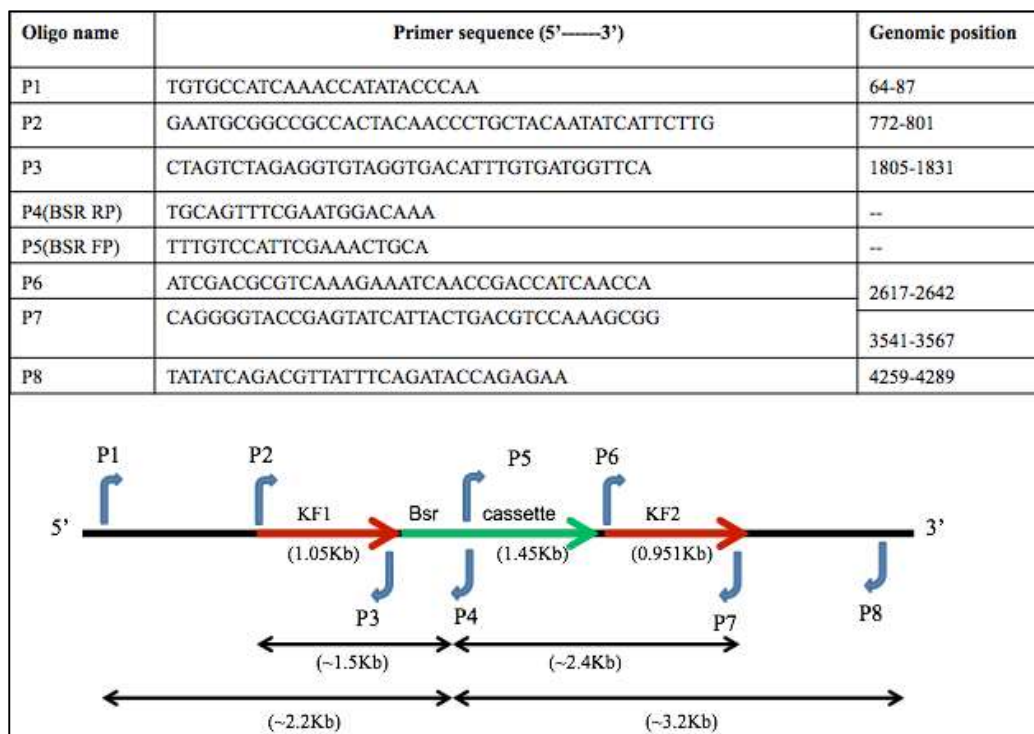


Figure 3.4: Schematic representation for the validation of [*PUFB*⁻/*Ax2*] knockout strain using various primer combinations. Primer combinations used for the confirmation of the knockout strain and their expected genomic sizes are mentioned. Upper panel shows the primer sequences and the lower panel shows the primer combinations and the expected amplicon sizes for the validation of knockout strain.

3.3.6 Confirmation of *PUFB* mutant strains through mRNA level measurement

Approximately 1×10^6 vegetative cells from wild type Ax2, *PUFB^{OE}* and *PUFB⁻* were harvested and washed twice with chilled 1x KK2 buffer. Cells were lysed in 1.0 mL TRI reagent (T9424, Sigma-Aldrich) and incubated for 20 minutes at room temperature. RNA was isolated, quantified and 1.0 μ g RNA from each sample was used to synthesize the respective cDNA. The gene-specific primer combinations (Table 3.3) were used for PCR amplification from cDNA template, which also ensures the purity of the preparation. PCR amplification for *PUFB* was carried out by initial denaturation at 98°C for 30 seconds followed by 24 cycles amplification of denaturation at 98°C for 45 seconds, primer annealing at 59.1°C for 1 minute and extension at 65°C for 1 minute. PCR amplification for *ig7* was carried out using an initial denaturation for 30 seconds at 98°C followed by amplification which was carried for 24 cycles of denaturation at 98°C for 15 seconds, primer annealing at 52°C for 45 seconds and extension at 68°C for 1 minute. PCR amplified DNA samples were run on 1.5% agarose gel and AlphaImager 3400 was used to calculate the IDV values of each DNA band along with blank. The relative abundance of *PUFB* in each sample was calculated with respect to *ig7* levels.

Oligo Name	Primer Sequence (5'--3')	Genomic position	Expected amplicon cDNA size(bp)	Expected amplicon gDNA size(bp)
<i>PufB</i> RT	FP:TAGGTGGTGGTGAATTATCAACAACA	1481-1507	537	614
	RP:TTGGTGTTGTATTAGTAGATGTTGCTGGTG	2065-2094		
<i>ig7</i> RT	FP: TGAATTGAAAGTCTGAGTAAACGG	1795-1815	723	1270
	RP: AGATAGGGACCAACTGTCTCAC	3065-3042		

Table 3.3: Primer combinations used for the amplification of cDNA for *PUFB* and *rnIA/ig7* genes for RT analyses. Expected amplicon sizes from cDNA and gDNA as templates are mentioned above [FP- Forward primer, RP- Reverse primer, bp-base pair].

3.3.7 Cell proliferation analysis

Ax2, *PUFB^{OE}* and *PUFB⁻* cells were grown in axenic HL5 media from fresh spores at 22°C. For growth analysis, logarithmic phase cells ($3-5 \times 10^6$ cells mL⁻¹) were diluted into fresh media at a seeding density of 5×10^5 cells mL⁻¹ and counted every 12 h up to 96 h as a measure of cell proliferation. Cell densities were measured by counting cells in a hemocytometer after appropriate dilutions in triplicates and were plotted as a function of time. Generation time was calculated as follows:

$$Td = (t_2 - t_1) \times \log_2 / \log (q_2/q_1)$$

Where: t1- initial time

t2- final time

q1-growth at t1

q2-growth at t2

3.3.8 Analysis of development

For development analyses, the logarithmic phase ($3\text{-}5 \times 10^6$ cells mL^{-1}) cells from wild type Ax2 and *PUFB* mutants were harvested, washed in 1xKK2 buffer and spotted (10-20 μL) as droplets at a density of 5×10^7 cells mL^{-1} on 1.5% NNA plates. The plated cells were kept at 4°C for 4–6 h to bring synchronization in development, followed by incubation at 22°C for comparison of developmental timings and morphologies between different strains. Developing structures were photographed every 4 h using Nikon SMZ1500 stereomicroscope and analyzed using NIS Elements AR v. 4.0.

3.3.9 Morphological analyses of multicellular structures formed during development

Upon starvation, cAMP signaling is triggered which leads to multicellular development. Cells tend to move towards each other in response to cAMP gradient forming aggregates. To analyze the effect of *PUFB* mutation in development we measured the size and number of the aggregates formed by the wild type Ax2 cells and the *PUFB* mutants using Nikon software (NIS Elements ARv.4.0). As the development proceeded to culmination *PUFB* mutants formed fruiting bodies showing different morphology than the wild type Ax2 cells. We measured the number of fruiting bodies formed in all the three strains and also measured the length of stalk and sorus and calculated the stalk to sorus ratio for each strains using NIS elements. Approximately 200 fruiting bodies from three individual experiments were analyzed.

3.3.10 Spore viability assay

Spore viability assay was performed as described in Maurya et al. (2017). Logarithmic phase ($3\text{-}5 \times 10^6$ cells mL^{-1}) cells from wild type Ax2 and *PUFB* mutants were harvested in 1x KK2 buffer and plated on 1.5% NNA and allowed to develop at 22°C . Spores were collected from fruiting bodies in spore buffer (40 mM KH_2PO_4 , 20 mM KCl, 2.5 mM MgCl_2), centrifuged at 12,000g for 2 minutes at 22°C and washed with spore storage buffer. Upon appropriate dilutions, spores were counted in a

haemocytometer and aliquots of 100 spores from each strain were then mixed with heat-killed *Klebsiella aerogenes* bacterial suspension and grown on NNA plates for 5-6 days. Clear plaques formed on the bacterial lawn were counted. The percent spore viability was measured by counting the number of clear plaques divided by total spores plated followed by multiplication of 100. All experiments were performed in triplicates.

3.3.11 Cell cycle and cell size analysis

To analyze the cell size and cell cycle of different *PUFB* mutant strain and wild type Ax2, BD FACS Aria with BD FACS DIVA software were used. For this purpose 1×10^7 cells mL^{-1} were harvested and washed with 1xKK2 buffer followed by resuspending in 1.5 mL buffer (0.9% NaCl, 5 mM EDTA, 2% sucrose in KK2 buffer). Fixing of the cells was done by using 75% ethanol drop wise then incubated at 22°C for 30 minutes and stored at 4°C. Just before analysis cells were washed and resuspended in 1 mL 1xKK2 buffer then $10 \mu\text{g mL}^{-1}$ RNase A (Sigma-Aldrich, USA) was added and incubated for 30 minutes at 37°C. After this, $50 \mu\text{g mL}^{-1}$ propidium iodide (Sigma-Aldrich, USA) was added and further incubated at room temperature for 30 minutes. Cells were washed with 1xKK2 buffer and resuspended in an appropriate volume of 1xKK2 buffer.

3.3.12 Pinocytosis and exocytosis assay

Endocytosis and exocytosis assay was performed according to Rivero and Maniak (2006). We inoculated 3×10^6 cells mL^{-1} of Ax2, *PUFB*⁻ and *PUFB*^{OE} and kept it for 15 minutes under shaken condition then 2 mg mL^{-1} of FITC dextran (Sigma Aldrich) was added and the samples were collected at different time points (0, 15, 30, 45, 60, 90, 120 and 180 minutes) and 1.5 mL of ice-cold Sorenson buffer (see Appendix) was added to it followed by washing (twice) with Sorenson buffer. After that cells were lysed with 500 μL of lysis buffer and then the fluorescence was measured in multiplate Reader (Thermoscientific Varioskan Flash) at $\lambda_{\text{Ex}} = 470 \text{ nm}$ and $\lambda_{\text{Em}} = 515 \text{ nm}$.

For exocytosis, 3×10^6 cells mL^{-1} cells of different strains were subjected to incubation in FITC-dextran for 3 h followed by washing then cells were resuspended in the growth medium again. Samples were collected at different time points (0, 15, 30, 45, 60, 90, 120 and 180 minutes) and 1.5 mL of ice-cold Sorenson buffer (see Appendix) was added to it followed by washing twice with Sorenson buffer. After that cells were lysed

with 500 μ L of lysis buffer then measured the fluorescence in multiplate Reader (Thermoscientific Varioskan Flash) at λ Ex = 470 nm and λ Em = 515 nm

3.3.13 Measurement of mRNA levels for developmental genes

Logarithmic phase wild type Ax2, *PUFB*^{OE}, and *PUFB*⁻ cells were harvested and developed on 1.5% NNA plates at a density of 5×10^7 cells mL⁻¹. Various developmental stages like vegetative, loose aggregate, mound, slug, early culminant and late culminant were collected and RNA was extracted. cDNA was prepared and RT-PCR was performed for various genes involved in early development like *cadA*, *csaA*, *ctnA*, *acaA*, *carA1*, *pdsA*, *cotA* and *cotB* using the specific primer combinations as shown in Table 3.4.

Oligo Name	Primer Sequence (5'—3')	Genomic position	Expected Amplicon cDNA size (bp)	Expected Amplicon gDNA size (bp)
<i>ig7 RT</i>	FP: TGAATTGAAGTCTGAGTAAACGG	1795-1815	723	1270
	RP: AGATAGGGACCAAACCTGTCTCAC	3065-3042		
<i>cadA RT</i>	TCTGTGATGCAAATAAAGTAAAA	1004-1027	468	579
	ATAGTCATATGGTGTATGTGTTG	1563-1586		
<i>csaA RT</i>	GTGAACGACTCTATTAACCTGCT	1406-1429	968	968
	AGTTGGAGTGTCTGGAATTGATA	2351-2371		
<i>ctnA RT</i>	ATTTAGCTTTATTCCTTGCAAC	1022-1045	356	470
	GTGTAAGCAATTGAGAGGGTGAAT	1468-1491		
<i>cotA RT</i>	TAATAAGCTTGAAAGATAATTGTGGAGAAGGTGGTGATG	1385-1414	1300	1329
	TTATCTCGAGGGAAGGCTTGATGATGCAGATGAAG	2687-2713		
<i>cotB RT</i>	GGTCAAGCTTAGAGATAGTAACGATTGTCTGCTAG	1468-1493	1112	1112
	TTACCTCGAGATAGTTGATGGATTGATACAGATTGG	2554-2579		
<i>carA RT</i>	TGTATGGCAGTGTGATTGGT	1082-1102	819	962
	ATGGTGATGGATTGTTATTGT	2024-2044		
<i>acaA RT</i>	AGTACACCACATAATAATAATCAT	1304-1327	1076	1201
	CTCTGGAATTACAATATCTCTCTT	2480-2503		
<i>pdsA RT</i>	ATGGCATTAAATAAAAAATT	1001-1020	1470	1500
	TAAATACAAATTGGATCACC	2492-2512		

Table 3.4: Primer combinations used for RT analyses of genes involved in the development of *Dictyostelium*. Expected amplicon sizes of genomic DNA and cDNA are mentioned.

3.3.14 cAMP level measurement

The total cAMP levels were measured using commercially available cAMP Enzyme Immunoassay Kit (CA200, Sigma Aldrich) as per the manufacturer's instructions. 1×10^6 cells from logarithmic phase cultures of Ax2 and *PUFB* mutants were harvested and washed twice in 1x KK2 buffer. Cells were starved in 1xKK2 buffer for 0,

4 and 6 h. Cells were harvested and treated with 0.1 M HCl. cAMP levels of each sample were calculated according to the kit manual.

3.4 RESULTS AND DISCUSSION

3.4.1 Preparation of *PUFB* overexpressing strain [*act15/PUFB-eYFP/Ax2*]

PCR amplification of *PUFB* gene (~2.66 Kb) using genomic DNA as the template was performed (Figure 3.5 A) and the amplified product was eluted using the gel elution kit available from Genetix as per the manufacturer's instructions and double digested with *SacI/XhoI* and further purified by gel elution kit. Similarly, pB17S vector (6.1 Kb) was double digested with *SacI/XhoI* and ligated with the digested 2.66 Kb amplicon (Figure 3.5 B). The ligated product was transformed into competent bacteria for amplification. Plasmid DNA of 5-6 colonies was isolated using alkaline lysis method (Sambrook and Russel, 2007) and confirmed for the presence of positive construct by restriction digestion with *SacI/XhoI* yielding 6.1 Kb fragment of vector and 2.66 Kb fragment of insert (Figure 3.5 C). The construct was also confirmed by sequencing. Plasmid DNA (2-10 μg) was then transformed by electroporation into *D. discoideum*, Ax2 cells (Gaudet et al., 2007). The transformed cells were sequentially selected on 10 $\mu\text{g mL}^{-1}$ of G418 and grown till 100 $\mu\text{g mL}^{-1}$. The transformed cells were cloned out on the bacterial lawn and the *Dictyostelium* cells overexpressing *PUFB* were now called as *PUFB^{OE}* strain.

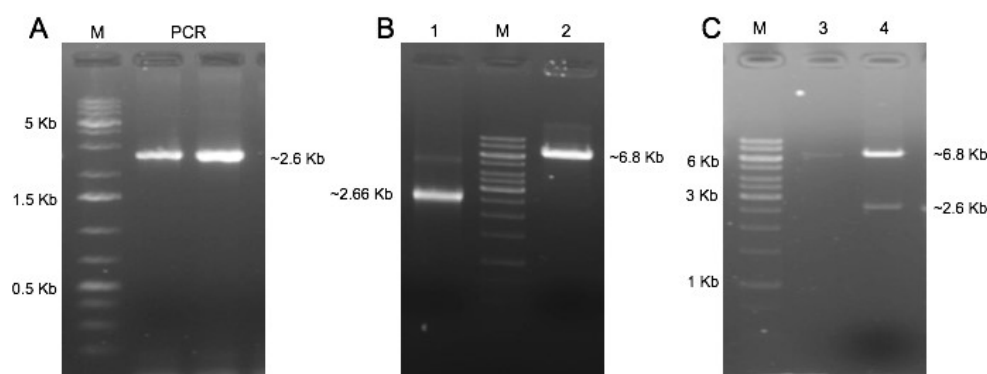


Figure 3.5: Construct preparation for the *PUFB* overexpressor (*PUFB^{OE}*). (A) PCR amplification of the full length *PUFB* (2.66 Kb) using gene-specific primers. (B) Restriction digestion of the *PUFB* amplified product (2.66 Kb) (Lane1) and pB17S vector (6.1 Kb) (Lane2) using *SacI/XhoI*. (C) Confirmation of clone; Lane 3- Digested vector (6.8 Kb); Lane 4: Restriction digestion of the plasmid with *SacI/XhoI* yields the vector fragment of 6.8 Kb and the insert of 2.66 Kb [M-DNA marker].

3.4.2 Subcellular localization of PUFB-eYFP fusion protein

To analyze the subcellular localization of PUFB expression of the fusion protein with the available *PUFB^{OE}* (*Dictyostelium PUFB* gene fused to eYFP as a reporter) cells. The cells were grown on coverslip overnight and then incubated in DAPI and Mitored. DAPI is a fluorescent stain that binds to AT-rich regions in DNA whereas Mito-Red binds to the mitochondria in live cells.

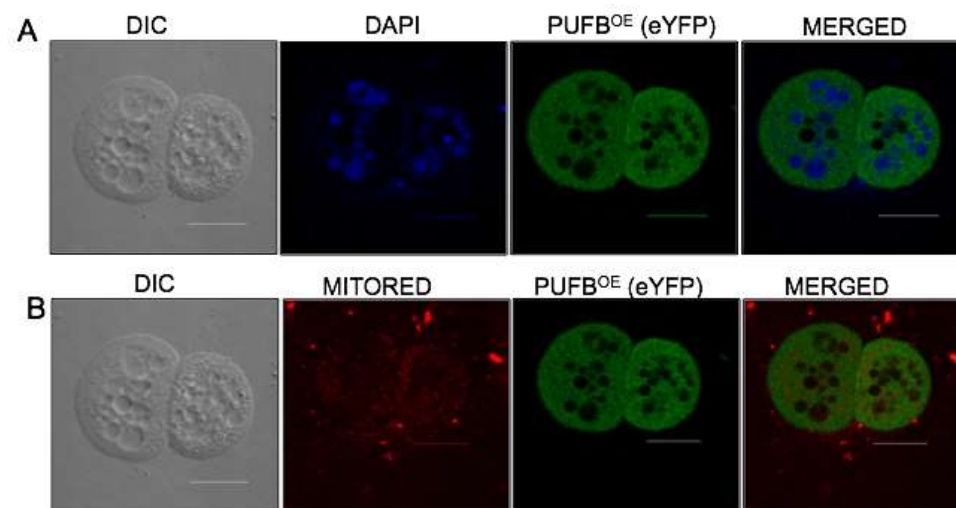


Figure 3.6: Subcellular colocalization studies in *PUFB^{OE}* cells. (A) The *PUFB^{OE}* cells expressing *PUFB* gene fused to eYFP as a reporter were stained with nuclear stain, DAPI (blue) and (B) Mitochondrial stain, Mitored (red) for 10 minutes and images were captured in confocal microscope. The PUFB fusion protein (green) showed cytosolic localization and did not colocalize with mitochondria. [Scale bar=10 μ m].

Through confocal microscopy analysis, we found that the eYFP fluorescence of PUFB-eYFP fusion protein was expressed in the cytosol (Figure 3.6 A). As reported in other organisms also, PUF protein is predominantly localized in the cytosol (Miller and Olivas, 2011). Except for PUF6p of *S. cerevisiae* which is localized in both cytoplasm and nucleus (Gu et al., 2004) and PUF7 of *T. brucei* which is present in the nucleolus (Droll et al., 2010). Microscopic examination showed that PUFB-eYFP fluorescence did not colocalize with the Mitored (Figure 3.6 B), a mitochondrial marker. Colocalization was determined through the analysis of merged images using NIS elements software.

3.4.3 Preparation of the *PUFB* knockout construct

PUFB knockout strain was created by gene disruption followed by homologous recombination. 5' and 3' targeting region (KF1 and KF2 respectively) of *PUFB* is cloned in such a way that it flanked the Bsr cassette of the pDrive vector, which was transformed

into Ax2 cells to create the knockout strain. Both 5' and 3' end of the gene (KF1 and KF2 respectively) were PCR amplified from the genomic DNA using the forward and reverse primer combination giving amplicon sizes of 1.05 Kb and 0.951 Kb respectively (Figure 3.7 A). The fragment 1 (KF1 from the 5' end) was digested with the restriction enzymes NotI/XbaI and ligated with the similarly digested vector. Also, fragment 2 (KF2 from the 3' end) was digested with the restriction enzymes KpnI/MluI and ligated with the similarly digested vector for directional cloning. The ligation product was then transformed in *E. coli* competent cells and grown on LB agar plates supplemented with $100 \mu\text{g mL}^{-1}$ ampicillin and incubated at 37°C .

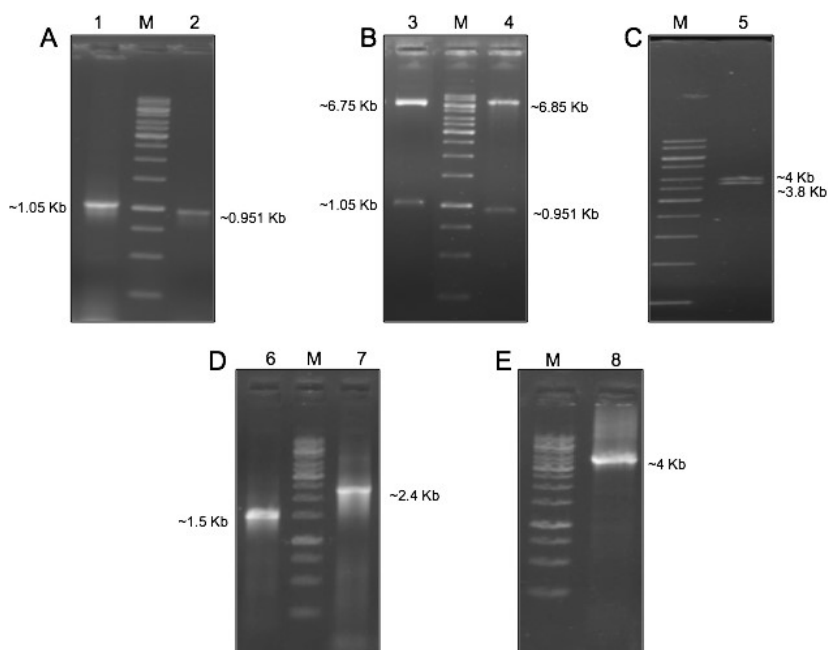


Figure 3.7: Cloning of *PUFB* knockout construct and validation of knockout construct via PCR amplification and restriction digestions. (A) PCR amplification of 5' targeting region Fragment 1 (KF1) and 3' targeting region Fragments 2 (KF2) from the genomic DNA yields a 1.05 Kb and 0.951 Kb products respectively. (B) Confirmation of *PUFB* knockout construct and Bsr cassette by restriction digestions. The restriction enzymes used along with the respective sizes of the release are as mentioned; Lane 3: NotI /XbaI (6.75 Kb vector backbone + 1.05 Kb insert); Lane 4: KpnI/MluI (6.85 Kb vector backbone + 0.951 Kb insert). (C) Lane 5: KpnI/NotI (~3.8 Kb vector backbone + ~4 Kb linearized product); (D) Confirmation of construct by PCR amplification. Lane 6 & 7: fragment 1 & 2 of size 1.5 & 0.95 Kb, respectively. (E) Lane 8: PCR amplification of linearized construct of ~4 Kb. All band sizes are approximate [M= DNA ladder].

Various combinations of restriction enzymes were used to confirm the positive clone. The plasmid was digested with KpnI/NotI enzymes to get the linearized construct

(fragment 1 + bsr cassette + fragment 2) of ~4 Kb (Figure 3.7 C). Digestion of plasmid with NotI/XbaI yield the fragments of size 6.75 Kb and 1.05 Kb (Fragment 1) while digestion with KpnI/MluI yield the fragments of size 6.85 Kb and 0.95 Kb (Fragment 1) respectively (Figure 3.7B). They were further confirmed by PCR using different primer combinations. Fragment 1 (1.05 Kb), fragment 2 (0.95 Kb) (Figure 3.7 D) and linearized construct (~4 Kb) (Figure 3.7 E) were successfully amplified from the plasmid further confirmed the construct preparation.

3.4.4 Preparation and validation knockout (*PUFB*⁻) strain by PCR

The knockout construct was linearized using KpnI/NotI restriction digestion (~4 Kb), eluted by gel extraction protocol and 2-10 µg of the linearized plasmid was transformed into Ax2 cells by electroporation method. Homologous recombination resulted in disruption of 2.62 Kb *PUFB* gene with the Blasticidin resistance (Bsr) cassette. Following transformation, cells were selected on 2 µg mL⁻¹ of Blasticidin S and selected until 10 µg mL⁻¹. After 10-15 days clear plaques were picked and transferred to 1mL of HL5 media (containing 10 µg mL⁻¹ of Blasticidin S) in 24-well culture plates. Around 500 independent resistant clones were isolated and their cell lysate was used as a template to screen for positional integrants by PCR amplification.

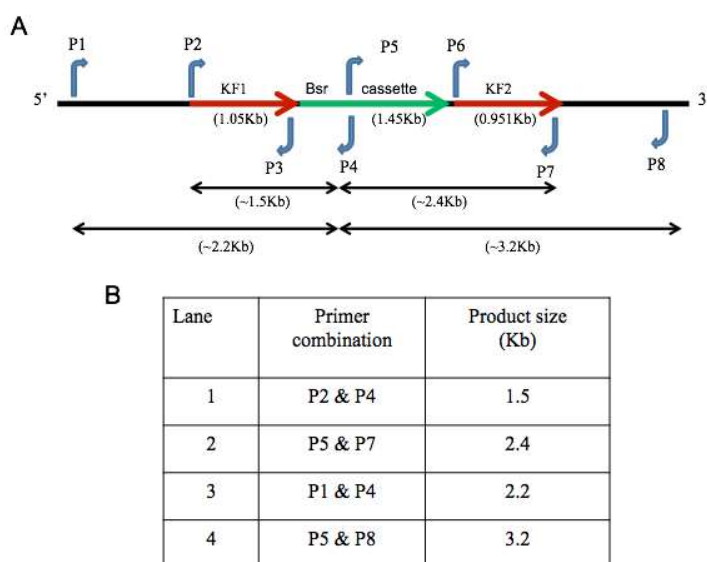


Figure 3.8: Schematic representation of various primers and a list of primer combinations used for the validation of positional integrant. Product size of the various PCR amplifications are mentioned in the table.

The schematic representation of various primers used for screening and the expected amplicon sizes are mentioned in Figure 3.8. Primer combinations to validate

PUFB⁻ strain by PCR amplification were mentioned in figure 3.4. Reverse complement primers of the blasticidin cassette were denoted as P4 and P5, respectively. P1 and P8 are primers upstream to fragment 1 and downstream to fragment 2 in the genomic DNA, respectively. Positional integrants (PI) were screened by the primer combinations P1/P4 and P5/P8 to yield amplicon sizes of 2.2 Kb and 3.2 Kb, respectively (Figure 3.9). Four positive clones were obtained from the screening that showed almost similar growth and development phenotype. One of these clones was chosen and designated as *PUFB*⁻ for further studies.

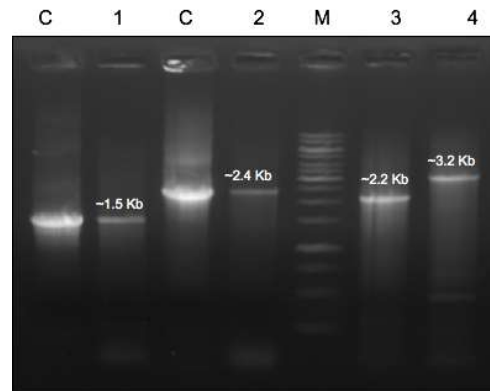


Figure 3.9: Screening of *PUFB*⁻ knockout strain by PCR amplifications. Confirmation of *PUFB* knockout strain by PCR from *PUFB*⁻ gDNA using various primer combinations; C: *PUFB*⁻ construct plasmid is used as control for the amplification of fragment 1+ Bsr and fragment 2+ Bsr (random integrants); Lane 1: Primer combination 2 and 4, amplicon size ~1.5 Kb; Lane 2: Primer combination 5 and 7, amplicon size ~2.4 Kb; Lane 3: Primer combination 1 and 4, amplicon size ~2.2 Kb; Lane 4: Primer combination 5 and 8, amplicon size ~3.2 Kb. [expected sizes are marked; M-DNA marker].

3.4.5 Confirmation of *PUFB* overexpressor (*PUFB*^{OE}) and knockout strain (*PUFB*⁻) by mRNA levels

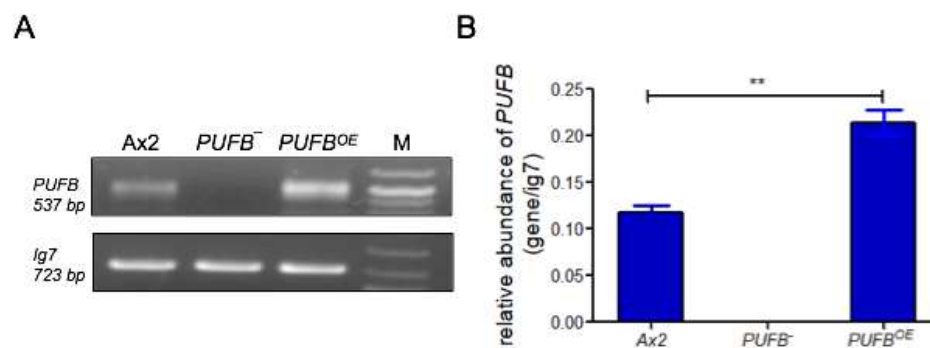


Figure 3.10: mRNA levels of *PUFB* in different strains. Semi-quantitative RT-PCR of *PUFB* mRNA in the vegetative stage of Ax2, *PUFB*⁻ and *PUFB*^{OE}. (A) Gel picture showing

PUFB mRNA levels and *ig7* mRNA levels (internal control) in Ax2, *PUF*⁻ and *PUF*^{OE} cells. (B) Relative expression of *PUFB* mRNA in graphical form. [The values represent mean \pm standard deviation; n=3; student t test].

mRNA expression pattern of *PUFB* in the vegetative stage of Ax2, *PUF*⁻ and *PUF*^{OE} confirmed the creation of both knockout and overexpressor strains. There was negligible mRNA in *PUF*⁻ strain while *PUF*^{OE} showed nearly 2-fold increase of *PUFB* mRNA (Figure 3.10).

3.4.6 Comparative cell proliferation and growth profile studies of Ax2, *PUF*⁻ and *PUF*^{OE} strains

To measure the cell proliferation rate in Ax2, *PUF*⁻ and *PUF*^{OE} cells, fresh spores of these strains were inoculated in 90 mm petri-plates. A primary culture was inoculated from the cells of different strains. Log phase cells of all three strains were then diluted into a fresh medium at an equal density of $\sim 5 \times 10^5$ cells mL⁻¹ and monitored for 4-5 days.

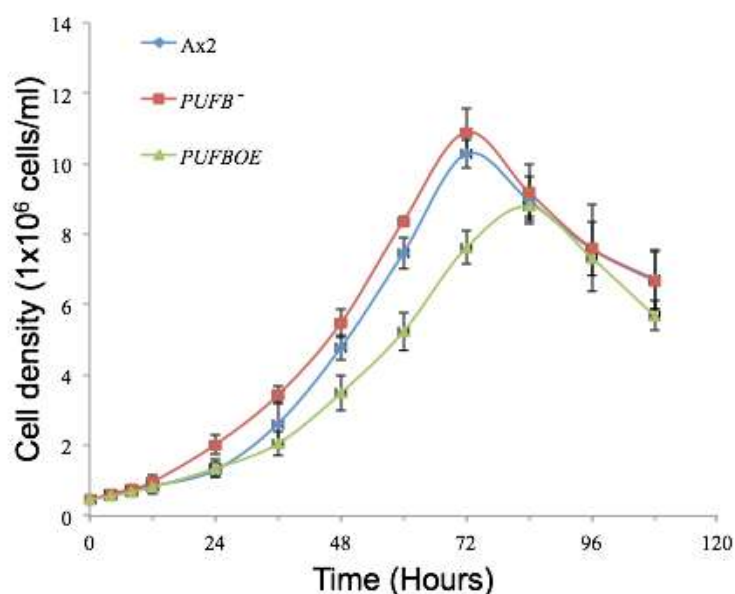


Figure 3.11: Effect of overexpression and deletion of *PUFB* on cell proliferation as compared to the wild type cells. The graph represents comparative cell proliferation of wild type Ax2, *PUF*^{OE}, and *PUF*⁻ cells. All strains were seeded at a density of 5×10^5 cells mL⁻¹ and monitored over 5-6 days; doubling time was calculated at logarithmic phase. The *PUF*^{OE} cells showed slower cell proliferation as compared to other strains. [The values represent mean \pm standard deviation; n=5; student t test].

Ax2 and *PUF*⁻ cells attained maximum cell density at 72 h while *PUF*^{OE} attained maximum cell density at 84 h. Wild type Ax2 cells acquired stationary phase at

$\sim 10.2 \times 10^6$ cell density, *PUFB*⁻ acquired stationary phase at $\sim 10.9 \times 10^6$ cell density while *PUFB*^{OE} acquired stationary phase at $\sim 8.79 \times 10^6$ cell density. We observed a slightly higher cell proliferation rate in *PUFB*⁻ cells as compared to the other strains, it reached a maximum cell density of $\sim 10.9 \times 10^6$ and thereafter decline phase was observed. *PUFB*^{OE} showed slower proliferation rate throughout and reached a maximum cell density of $\sim 8.79 \times 10^6$ at 84 h, 12 h later than the Ax2 and *PUFB*⁻ (Figure 3.11). Doubling time for Ax2, *PUFB*⁻ and *PUFB*^{OE} was found to be 12.66 ± 0.7 , 11.10 ± 0.35 , 18.34 ± 0.91 h, respectively. It shows that overexpression or knockout of *PUFB* gene leads to aberration in cell proliferation rate.

Next, we wanted to know whether this aberration in cell proliferation was due to alteration in cell cycle or defect in pinocytosis and exocytosis.

3.4.7 Cell cycle analysis of *PUFB* mutants

To know if the aberration observed in the cell proliferation of *PUFB*⁻ and *PUFB*^{OE} was due to changes in the cell cycle, we checked for the percentage of cells in each phase of the cell cycle. To investigate the effect of *PUFB* mutation on the phases of cell cycle flow cytometry was used. For this, cells were fixed with 75% ethanol at a different time point (0-96 h) during cell cycle progression. Cells were then stained with PI (Propidium iodide) and subjected to analysis in flow cytometer.

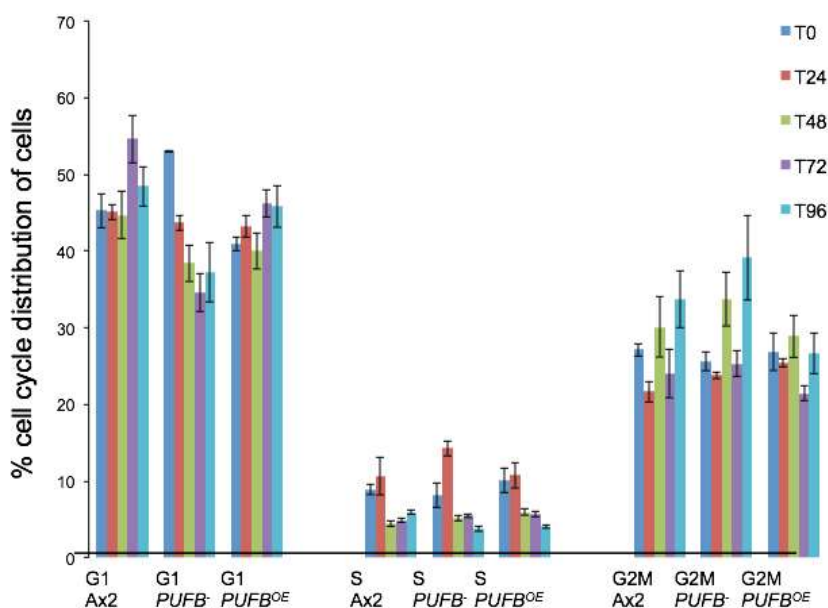


Figure 3.12: Cell cycle analyses in *PUFB* mutants. Cell cycle analyses were performed using FACS in wild type Ax2, *PUFB*^{OE}, and *PUFB*⁻ cells at different time points. The

bar graph represents the percentage of cells in G1, S and G2/M phases of the cell cycle at 0 h, 24 h, 48 h, 72 h and 96 h (The values represent mean \pm S.D.; n=3; Student t-test).

We observed that the percentage of *PUFB*⁻ cells present in the G1 phase of the cell cycle are significantly less when compared to wild type while in case of *PUFB*^{OE} no significant difference was observed. During S-phase, *PUFB*⁻ at the time point t24 and t48 showed a increase in the percentage of cells as compared to the wild type (Figure 3.12). This suggests that knockout of *PUFB* leads to an increase in cell proliferation possibly by suppressing G1 arrest and initiating the G1-S transition.

3.4.8 Endocytosis and exocytosis studies in *PUFB* mutants

Dictyostelium internalize particles and fluid by the process of endocytosis (also called macropinocytosis or cell drinking) that involves the function of the actin cytoskeleton. This is then surrounded by plasma membrane to form endosome which fuses with lysosome where internalized material is acted upon by various enzymes to digest it and undigested remnants are released outside by exocytosis (Maniak et al., 1995; Hacker et al., 1997). Thus we measured the pinocytosis rate of FITC dextran, which is a fluid phase marker. We inoculated 3×10^6 cells mL⁻¹ of Ax2, *PUFB*⁻ and *PUFB*^{OE} and kept it for 15 minutes under shaken condition then 2mg mL⁻¹ of FITC dextran was added and the samples were collected at different time points (0, 15, 30, 45, 60, 90, 120 and 180 minutes) to measure the intracellular fluorescence. The intracellular fluorescence was normalized with protein content to account for any differences in cell size. The maximum value of intracellular fluorescence was taken as 100 percent (for pinocytosis) and values at different time points were compared to it. We observed no significant difference in the pinocytosis rate of Ax2, *PUFB*⁻ and *PUFB*^{OE} cells (Figure 3.13 A).

For exocytosis, 3×10^6 cells mL⁻¹ cells of different strains were subjected to incubation in FITC-dextran for 3 h followed by washing then cells were resuspended in the growth medium again. Samples were collected at different time points (0, 15, 30, 45, 60, 90, 120 and 180 minutes) to measure the intracellular fluorescence. Percent fluorescence was determined by taking maximum fluorescence as 100% and the values at each time points were compared.

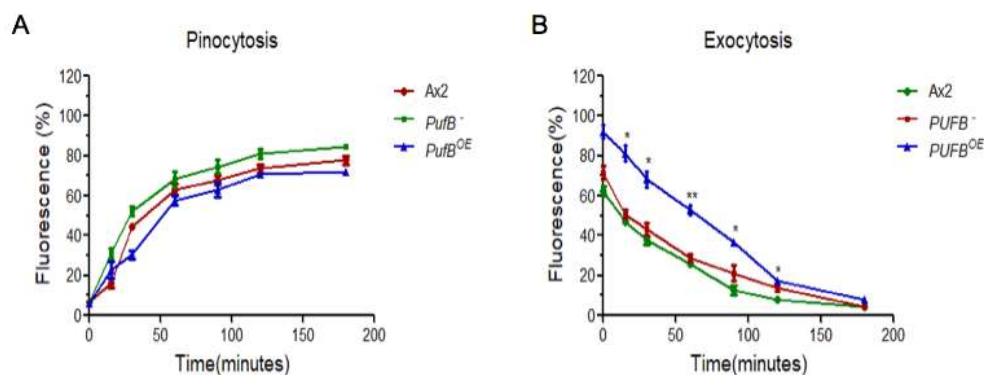


Figure 3.13: Pinocytosis and exocytosis analysis in *Ax2* and *PUFB* mutants by using FITC-labeled dextran (A) For pinocytosis analysis, *Ax2* and *PUFB* mutants strain at a cell density of 3×10^6 cells mL^{-1} were incubated with FITC-dextran (2 mg mL^{-1}) and intracellular fluorescence of internalized fluorescent marker was measured at various time points using a spectrofluorimeter (excitation at 544 nm and emission at 574 nm). (B) Exocytosis analysis was done in all three strains by incubation of 3×10^6 cells mL^{-1} with FITC-dextran for 3 h, washed and cell suspension was used to measure the fluorescence from the marker that remained in the cell at various time points (The values represents the average \pm standard deviation; $n=3$; experiments were carried out in triplicate).

PUFB^{OE} cells showed an increase in intracellular fluorescence representing reduced exocytosis as compared to the wild type *Ax2* while fluorescence in *PUFB⁻* appeared to be comparable to wild type cells. This result suggests that in *PUFB^{OE}* pinocytosis is normally operating inside the cells i.e. there is no defect in the uptake of food but there is a defect in exocytosis process as the rate is slower as compared to the wild type (13.3B). Due to defects in exocytosis process, undigested remnants or other excretory products may not be released outside at a proper rate and accumulate inside the cells that could be toxic to the cells and this may lead to the decreased cell proliferation and growth. This could be the reason that the *PUFB^{OE}* cells are slow proliferating.

Cell proliferation and cell growth are regulated independently in *Dictyostelium*. To determine the role of *PUFB* in regulating growth (increase in cell mass or size) we measured the cell mass of *Ax2*, *PUFB⁻* and *PUFB^{OE}*. Increase in cell mass represents the increase in growth of cell over time due to which protein content of cell increases. The average cell mass of *Ax2* was found to be 10.3 ± 0.33 mg while the *PUFB^{OE}* showed a significant decrease in cell mass having 7.6 ± 0.33 mg. The average cell mass of *PUFB⁻* was observed to be 11 ± 0.57 mg (Figure 3.14 A). The average cell mass of *PUFB⁻* cells was insignificant as compared to *Ax2* cells. In other words, this result suggests that

PUFB^{OE} cells accumulate less mass because of decreased cell growth while the non-significant increase in growth of *PUFB⁻* cells was observed.

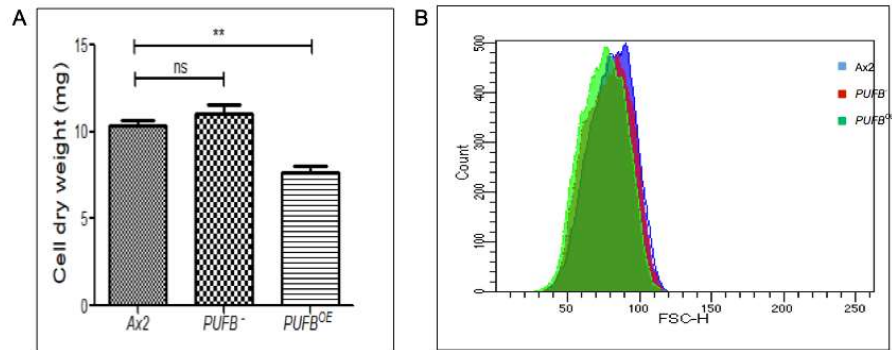


Figure 3.14: Cell dry weight and cell size analysis of *PUFB⁻* and Ax2, *PUFB^{OE}* cells. (A) 5×10^7 cells of Ax2, *PUFB⁻* and *PUFB^{OE}* were harvested for dry weight analysis. (B) Cell size analysis of Ax2, *PUFB⁻* and *PUFB^{OE}* cells were done using BD FACS Calibur flow cytometer. [The values represent mean \pm standard deviation; One way ANOVA: p value ≤ 0.05 , ≤ 0.01 and ≤ 0.001 has been symbolized as *, ** and ***, respectively; n=3].

Further to know whether *PUFB⁻* cells affect cell size, we performed flow cytometry analysis (Figure 3.14 B). No significant difference between cell sizes of Ax2, *PUFB⁻* and *PUFB^{OE}* was observed.

3.4.9 Comparative developmental profile study of Ax2, *PUFB⁻* and *PUFB^{OE}*

To understand the role of PUFB in multicellular development, cells of mutant strains of *PUFB* i.e. *PUFB⁻* and *PUFB^{OE}* along with wild type were developed on NNA plates at a final density of 5×10^7 cells mL^{-1} . After synchronization at 4°C for 4-6 h, the cells were allowed to develop at 22°C and pictures were taken at different time interval as shown in figure 3.15.

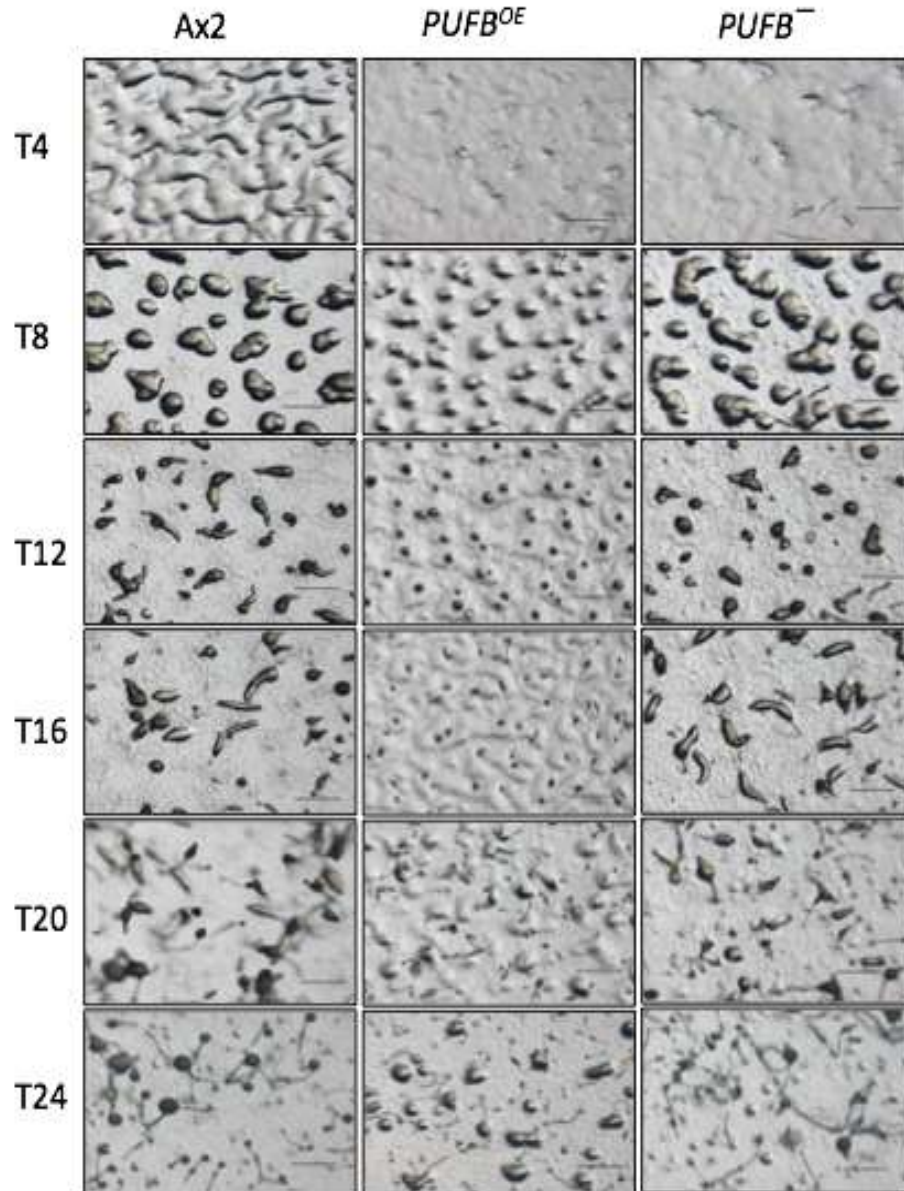


Figure 3.15: Developmental profile of *PUFB⁻* and *PUFB^{OE}* as compared to the wild type *Ax2* cells. All the strains were grown till log phase ($\sim 3\text{-}5 \times 10^6$ cells mL^{-1}), washed and spotted on NNA plates at a density of $\sim 5 \times 10^7$ cell mL^{-1} and kept for synchronization of development. Different developmental stages were photographed using Nikon- SMZ1500 microscope. The timings after starvation is also indicated. scale bar; 500 μm [n=3].

Wild type *Ax2* develop synchronously and start streaming at 4 h while in case of *PUFB⁻* and *PUFB^{OE}* streaming did not occur till 4 h, suggesting a delay in the initiation of development of both the mutant strain. After 8 h of development wild type *Ax2* cells formed tight aggregates while *PUFB⁻* and *PUFB^{OE}* cells formed loose aggregate. The number of loose aggregates formed by the overexpressing strain was much less (~ 2.5 fold

decrease) as compared to wild type and also in *PUFB* null strain number of loose aggregates formed were significantly lower (~1.5 fold decrease) (Figure 3.16 B). Also, the size of loose aggregate formed by the *PUFB*^{OE} cells are smaller (~4.5 fold decrease) as compared to the wild type while in case of *PUFB*⁻ cells, relatively larger aggregates (~1.3 fold increase) are formed (Figure 3.16 A and C).

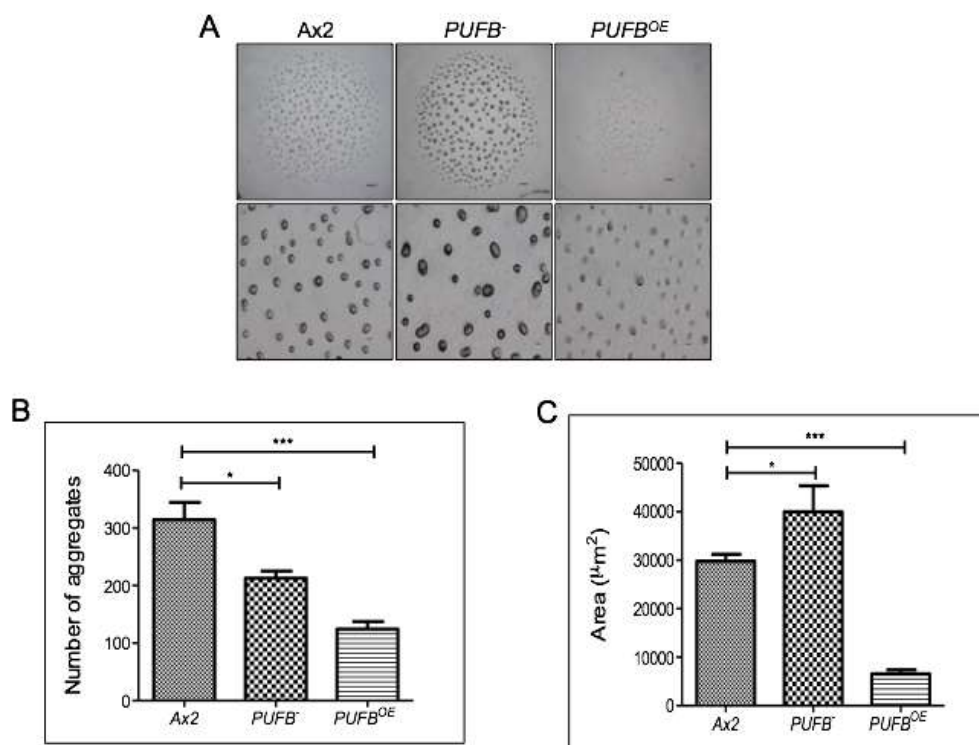


Figure 3.16: Analysis of aggregate size in Ax2, *PUFB*⁻ and *PUFB*^{OE} strains (A) The image shows the complete spot of cells plated for development on NNA plate. (B) The graph shows the number of aggregates formed by each strain. (C) The graph representing the area of mounds in Ax2 *PUFB*⁻ and *PUFB*^{OE} cells. [The values represent mean \pm standard deviation; ***p < 0.001, **p < 0.01(Student's t-test); n=3].

At 12 h in Ax2, the formation of slug began but in case of *PUFB*⁻ and *PUFB*^{OE} strains they were still in the mound stage suggesting the delayed development of the mutant strains during the initial part of the developmental life cycle. But as time progressed the mutant strain matched up to the developmental timing and formed slug at 16 h, comparable to the slug formed by wild type cells. The slugs formed by the overexpressor strain are smaller in size as compared to wild type Ax2 and *PUFB*⁻ strain. Finally, they all culminated into the fruiting body at 24 h.

3.4.10 Morphological analysis of the fruiting bodies in *Ax2* and *PUFB* mutants

Fruiting bodies formed by the overexpressing strain are smaller in size having relatively large sorus while *PUFB* null cells formed large fruiting bodies as compared to the wild type (Figure 3.17A).

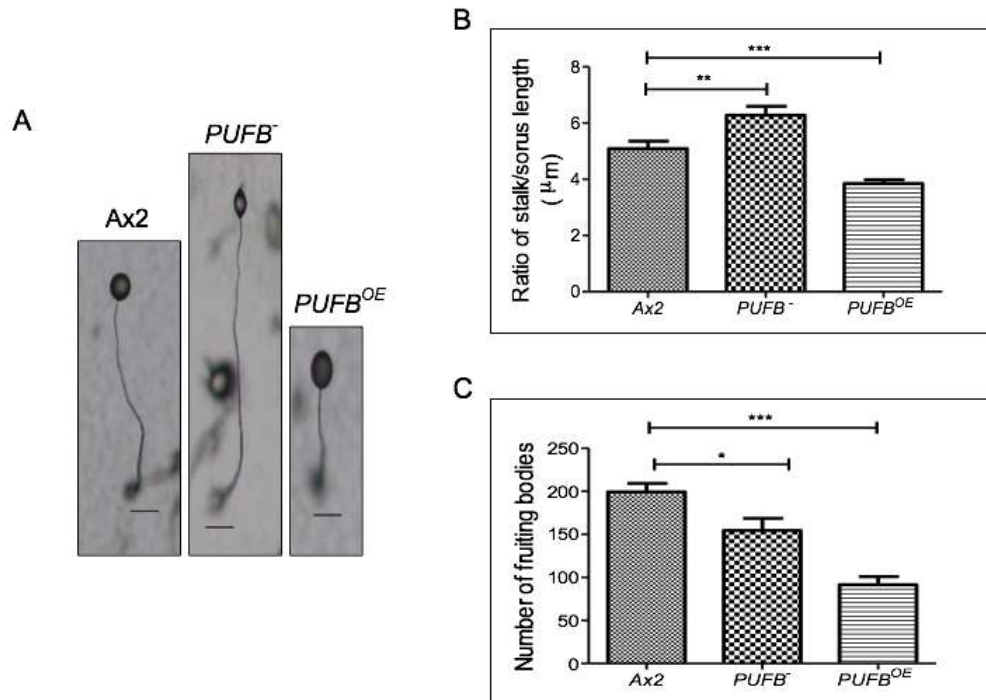


Figure 3.17: Morphological analyses of the fruiting bodies formed by *PUFB* mutants and its comparison with wild type cells. (A) Images showing the fruiting body of *Ax2*, *PUFB⁻* and *PUFB^{OE}* strains. (B) The graph represents the stalk to sorus ratio of fruiting bodies formed by each strain (C) The graph represents the number of fruiting bodies formed by each strain. [The values represent mean \pm standard error; One way ANOVA: p-value ≤ 0.05 , ≤ 0.01 and ≤ 0.001 has been symbolized as *, **, and ***, respectively; number of fruiting body analyzed ~ 200 ; $n = 3$].

Stalk to spore ratio of *PUFB⁻* was found to be 1.25 fold more than the wild type suggesting that *PUFB⁻* formed stalky fruiting body while in case of *PUFB^{OE}* the ratio was found to be ~ 1.6 fold less than the wild type suggesting that the fruiting body formed by the *PUFB^{OE}* had small stalk and relatively large sori (Figure 3.17B). The numbers of fruiting bodies formed by *PUFB⁻* (~ 1.3 fold decrease) and *PUFB^{OE}* (~ 2.2 fold decrease) are lower in number as compared to the wild type (Figure 3.17 C). Both *PUFB⁻* and *PUFB^{OE}* mutant strains showed asynchronous development as all the structures formed during the intermediate stage of development did not culminate into fruiting bodies.

3.4.11 mRNA expression of genes involved in aggregate formation

Defects observed in the aggregation of *PUFB* mutants could be due to the number of cells that participate in the formation of multicellular structure, any alteration in cell adhesion, the counting mechanism that is responsible for controlling the aggregation size in *Dictyostelium* and intracellular as well as extracellular cAMP level (Jang et al., 2002; Jang and Gomer, 2008).

Counting factor (CF), a 450 kDa complex is composed of about five polypeptides including Countin and CF50 that plays a major role in regulating the number of cells within the mounds. It regulates group size by down-regulating cell-cell adhesion proteins Gp24 (CadA) (Roisin-Bouffay et al., 2000). A gene called *smlA* which regulates the expression of CF as in the absence of *smlA* gene the level of CF increases, resulting in the formation of smaller aggregates and fruiting body than wild type (Brock et al., 1996; Brock and Gomer, 1999). Countin, a 40 kDa hydrophilic protein negatively regulates the aggregates size and cell adhesion. By regulating the number of cells that participates in the aggregate formation Countin regulates the size of aggregates. Elevated Countin levels cause breaking of aggregates that eventually results in small-sized fruiting bodies with less number of spores per sorus (Spratt Jr and Haas, 1961). The mRNA level of *ctnA* was found to be high during early stages of development in case of *PUFB^{OE}* which contributes to the formation of small-sized aggregates and thus small sized fruiting bodies as well. In the case of *PUFB* an expression of *ctnA* was low during the early stages of development, which leads to the formation of relatively large-sized aggregates as compared to Ax2 (Figure 3.18A).

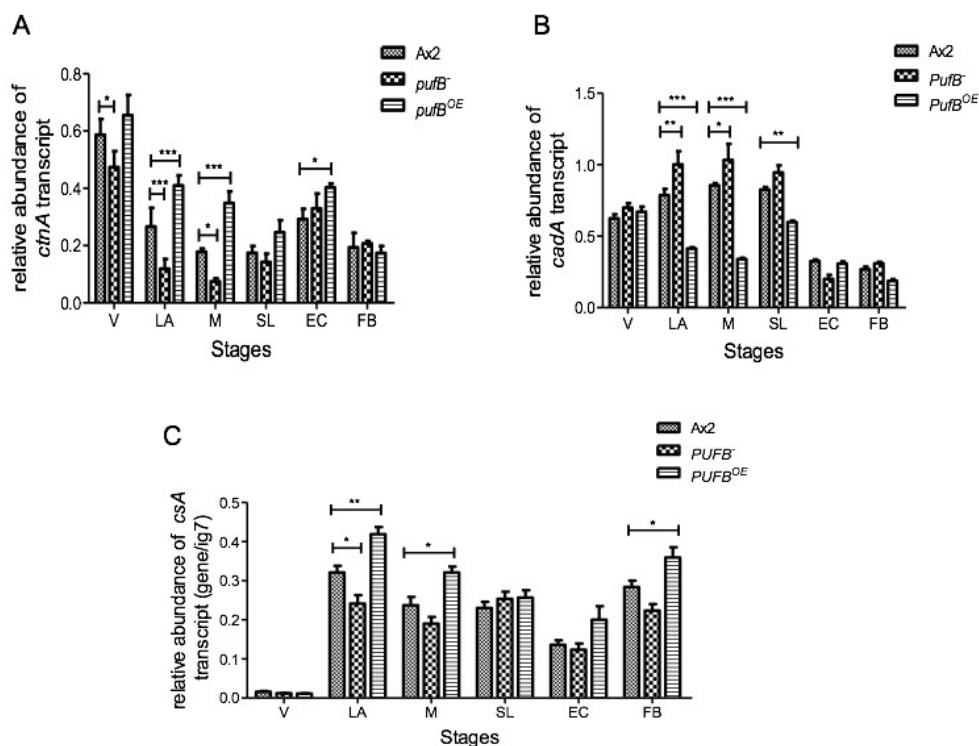


Figure 3.18: mRNA expression of genes involved in early development. The relative abundance of the various transcripts involved in the formation of aggregates during early development in wild type Ax2. *PUFB*^{OE} and *PUFB*⁻ were analyzed. (A) The relative abundance of *ctnA* in Ax2, *PUFB*⁻ and *PUFB*^{OE} cells (B) Relative abundance of *cadA* in Ax2, *PUFB*⁻ and *PUFB*^{OE} cells. (C) The relative abundance of *csA* in Ax2, *PUFB*⁻ and *PUFB*^{OE} [ctnA- CounTiN; csA- Contact Site A protein and cadA- Calcium-dependent ADhesion molecule A. [V- Vegetative stage, LA- Loose aggregate, M- Mound, S- Slug, EC- Early Culminant, FB- Fruiting body; The value represents mean \pm standard deviation; Two way ANOVA: p-value ≤ 0.05 , ≤ 0.01 and ≤ 0.001 has been symbolized as *, ** and ***, respectively; n=3].

Two cell adhesion proteins namely Gp24 (CadA) and Gp80 (CsA) that play an important role in regulating the size of the aggregates are expressed during early development. CadA, like Cadherins is calcium-dependent cell adhesion molecule. In *Dictyostelium* *CadA* gene codes for DdCAD-1, a calcium-dependent cell adhesion molecule. If *cadA* is deleted, it leads to a reduction in EDTA-sensitive cell adhesion, cell-type proportioning and pattern formation (Wong et al., 2002). The contact site A (CsA) glycoprotein is a Ca²⁺-independent cell adhesion protein in *Dictyostelium discoideum*. Both CadA and CsA mediate EDTA-sensitive cell adhesion. It had been reported that the overexpression of *CsA* leads to the fragmentation of aggregates i.e. it causes aggregation stream to break up leads to the formation of small size aggregates (Faix et al., 1992). The

expression of *CadA* mRNA in *PUFB*⁻ was found to be significantly high in early developmental stages i.e. in loose aggregate and mound resulting in increased cell-cell adhesion and thus form the relatively large size aggregate while in case of *PUFB*^{OE} the expression was significantly low as compared to wild type Ax2 (Figure 3.18 B) suggesting that the cell-cell adhesion is low and thus form small-sized aggregates. The level of *CsA* in *PUFB*⁻ was found to be significantly low in loose aggregate stage and leads to the formation of large sized aggregate along with the activity of *CadA*. While in other stages the decrease in *CsA* level was not significant. In *PUFB*^{OE} the expression of *CsA* was observed to be high (Figure 18 C) in the loose aggregate, mound resulting in the formation of small-sized aggregates.

3.4.12 Expression levels of spore coat proteins and spore viability in *PUFB* mutants

As we observed that very less number of fruiting bodies formed by *PUFB*⁻ and *PUFB*^{OE} strains, we were interested to check the viability of spores formed by these mutants.

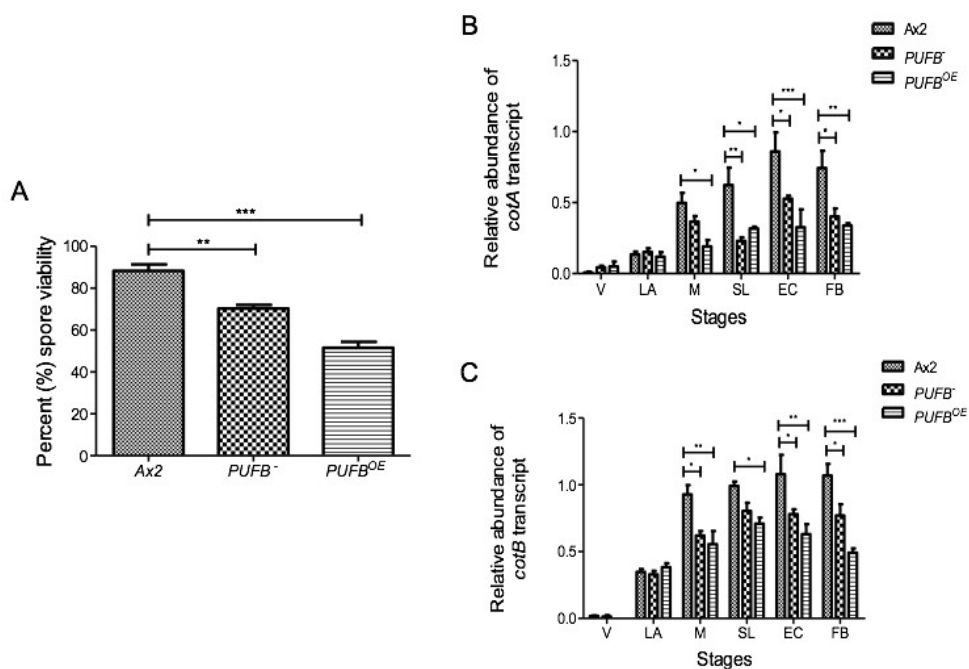


Figure 3.21: Spore viability and mRNA expression of genes involved in development. (A) Spore viability of Ax2, *PUFB*⁻ and *PUFB*^{OE} strains. (B) RT-PCR analyses of spore coat gene (*cotA*) (C) RT-PCR analyses of spore coat gene *cotB* during the development of Ax2, *PUFB*⁻ and *PUFB*^{OE} using *ig7* as an internal control. [V-Vegetative, LA-Loose aggregate, M- Mound, S- Slug, EC-Early Culminant, FB- Fruiting body; The values

represent mean \pm standard error; Two way ANOVA: p-value ≤ 0.05 , ≤ 0.01 and ≤ 0.001 has been symbolized as *, ** and ***, respectively; n=3]

The average spore viability of Ax2 was $88.25 \pm 3.025\%$, similar to earlier studies (Brock and Gomer, 2005; Myre et al., 2011). While the average spore viability of *PUFB*⁻ and *PUFB*^{OE} were significantly reduced to $70.25 \pm 1.7\%$ and $51.5 \pm 2.8\%$, respectively (Figure 3.19 A). Therefore, it suggests that PUFB protein should be present in optimal concentration for spore germination as very high or very low concentration of this protein reduces the efficiency of spores to germinate properly. This led us to investigate the expression of two proteins that are present specifically in spores, SP96 and SP70. *cotA* and *cotB* genes encode spore coat proteins SP96 and SP70, respectively that are expressed throughout the post-aggregation stages of development in *Dictyostelium* and are required for maintaining the integrity of spore coat. *cotA* expression is dependent on extracellular cAMP while cAMP-dependent protein kinase regulates the expression of *cotB* (Hopper et al., 1995). Deletion of *cotA* and *cotB* leads to reduced spore viability due to increased porosity of the spore coat (Fosnaugh et al., 1994). We analyzed the expression of *cotA* and *cotB* mRNA during the development of *PUFB*⁻ and *PUFB*^{OE} along with wild type Ax2. We found the expression of both *cotA* and *cotB* were significantly decreased in *PUFB*⁻ and *PUFB*^{OE} as compared to the wild type Ax2 cells (Figure 3.19 B and C).

3.4.13 *PUFB* mutants show reduced cAMP signaling

As we observed that the development was delayed in both *PUFB*⁻ and *PUFB*^{OE} strains as compared to the wild type, it led us to investigate whether it involves any change in cAMP level. It is well known that cAMP and cell adhesion molecules are essentially required during the early development in *Dictyostelium discoideum*. The cAMP-mediated cell signaling and chemotaxis to cAMP (chemoattractant) are two important mechanisms that control aggregation in *Dictyostelium* (Manahan et al., 2004). Defects observed in the aggregation of *PUFB*⁻ and *PUFB*^{OE} may involve the alteration in cAMP signaling.

For this, we measured cAMP levels in wild type Ax2 and both *PUFB* mutant strains. Cells from the log phase culture of Ax2, *PUFB*⁻ and *PUFB*^{OE} were starved for 0,

4 and 6 h and the levels of cAMP were measured by using cAMP Enzyme Immunoassay Kit. For the quantitative estimation of cAMP, this kit uses polyclonal antibody specific to cAMP that binds to cAMP in a competitive manner. We harvested the samples and treated them with 0.1 M HCl and incubated at room temperature in 96 well plate coated with a secondary antibody. Thereafter, the substrate was added which gives a yellow colour that represents an inversely proportional relationship with the concentration of cAMP in the samples. Reading was taken at 405 nm and cAMP concentration (pmol mL^{-1}) was calculated as per the manufacturer's instructions. Optical density obtained from the standard and samples were used to plot the graph.

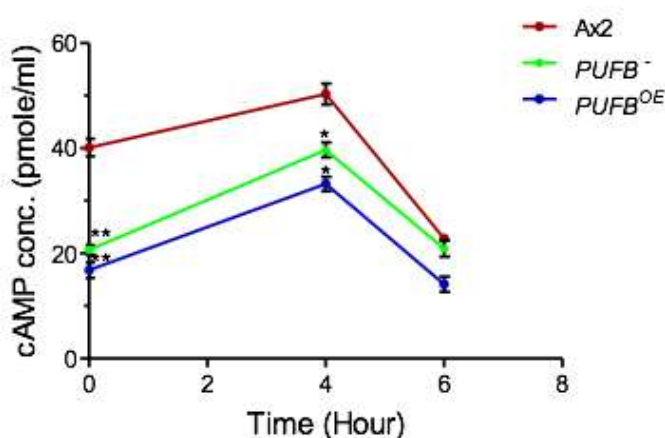


Figure 3.19: cAMP level measurements in Ax2, *PUFB*⁻ and *PUFB*^{OE} cells. The graph shows intracellular cAMP levels in various strains. cAMP concentrations in *PUFB*⁻ and *PUFB*^{OE} cells upon starvation was reduced when compared to the wild type cells. [The values represent mean \pm standard error; Student t-test: p-value ≤ 0.05 , ≤ 0.01 and ≤ 0.001 has been symbolized as *, ** and ***, respectively; ns: non-significant; n = 3].

It revealed that both the *PUFB* mutant strains showed a significant decrease in the cAMP level under starved condition. *PUFB*⁻ showed ~ 1.3 fold decrease in cAMP level while *PUFB*^{OE} showed ~ 1.5 fold decrease in cAMP level as compared to Ax2. Low levels of cAMP in both the *PUFB* mutant strains could be the possible reason for the delayed development. Low levels of cAMP slow down the chemotactic movement of cells and that could also be one of the possible reasons for the small-sized aggregates formed by the *PUFB*^{OE} cells (Figure 3.20). Interestingly the levels reached to near normal by 6 h, suggesting that normal development may proceed thereafter.

3.4.14 Expression level of genes involved in the cAMP signaling

We further analyzed the expression of genes involved in cAMP signaling. In response to starvation, cells undergo cAMP-mediated chemotaxis in *Dictyostelium*. cAMP signaling plays a very important role in the expression of genes required for aggregation and in the induction of post-aggregative differentiation in *Dictyostelium discoideum* (Kay, 1982; Schaap and van Driel, 1985). Under starvation condition conversion of ATP to cAMP by aggregation stage adenylyl cyclase (*AcaA*) leads to the release of extracellular cAMP that functions as a chemoattractant by binding to the high-affinity cAMP receptor (*CarA*) on the surface of neighboring cells that triggers chemotaxis, streaming and aggregation (Huber et al., 2017). To understand the cAMP signaling in *PUFB* mutant strains, we analyzed the mRNA expression pattern of *acaA* (*adenylyl cyclaseA*), *carA1* (*cyclic AMP receptor1*) and *pdsA* (*extracellular cAMP phosphodiesterase*) genes.

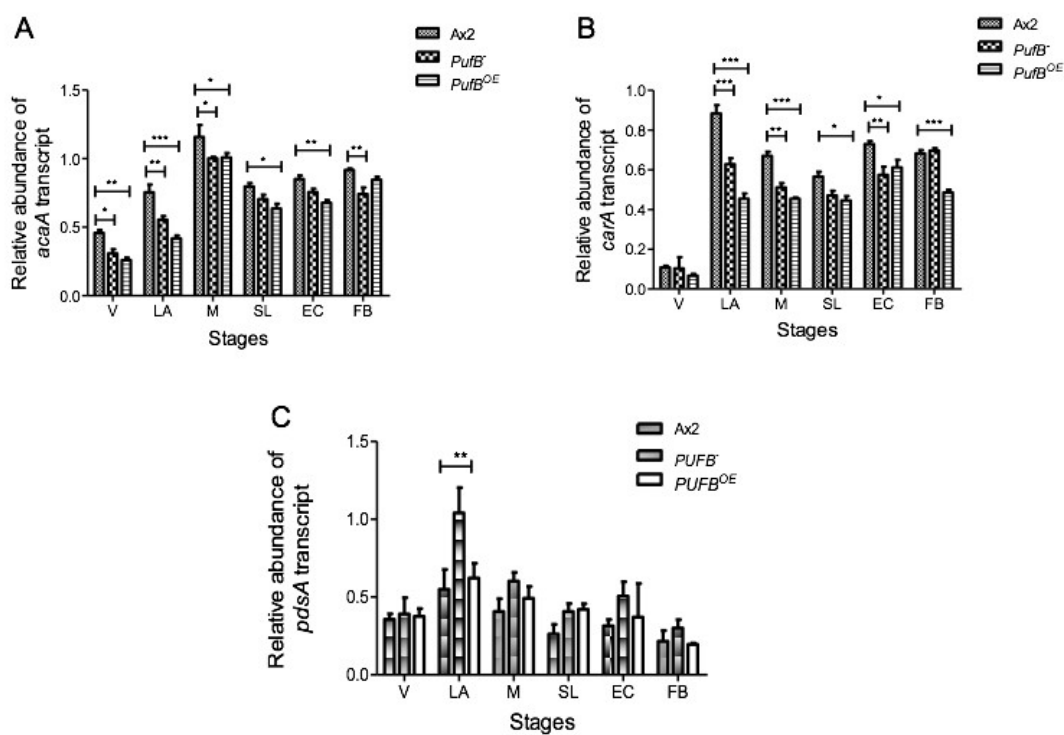


Figure 3.20: mRNA expression of genes involved in cAMP signaling. (A) The relative abundance of *acaA* in Ax2, *PUFB*⁻ and *PUFB*^{OE} cells. (B) The relative abundance of *carA1* in Ax2, *PUFB*⁻ and *PUFB*^{OE} cells and (C) Relative abundance of *pdsA* in Ax2 *PUFB*⁻ and *PUFB*^{OE} cells. [V- Vegetative, LA-Loose aggregate, M- Mound, S- Slug, EC-Early Culminant, FB- Fruiting body. The values represent mean \pm standard error; Two way ANOVA: p-value ≤ 0.05 , ≤ 0.01 and ≤ 0.001 has been symbolized as *, ** and ***, respectively; ns: non-significant; n = 3].

The mRNA expression of *acaA* and *carA* was found to be significantly low during the initial stages of development in both *PUFB*⁻ and *PUFB*^{OE} mutant strains responsible for the delay in development and also less number of aggregate formation (Figure 3.21 A and B). Low levels of *acaA* and *carA* cause low cAMP levels during culmination stage, which results in the reduced viability of spores formed by *PUFB*⁻ and *PUFB*^{OE} mutant strains. The cAMP level is further regulated by a cAMP phosphodiesterase (PdsA) which is responsible for the degradation of extracellular cAMP (Darmon et al., 1978). We checked the expression pattern of *PdsA* in both *PUFB* mutant strains. We found the expression was significantly high only in loose aggregates while in other stages its expression was non-significantly high in *PUFB*⁻. While in case of *PUFB*^{OE} no significant difference was observed (Figure 3.21 C) when compared to wild type, which could be because the level of cAMP is already less so it further does not need to be down regulated so that a certain level of cAMP is maintained to complete the development process.

3.5 CONCLUSIONS

As discussed earlier, *PUFB* is expressed in both growth and development. So it is expected to have a role in both cell proliferation and development of *Dictyostelium discoideum*. In this chapter, we have characterized the *PUFB* by successfully creating overexpressor and knockout strains.

The *PUFB*^{OE} strain was successfully created by expressing full length *PUFB* gene under constitutive *actin15* promoter fused with an *eYFP* reporter gene. This was confirmed by mRNA expression and microscopy studies. *PUFB* fusion protein showed localization in the cytosol. On the other hand knockout of *PUFB* was also successfully made by gene disruption method, which was confirmed by various PCR and mRNA expression studies. Both *PUFB*^{OE} and *PUFB*⁻ strains were further used to study the growth and development in *Dictyostelium discoideum*.

Cell proliferation and cell growth studies were performed and found that *PUFB*⁻ strain showed an increased proliferation rate as compared to wild type and cell cycle analysis showed that it could be possibly by suppressing G1 arrest and initiating the G1-S transition. While *PUFB*^{OE} strain showed decreased proliferation rate as compared to the wild type. Any significant difference was not observed during the cell cycle but showed

defects in exocytosis rate, which was found to be reduced as compared to wild type suggesting that reduced exocytosis leads to increased accumulation of undigested remnants which may cause toxicity to the cells affecting both cell proliferation and cell growth of *PUFB^{OE}* cells. We also showed cell growth analysis in which the cell mass of *PUFB^{OE}* was found to be significantly low as compared to Ax2 and *PUFB⁻* strain suggesting decreased cell growth of *PUFB^{OE}* cells.

We showed that mutation of *PUFB* leads to defects in the multicellular development of *Dictyostelium*. We observed that there was a defect in the aggregation size determination mechanism as *PUFB^{OE}* strain formed very less number of small-sized aggregates as compared to the wild type while *PUFB⁻* strain formed less number of relatively large size aggregates. And this defect was found to be because of misregulation of certain genes involved in aggregation. In *PUFB^{OE}* less number of small-sized aggregates formation was due to increased expression of *Countin* and *csA*, a cell adhesion molecule and lower expression of *cadA* another cell adhesion molecules. While in case of *PUFB⁻*, *countin* and *csA* expression was found to be low and lower expression of *cadA* leads to relatively large-sized aggregates.

Because of the mutation of *PUFB*, defect in cAMP signaling was observed as the levels of cAMP was low in both the mutant strains and also there was misregulation of cAMP signaling mRNA of *acaA*, *carA* was observed. Due to this development of both the strains are delayed and also contribute to defects in aggregation size and number. Formation of the fruiting body is one of the important aspects in the life cycle of *Dictyostelium* to maintain their generation. We found an alteration in the morphology of fruiting body as *PUFB⁻* forms large fruiting bodies while *PUFB^{OE}* forms a smaller fruiting body having a small stalk and relatively large sorus. Also, the spore viability of both the mutant strains was found to be significantly low because of the reduced expression of *cotA* and *cotB*. It suggests that an optimum level of *PUFB* protein is required for the efficient spore formation. Thus, our study suggests the important role of *PUFB* during growth and development by regulating the expression of genes important in growth and development of *Dictyostelium discoideum*.

4.1 INTRODUCTION

Dictyostelium cells exist as a unicellular haploid amoeba/myxamoeba that *via* phagocytosis feeds on bacteria and grow vegetatively through mitotic division (binary fission). Starvation is the major factor that triggers the vegetative unicellular cells towards multicellular development and leads to the expression of a variety of new genes, which are responsible for chemotaxis both towards folic acid (factors from bacteria) and cAMP. Each and every amoeba can sense the cAMP, respond by releasing cAMP and leads to the signal amplification and relay. In response to cAMP, millions (10,000-1,00,000) of highly polarized chemotactic amoeba undergo head to tail streaming to a common point to form a multicellular structure called loose aggregate (Kimmel and Firtel, 1991). From this very stage onwards differentiation of cell into prestalk and prespore cells starts in response to cAMP signaling and cell-specific gene expression can be observed (Araki et al., 1997). Cellular movements in the mound stage lead to the formation of distinct prestalk (having prestalk cells) and prespore zones (having prespore cells). Some cells at the tip-organizer secrete cAMP due to which *pstA* and *pstO* cells move towards the tip and lead to the formation of tipped-mound (Dormann and Weijer, 2001). Reports suggest that deletion of Disintegrin family proteins that are crucial for differential, cell adhesion and movement of prestalk cells leads to defects in cell sorting and cell-type specific patterning (Varney et al., 2002). Migrating slug has been considered as the best stage to study pattern formation as the two specified prestalk and prespore forms a typical pattern where the anterior is composed of prestalk cells and the posterior is composed of prespore. Prestalk cells show expression of specific marker genes, *ecmA* and *ecmB*. *PstB* cells express *ecmB* gene. *PstAB* cells express both *ecmA* and *ecmB* genes (Jermyn et al., 1987). Prestalk cells expressing both *ecmA* and *ecmB* are present in the core of anterior region called *pstAB* cells (Gaskell et al., 1992). During culmination, it moves to the posterior position of the fruiting body forming the stalk region that makes the basal disc (Ceccarelli et al., 1991). Prespore cells express *cotB* gene (Loomis, 1993), the prespore region consists of *pstA*, *pstB* and ALCs (anterior-like cells) (Figure 4.1).

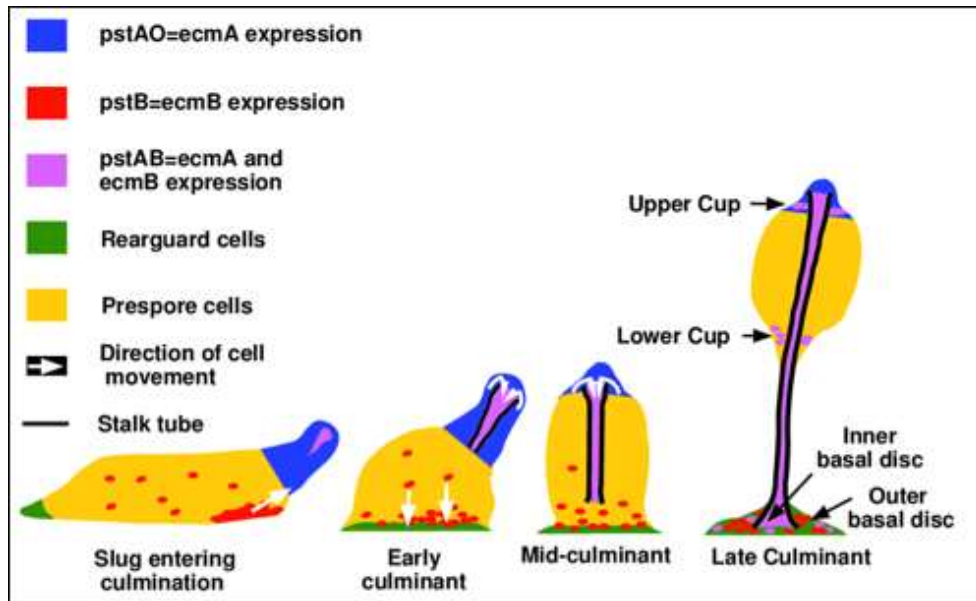


Figure 4.1: Diagrammatic representation of morphogenesis and cell differentiation in *Dictyostelium*. Spatial expression pattern of different prestalk and prespore cell-types in the slug, early culminant and fruiting body. Different cells are shown as blocks of colour. The fate of different cells in various multicellular structures are shown (adapted from Jermyn *et al.*, 1996)

Various studies suggest the important role of PUF protein in the differentiation and patterning of organisms. In *Drosophila*, PUF protein is responsible for maintaining the anterior-posterior patterning of embryo where mutation of this gene leads to the abnormal segmentation of the early embryo (Lehmann and Nüsslein-Volhard, 1987; Barker *et al.*, 1992). In *C. elegans*, PUF protein is responsible for maintaining spermatogenesis to oogenesis transition (Zhang *et al.*, 1997) and also for maintaining the pool of Germline stem cell (Shin *et al.*, 2017). In *Arabidopsis thaliana*, it plays a role in the growth and development, morphogenesis of leaves (Huang *et al.*, 2014; Reichel *et al.*, 2016). In *Dictyostelium*, patterning and cell-type differentiation plays a crucial role in the multicellular development and terminal differentiation into the fruiting body and as discussed above the role of PUF in cell differentiation and patterning. So in this chapter, we would explore the functions of PUFB in cell-type differentiation and patterning of this organism. As discussed in the previous chapter that mutation in PUFB leads to aberrant development and multicellular structures formed, thus we hypothesized that this defect would be due to the improper proportioning of the cells or alteration in the prestalk to the prespore ratio of cells.

4.1.1 Cell death and autophagy in *Dictyostelium*

In the life cycle of *Dictyostelium*, starvation-induced multicellular development leads to the formation of the fruiting body which is composed of dead vacuolated stalk cells and live spore cells (Whittingham and Raper, 1960; Schaap et al., 1981). Since in *Dictyostelium* cell death by apoptosis does not occur because of the absence of caspases or metacaspases (Eichinger and Noegel, 2003), thus cell death by means of developmental programmed cell death is the only process that leads to the formation of stalk cells (Laporte et al., 2007). *Dictyostelium* can undergo either autophagic or necrotic cell death depending upon the environmental conditions (Levraud et al., 2003; Kosta et al., 2004; Laporte et al., 2007). *D. discoideum* has been considered as a good model system for caspase-independent cell death or developmental autophagic cell death (ACD) which occurs in the absence of apoptosis. Starvation induces the Atg1 required for autophagosome formation (De Chastellier and Ryter, 1977; Tresse et al., 2007) and DIF promotes the stalk cell differentiation (Town et al., 1976; Town and Stanford, 1979) are the two mechanisms in *Dictyostelium* on which ACD depends.

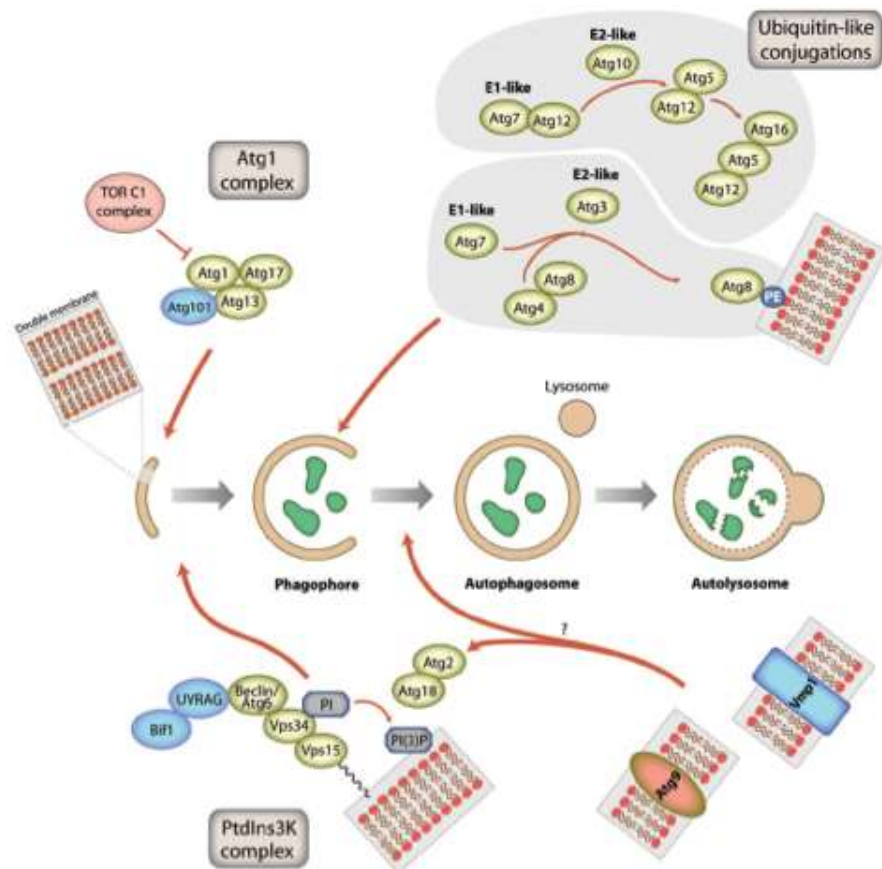


Figure 4.2: Autophagy signaling pathways of *Dictyostelium*. Phagophore engulfs the cytoplasmic materials, which then fuse with the lysosome, to degrade the

cytoplasmic materials and then recycled for later utilization. Role of *Dictyostelium* autophagy proteins in this signaling process hypothesized (Calvo- Garrido *et al.*, 2010).

TOR (target of rapamycin) regulates autophagy in *Dictyostelium*. It belongs to the serine/threonine kinase family made up of TOR, Kog1 (Raptor) and Lst8. It functions upstream of Atg1 complex and regulates cell metabolism and cell growth (Schmelzle and Hall, 2000; Mizushima, 2010). TORC1 and TORC2 are the two complexes formed by TOR after interacting with different proteins and it is TORC1, which is involved in autophagy. It regulates autophagy *via* the phosphorylation of Atg13 and Atg1 or through a signal transduction pathway with other proteins (Figure 4.2) (He and Klionsky, 2009). Autophagic mutants in *Dictyostelium* show aberrant development as it does not aggregate normally and forms defective fruiting bodies (Otto *et al.*, 2004). In mammalian cells, Atg8 (known as LC3 in mammals) is present in phagophore membrane in cytosolic form and on autophagosome present in the lipidated form. The conversion of LC1 to LC3 is used to study the process of autophagic flux while in *Dictyostelium* it is difficult to interpret autophagic induction as Atg8 can be observed in one form only. *Dictyostelium* Atg1 is a serine/threonine protein kinase having a conserved kinase domain and conserved C-terminal domain that is essential for the induction and development of autophagosome. DdAtg1 and DdAtg8 colocalize on the autophagosome and recruit other proteins to the assembly site, which is required for the induction and maturation of autophagosomes (Tekinay *et al.*, 2006). DdAtg8 is an ubiquitin-like protein used as an autophagosome marker to study autophagic induction as it is attached to the autophagosome membrane upon lipidation by phosphatidylethanolamine (PE) (Mizushima, 2010). Autophagy can be monitored using GFP-Atg8 as a marker where GFP-Atg8 puncta represent the autophagosome formation and autophagy defect can be studied by monitoring variation in the GFP-Atg8 puncta formation (Klionsky *et al.*, 2008). In *Dictyostelium* ubiquitin-like protein conjugation system is formed by Atg5, Atg12 and Atg16 along with Atg8 and is required for the expansion of phagosome membrane into autophagosome (Webber *et al.*, 2007; Calvo-Garrido *et al.*, 2010). Interaction between Atg18 and Atg2 is mediated by phosphatidylinositol 3-phosphate, which is essential for the recruitment of other autophagic proteins to the assembly site and for autophagy to proceed (Figure 4.2).

Since *Dictyostelium* is a good model system to study autophagy and there are no reports of autophagy related to PUF proteins so we were interested to know its role in the autophagy process. Based on the above information we laid down the following objectives for this chapter.

4.2 OBJECTIVES

- To explore the role of PUFB in cell-type differentiation and patterning.

Following strains were prepared in Ax2 and *PUFB*⁻ cells:

- Ax2 cells: *ecmA-lacZ/Ax2*, *ecmB-lacZ/Ax2*, *ecmO-lacZ/Ax2*, *ecmAO-lacZ/Ax2* and *pspA-lacZ/Ax2*.
 - *PUFB*⁻ cells: *ecmA-lacZ/PUFB*⁻, *ecmB-lacZ/PUFB*⁻, *ecmO-lacZ/PUFB*⁻, *ecmAO-lacZ/PUFB*⁻ and *pspA-lacZ/PUFB*⁻.
- Exploring the role of PUFB in cell-lineage tracing in *Dictyostelium* by making chimeras. To perform this study *act15-GFP/Ax2* and *act15-RFP/PUFB*⁻ strains were prepared.
 - To explore the role of PUFB in the autophagy process by performing the autophagic flux study and expression level of different genes involved in the autophagy.
To achieve this objective Ax2 and *PUFB*⁻ cells were transformed with RFP-GFP-Atg8 to study autophagic flux.

4.3 MATERIAL AND METHODS

4.3.1 Storage of *Dictyostelium* spores

Dictyostelium Ax2 cells were grown in HL5 medium at 22°C and developed on SM agar plates to form fruiting bodies. Spores from sorus of fruiting bodies were collected in spore storage solution (pre-chilled) having 0.45 mL H-50 buffer, 0.1 mL DMSO and 0.45 mL horse serum. Aliquots of spore suspension were stored in 1.5 ml micro centrifuge tubes, slow freezing at -20°C for 1-2 h and finally stored in -80°C until further use.

4.3.2 mRNA expression analysis of cell-type specific marker using semi-quantitative RT-PCR

Log phase Ax2 and *PUFB*⁻ cells were developed on NNA plates at an equal cell density of 5×10^7 cells mL⁻¹. Various multicellular structures at different stages/timings

were collected and RNA isolation was done as mentioned in chapter 3. cDNA was prepared using Verso cDNA synthesis kit and further used for semi-quantitative RT-PCR of the cell-type specific marker genes. Expression analyses of mRNA levels of the cell-type specific marker genes *ecmA*, *ecmB* and *d19* were done using specific primer combinations as mentioned in Table 4.1

Gene Name	Primer Sequence (5'→3')	Genomic position	Expected amplicon cDNA size(bp)	Expected amplicon gDNA size(bp)
<i>ecmA</i> RT	FP: GATGATGGAAATAGATGGTCAACA	220-243	821	1017
	RP: GTACATTGGTTATTATCATCGACA	1236-1213		
<i>ecmB</i> RT	FP: GTGGTGTTACTCATACTCCAATTCGTT	2611-2637	674	756
	RP: CATTGGAACATGAATACATTACCACC	3366-3340		
<i>pspA</i> RT	FP:GATAGGATCCCCAGTTTGTGCTTCAGTAGATGTC	94-117	341	341
	RP:ACTTCTCGAGGTTGTTGTTGATGTTTGGGATGG	434-415		

Table 4.1: List of primer combinations used for the semi-quantitative RT-PCR expression analyses of cell-type specific markers. It shows the genomic positions of primers used for expression analysis of ExtraCellular Matrix protein (*ecmA*), ExtraCellular Matrix protein (*ecmB*), PreSPore-specific gene A (*pspA*); expected amplicons sizes in bp from cDNA and gDNA are mentioned.

4.3.3 β -galactosidase staining in multicellular structure for cell type patterning studies

Cell-type patterning using β -galactosidase staining was performed as mentioned by Gosain et al. (2012) with slight modifications from the protocol described by Escalante and Sastre (2006). The log phase cells of wild type Ax2 and *PUFB*⁻ cells were transformed with cell-type specific prestalk marker genes like *ecmA*, *ecmB*, *ecmO* and *ecmA*O and fused to LacZ reporter. Also, transformed with cell-type specific prespore marker gene *pspA* (*d19*) fused to LacZ reporter. Log phase cells ($3-5 \times 10^6$ cells mL⁻¹) expressing *ecmA*, *ecmB*, *ecmO*, *ecmA*O and *pspA* (*d19*) fused to LacZ reporter from Ax2 and *PUFB*⁻ were collected and washed with 1xKK2 buffer (ice cold) and resuspended in 1xKK2 at an equal cell density of 5×10^7 cells mL⁻¹. Cell suspension of Ax2 and *PUFB*⁻ were spotted (15-20 μ L) on dialysis membrane placed on 1.5% non-nutrient agar plates. Cells were kept at 22°C to develop and form various multicellular structures that were collected in 24 well plates. Various developmental structures collected on dialysis membrane were fixed with methanol at room temperature for 30 minutes. Structures were then washed twice with Z buffer to remove the methanol completely and incubated for 1 h in permeabilization buffer containing 0.1% NP40 in Z-buffer. This was followed by washing the structures with Z-buffer for 2-3 times and staining the structure using

staining solution containing X-gal (20 mg mL⁻¹), potassium ferrocyanide (133 mM) and potassium ferricyanide (133 mM). Colour reaction was stopped after evident staining was observed in structures by washing the structures with Z buffer for 2-3 times. Images of stained structures of Ax2 and *PUFB*⁻ were captured using Nikon AZ100 microscope.

4.3.4 Development of chimeras of Ax2 cells tagged with GFP and *PUFB*⁻ cells tagged with RFP

Log phase Ax2 cells tagged with GFP and *PUFB*⁻ tagged with RFP were collected, washed with ice-cold 1xKK2 buffer twice and resuspended in 1xKK2 buffer at a cell density of 1x10⁶ cells mL⁻¹. Cells from each strain were then mixed in various proportions (10% to 100%), collected by centrifugation at 3000 rpm for 2-3 minutes, washed with ice-cold 1xKK2 and resuspended in 1xKK2 to a final dilution of 5x10⁷ cells mL⁻¹. Cell suspensions in various proportions were then spotted (15-20 µL) on 1.5% NNA plates and kept at 22°C to develop. Developmental structures formed by mixing of tagged Ax2 and *PUFB*⁻ cells in various proportions were observed at different developmental timings and photographed (both DIC and fluorescent images) using Nikon SMZ1500 microscope.

4.3.5 Spore count from fruiting bodies developed from the chimeras

Fruiting bodies formed from chimeras of Ax2 cells tagged with GFP and *PUFB*⁻ tagged with RFP in various proportion from 10% to 100% were used for spore count by picking spore-heads from the individual fruiting body on a glass slide. Spores were visualized under Nikon eclipse 80i fluorescence microscope and photographed using DIC, TRITC and FITC filter to count the number of red and green fluorescent spore. 10–15 fruiting bodies from each proportion per experiment were counted.

4.3.6 mRNA levels of autophagy-related genes in wild type Ax2 and *PUFB*⁻ cells

cDNA was prepared using Verso cDNA synthesis kit (Thermo Scientific) as mentioned earlier and semi-qualitative RT-PCR was carried for various genes that are involved in autophagy like *atg1*, *atg5*, *atg18*, and *atg8*. The specific primer combinations used are mentioned in Table 4.2.

Oligo Name	Primer Sequence (5'.....3')	Genomic Position	Expected amplicon cDNA size(bp)	Expected amplicon gDNA size(bp)
<i>atg1</i> RT	FP: ATGAAACGAGTAGGAGAT	1001-1018	661	788
	RP: TAATAGGTCTGGTACTGAACC	1768-1788		
<i>atg8</i> RT	FP: ATGTATCAAGCTTTAAAAACGACCAC	1008-1033	362	590
	RP: TTATAAATCACTACCAAAAAGTATTCACC	1568-1597		
<i>atg5</i> RT	FP: ATGTCATTTGACGAA	1001-1018	494	618
	RP: GGGTATGATTGGAAATGAAC	1599-1618		
<i>atg16</i> RT	FP: ATGTTTTTCATCACAAAATAA	1001-1020	719	800
	RP: TCTTCAACTAACTACTA	1782-1800		
<i>atg18</i> RT	FP: ATGAATGTTGGAGGTAAATT	1001-1020	685	920
	RP: TACTATGAATGATTGCAGGT	1901-1920		

Table 4.2: List of primer combinations used for semi-quantitative RT-PCR analyses of autophagy-related genes. Expected amplicon sizes of cDNA and gDNA are mentioned.

4.3.7 Analysis of autophagic flux using *RFP-GFP-Atg8* assay

Autophagic flux was measured in both wild type Ax2 cells and *PUFB*⁻ cells that were transformed with plasmid containing tandemly fused *RFP-GFP-Atg8*, selected on antibiotic (G418) (Calvo-Garrido et al., 2011; Lohia et al., 2017). Autophagic flux was analysed by confocal microscopy under different stimuli like control, starvation for 4 h and treatment with 100 mM NH₄Cl (lysosomotropic agent) for 4 h in both wild type Ax2 cells and *PUFB*⁻ cells. Autophagic flux was calculated by counting the number of fluorescent puncta formed per cell in both the samples. For preparation of starvation sample, log phase cells from both wild type Ax2 cells and *PUFB*⁻ cells were collected by centrifugation at 3,000 rpm for 3 minutes in 1x KK2 at 22°C and incubated for 4 h at 22°C under shaken conditions (120 rpm). For preparation of NH₄Cl treated sample, harvested wild type Ax2 cells and *PUFB*⁻ cells were resuspended in HL5 media at a cell density of 1x10⁶ cells mL⁻¹ and 1 mL of cell suspensions were placed in a sterile 6-well plate. 100 mM NH₄Cl was added twice to the cells at an interval of 2 h and incubated at 22°C. The NH₄Cl treated cells from each well were collected by centrifuged at 3,000 rpm for 3 minutes. Treated as well as control samples were placed on thin layer of 1% agarose slides for visualization under Nikon confocal microscope using Andor iQ 2.7.1 software. The fluorescent puncta (Red or Green)/cell were analyzed by NIS Elements AR version 4.0.

4.4 RESULTS AND DISCUSSION

4.4.1 Cell-type differentiation and patterning in *PUFB*⁻

Till there is surplus food, *Dictyostelium* cells grow and divide mitotically but as food becomes limited they initiate multicellular developmental. In response to cAMP, *Dictyostelium* cells move towards each other to form aggregates (Kay, 1982; Loomis, 1993). During multicellular development cell differentiation in *Dictyostelium* occurs forming prestalk and prespore cells which finally forms terminally differentiated stalk and spore cells, respectively. Thus, during development, cAMP signaling plays a crucial role in cellular differentiation and pattern formation (Louis et al., 1994; Williams, 1995; Bretschneider et al., 1997). The differentiated cell-types show characteristic expression patterns of specific marker genes and during development, the ratio of prestalk and prespore cells remain constant regardless of the size of the slug and any alteration in this leads to the aberrant differentiation (Chung et al., 1998; Jaffer et al., 2001). Prestalk cells are distinguished by the expression of two specific markers, *ecmA* and *ecmB* (extracellular matrix) (Jermyn et al., 1987). PstA (*ecmA*-expressing prestalk cells) cells are scattered in the aggregate but during mound stage, it migrate upwards forming the tip. PstB (*ecmB*-expressing cells) cells are present in the basal region of the mound while the prespore cells are present in the posterior region of slug except at the base and the tip region (Williams et al., 1989).

To elucidate the role of *PUFB* in cell-type differentiation and patterning, cell-type specific marker expression studies were performed by RT-PCR and *lacZ* reporter assay during the development of Ax2 and *PUFB*⁻ cells. We analyzed the mRNA levels of prestalk specific marker (*ecmA* and *ecmB*) and prespore specific marker (*pspA* or *d19*) using specific primer combinations (Table 4.1). The mRNA expression level of prestalk-specific gene *ecmA* in *PUFB*⁻ shows a significant increase from the mound stage to the fruiting body as compared to the wild type Ax2. The mRNA expression level of the prespore marker, *pspA* was significantly reduced during later stages of development but in mound stage, it showed an insignificant decrease in *PUFB*⁻ cells as compared to wild type Ax2 cells (Figure 4.3).

To substantiate our results, we examined the spatial cell-type patterning in both Ax2 and *PUFB*⁻ cells by using cell-type specific promoters fused to *LacZ* reporter.

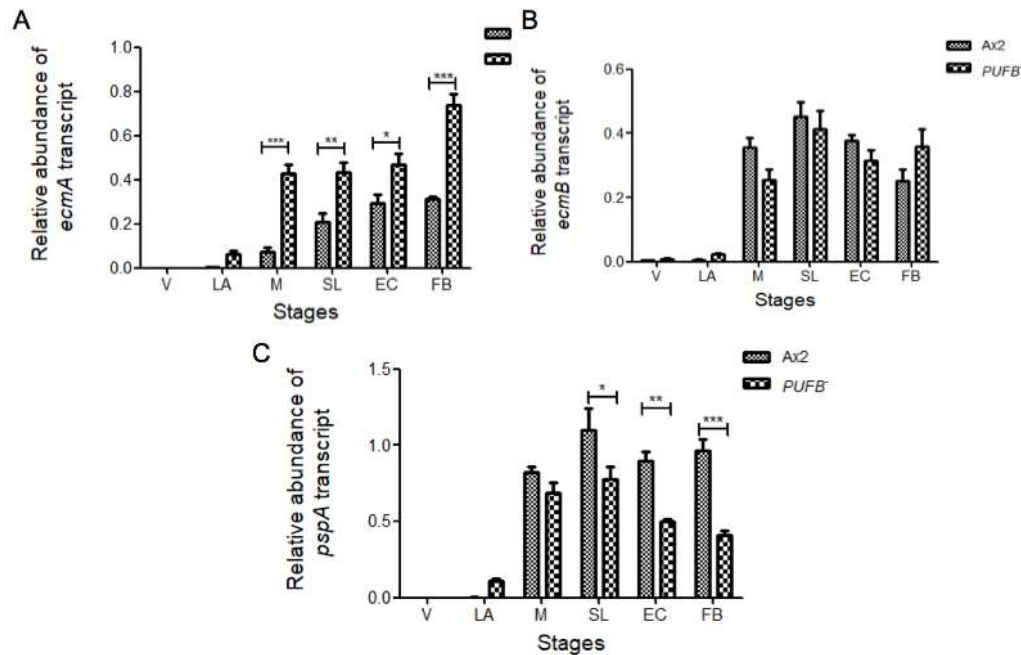


Figure 4.3: mRNA expression analysis of cell-type-specific marker genes during the development of Ax2 and *PUFB⁻* cells. Relative abundance of cell-type specific genes (A) *ecmA* (ExtraCellular Matrix protein A), (B) *ecmB* (ExtraCellular Matrix protein B) and (C) *d19* (*pspA*; PreSPore-specific gene) during developmental stages of Ax2 and *PUFB⁻* was analyzed using RT-PCR after normalization to *ig7*. [V: vegetative; LA: loose aggregate; M: mound; EC: early culminant; FB: fruiting body. The values represent mean; standard deviation; Two way ANOVA, p-value ≤ 0.05 , ≤ 0.01 and ≤ 0.001 has been symbolized as *, **, and ***, respectively; n=3].

Spatial expression pattern study of *ecmA/lacZ*

The wild type Ax2 cells were transformed with prestalk-specific *ecmA* promoter fused to *LacZ* reporter gene and selected at $40 \mu\text{g mL}^{-1}$ of G418 and the *PUFB⁻* cells were transformed with the same and selected at $40 \mu\text{g mL}^{-1}$ of G418 and $10 \mu\text{g mL}^{-1}$ of Blasticidin S. Various multicellular structures formed during development were collected in 24 well culture plates and fixed in methanol. Structures were permeabilized and stained with X-gal to analyze the staining pattern in both strains (Figure 4.4).

In case of Ax2, the expression in slug was found to be at the tip, which is formed by the prestalk cells and also in the fruiting body the expression was present in the anterior prestalk region (Figure 4.4 a & a'). In *PUFB⁻* the staining region in slug was found expanded as compared to Ax2 while in case of the fruiting body the staining was present in the anterior prestalk region which found to be expanded. Staining was also

present in the lower cup, stalk and basal disc as compared to wild type (Figure 4.4). In all the structures developed staining was found to be more pronounced than the wild type as is also revealed by RT-PCR.

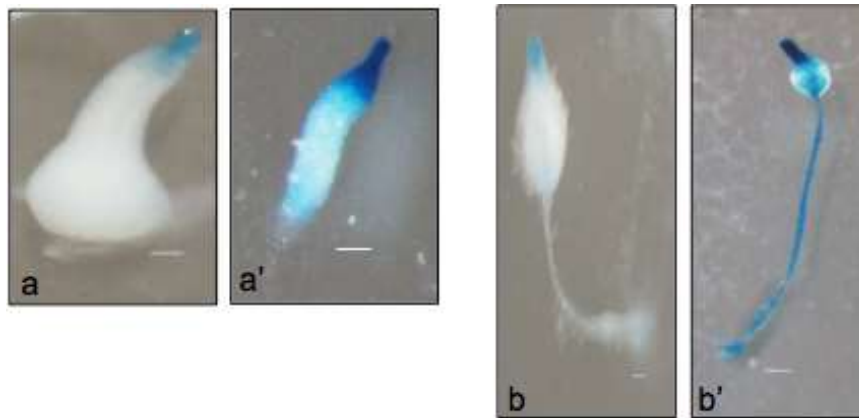


Figure 4.4: Expression pattern of prestalk specific marker *ecmA/lacZ* in wild type Ax2 and *PUFB⁻* multicellular structures. Wild type Ax2 cells and *PUFB⁻* were transformed with *ecmA/lacZ* and developed on dialysis membrane placed on NNA plates. Structures were collected, fixed with methanol and X-gal staining of *ecmA/lacZ* in wild type Ax2 and (a and b) and *PUFB⁻* (a' and b') in the multicellular structure was performed. Structures were visualized and photographed under Nikon AZ100 microscope. [slug (a-a'), Fruiting body (b-b')]; Scale bar- 50 μm ; n=3].

Spatial expression pattern study of *ecmB/lacZ*

The wild type Ax2 cells were transformed with prestalk-specific *ecmB* promoter fused to *LacZ* reporter gene and selected at 40 $\mu\text{g mL}^{-1}$ of G418 and the *PUFB⁻* cells were transformed with the same and selected at 40 $\mu\text{g mL}^{-1}$ of G418 and 10 $\mu\text{g mL}^{-1}$ of Blasticidin S. Various multicellular structures formed during development were collected in 24 well culture plates and fixed in methanol. Structures were permeabilized and stained with X-gal to analyze the staining pattern in both strains (Figure 4.4).

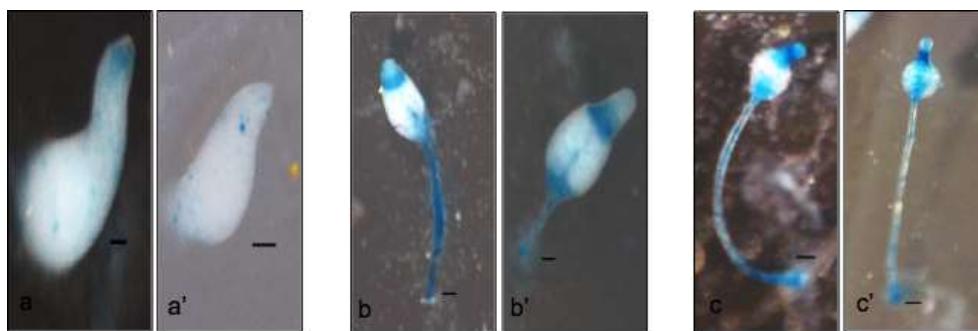


Figure 4.5: Expression pattern of prestalk specific marker *ecmB/lacZ* in wild type Ax2 and *PUFB⁻* multicellular structures. Wild type Ax2 cells and *PUFB⁻* were transformed with *ecmB/lacZ* and developed on dialysis membrane placed on NNA

plates. Structures were collected, fixed with methanol and X-gal staining of *ecmB/lacZ* in wild type Ax2 (a-c) and *PUFB*⁻ (a'-c') in the multicellular structure was performed. Structures were visualized and photographed under Nikon AZ100 microscope. [Slug (a-a'), Early culminants (b-b'), Fruiting bodies (c-c'); Scale bar- 50 μ m; n=3].

We observed that in Ax2 the expression of *ecmB* was present at the anterior region of the slug while in the early culminant and culminant there was staining in the upper and lower cups and was also present throughout the stalk and base (Figure 4.5 a-c). In case of *PUFB*⁻, no noticeable difference in the spatial localization of *ecmB* was observed as was also observed in RT-PCR analysis (Figure 4.4 a'-c').

Spatial expression pattern study of *ecmO/lacZ*

The wild type Ax2 cells were transformed with prestalk-specific *ecmO* promoter fused to *lacZ* reporter gene and selected at 40 μ g mL⁻¹ of G418 and the *PUFB*⁻ cells transformed with the same were selected at 40 μ g mL⁻¹ of G418 and 10 μ g mL⁻¹ of Blasticidin S. Various multicellular structures formed during development were collected in 24 well culture plates and fixed with methanol. Structures were permeabilized and stained with X-gal to analyze the staining pattern.

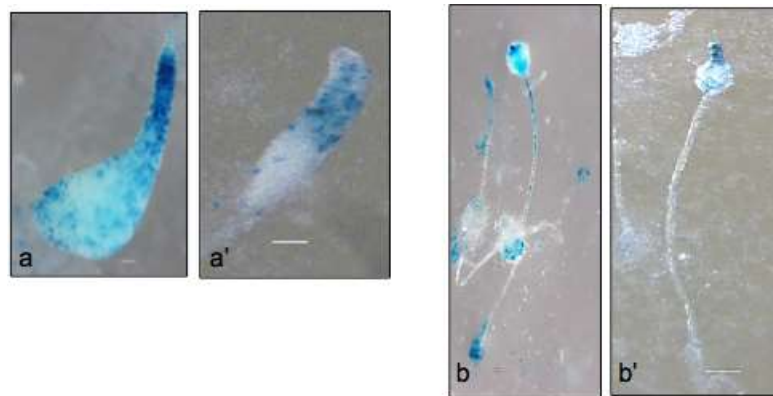


Figure 4.6: Expression pattern of prestalk specific marker *ecmO/lacZ* in wild type Ax2 and *PUFB*⁻ multicellular structures. Wild type Ax2 cells and *PUFB*⁻ were transformed with *ecmO/lacZ* and developed on dialysis membrane placed on NNA plates. Structures were collected, fixed with methanol and X-gal staining of *ecmO/lacZ* in wild type Ax2 (a and b) and *PUFB*⁻ (a' and b') in the multicellular structure was performed. Structures were visualized and photographed under Nikon AZ100 microscope. [Slug (a-a'), Fruiting body (b-b'); Scale bar- 50 μ m; n=3].

We observed that the *ecmO/lacZ* expression in wild type Ax2 slug was present at the neck region in the anterior prestalk region while expression is also present at towards the posterior basal region. In *PUFB*⁻ an expression of *ecmO/lacZ* in the slug stage was expanded more towards the prespore region while the expression was absent at the base in the posterior region. In Ax2, the fruiting body shows the expression of *ecmO* in the anterior region and also in the stalk region. While in *PUFB*⁻ the staining was present at the anterior prestalk region extending towards the tip while in the stalk region staining was present as comparable to the wild type (Figure 4.6).

Spatial expression pattern study of *ecmA0/lacZ*

The wild type Ax2 cells were transformed with prestalk-specific *ecmA0* promoter fused to *lacZ* reporter gene and selected at 40 $\mu\text{g mL}^{-1}$ of G418 and the *PUFB*⁻ cells transformed with the same were selected at 40 $\mu\text{g mL}^{-1}$ of G418 and 10 $\mu\text{g mL}^{-1}$ of Blasticidin S. Various multicellular structures formed during development were collected in 24 well culture plates and fixed with methanol. Structures were permeabilized and stained with X-gal to analyze the staining pattern in both Ax2 and *PUFB*⁻ cells.

The *ecmA0/lacZ* expression was present in the anterior prestalk region covering the tip and neck region of slug in Ax2 while in case of *PUFB*⁻ this region was further extended. Expression was also found in the rear-guard region of *PUFB*⁻ slug as compared to Ax2 slug. Fruiting body shows the expression of *ecmA0* in the anterior region, lower cup and stalk region in Ax2 while *PUFB*⁻ shows a similar type of expression (Figure 4.7).

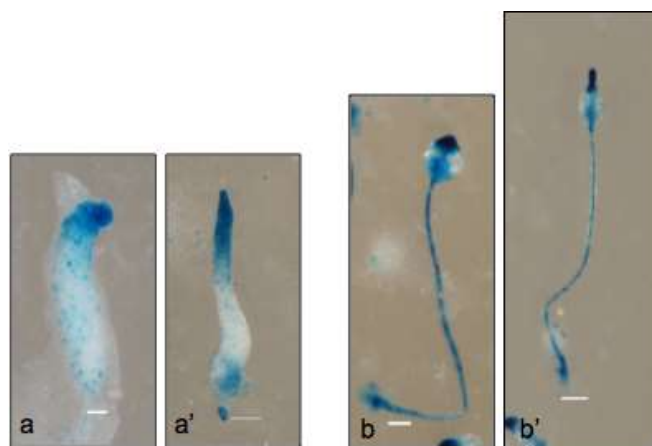


Figure 4.7: Expression pattern of prestalk specific marker *ecmA0/lacZ* in wild type Ax2 and *PUFB*⁻ multicellular structures. Wild type Ax2 cells and *PUFB*⁻ were transformed with *ecmA0/lacZ* and developed on dialysis membrane placed on NNA plates. Structures were collected, fixed with methanol and X-gal staining of

*ecmA*O/*lacZ* in wild type Ax2 (a and b), and *PUFB*⁻ (a' and d') in the multicellular structure was performed. Structures were visualized and photographed under Nikon AZ100 microscope. [Slug (a-a'), Fruiting body (b-b'); Scale bar- 50 μ m; n=3].

Spatial expression pattern study of *pspA/lacZ*

The wild type Ax2 cells were transformed with prespore-specific *pspA* promoter fused to *lacZ* reporter gene and selected at 40 μ g mL⁻¹ of G418 and the *PUFB*⁻ cells transformed with the same were selected at 40 μ g mL⁻¹ of G418 and 10 μ g mL⁻¹ of Blasticidin S. Various multicellular structures formed during development were collected in 24 well culture plates and fixed with methanol. Structures were permeabilized and stained with X-gal to analyze the staining pattern in both Ax2 and *PUFB*⁻ cells

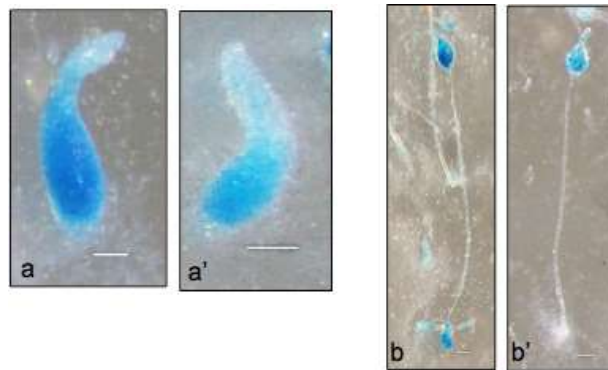


Figure 4.8: Expression pattern of prestalk specific marker *pspA/lacZ* in wild type Ax2 and *PUFB*⁻ multicellular structures. Wild type Ax2 cells and *PUFB*⁻ were transformed with *pspA/lacZ* and developed on dialysis membrane placed on NNA plates. Structures were collected, fixed with methanol and X-gal staining of *pspA/lacZ* in wild type Ax2 and (a and b), and *PUFB*⁻ (a' and b') in the multicellular structure was performed. Structures were visualized and photographed under Nikon AZ100 microscope. [Slug (a-a'), Fruiting body (b-b'); Scale bar- 50 μ m; n=3].

In Ax2, the *lacZ* staining of *pspA* showed the expression of *pspA* primarily localized in the prespore region of slug while in the fruiting body it is located in the sorus. In case of *PUFB*⁻ the expression of *pspA* was present in the prespore/spore region of both slug and fruiting body but the expression was less than the wild type (Figure 4.8), also suggested by the RT-PCR analysis in figure 4.3. The staining was observed only in the posterior region of prespore suggesting that the boundary between the prestalk and prespore was lost in the slugs developed.

Our results suggest the important role of *PUFB*⁻ in maintaining distinct boundaries between the two cell types during development and differentiation of *Dictyostelium*. *PUFB* mutant showed misregulation of some of the prestalk marker suggesting that there is a defect in the normal prestalk cell-type patterning and this is due to the disturbed prestalk/prespore ratio that leads to loss of clear boundaries in *PUFB*⁻ structures. As we observed that in *PUFB*⁻ the multicellular structures formed showed the aberration in the prespore region and prestalk region which resulted in the fruiting bodies formed with small sori and long stalk due to reduced prespore region suggesting the role of *PUFB*⁻ in cell-type differentiation, proper proportioning of prestalk/prespore ratio and patterning during multicellular development in *Dictyostelium*.

4.4.2 Cell lineage tracing by chimera formation of GFP marked Ax2 cells and RFP marked *PUFB*⁻ cells

In order to have a better understating of cell lineage tracing and the fate of *PUFB*⁻ cells in the chimeras cell-mixing experiments were performed. Structures formed by mixing two or more types of cells from different genetic backgrounds are called chimeras. Wild type Ax2 cells tagged with GFP and *PUFB*⁻ cells tagged with RFP in different proportions to form chimeras. Chimera study in various organisms revealed that under the influence of various factors and differential gene expression, cells show differential preferences in cell patterning resulting in aberrant development and mislocalization during cell differentiation.

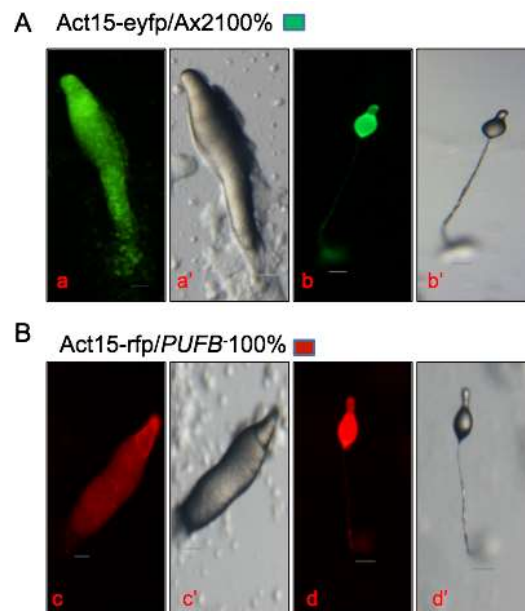


Figure 4.9: GFP tagged Ax2 cells and RFP tagged *PUFB*⁻ cells in the pure populations (100%) in slugs and fruiting bodies. Wild-type, Ax2 cells expressing GFP and *PUFB*⁻ cells expressing RFP were used as controls. (A) Multicellular structures formed by Ax2 cells expressing GFP in pure population. (B) Multicellular structures formed by *PUFB*⁻ cells expressing RFP in pure population. [DIC image – (a'-d'), TRITC image (c and d) and images capture in FITC image (a-b); Slug stage (a-a' and c-c'); and Fruiting body (b-b' and d-d'); Scale bar- 50 μ m; n=3].

For the chimera studies, multicellular structures formed by 100% GFP marked Ax2 cells and 100% RFP marked *PUFB*⁻ cells were used as controls (Figure 4.9 A, B). RFP tagged *PUFB*⁻ cells and GFP tagged Ax2 cells were mixed in various ratios (10 to 90%) and cell suspensions of equal densities (5×10^7) were prepared in 1xKK2 buffer, spotted on NNA plates and allowed to develop at 22°C. The various developmental structures formed by the chimeras were visualized under SMZ1500 fluorescence microscope.

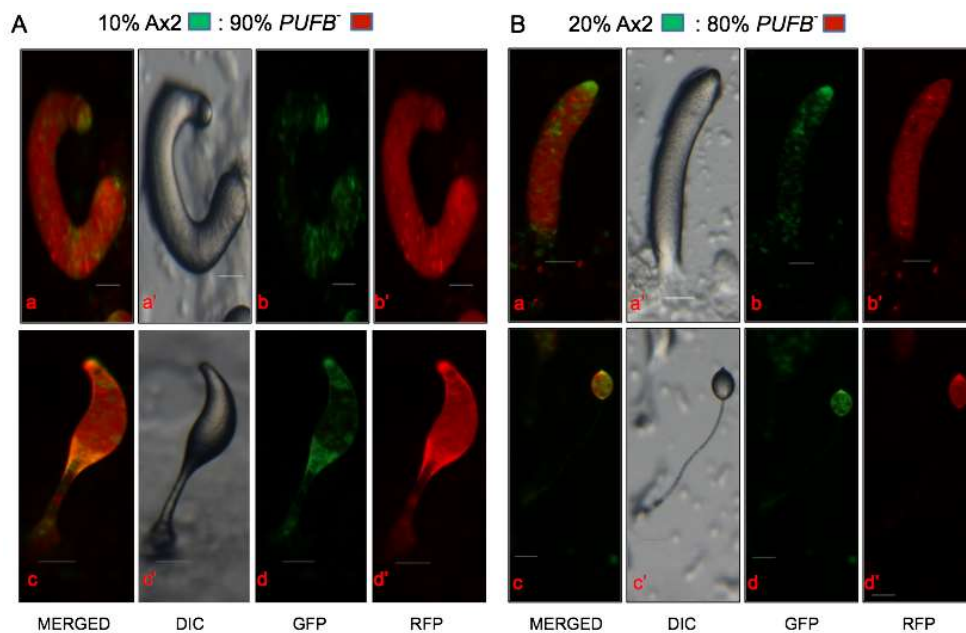


Figure 4.10: Cell fate of *PUFB*⁻ cells in chimeric structures. (A) 10% GFP-tagged wild type Ax2 cells and 90% RFP- tagged *PUFB*⁻ cells, (B) 20% GFP-tagged wild type cells and 80% RFP tagged *PUFB*⁻ cells were mixed and developed on NNA plates. Position of Ax2 cells and *PUFB*⁻ cells in the chimaeric structure was monitored using Nikon SMZ1500 fluorescence microscope. Multicellular structures (slug and fruiting body) were imaged under DIC, FITC and TRITC filter [Scale bar- 50 μ m; n=3].

When cells were mixed in the ratio of 10% GFP tagged Ax2 (Green) and 90% RFP tagged *PUFB*⁻ (Red) Ax2 cells distribute themselves at the tip and posterior part of

the slug while *PUFB*⁻ cells are present throughout the structure while in early culminants *Ax2* is primarily localized in the upper, lower cups and in the stalk while prespore region is occupied by *PUFB*⁻ cells (Figure 4.10A). When 20% *Ax2* and 80% *PUFB*⁻ cells were mixed then also wild type *Ax2* is present at the tip and rear-guard cell of the prestalk region while the prespore region is once again occupied mainly by the *PUFB*⁻ cells (Figure 4.10B).

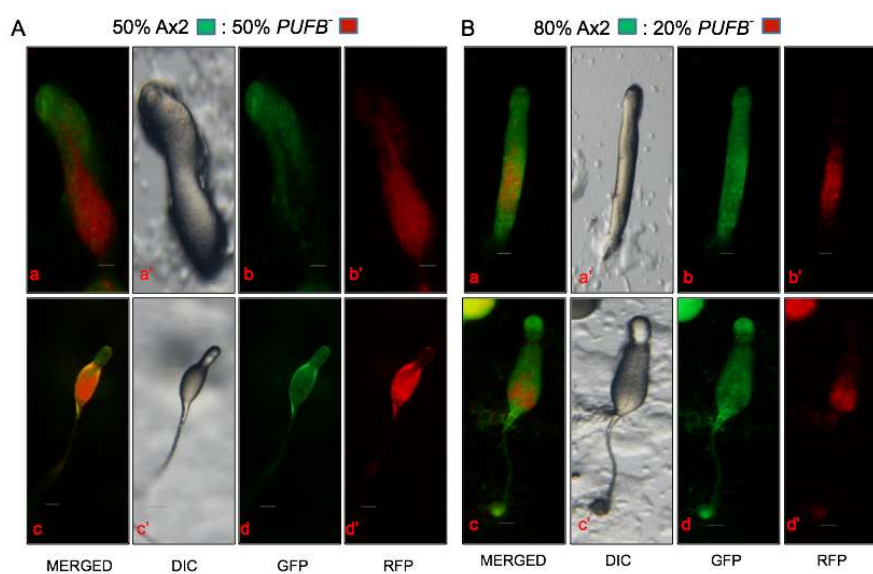


Figure 4.11: Cell fate of *PUFB*⁻ cells in chimeric structures. (A) 50% GFP-tagged wild-type *Ax2* cells and 50% RFP- tagged *PUFB*⁻ cells, (B) 80% GFP-tagged wild type cells and 20% RFP tagged *PUFB*⁻ cells were mixed and developed on NNA plates. Position of *Ax2* cells and *PUFB*⁻ cells in the chimeric structure was monitored using Nikon SMZ1500 fluorescence microscope. Multicellular structures (slug and fruiting body) were imaged under DIC, FITC and TRITC filter [Scale bar- 50 μ m; n=3].

The distribution pattern of *PUFB*⁻ cells appeared more pronounced as the percentage of *PUFB*⁻ cells become less and the percentage of *Ax2* increases. In 1:1 ratio i.e. when an equal number of cells were taken, *PUFB*⁻ cells distribute itself in the prespore region while the wild type cells occupy the anterior prestalk region in both the slug and early culminants. But as the percentage of *PUFB*⁻ cells decreases further in the ratio to 20% (Figure 4.11B) and 10% (Figure 4.12B) the picture becomes clearer as *PUFB*⁻ cells occupy the prespore region in slug and early culminants despite such low percentage.

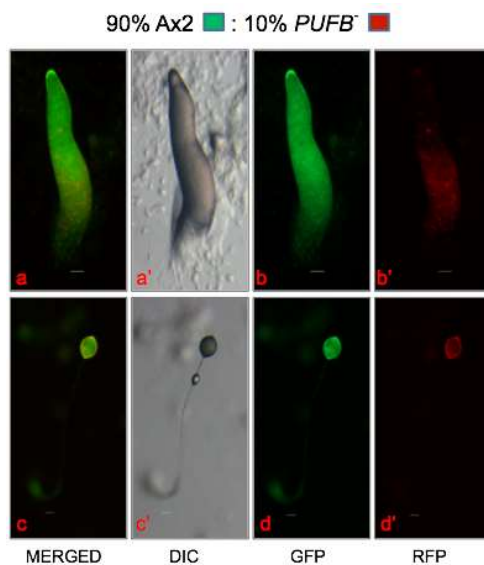


Figure 4.12: Cell fate of *PUFB*⁻ cells in chimeras. 90% GFP-tagged wild type cells and 10% RFP tagged *PUFB*⁻ cells were mixed and developed on NNA plates. DIC, TRITC and FRITC images of multicellular structure (migratory slugs and fruiting body) were captured using Nikon SMZ1500 fluorescence microscope. [Scale bar- 50 μ m; n=3].

Our results showed that the *PUFB*⁻ cells have the tendency to distribute itself in the prespore region in different chimeric multicellular structures formed with wild type Ax2 cells.

4.4.3 Contribution of *PUFB*⁻ cells in spore formation in the chimeras developed

GFP marked Ax2 cells and RFP marked *PUFB*⁻ cells were mixed in different proportions and allowed to develop on NNA plates at 22°C to form fruiting bodies. Fruiting bodies formed by the chimeras in all the ratios, 10%, 20%, 50%, 80%, 90 and 100% *PUFB*⁻ cells were mixed with wild type. Fruiting bodies were analyzed for the spore-forming tendencies of *PUFB*⁻ cells in the chimeric mixtures. Approximately, 10-15 spore heads from the chimeric fruiting bodies from all ratios were counted for each experiment.

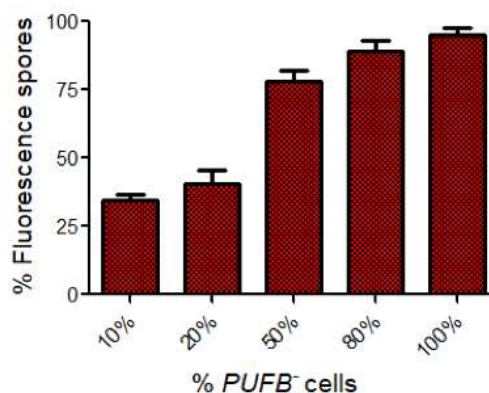


Figure 4.13: Percentage (%) spore count of *PUFB*⁻ in chimeric fruiting bodies. RFP tagged *PUFB*⁻ cells were mixed in various proportions from 10%, 20%, 50% and 80% with GFP-tagged wild-type cells and cell suspensions were allowed to co-develop till the culminant formation. About 10-15 fruiting bodies per ratio per experiment were scored. The values represent mean ± standard deviation].

We found that *PUFB*⁻ cells contributed $34.6 \pm 2.06\%$, $40.8 \pm 4.85\%$, $78.3 \pm 3.6\%$, $89.2 \pm 3.6\%$, $95.2 \pm 2.39\%$ spores from 10%, 20%, 50%, 80%, 90 and 100% *PUFB*⁻ cells, respectively in chimeric mixtures with wild type (Figure 4.12). This suggests that in the chimeric mixtures *PUFB*⁻ cells show more spore-forming tendency as compared to the wild type.

Cell lineage study with chimeric mixtures of *PUFB*⁻ and Ax2 cells in various proportions showed the tendency of Ax2 and *PUFB*⁻ cells to occupy the different regions in the multicellular structure formed. We found that the distribution of *PUFB*⁻ cells was found to be more in the prespore region in the multicellular structures as compared to the wild type. Also, the spore-forming tendency of *PUFB*⁻ cells was found to be more as compared to the wild type.

4.4.4 Expression of autophagy-related genes in Ax2 and *PUFB*⁻ cells

Autophagy is a degradative process which maintains the cellular homeostasis of the cell such as stress or DNA damage. It eliminates long-lived misfolded or unfolded proteins or even entire organelle (via lysosomal degradation) that the ubiquitin-proteasome system cannot degrade (Decuyper et al., 2011). In *Dictyostelium*, during multicellular development under starvation condition autophagy is required.

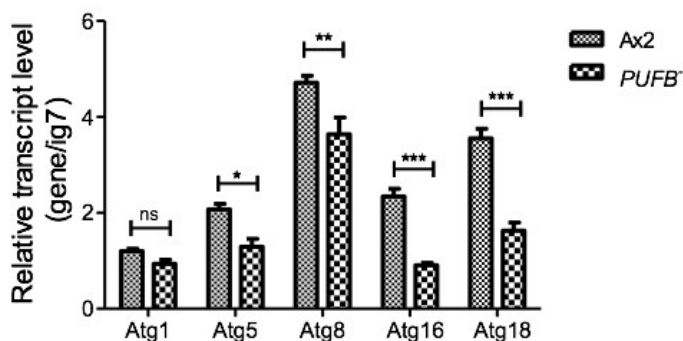


Figure 4.14: mRNA expression of autophagy-related genes in Ax2 and *PUFB⁻* cells. Semi-quantitative RT-PCR analysis in wild type Ax2 and *PUFB⁻* cells. mRNA expression of autophagy-related genes *atg1*, *atg5*, *atg8*, *atg16* and *atg18* with *ig7* as internal control are shown in the graph. [The values represent mean; \pm standard deviation; Two way ANOVA, p-value ≤ 0.05 , ≤ 0.01 and ≤ 0.001 has been symbolized as *, ** and ***, respectively; n=3].

We found a significant decrease in the mRNA expression of *atg5*, *atg8* and *atg16* and *atg18* in *PUFB⁻* cells in the vegetative stage as compared to the wild type Ax2 cells. Thus, we can say that in *Dictyostelium* *PUFB* affects the process of autophagy by regulating the autophagy-related genes that are important in the formation of autophagosome, membrane trafficking and ultimately autolysosome formation. To further this we performed autophagic flux study in Ax2 and *PUFB⁻* cells.

4.4.5 *PUFB* knockout leads to suppression of autophagy and autophagic flux in *Dictyostelium*

To determine whether deletion of *PUFB* has any effect on autophagic process Ax2 cells and *PUFB⁻* cells were transfected with a tandemly tagged *mRFP-GFP-Atg8* plasmid. *Atg8* is an autophagic marker used for monitoring autophagic flux in *Dictyostelium*. On autophagy induction, *Atg8* (known as LC3 in mammals) becomes lipidated and become integrated to cytosolic side of the autophagosome and remain attached to the autophagosome membrane until cleaved from phosphatidylethanolamine (PE) by *Atg4* and recycled (Mesquita et al., 2017). The process of autophagosome formation to fusion of autophagosome to lysosome can be monitored using *RFP-GFP-Atg8* autophagic marker with NH_4Cl treatment that facilitates autophagic flux assessment by measuring the number of fluorescent puncta under confocal microscopy (Calvo-Garrido et al., 2011). GFP fluorescence is rapidly quenched in acidic environment of lysosome but the RFP

fluorescence is more resistant to the acidic and protease-rich conditions of the lysosome. So the formation of red-green puncta is indicative to early autophagosome whereas presence of red puncta in the absence of green puncta suggests the fusion of autophagosomes with lysosome (Kimura et al., 2007). When the cells were treated with NH_4Cl , a lysosomotropic agent that increases lysosomal pH leads to inhibition of autophagosome-lysosome fusion.

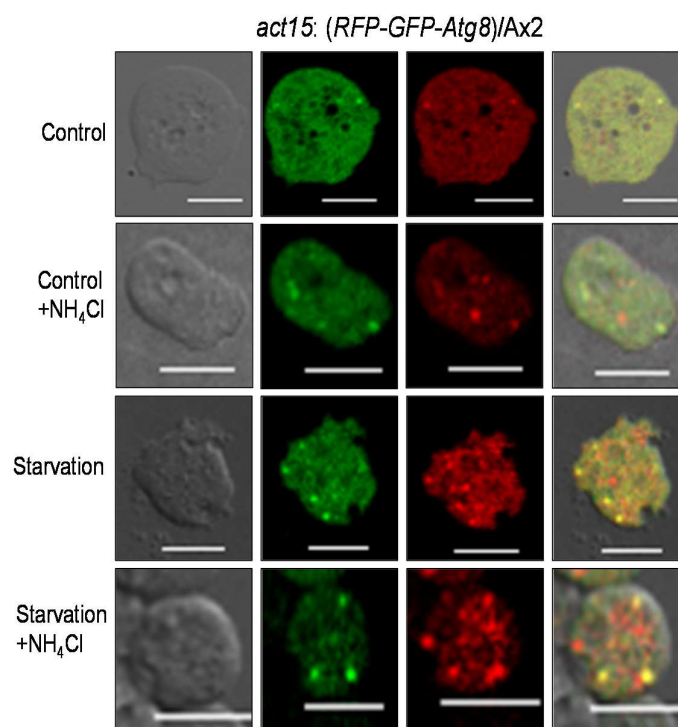


Figure 4.15: Analysis of autophagic flux measurement in wild type Ax2 cells using confocal microscopy. Ax2 cells expressing *RFP-GFP-Atg8* marker were diluted at a cell density of 1×10^6 cells mL^{-1} and the cell suspension was placed in a 6 well plate having HL5 and in 1xKK2 buffer to induce starvation. 100 mM NH_4Cl was added to the cell for 2 h and incubated at 22°C . After 2 hours cells were washed and again 100 mM NH_4Cl was added and incubated at 22°C for another 2 h. After incubation cells were visualized under confocal microscopes and photographs were captured in DIC, FITC and TRITC filters. [Scale bar- 10 μm ; n=3].

Quantitative analysis of autophagic puncta formed per cell using confocal microscopy revealed that Ax2 cells expressing *RFP-GFP-Atg8* in HL5 media showed a typical green/red puncta formation although very few cells showed red/not green puncta indicating basal autophagy (Figure 4.15 and 4.17). However, starvation induces autophagy in *Dictyostelium* as the Ax2 cells starved for 4 h showed increased number of red puncta that indicates autolysosomes over yellow puncta that indicates

autophagosomes, thus increased autophagic flux than the basal level was observed. Upon NH_4Cl treatment, Ax2 cells expressing *RFP-GFP-Atg8* marker showed a significant increase in number of red puncta that indicates a rapid increase in autophagy flux (Figure 4.15 and 4.17).

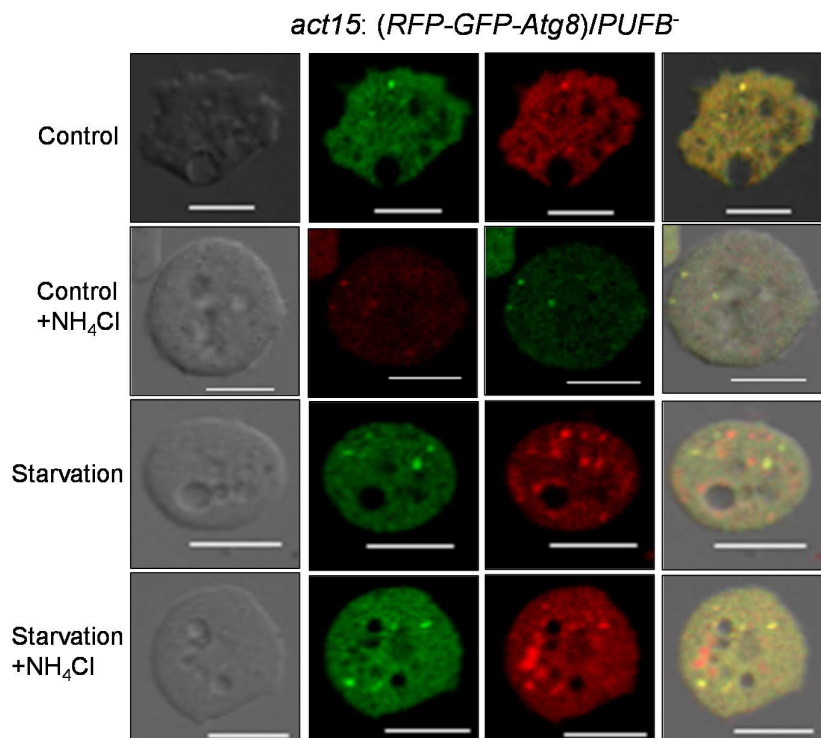


Figure 4.16: Analysis of autophagic flux measurement in *PUFB⁻* cells using confocal microscopy. *PUFB⁻* cells expressing *RFP-GFP-Atg8* marker were diluted at a cell density of 1×10^6 cells mL^{-1} and the cell suspension was placed in a 6 well plate having HL5 and in 1xKK2 buffer to induce starvation. 100 mM NH_4Cl was added to the cell for 2 h and incubated at 22°C . After 2 h cells were washed and again 100 mM NH_4Cl was added and incubated at 22°C for another 2 h. After incubation cells were visualized under confocal microscopes and photographs were captured in DIC, FITC and TRITC filters. [Scale bar- 10 μm ; n=3].

In *PUFB⁻* cells expressing *RFP-GFP-Atg8*, number of yellow or red puncta per cell were very low but starvation and/or NH_4Cl treatment lead to an increase in the number of yellow or red puncta per cell which still is significantly less when compared to the Ax2 cells under starvation and NH_4Cl treatment (Figure 4.16 and 4.17). Thus, reduced autophagy flux suggests that *PUFB* play a regulatory role during basal and starvation-induced autophagy in *Dictyostelium*. Therefore, we postulate that *PUFB* is required during autophagy in *Dictyostelium*.

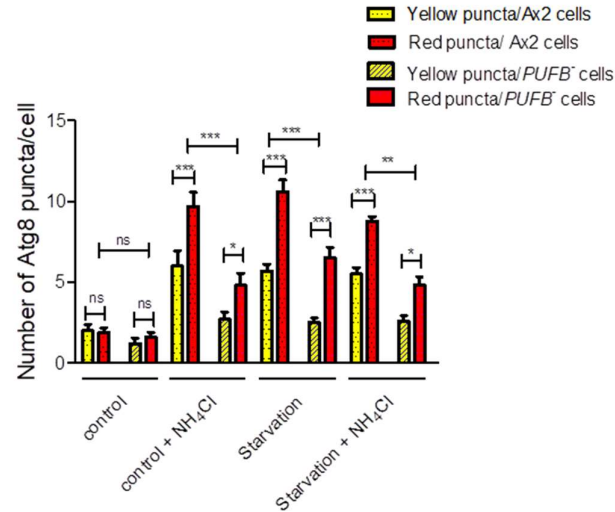


Figure 4.17: Quantitative measurement of yellow and red puncta formed in Ax2 and *PUFB⁻* cells. Wild type and *PUFB⁻* cells expressing the *RFP-GFP-Atg8* marker were starved for 4 h and treated with 100 mM NH_4Cl in HL5 for 2+2 h. Both treated and control samples were visualized under confocal microscope. Graph represents the score of yellow and red puncta. Nearly 30-40 cells per experiment for each condition were scored. [The values represent mean; standard deviation; Two way ANOVA, p-value ≤ 0.05 , ≤ 0.01 and ≤ 0.001 has been symbolized as *, ** and ***, respectively; n=3].

4.5 CONCLUSIONS

To know the role of *PUFB⁻* cells in cell-type differentiation and patterning, cell-type specific marker expression studies were performed during the development of Ax2 and *PUFB⁻* cells were performed. We found out that the expression of prestalk specific gene *ecmA* was higher than the wild type. And also the expression is mislocalized in the slug and fruiting body. As their staining region was extended than the wild type in the slug, the fruiting body also showed expression in the stalk region. While other prestalk markers like *ecmO* and *ecmA0* were mislocalized as their staining region was extended to the prespore region in slug. Prespore marker *pspA* showed decreased expression along with a decrease in the staining region in the slug and the fruiting body. This result suggests that there was a loss of boundary between the prespore and the prestalk cell types. There was misregulated prestalk cell-type patterning due to disturbed prestalk/prespore ratio, which results in the formation of fruiting bodies with long stalk and small sori due to reduced prespore region. Our results suggest the important role of *PUFB⁻* in cell-type differentiation, proper proportioning of prestalk/prespore ratio and patterning during multicellular development in *Dictyostelium*.

Our study demonstrates that *PUFB*⁻ cells in the chimeric mixtures formed with Ax2 tend to distribute themselves in the prespore region of the multicellular structure formed in the ratio ranging from 10% to 100%. In all the ratios tested, *PUFB* null cells distributed themselves in the prespore region, They also contributed majorly in the spore formation in the chimeric mixtures with wild type. Lastly, we observed that the expression of autophagy-related genes was found to be less than the wild type, which suggests its role in the autophagy. In *PUFB*⁻ cells expressing *RFP-GFP-Atg8*, number of yellow or red puncta per cell were very low but starvation and/or NH_4Cl treatment lead to an increase in the number of yellow or red puncta per cell which still was significantly less when compared to the Ax2 cells under starvation and NH_4Cl treatment. Reduced autophagy flux suggests that *PUFB* play a regulatory role during basal and starvation-induced autophagy in *Dictyostelium*. Therefore, we postulate that *PUFB* is required during autophagy in *Dictyostelium*. Further studies are required to better understand the role of *PUFB* in autophagic process.

PUF (Pumilio and FBF) proteins are the conserved RNA binding proteins present in all eukaryotes. They are known to be post-transcriptional regulators where they interact with 3' UTR of their target mRNA through specific recognition sequence present at the 3'UTR of mRNA to control the stability and translation of transcripts. PUF proteins are characterized by the presence of evolutionarily highly conserved domain called PUF domain comprising of eight repeats present at the C-terminal part of protein. It plays important roles in cell development, stem cell maintenance and differentiation. For example, In *Drosophila* it is involved in the anterior-posterior patterning of early embryo, maintenance of germline stem cells and germline switch from spermatogenesis to oogenesis in case of *C. elegans*, aging, mitochondrial function and mating type switching in yeast, etc. Thus it has been shown to be involved in the development and differentiation of organisms. *Dictyostelium* being the good model organism for the study of growth, development and differentiation, it serves as a preferable model organism to understand the role of PUF in *Dictyostelium*.

Dictyostelium a soil living social amoeba exist in two life forms i.e. unicellular and multicellular. This enables us to study growth and development independent of each other. Upon starvation unicellular amoeba in response to the cAMP signal, aggregate to form multicellular structure which finally leads to the formation of the terminally differentiated fruiting body consisting of the stalk (dead vacuolated cells) and sorus (spores). Many fundamental processes like chemotaxis, cell motility, cell sorting and pattern formation, endocytic vesicle traffic, cell adhesion, autophagy-associated cell death can be studied in this organism. Recently it has emerged as a valuable tool for studying the molecular basis of pathogenic human diseases.

In the genome of *Dictyostelium* 5 PUF genes are present named as *PUFA*, *PUFB*, *PUFC*, *PUFD* and *PUFE*. Based on the bioinformatics analysis we found out that *PUFA*, *PUFB* and *PUFC* showed more closeness with yeast and plant PUF protein while *PUFA* also show similarity with human PUF. But *PUFC* and *PUFE* are distantly related to PUF proteins of other organisms. We observed three highly conserved motifs in the promoter region of all the 5 PUF which could act as the binding site for different transcription factors. Tertiary structure modeling of all the 5 *Dd*PUF protein suggests that they consist mainly of alpha-helix. *PUFA*, *PUFB* and *PUFD* showed the presence of eight repeats in their PUF domain while *PUFC* and *PUFE* have six domains only. This could be the

reason that PUF_C and PUF_E are distantly related to PUF proteins of other organisms in the phylogenetic tree. It has been studied that PUFA plays an important role during growth to development transition. We chose PUF_B to work upon further based on the better structural and stereochemical quality and also possesses eight repeats in their PUF domain as suggested by the structural modeling data and also it shows the more similarity with yeast and plant PUF. We have performed the temporal and spatial expression pattern of *PUFB* gene during growth and differentiation using semi-quantitative RT-PCR and *in situ* hybridization analysis. mRNA expression of *PUFB* was found to be high during early and later stages of development suggest that it may have a role in cell division, growth to development transition and terminal differentiation of cell types. Whole-mount *in situ* hybridization analysis showed that *PUFB* mRNA is expressed in the tip of the mound, anterior prestalk region of slug and culminants. Prestalk specific localization of *PUFB* mRNA suggests it may have a role in autophagic cell death and stalk cell differentiation.

To study the functional aspects of PUF_B during growth, development and differentiation of *Dictyostelium* two mutant strains (*PUFB*⁻ and *PUFB*^{OE}) were created. Overexpressor strain of PUF_B was created by expressing full-length *PUFB* gene under constitutive *actin15* promoter fused with an *eYFP* reporter gene at the C-terminus. PUF_B knockout strain was prepared by gene disruption method which was confirmed by various PCR and RT-PCR expression studies.

Cell proliferation studies of both the mutant strains along with wild type Ax2 was carried out by monitoring the cell density for 5 days. *PUFB*⁻ strain showed slightly higher proliferation rate while *PUFB*^{OE} showed decreased proliferation rate. Cell cycle analysis showed that the higher proliferation rate of *PUFB*⁻ could be possibly by suppressing G1 arrest and initiating the G1-S transition while in case of *PUFB*^{OE} no significant difference was observed. Defect in the exocytosis rate of *PUFB*^{OE} was found which suggest that may be because of reduced exocytosis, toxicity by the accumulation of undigested remnants occurs which affects both cell proliferation and cell growth of *PUFB*^{OE} cells. Also, the cell mass of *PUFB*^{OE} was found to be less than the wild type suggesting a decrease in growth of overexpressor cells.

Multicellular development of both the mutant strains along with wild type Ax2 was analyzed. The development of *PUFB*⁻ and *PUFB*^{OE} was found to be delayed early as

control to wild type. *PUFB^{OE}* formed small sized less number of aggregate while *PUFB⁻* formed relatively large sized and less number of aggregate. Also, the development of *PUFB^{OE}* was asynchronous in nature as all the cells did not culminate into fruiting body. Formation of the fruiting body is one of the important aspects in the life cycle of *Dictyostelium* to maintain their generation. We found an alteration in the morphology of fruiting body as the fruiting body formed by *PUFB⁻* cells are relatively large having high stalk/spore ratio while the fruiting body formed by *PUFB^{OE}* was small having large sorus and thus lower stalk/spore ratio as compared to wild type. Both the mutant strain formed less number of fruiting body as compared to the wild type. This defect in terminal differentiation (fruiting body formation) of *PUFB⁻* and *PUFB^{OE}* was associated with the reduced spore viability of spores because of the decrease in expression of two spore coat proteins, *cotA* and *cotB*. It suggests that an optimum level of *PUFB* protein is required for the efficient spore formation. There is a defect in the aggregation size and number formed by both the mutant strains. This defect was found to be because of misregulation of certain genes involved in aggregation. In *PUFB^{OE}* less number of small-sized aggregates formation was due to increased expression of *Countin* and *csA*, a cell adhesion molecule and lower expression of *cadA* another cell adhesion molecules. While in case of *PUFB⁻*, *countin* and *csA* expression was found to be low and higher expression of *cadA* leads to relatively large-sized aggregates. Because of the mutation of *PUFB*, defect in cAMP signaling was observed as the levels of cAMP were low in both the mutant strains and also there was misregulation of cAMP signaling. The decrease in the mRNA level of *acaA*, *carA* was observed. Due to this development of both the strains are delayed and also contribute to defects in aggregation size and number. Thus, our study suggests the important role of *PUFB* during growth and development by regulating the expression of genes important in growth and development of *Dictyostelium discoideum*.

To decipher the role of *PUFB⁻* cells in cell-type differentiation and patterning, cell-type specific marker expression studies were performed during the development of Ax2 and *PUFB⁻*. For this β -galactosidase staining was carried using cell-type specific promoter gene fused to *lacZ* reporter in both Ax2 and *PUFB⁻* cells. We found out that the expression of prestalk-specific gene *ecmA* was higher than the wild type. And also the expression is mislocalized in the slug and fruiting body. As their staining region was extended than the wild type in the slug, the fruiting body also showed expression in the stalk region. While other prestalk markers like *ecmO* and *ecmA*O were mislocalized as

their staining region was extended to the prespore region in the slug. Prespore marker *pspA* showed decreased expression along with a decrease in the staining region in the slug and the fruiting body. This result suggests that there was a loss of boundary between the prespore and the prestalk cell types. There was misregulated prestalk cell-type patterning due to disturbed prestalk/prespore ratio, which results in the formation of fruiting bodies with long stalk and small sori due to reduced prespore region. Our results suggest the important role of *PUFB*⁻ in cell-type differentiation, proper proportioning of prestalk/prespore ratio and patterning during multicellular development in *Dictyostelium*.

To know the role of *PUFB* in cell lineage tracing, chimera studies were performed. When Wild type Ax2 cells tagged with GFP and *PUFB*⁻ cells tagged with RFP in different proportions ranging from 10% to 90% to form chimeras, *PUFB*⁻ cells tend to distribute themselves in the prespore region of the multicellular structure formed. They also contributed majorly in the spore formation in the chimeric mixtures with wild type.

Further, the role of *PUFB* in autophagy was observed by monitoring the autophagic flux using a molecular marker of autophagy Atg8/LC3 (early autophagosome marker). *PUFB*⁻ cells showed a decrease in , number of yellow or red puncta per cell was very low but starvation and/or NH₄Cl treatment leads to an increase in the number of yellow or red puncta per cell which still was significantly less when compared to the Ax2 cells under starvation and NH₄ Cl treatment. Also the mRNA expression level of autophagy-related genes in the *PUFB*⁻ was found to be less than the wild type. Thus we can conclude that *PUFB* plays a regulatory role during basal and starvation-induced autophagy and is required during autophagy in *Dictyostelium*.

So we conclude that *PUFB* suppress cell proliferation and growth, and also regulate aggregation size by modulating the early developmental gene expression and cAMP signaling. It is involved in the regulation of development, differentiation and cell type patterning by maintaining the boundary between prestalk and prespore region. It also play a crucial role in the starvation-induced autophagy.

1. Abbasi, N. et al. 2010. APUM23, a nucleolar Puf domain protein, is involved in pre-ribosomal RNA processing and normal growth patterning in Arabidopsis. *The Plant Journal* 64: 960-976.
2. Ahringer, J., and J. Kimble. 1991. Control of the sperm–oocyte switch in *Caenorhabditis elegans* hermaphrodites by the fem-3 3' untranslated region. *Nature* 349: 346.
3. Amrani, N., S. Ghosh, D. A. Mangus, and A. Jacobson. 2008. Translation factors promote the formation of two states of the closed-loop mRNP. *Nature* 453: 1276.
4. Anjard, C., Y. Su, and W. F. Loomis. 2009. Steroids initiate a signaling cascade that triggers rapid sporulation in *Dictyostelium*. *Development* 136: 803-812.
5. Anjard, C., Y. Su, and W. F. Loomis. 2011. The polyketide MPBD initiates the SDF-1 signaling cascade that coordinates terminal differentiation in *Dictyostelium*. *Eukaryotic cell* 10: 956-963.
6. Anjard, C., C. Zeng, W. F. Loomis, and W. Nellen. 1998. Signal Transduction Pathways Leading to Spore Differentiation in *Dictyostelium discoideum*. *Developmental biology* 193: 146-155.
7. Araki, T., T. Abe, J. G. Williams, and Y. Maeda. 1997. Symmetry Breaking in *Dictyostelium* Morphogenesis: Evidence That a Combination of Cell Cycle Stage and Positional Information Dictates Cell Fate. *Developmental biology* 192: 645-648.
8. Archer, S. K., V.-D. Luu, R. A. de Queiroz, S. Brems, and C. Clayton. 2009. *Trypanosoma brucei* PUF9 regulates mRNAs for proteins involved in replicative processes over the cell cycle. *PLoS pathogens* 5: e1000565.
9. Arya, R., A. Bhattacharya, and K. S. Saini. 2008. *Dictyostelium discoideum*—a promising expression system for the production of eukaryotic proteins. *The FASEB Journal* 22: 4055-4066.
10. Asaoka-Taguchi, M., M. Yamada, A. Nakamura, K. Hanyu, and S. Kobayashi. 1999. Maternal Pumilio acts together with Nanos in germline development in *Drosophila* embryos. *Nature cell biology* 1: 431.
11. Bailey, T. L. et al. 2009. MEME SUITE: tools for motif discovery and searching. *Nucleic acids research* 37: W202-W208.
12. Bakthavatsalam, D. et al. 2008. The secreted *Dictyostelium* protein CfaD is a chalone. *Journal of cell science* 121: 2473-2480.
13. Bakthavatsalam, D., J. M. Choe, N. E. Hanson, and R. H. Gomer. 2009. A *Dictyostelium* chalone uses G proteins to regulate proliferation. *BMC biology* 7: 44.
14. Barker, D. D., C. Wang, J. Moore, L. K. Dickinson, and R. Lehmann. 1992. Pumilio is essential for function but not for distribution of the *Drosophila* abdominal determinant Nanos. *Genes & Development* 6: 2312-2326.
15. Barton, M. K., T. B. Schedl, and J. Kimble. 1987. Gain-of-function mutations of fem-3, a sex-determination gene in *Caenorhabditis elegans*. *Genetics* 115: 107-119.
16. Berks, M., and R. R. Kay. 1988. Cyclic AMP is an inhibitor of stalk cell differentiation in *Dictyostelium discoideum*. *Developmental biology* 126: 108-114.
17. Bernstein, D., B. Hook, A. Hajarnavis, L. Opperman, and M. Wickens. 2005. Binding specificity and mRNA targets of a *C. elegans* PUF protein, FBF-1. *Rna* 11: 447-458.
18. Bimboim, H., and J. Doly. 1979. A rapid alkaline extraction procedure for screening recombinant plasmid DNA. *Nucleic acids research* 7: 1513-1523.

19. Bonner, J. T. 1952. The pattern of differentiation in amoeboid slime molds. *The American Naturalist* 86: 79-89.
20. Bonner, J. T., and L. Savage. 1947. Evidence for the formation of cell aggregates by chemotaxis in the development of the slime mold *Dictyostelium discoideum*. *Journal of Experimental Zoology* 106: 1-26.
21. Bray, S. J. 2016. Notch signalling in context. *Nature reviews Molecular cell biology* 17: 722.
22. Bretschneider, T., B. Vasiev, and C. J. Weijer. 1997. A model for cell movement during *Dictyostelium* mound formation. *Journal of Theoretical Biology* 189: 41-51.
23. Brock, D. A. et al. 1996. A *Dictyostelium* mutant with defective aggregate size determination. *Development* 122: 2569-2578.
24. Brock, D. A., and R. H. Gomer. 1999. A cell-counting factor regulating structure size in *Dictyostelium*. *Genes & development* 13: 1960-1969.
25. Brock, D. A., and R. H. Gomer. 2005. A secreted factor represses cell proliferation in *Dictyostelium*. *Development* 132: 4553-4562.
26. Cai, H. et al. 2014. Nucleocytoplasmic shuttling of a GATA transcription factor functions as a development timer. *Science* 343: 1249-1253.
27. Calvo-Garrido, J. et al. 2010. Autophagy in *Dictyostelium*: genes and pathways, cell death and infection. *Autophagy* 6: 686-701.
28. Calvo-Garrido, J., S. Carilla-Latorre, A. Mesquita, and R. Escalante. 2011. A proteolytic cleavage assay to monitor autophagy in *Dictyostelium discoideum*. *Autophagy* 7: 1063-1068.
29. Cao, Q., K. Padmanabhan, and J. D. Richter. 2010. Pumilio 2 controls translation by competing with eIF4E for 7-methyl guanosine cap recognition. *Rna* 16: 221-227.
30. Ceccarelli, A., H. Mahbubani, and J. G. Williams. 1991. Positively and negatively acting signals regulating stalk cell and anterior-like cell differentiation in *Dictyostelium*. *Cell* 65: 983-989.
31. Chagnovich, D., and R. Lehmann. 2001. Poly (A)-independent regulation of maternal hunchback translation in the *Drosophila* embryo. *Proceedings of the National Academy of Sciences* 98: 11359-11364.
32. Charette, S., and P. Cosson. 2004. Preparation of genomic DNA from *Dictyostelium discoideum* for PCR analysis. *Biotechniques* 36: 574-575.
33. Chen, D. et al. 2012. Pumilio 1 suppresses multiple activators of p53 to safeguard spermatogenesis. *Current Biology* 22: 420-425.
34. Cho, P. F. et al. 2006. Cap-dependent translational inhibition establishes two opposing morphogen gradients in *Drosophila* embryos. *Current Biology* 16: 2035-2041.
35. Cho, P. F. et al. 2005. A new paradigm for translational control: inhibition via 5'-3' mRNA tethering by Bicoid and the eIF4E cognate 4EHP. *Cell* 121: 411-423.
36. Chritton, J. J., and M. Wickens. 2010. Translational repression by PUF proteins in vitro. *Rna* 16: 1217-1225.
37. Chung, C., S. L. Niemela, and R. H. Miller. 1989. One-step preparation of competent *Escherichia coli*: transformation and storage of bacterial cells in the same solution. *Proceedings of the National Academy of Sciences* 86: 2172-2175.
38. Chung, C. Y., T. Reddy, K. Zhou, and R. A. Firtel. 1998. A novel, putative MEK kinase controls developmental timing and spatial patterning in *Dictyostelium* and is regulated by ubiquitin-mediated protein degradation. *Genes & development* 12: 3564-3578.

39. Clarke, M., and R. Gomer. 1995. PSF and CMF, autocrine factors that regulate gene expression during growth and early development of *Dictyostelium*. *Experientia* 51: 1124-1134.
40. Collier, J., and R. Parker. 2005. General translational repression by activators of mRNA decapping. *Cell* 122: 875-886.
41. Collier, J. M., M. Tucker, U. Sheth, M. A. Valencia-Sanchez, and R. Parker. 2001. The DEAD box helicase, Dhh1p, functions in mRNA decapping and interacts with both the decapping and deadenylase complexes. *Rna* 7: 1717-1727.
42. Crittenden, S. L. et al. 2002. A conserved RNA-binding protein controls germline stem cells in *Caenorhabditis elegans*. *Nature* 417: 660.
43. Darmon, M., J. Barra, and P. Brachet. 1978. The role of phosphodiesterase in aggregation of *Dictyostelium discoideum*. *Journal of cell science* 31: 233-243.
44. De Chastellier, C., and A. Ryter. 1977. Changes of the cell surface and of the digestive apparatus of *Dictyostelium discoideum* during the starvation period triggering aggregation. *The Journal of cell biology* 75: 218-236.
45. Decuypere, J.-P., G. Bultynck, and J. B. Parys. 2011. A dual role for Ca²⁺ in autophagy regulation. *Cell calcium* 50: 242-250.
46. Deng, Y., R. H. Singer, and W. Gu. 2008. Translation of ASH1 mRNA is repressed by Puf6p–Fun12p/eIF5B interaction and released by CK2 phosphorylation. *Genes & development* 22: 1037-1050.
47. Dereeper, A. et al. 2008. Phylogeny. fr: robust phylogenetic analysis for the non-specialist. *Nucleic acids research* 36: W465-W469.
48. Dormann, D., and C. J. Weijer. 2001. Propagating chemoattractant waves coordinate periodic cell movement in *Dictyostelium* slugs. *Development* 128: 4535-4543.
49. Droll, D. et al. 2010. The trypanosome Pumilio-domain protein PUF7 associates with a nuclear cyclophilin and is involved in ribosomal RNA maturation. *FEBS letters* 584: 1156-1162.
50. Durston, A. 1976. Tip formation is regulated by an inhibitory gradient in the *Dictyostelium discoideum* slug. *Nature* 263: 126.
51. Durston, A., and F. Vork. 1979. A cinematographical study of the development of vitally stained *Dictyostelium discoideum*. *Journal of Cell Science* 36: 261-279.
52. Early, A., T. Abe, and J. Williams. 1995. Evidence for positional differentiation of prestalk cells and for a morphogenetic gradient in *Dictyostelium*. *Cell* 83: 91-99.
53. Early, A. E., M. J. Gaskell, D. Traynor, and J. G. Williams. 1993. Two distinct populations of prestalk cells within the tip of the migratory *Dictyostelium* slug with differing fates at culmination. *Development* 118: 353-362.
54. Edgar, R. C. 2004. MUSCLE: multiple sequence alignment with high accuracy and high throughput. *Nucleic acids research* 32: 1792-1797.
55. Edwards, T. A., S. E. Pyle, R. P. Wharton, and A. K. Aggarwal. 2001. Structure of Pumilio reveals similarity between RNA and peptide binding motifs. *Cell* 105: 281-289.
56. Eichinger, L., and A. A. Noegel. 2003. Crawling into a new era—the *Dictyostelium* genome project. *The EMBO journal* 22: 1941-1946.
57. Eichinger, L. et al. 2005. The genome of the social amoeba *Dictyostelium discoideum*. *Nature* 435: 43.

58. Faix, J., G. Gerisch, and A. A. Noegel. 1992. Overexpression of the csA cell adhesion molecule under its own cAMP-regulated promoter impairs morphogenesis in *Dictyostelium*. *Journal of Cell Science* 102: 203-214.
59. Farnsworth, P. A., and W. Loomis. 1975. A gradient in the thickness of the surface sheath in pseudoplasmodia of *Dictyostelium discoideum*. *Developmental biology* 46: 349-357.
60. Felsenstein, J. 1993. PHYLIP (phylogeny inference package), version 3.5 c. Joseph Felsenstein.
61. Fosnaugh, K., D. Fuller, and W. F. Loomis. 1994. Structural roles of the spore coat proteins in *Dictyostelium discoideum*. *Developmental biology* 166: 823-825.
62. Francischini, C. W., and R. B. Quaggio. 2009. Molecular characterization of *Arabidopsis thaliana* PUF proteins—binding specificity and target candidates. *The FEBS journal* 276: 5456-5470.
63. Franke, J., and R. H. Kessin. 1992. The cyclic nucleotide phosphodiesterases of *Dictyostelium discoideum*: Molecular genetics and biochemistry. *Cellular signalling* 4: 471-478.
64. Freeze, H., and W. F. Loomis. 1977. Isolation and characterization of a component of the surface sheath of *Dictyostelium discoideum*. *Journal of Biological Chemistry* 252: 820-824.
65. Galgano, A. et al. 2008. Comparative analysis of mRNA targets for human PUF-family proteins suggests extensive interaction with the miRNA regulatory system. *PloS one* 3: e3164.
66. Gaskell, M. J., K. A. Jermyn, D. J. Watts, T. Treffry, and J. G. Williams. 1992. Immunolocalization and separation of multiple prestalk cell types in *Dictyostelium*. *Differentiation* 51: 171-176.
67. Gennarino, V. A. et al. 2015. Pumilio1 haploinsufficiency leads to SCA1-like neurodegeneration by increasing wild-type Ataxin1 levels. *Cell* 160: 1087-1098.
68. George, R., H. Hohl, and K. Raper. 1972. Ultrastructural development of stalk-producing cells in *Dictyostelium discoideum*, a cellular slime mould. *Microbiology* 70: 477-489.
69. Gerber, A. P., D. Herschlag, and P. O. Brown. 2004. Extensive association of functionally and cytologically related mRNAs with Puf family RNA-binding proteins in yeast. *PLoS biology* 2: e79.
70. Gerber, A. P., S. Luschnig, M. A. Krasnow, P. O. Brown, and D. Herschlag. 2006. Genome-wide identification of mRNAs associated with the translational regulator PUMILIO in *Drosophila melanogaster*. *Proceedings of the National Academy of Sciences* 103: 4487-4492.
71. Gezelius, K., and B. G. Rånby. 1957. Morphology and fine structure of the slime mold *Dictyostelium discoideum*. *Experimental cell research* 12: 265-289.
72. Glisovic, T., J. L. Bachorik, J. Yong, and G. Dreyfuss. 2008. RNA-binding proteins and post-transcriptional gene regulation. *FEBS letters* 582: 1977-1986.
73. Goldstrohm, A. C., B. A. Hook, D. J. Seay, and M. Wickens. 2006. PUF proteins bind Pop2p to regulate messenger RNAs. *Nature structural & molecular biology* 13: 533.
74. Goldstrohm, A. C., and M. Wickens. 2008. Multifunctional deadenylase complexes diversify mRNA control. *Nature reviews Molecular cell biology* 9: 337.
75. Grabel, L., and W. F. Loomis. 1978. Effector controlling accumulation of N-acetylglucosaminidase during development of *Dictyostelium discoideum*. *Developmental biology* 64: 203-209.

76. Grimson, M. J., C. H. Haigler, and R. L. Blanton. 1996. Cellulose microfibrils, cell motility, and plasma membrane protein organization change in parallel during culmination in *Dictyostelium discoideum*. *Journal of cell science* 109: 3079-3087.
77. Gu, W., Y. Deng, D. Zenklusen, and R. H. Singer. 2004. A new yeast PUF family protein, Puf6p, represses *ASH1* mRNA translation and is required for its localization. *Genes & development* 18: 1452-1465.
78. Guindon, S., and O. Gascuel. 2003. A simple, fast, and accurate algorithm to estimate large phylogenies by maximum likelihood. *Systematic biology* 52: 696-704.
79. Guindon, S., F. Lethiec, P. Duroux, and O. Gascuel. 2005. PHYML Online—a web server for fast maximum likelihood-based phylogenetic inference. *Nucleic acids research* 33: W557-W559.
80. Hacker, U., R. Albrecht, and M. Maniak. 1997. Fluid-phase uptake by macropinocytosis in *Dictyostelium*. *Journal of Cell Science* 110: 105-112.
81. He, C., and D. J. Klionsky. 2009. Regulation mechanisms and signaling pathways of autophagy. *Annual review of genetics* 43.
82. Herskowitz, I. 1988. Life cycle of the budding yeast *Saccharomyces cerevisiae*. *Microbiological reviews* 52: 536.
83. Hodgkin, J. 1986. Sex determination in the nematode *C. elegans*: analysis of *tra-3* suppressors and characterization of *fem* genes. *Genetics* 114: 15-52.
84. Hohl, H. R., and S. T. Hamamoto. 1969. Ultrastructure of spore differentiation in *Dictyostelium*: the prespore vacuole. *Journal of ultrastructure research* 26: 442-453.
85. Hook, B. A., A. C. Goldstrohm, D. J. Seay, and M. Wickens. 2007. Two yeast PUF proteins negatively regulate a single mRNA. *Journal of Biological Chemistry* 282: 15430-15438.
86. Hopper, N., A. Harwood, S. Bouzid, M. Veron, and J. Williams. 1993. Activation of the prespore and spore cell pathway of *Dictyostelium* differentiation by cAMP-dependent protein kinase and evidence for its upstream regulation by ammonia. *The EMBO Journal* 12: 2459-2466.
87. Hopper, N. A., G. M. Sanders, K. L. Fosnaugh, J. G. Williams, and W. F. Loomis. 1995. Protein kinase A is a positive regulator of spore coat gene transcription in *Dictyostelium*. *Differentiation* 58: 183-188.
88. Huang, T., R. A. Kerstetter, and V. F. Irish. 2014. APUM23, a PUF family protein, functions in leaf development and organ polarity in *Arabidopsis*. *Journal of experimental botany* 65: 1181-1191.
89. Huber, R. J., M. A. Myre, and S. L. Cotman. 2017. Aberrant adhesion impacts early development in a *Dictyostelium* model for juvenile neuronal ceroid lipofuscinosis. *Cell adhesion & migration* 11: 399-418.
90. Hubstenberger, A., C. Cameron, R. Shtofman, S. Gutman, and T. C. Evans. 2012. A network of PUF proteins and Ras signaling promote mRNA repression and oogenesis in *C. elegans*. *Developmental biology* 366: 218-231.
91. Huh, S. U., M. J. Kim, and K.-H. Paek. 2013. *Arabidopsis* Pumilio protein APUM5 suppresses Cucumber mosaic virus infection via direct binding of viral RNAs. *Proceedings of the National Academy of Sciences* 110: 779-784.
92. Huh, S. U., and K.-H. Paek. 2014. APUM5, encoding a Pumilio RNA binding protein, negatively regulates abiotic stress responsive gene expression. *BMC plant biology* 14: 75.

93. Jaffer, Z. M., M. Khosla, G. B. Spiegelman, and G. Weeks. 2001. Expression of activated Ras during Dictyostelium development alters cell localization and changes cell fate. *Development* 128: 907-916.
94. Jain, R., and R. Gomer. 1994. A developmentally regulated cell surface receptor for a density-sensing factor in Dictyostelium. *Journal of Biological Chemistry* 269: 9128-9136.
95. Jalal Kiani, S., T. Taheri, S. Rafati, and K. Samimi-Rad. 2017. PUF proteins: Cellular functions and potential applications. *Current Protein and Peptide Science* 18: 250-261.
96. Jang, W., B. Chiem, and R. H. Gomer. 2002. A secreted cell number counting factor represses intracellular glucose levels to regulate group size in Dictyostelium. *Journal of Biological Chemistry* 277: 39202-39208.
97. Jang, W., and R. H. Gomer. 2008. Combining experiments and modelling to understand size regulation in Dictyostelium discoideum. *Journal of The Royal Society Interface* 5: S49-S58.
98. Jermyn, K., M. Berks, R. Kay, and J. Williams. 1987. Two distinct classes of prestalk-enriched mRNA sequences in Dictyostelium discoideum. *Development* 100: 745-755.
99. Jermyn, K., K. Duffy, and J. Williams. 1989. A new anatomy of the prestalk zone in Dictyostelium. *Nature* 340: 144.
100. Jermyn, K., D. Traynor, and J. Williams. 1996. The initiation of basal disc formation in Dictyostelium discoideum is an early event in culmination. *Development* 122: 753-760.
101. Jermyn, K., and J. Williams. 1991. An analysis of culmination in Dictyostelium using prestalk and stalk-specific cell autonomous markers. *Development* 111: 779-787.
102. Jiang, L. et al. 2017. A Puf RNA-binding protein encoding gene PIM90 regulates the sexual and asexual life stages of the litchi downy blight pathogen *Peronosphythora litchii*. *Fungal genetics and biology* 98: 39-45.
103. Kadyrova, L. Y., Y. Habara, T. H. Lee, and R. P. Wharton. 2007. Translational control of maternal Cyclin B mRNA by Nanos in the Drosophila germline. *Development* 134: 1519-1527.
104. Kay, R. R. 1982. cAMP and spore differentiation in Dictyostelium discoideum. *Proceedings of the National Academy of Sciences* 79: 3228-3231.
105. Keene, J. D. 2007. RNA regulons: coordination of post-transcriptional events. *Nature Reviews Genetics* 8: 533.
106. Kershner, A. et al. 2013. Germline stem cells and their regulation in the nematode *Caenorhabditis elegans* *Transcriptional and Translational Regulation of Stem Cells*. p 29-46. Springer.
107. Kershner, A. M., H. Shin, T. J. Hansen, and J. Kimble. 2014. Discovery of two GLP-1/Notch target genes that account for the role of GLP-1/Notch signaling in stem cell maintenance. *Proceedings of the National Academy of Sciences* 111: 3739-3744.
108. Kimmel, A. R., and R. A. Firtel. 1991. cAMP signal transduction pathways regulating development of Dictyostelium discoideum. *Current opinion in genetics & development* 1: 383-390.
109. Kimmel, A. R., and C. A. Parent. 2003. The signal to move: D. discoideum go orienteering. *Science* 300: 1525-1527.
110. Kimura, S., T. Noda, and T. Yoshimori. 2007. Dissection of the autophagosome maturation process by a novel reporter protein, tandem fluorescent-tagged LC3. *Autophagy* 3: 452-460.
111. Klionsky, D. J. et al. 2008. Guidelines for the use and interpretation of assays for monitoring autophagy in higher eukaryotes. *Autophagy* 4: 151-175.

112. Konijn, T. M., J. Van De Meene, J. T. Bonner, and D. S. Barkley. 1967. The acrasin activity of adenosine-3', 5'-cyclic phosphate. *Proceedings of the National Academy of Sciences of the United States of America* 58: 1152.
113. Kosta, A. et al. 2004. Autophagy gene disruption reveals a non-vacuolar cell death pathway in *Dictyostelium*. *Journal of Biological Chemistry* 279: 48404-48409.
114. Kreppel, L., and A. R. Kimmel. 2002. Genomic database resources for *Dictyostelium discoideum*. *Nucleic acids research* 30: 84-86.
115. Kuhlmann, M., B. Popova, and W. Nellen. 2006. RNA interference and antisense-mediated gene silencing in *Dictyostelium*. *Dictyostelium discoideum protocols*. p 211-226. Springer.
116. Laporte, C. et al. 2007. A necrotic cell death model in a protist. *Cell death and differentiation* 14: 266.
117. Laub, M. T., and W. F. Loomis. 1998. A molecular network that produces spontaneous oscillations in excitable cells of *Dictyostelium*. *Molecular biology of the cell* 9: 3521-3532.
118. Lee, D. et al. 2010. PUF3 acceleration of deadenylation in vivo can operate independently of CCR4 activity, possibly involving effects on the PAB1-mRNP structure. *Journal of molecular biology* 399: 562-575.
119. Lee, M.-H. et al. 2007. Conserved regulation of MAP kinase expression by PUF RNA-binding proteins. *PLoS genetics* 3: e233.
120. Lehmann, R., and C. Nüsslein-Volhard. 1987. Involvement of the *pumilio* gene in the transport of an abdominal signal in the *Drosophila* embryo. *Nature* 329: 167.
121. Leichtling, B. et al. 1984. A cytosolic cyclic AMP-dependent protein kinase in *Dictyostelium discoideum*. II. Developmental regulation. *Journal of Biological Chemistry* 259: 662-668.
122. Levraud, J.-P. et al. 2003. *Dictyostelium* cell death: early emergence and demise of highly polarized paddle cells. *The Journal of cell biology* 160: 1105-1114.
123. Lin, K.-b. et al. 2018a. Generation and functional characterization of a conditional *Pumilio2* null allele. *Journal of biomedical research* 32: 434.
124. Lin, K. et al. 2018b. Essential requirement of mammalian *Pumilio* family in embryonic development. *Molecular biology of the cell* 29: 2922-2932.
125. Lohia, R. et al. 2017. *Dictyostelium discoideum* Sir2D modulates cell-type specific gene expression and is involved in autophagy. *Int. J. Dev. Biol* 61: 95-104.
126. Loomis, W. F. 1993. 1 Lateral Inhibition and Pattern Formation in *Dictyostelium* *Current topics in developmental biology* No. 28. p 1-46. Elsevier.
127. Loomis, W. F. 1998. Role of PKA in the timing of developmental events in *Dictyostelium* cells. *Microbiol. Mol. Biol. Rev.* 62: 684-694.
128. Louis, J. M., G. T. Ginsburg, and A. R. Kimmel. 1994. The cAMP receptor CAR4 regulates axial patterning and cellular differentiation during late development of *Dictyostelium*. *Genes & Development* 8: 2086-2096.
129. Lu, G., and T. M. T. Hall. 2011. Alternate modes of cognate RNA recognition by human PUMILIO proteins. *Structure* 19: 361-367.
130. Macdonald, P. M. 1992. The *Drosophila pumilio* gene: an unusually long transcription unit and an unusual protein. *Development* 114: 221-232.
131. Machin, N. A., J. M. Lee, and G. Barnes. 1995. Microtubule stability in budding yeast: characterization and dosage suppression of a benomyl-dependent tubulin mutant. *Molecular biology of the cell* 6: 1241-1259.

132. MAEDA, Y., and I. TAKEUCHI. 1969. CELL DIFFERENTIATION AND FINE STRUCTURES IN THE DEVELOPMENT OF THE CELLULAR SLIME MOLDS 1. *Development, growth & differentiation* 11: 232-245.
133. Maillet, L., and M. A. Collart. 2002. Interaction between Not1p, a component of the Ccr4-not complex, a global regulator of transcription, and Dhh1p, a putative RNA helicase. *Journal of Biological Chemistry* 277: 2835-2842.
134. Manahan, C. L., P. A. Iglesias, Y. Long, and P. N. Devreotes. 2004. Chemoattractant signaling in *Dictyostelium discoideum*. *Annu. Rev. Cell Dev. Biol.* 20: 223-253.
135. Maniak, M., R. Rauchenberger, R. Albrecht, J. Murphy, and G. Gerisch. 1995. Coronin involved in phagocytosis: dynamics of particle-induced relocalization visualized by a green fluorescent protein Tag. *Cell* 83: 915-924.
136. Mann, S., W. M. Yonemoto, S. S. Taylor, and R. A. Firtel. 1992. DdPK3, which plays essential roles during *Dictyostelium* development, encodes the catalytic subunit of cAMP-dependent protein kinase. *Proceedings of the National Academy of Sciences* 89: 10701-10705.
137. Mesquita, A. et al. 2017. Autophagy in *Dictyostelium*: Mechanisms, regulation and disease in a simple biomedical model. *Autophagy* 13: 24-40.
138. Miller, M. A., and W. M. Olivas. 2011. Roles of Puf proteins in mRNA degradation and translation. *Wiley Interdisciplinary Reviews: RNA* 2: 471-492.
139. Miller, M. T., J. J. Higgin, and T. M. T. Hall. 2008. Basis of altered RNA-binding specificity by PUF proteins revealed by crystal structures of yeast Puf4p. *Nature structural & molecular biology* 15: 397.
140. Mizushima, N. 2010. The role of the Atg1/ULK1 complex in autophagy regulation. *Current opinion in cell biology* 22: 132-139.
141. Moore, F. L. et al. 2003. Human Pumilio-2 is expressed in embryonic stem cells and germ cells and interacts with DAZ (Deleted in AZoospermia) and DAZ-like proteins. *Proceedings of the National Academy of Sciences* 100: 538-543.
142. Morris, H. R., G. W. Taylor, M. S. Masento, K. A. Jermyn, and R. R. Kay. 1987. Chemical structure of the morphogen differentiation inducing factor from *Dictyostelium discoideum*. *Nature* 328: 811.
143. Murata, Y., and T. Ohnishi. 1980. *Dictyostelium discoideum* fruiting bodies observed by scanning electron microscopy. *Journal of bacteriology* 141: 956-958.
144. Murata, Y., and R. P. Wharton. 1995. Binding of pumilio to maternal hunchback mRNA is required for posterior patterning in *Drosophila* embryos. *Cell* 80: 747-756.
145. Myre, M. A. et al. 2011. Deficiency of huntingtin has pleiotropic effects in the social amoeba *Dictyostelium discoideum*. *PLoS genetics* 7: e1002052.
146. Narita, R. et al. 2014. A novel function of human Pumilio proteins in cytoplasmic sensing of viral infection. *PLoS pathogens* 10: e1004417.
147. Newell, P. C., A. Telser, and M. Sussman. 1969. Alternative developmental pathways determined by environmental conditions in the cellular slime mold *Dictyostelium discoideum*. *Journal of bacteriology* 100: 763-768.
148. Opperman, L., B. Hook, M. DeFino, D. S. Bernstein, and M. Wickens. 2005. A single spacer nucleotide determines the specificities of two mRNA regulatory proteins. *Nature structural & molecular biology* 12: 945.
149. Orlow, S. J., R. I. Shapiro, J. Franke, and R. H. Kessin. 1981. The extracellular cyclic nucleotide phosphodiesterase of *Dictyostelium discoideum*. Purification and characterization. *Journal of Biological Chemistry* 256: 7620-7627.

150. Otto, G. P., M. Y. Wu, N. Kazgan, O. R. Anderson, and R. H. Kessin. 2004. Dictyostelium macroautophagy mutants vary in the severity of their developmental defects. *Journal of Biological Chemistry* 279: 15621-15629.
151. Poff, K., and W. Loomis Jr. 1973. Control of phototactic migration in Dictyostelium discoideum. *Experimental cell research* 82: 236-240.
152. PREISS, T., M. MUCKENTHALER, and M. W. HENTZE. 1998. Poly (A)-tail-promoted translation in yeast: implications for translational control. *Rna* 4: 1321-1331.
153. Qiu, C., K. L. McCann, R. N. Wine, S. J. Baserga, and T. M. T. Hall. 2014. A divergent Pumilio repeat protein family for pre-rRNA processing and mRNA localization. *Proceedings of the National Academy of Sciences* 111: 18554-18559.
154. Quenault, T., T. Lithgow, and A. Traven. 2011. PUF proteins: repression, activation and mRNA localization. *Trends in cell biology* 21: 104-112.
155. Raper, K. B. 1935. Dictyostelium discoideum, a new species of slime mold from decaying forest leaves. *J. Agricul. Res.* 50: 135-147.
156. Raper, K. B. 1940. Pseudoplasmodium formation and organization in Dictyostelium discoideum. *Journal of the Elisha Mitchell Scientific Society* 56: 241-282.
157. Raper, K. B., and D. I. Fennell. 1952. Stalk formation in Dictyostelium. *Bulletin of the Torrey Botanical Club*: 25-51.
158. Rathi, A., S. C. Kayman, and M. Clarke. 1991. Induction of gene expression in Dictyostelium by prestarvation factor, a factor secreted by growing cells. *Developmental genetics* 12: 82-87.
159. Ray, D. et al. 2013. A compendium of RNA-binding motifs for decoding gene regulation. *Nature* 499: 172.
160. Reichel, M. et al. 2016. In planta determination of the mRNA-binding proteome of Arabidopsis etiolated seedlings. *The Plant Cell* 28: 2435-2452.
161. Roisin-Bouffay, C., W. Jang, D. R. Caprette, and R. H. Gomer. 2000. A precise group size in Dictyostelium is generated by a cell-counting factor modulating cell-cell adhesion. *Molecular cell* 6: 953-959.
162. Roisin-Bouffay, C. et al. 2004. Developmental cell death in Dictyostelium does not require paracaspase. *Journal of Biological Chemistry* 279: 11489-11494.
163. Rose, P. W. et al. 2010. The RCSB Protein Data Bank: redesigned web site and web services. *Nucleic acids research* 39: D392-D401.
164. Roy, A., A. Kucukural, and Y. Zhang. 2010. I-TASSER: a unified platform for automated protein structure and function prediction. *Nature protocols* 5: 725.
165. Rubin, J., and A. Robertson. 1975. The tip of the Dictyostelium discoideum pseudoplasmodium as an organizer. *Development* 33: 227-241.
166. Saito, T., A. Kato, and R. R. Kay. 2008. DIF-1 induces the basal disc of the Dictyostelium fruiting body. *Developmental biology* 317: 444-453.
167. Salazar, A. M., E. J. Silverman, K. P. Menon, and K. Zinn. 2010. Regulation of synaptic Pumilio function by an aggregation-prone domain. *Journal of Neuroscience* 30: 515-522.
168. Sasaki, K. et al. 2008. An immediate-early gene, srsA: its involvement in the starvation response that initiates differentiation of Dictyostelium cells. *Differentiation* 76: 1093-1103.
169. Schaap, P. 2011. Evolutionary crossroads in developmental biology: Dictyostelium discoideum. *Development* 138: 387-396.

170. Schaap, P. 2016. Evolution of developmental signalling in Dictyostelid social amoebas. *Current opinion in genetics & development* 39: 29-34.
171. Schaap, P., L. van der Molen, and T. M. Konijn. 1981. Development of the simple cellular slime mold *Dictyostelium minutum*. *Developmental biology* 85: 171-179.
172. Schaap, P., and R. van Driel. 1985. Induction of post-aggregative differentiation in *Dictyostelium discoideum* by cAMP: evidence of involvement of the cell surface cAMP receptor. *Experimental cell research* 159: 388-396.
173. Schmelzle, T., and M. N. Hall. 2000. TOR, a central controller of cell growth. *Cell* 103: 253-262.
174. Schneider, T. D., and R. M. Stephens. 1990. Sequence logos: a new way to display consensus sequences. *Nucleic acids research* 18: 6097-6100.
175. Schulkes, C., and P. Schaap. 1995. cAMP-dependent protein kinase activity is essential for preaggregative gene expression in *Dictyostelium*. *FEBS letters* 368: 381-384.
176. Serafimidis, I., G. Bloomfield, J. Skelton, A. Ivens, and R. R. Kay. 2007. A new environmentally resistant cell type from *Dictyostelium*. *Microbiology* 153: 619.
177. Shin, H. et al. 2017. SYGL-1 and LST-1 link niche signaling to PUF RNA repression for stem cell maintenance in *Caenorhabditis elegans*. *PLoS genetics* 13: e1007121.
178. Shrestha, S., X. Li, G. Ning, J. Miao, and L. Cui. 2016. The RNA-binding protein Puf1 functions in the maintenance of gametocytes in *Plasmodium falciparum*. *J Cell Sci* 129: 3144-3152.
179. Smith, E., and K. L. Williams. 1980. Evidence for tip control of the 'slug/fruit' switch in slugs of *Dictyostelium discoideum*. *Development* 57: 233-240.
180. Souza, G. M., A. M. Da Silva, and A. Kuspa. 1999. Starvation promotes *Dictyostelium* development by relieving PufA inhibition of PKA translation through the Yaka kinase pathway. *Development* 126: 3263-3274.
181. Souza, G. M., S. Lu, and A. Kuspa. 1998. Yaka, a protein kinase required for the transition from growth to development in *Dictyostelium*. *Development* 125: 2291-2302.
182. Spassov, D., and R. Jurecic. 2003a. The PUF family of RNA-binding proteins: does evolutionarily conserved structure equal conserved function? *IUBMB life* 55: 359-366.
183. Spassov, D. S., and R. Jurecic. 2003b. Mouse Pum1 and Pum2 genes, members of the Pumilio family of RNA-binding proteins, show differential expression in fetal and adult hematopoietic stem cells and progenitors. *Blood Cells, Molecules, and Diseases* 30: 55-69.
184. Spratt Jr, N. T., and H. Haas. 1961. Integrative mechanisms in development of the early chick blastoderm. II. Role of morphogenetic movements and regenerative growth in synthetic and topographically disarranged blastoderms. *Journal of Experimental Zoology* 147: 57-93.
185. Sternfeld, J. 1992. A study of pstB cells during *Dictyostelium* migration and culmination reveals a unidirectional cell type conversion process. *Roux's archives of developmental biology* 201: 354-363.
186. Sternfeld, J., and C. N. David. 1981. Cell sorting during pattern formation in *Dictyostelium*. *Differentiation* 20: 10-21.
187. Sternfeld, J., and C. N. David. 1982. Fate and regulation of anterior-like cells in *Dictyostelium* slugs. *Developmental biology* 93: 111-118.
188. Stewart, M. S., S. A. Krause, J. McGhie, and J. V. Gray. 2007. Mpt5p, a stress tolerance- and lifespan-promoting PUF protein in *Saccharomyces cerevisiae*, acts upstream of the cell wall integrity pathway. *Eukaryotic cell* 6: 262-270.

189. Stumpf, C. R., J. Kimble, and M. Wickens. 2008. A *Caenorhabditis elegans* PUF protein family with distinct RNA binding specificity. *Rna* 14: 1550-1557.
190. Sugang, R., C. J. Weijer, F. Siegert, J. Franke, and R. H. Kessin. 1997. Null Mutations of the *Dictyostelium* Cyclic Nucleotide Phosphodiesterase Gene Block Chemotactic Cell Movement in Developing Aggregates. *Developmental biology* 192: 181-192.
191. Tam, P. P. et al. 2010. The Puf family of RNA-binding proteins in plants: phylogeny, structural modeling, activity and subcellular localization. *BMC plant biology* 10: 44.
192. Tang, L. et al. 2002. A cell number-counting factor regulates the cytoskeleton and cell motility in *Dictyostelium*. *Proceedings of the National Academy of Sciences* 99: 1371-1376.
193. Tautz, D. 1988. Regulation of the *Drosophila* segmentation gene *hunchback* by two maternal morphogenetic centres. *Nature* 332: 281.
194. Tekinay, T., M. Y. Wu, G. P. Otto, O. R. Anderson, and R. H. Kessin. 2006. Function of the *Dictyostelium discoideum* Atg1 kinase during autophagy and development. *Eukaryotic cell* 5: 1797-1806.
195. Town, C., J. Gross, and R. Kay. 1976. Cell differentiation without morphogenesis in *Dictyostelium discoideum*. *Nature* 262: 717.
196. Town, C., and E. Stanford. 1979. An oligosaccharide-containing factor that induces cell differentiation in *Dictyostelium discoideum*. *Proceedings of the National Academy of Sciences* 76: 308-312.
197. Tresse, E., A. Kosta, M.-F. Luciani, and P. Golstein. 2007. From autophagic to necrotic cell death in *Dictyostelium*. In: *Seminars in cancer biology*. p 94-100.
198. Van Der Spoel, D. et al. 2005. GROMACS: fast, flexible, and free. *Journal of computational chemistry* 26: 1701-1718.
199. Varney, T. R., H. Ho, and D. D. Blumberg. 2002. A novel disintegrin domain protein affects early cell type specification and pattern formation in *Dictyostelium*. *Development* 129: 2381-2389.
200. Vessey, J. P. et al. 2006. Dendritic localization of the translational repressor Pumilio 2 and its contribution to dendritic stress granules. *Journal of Neuroscience* 26: 6496-6508.
201. Wang, X., J. McLachlan, P. D. Zamore, and T. M. T. Hall. 2002. Modular recognition of RNA by a human pumilio-homology domain. *Cell* 110: 501-512.
202. Wang, X., P. D. Zamore, and T. M. T. Hall. 2001. Crystal structure of a Pumilio homology domain. *Molecular cell* 7: 855-865.
203. Wang, Y., L. Opperman, M. Wickens, and T. M. T. Hall. 2009. Structural basis for specific recognition of multiple mRNA targets by a PUF regulatory protein. *Proceedings of the National Academy of Sciences* 106: 20186-20191.
204. Webber, J. L., A. R. Young, and S. A. Tooze. 2007. Atg9 trafficking in mammalian cells. *Autophagy* 3: 54-56.
205. Weidmann, C. A., and A. C. Goldstrohm. 2012. *Drosophila* Pumilio protein contains multiple autonomous repression domains that regulate mRNAs independently of Nanos and brain tumor. *Molecular and cellular biology* 32: 527-540.
206. West, C. M., and G. W. Erdos. 1990. Formation of the *Dictyostelium* spore coat. *Developmental genetics* 11: 492-506.
207. Wharton, R. P., J. Sonoda, T. Lee, M. Patterson, and Y. Murata. 1998. The Pumilio RNA-binding domain is also a translational regulator. *Molecular cell* 1: 863-872.

208. Wharton, R. P., and G. Struhl. 1991. RNA regulatory elements mediate control of *Drosophila* body pattern by the posterior morphogen nanos. *Cell* 67: 955-967.
209. Whittingham, W. F., and K. B. Raper. 1960. Non-viability of stalk cells in *Dictyostelium*. *Proceedings of the National Academy of Sciences of the United States of America* 46: 642.
210. Wickens, M., D. S. Bernstein, J. Kimble, and R. Parker. 2002. A PUF family portrait: 3' UTR regulation as a way of life. *TRENDS in Genetics* 18: 150-157.
211. Wilinski, D. et al. 2015. RNA regulatory networks diversified through curvature of the PUF protein scaffold. *Nature communications* 6: 8213.
212. Williams, J. 1995. Morphogenesis in *Dictyostelium*: New twists to a not-so-old tale. *Current opinion in genetics & development* 5: 426-431.
213. Williams, J. G. 2006. Transcriptional regulation of *Dictyostelium* pattern formation. *EMBO reports* 7: 694-698.
214. Williams, J. G. et al. 1989. Origins of the prestalk-prespore pattern in *Dictyostelium* development. *Cell* 59: 1157-1163.
215. Wong, E. et al. 2002. Disruption of the gene encoding the cell adhesion molecule DdCAD-1 leads to aberrant cell sorting and cell-type proportioning during *Dictyostelium* development. *Development* 129: 3839-3850.
216. Wreden, C., A. C. Verrotti, J. A. Schisa, M. E. Lieberfarb, and S. Strickland. 1997. Nanos and pumilio establish embryonic polarity in *Drosophila* by promoting posterior deadenylation of hunchback mRNA. *Development* 124: 3015-3023.
217. Wu, Z. et al. 2016. RNA binding proteins RZ-1B and RZ-1C play critical roles in regulating pre-mRNA splicing and gene expression during development in *Arabidopsis*. *The Plant Cell* 28: 55-73.
218. Xu, E. Y., R. Chang, N. A. Salmon, and R. A. Reijo Pera. 2007. A gene trap mutation of a murine homolog of the *Drosophila* stem cell factor Pumilio results in smaller testes but does not affect litter size or fertility. *Molecular reproduction and development* 74: 912-921.
219. Yagi, Y. et al. 2013. Pentatricopeptide repeat proteins involved in plant organellar RNA editing. *RNA biology* 10: 1419-1425.
220. Yamada, Y., B. Nuñez-Corcuera, and J. G. Williams. 2011. DIF-1 regulates *Dictyostelium* basal disc differentiation by inducing the nuclear accumulation of a bZIP transcription factor. *Developmental biology* 354: 77-86.
221. Yamada, Y., H. Sakamoto, S. Ogihara, and M. Maeda. 2005. Novel patterns of the gene expression regulation in the prestalk region along the antero-posterior axis during multicellular development of *Dictyostelium*. *Gene expression patterns* 6: 63-68.
222. Yang, J., and Y. Zhang. 2015. I-TASSER server: new development for protein structure and function predictions. *Nucleic acids research* 43: W174-W181.
223. Ye, B. et al. 2004. Nanos and Pumilio are essential for dendrite morphogenesis in *Drosophila* peripheral neurons. *Current biology* 14: 314-321.
224. Yin, P. et al. 2013. Structural basis for the modular recognition of single-stranded RNA by PPR proteins. *Nature* 504: 168.
225. Yuen, I. S. et al. 1995. A density-sensing factor regulates signal transduction in *Dictyostelium*. *The Journal of cell biology* 129: 1251-1262.
226. Zamore, P., J. Williamson, and R. Lehmann. 1997. The Pumilio protein binds RNA through a conserved domain that defines a new class of RNA-binding proteins. *Rna* 3: 1421.

227. Zamore, P. D., D. P. Bartel, R. Lehmann, and J. R. Williamson. 1999. The PUMILIO–RNA Interaction: A Single RNA-Binding Domain Monomer Recognizes a Bipartite Target Sequence. *Biochemistry* 38: 596-604.
228. Zhang, B. et al. 1997. A conserved RNA-binding protein that regulates sexual fates in the *C. elegans* hermaphrodite germ line. *Nature* 390: 477.
229. Zhang, C., and D. G. Muench. 2015. A nucleolar PUF RNA-binding protein with specificity for a unique RNA sequence. *Journal of Biological Chemistry* 290: 30108-30118.
230. Zhang, J. et al. 2016. Nop9 is a PUF-like protein that prevents premature cleavage to correctly process pre-18S rRNA. *Nature communications* 7: 13085.
231. Zhu, D., C. R. Stumpf, J. M. Krahn, M. Wickens, and T. M. T. Hall. 2009. A 5' cytosine binding pocket in Puf3p specifies regulation of mitochondrial mRNAs. *Proceedings of the National Academy of Sciences* 106: 20192-20197.

Media, Chemicals and Reagents

Growth media, buffers and reagents:

HL5 (for 1 litre)

Proteose peptone	14.3 g
Yeast extract	7.15 g
Glucose	16 g
Na ₂ HPO ₄ ·2H ₂ O	0.626 g
KH ₂ PO ₄	0.485 g

pH was adjusted to 6.5 with dilute HCl and the volume made up with double distilled water

Luria Broth (LB) for 100 mL

Bacteriological Peptone	1.0 g
Yeast Extract	0.5 g
NaCl	1.0 g

pH was adjusted to 7.5 with NaOH and the volume made up to 100 mL

For LB agar 2 % of Agar was added

KK₂ buffer (for 1 litre) (10x)

KH ₂ PO ₄	22.5 g
K ₂ HPO ₄	6.2 g

pH adjusted to 6.2 and the volume made up to 1 litre. Autoclaved and stored at 4°C

H-50 electroporation buffer

20 mM HEPES
50 mM KCl
10 mM NaCl
1 mM MgSO ₄
5 mM NaHCO ₃
1 mM NaH ₂ PO ₄ ·2H ₂ O
pH 7.0

Spore buffer

40 mM KH ₂ PO ₄
20 mM KCl
2.5 mM MgCl ₂

NNA plates

1.5% Agar per 500 mL of 1xKK₂

Alkaline Lysis solution I

50 mM glucose

25 mM Tris -Cl pH 8.0

10 mM EDTA, pH 8.0

Autoclaved and stored at 4°C

Alkaline Lysis solution II

0.2N NaOH

1% SDS

Solution II is always prepared just before use.

Alkaline Lysis solution III

5 M Potassium Acetate solution 60 mL

Glacial Acetic Acid 11.5 mL

Water 28.5 mL

The resulting solution is 3M with respect to Potassium and 5 M with respect to Acetate.

Buffer 1

10 mM EDTA

10 mM Tris (pH 7.5)

1x carbonate buffer

120 mM Na₂CO₃

80 mM NaHCO₃

DB

10 mM phosphate buffer (pH 6.5)

2 mM MgSO₄

0.2 mM CaCl₂

50x Denhardt's reagent

1% w/v Ficoll type 400 (Pharmacia)

1% w/v bovine serum albumin (fraction V, Sigma)

1% w/v polyvinylpyrrolidone

DEPC-treated water

0.1% DEPC in double distilled water

Mixed, allowed to remain at 37°C overnight
Autoclaved and stored at RNase free conditions

DNA loading Dye (6x)

0.25% Bromophenol Blue
30% Glycerol

Ethidium Bromide (EtBr)

10mg/mL

Z buffer

60 mM Na₂HPO₄
40 mM NaH₂PO₄
10 mM KCl
1 mM MgSO₄
Adjust the pH to 7.0, sterilize by autoclaving and store at 4°C

Fixing solution

3.7% formaldehyde solution prepared in Z buffer (freshly prepare before use)

Hybridization buffer

4x SSC
0.5 mg/mL sonicated denatured calf thymus DNA (Sigma)
0.25 mg/mL yeast RNA (Sigma)
60% formamide

Staining solution

5 mM potassium ferrocyanide
5 mM potassium ferricyanide
0.4 mg/mL X-Gal in Z buffer
Prepare immediately before use by mixing 680 µL Z buffer, 150 µL potassium ferrocyanide stock solution, 150 µL potassium ferricyanide stock solution and 20 µL X-Gal stock solution per mL of staining solution.

10x SSC

1.5 M NaCl
150 mM sodium citrate, pH 7.0

Permeabilization solution

0.1% NP40 in Z buffer

Potassium ferrocyanide

33 mM dissolved in double distilled water, in dark and stored at 4°C

Potassium ferricyanide

33mM dissolved in double distilled water, in dark and stored at 4°C

Prehybridization buffer

4x SSC

1x Denhardt's solution

0.5 mg/mL sonicated denatured calf thymus DNA (Sigma)

0.25 mg/mL yeast RNA (Sigma)

60% formamide

RLB

0.32 M Sucrose,

5 mM MgCl₂,

1% Triton-100

10 mM Tris (pH 7.5)

Bradford Reagent

10 mg Coomassie Brilliant blue G-250

5 mL ethanol

10 mL conc. H₃PO₄

Total volume 100 mL with water

50x TAE buffer

242 g Tris Base

57.1 mL Glacial Acetic Acid

100 mL of 0.5 M EDTA (pH 8.0)

Volume 1000 mL

Lysis buffer

50 mM Tris-HCl (pH 7.5)

150 mM NaCl

0.1% Triton X-100

5% Glycerol

1mM Phenylmethylsulfonyl fluoride (PMSF)

0.2 mg/ml Lysozyme

EDTA free 1x protease inhibitor cocktail

5xTBE buffer

54 g of Tris base
27.5 g of boric acid
20 mL of 0.5 M EDTA (pH 8.0)
Volume 1000 mL

TE, pH 8.0

10 mM Tris-Cl, pH 8.0
1 mM EDTA, pH 8.0

X-Gal (5-Bromo-4-chloro-3-indolyl β -D-galactopyranoside)

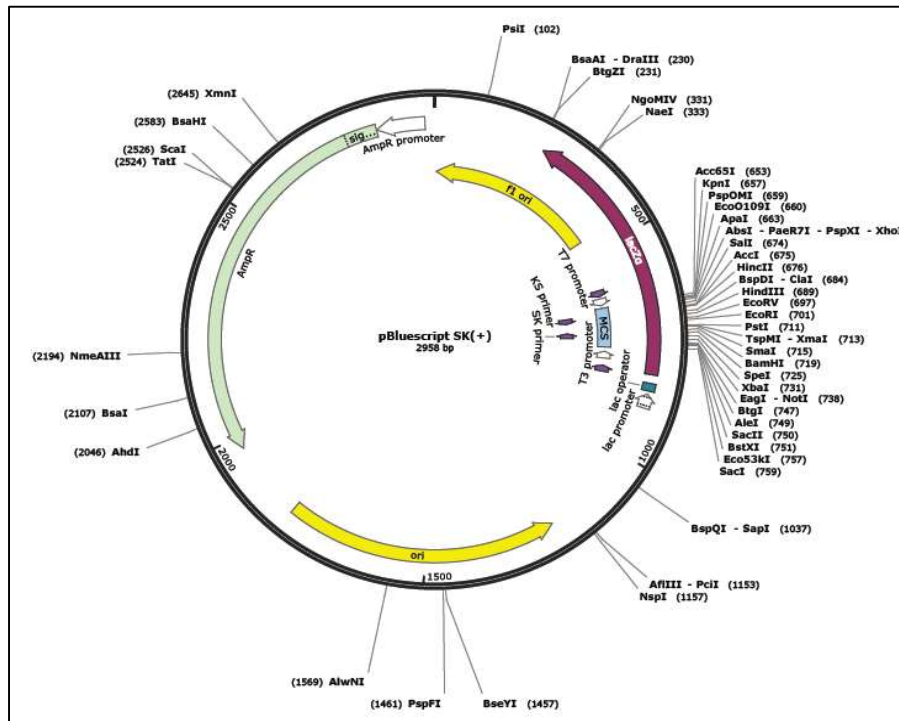
20mg/mL in dimethyl formamide. Store at -20°C in dark.

Cell cycle buffer

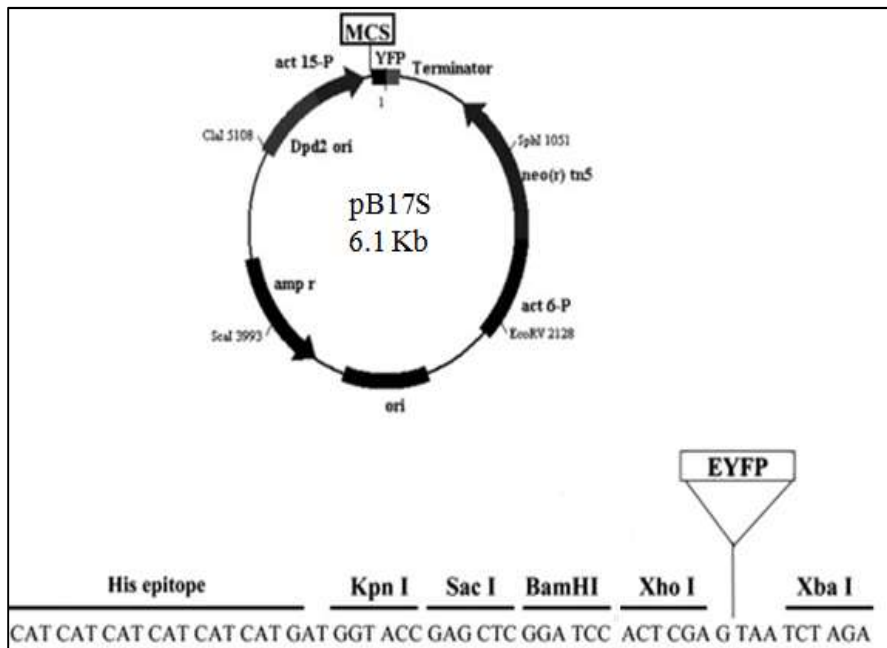
0.9% NaCl,
2% Sucrose,
5 mM EDTA in 1xKK₂ buffer

Vector Maps

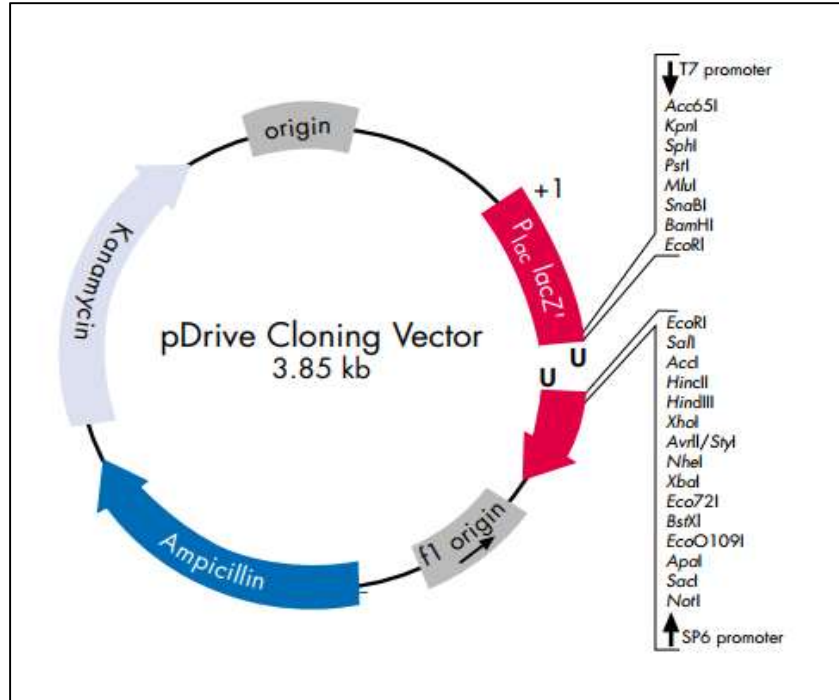
1. pBluescript SK(+)



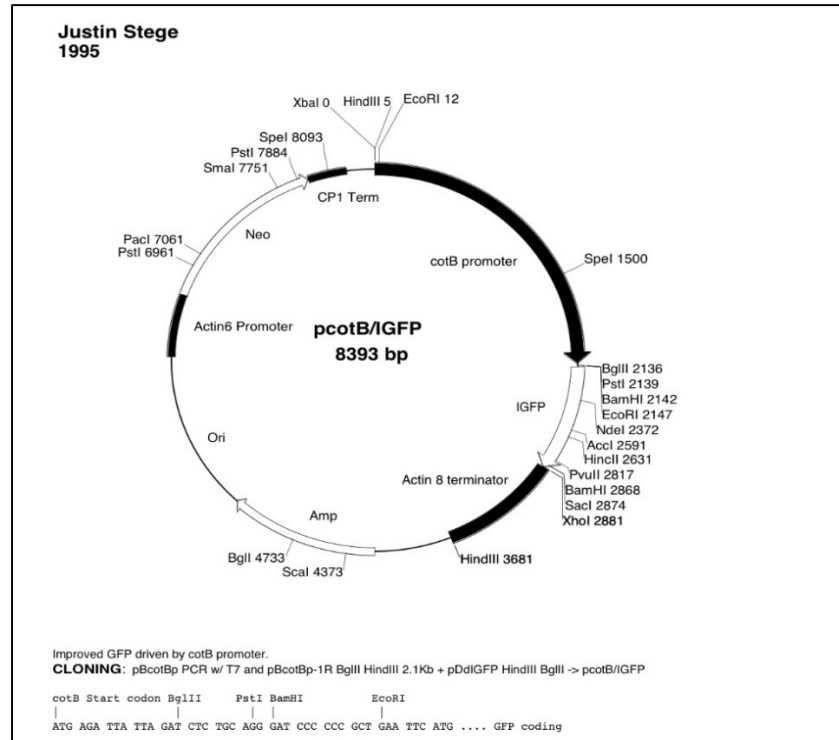
2. pB17S



3. pDrive



4. pcotB/IGFP



Conferences and Seminars

1. **Karan Singh Rajput**, Shweta Saran. Title: characterization of *D. discoideum* PUF protein. XL ALL INDIA CELL BIOLOGY CONFERENCE & INTERNATIONAL SYMPOSIUM on Functional Genomics and Epigenomics Jiwaji University, Gwalior (November 17-19, 2016) (**Poster Presentation**).
2. **Karan Singh Rajput**, Shweta Saran. Title: Role of PUF in *Dictyostelium Discoideum*. NATIONAL SCIENCE DAY 2018 Organized by Department of Science and Technology & Jawaharlal Nehru University, New Delhi. “Science and Technology for Sustainable Future” (28th February, 2018) (**Poster Presentation**)
3. **Karan Singh Rajput**, Shweta Saran. Title: Functional Characterization of PUF Protein in *Dictyostelium Discoideum*. 1st INTERNATIONAL CONFERENCE on Integrative Chemistry, Biology and Translational Medicine (ICBTM-2019). Centre for Global Health, Hansraj College, University of Delhi, India & Loyola University Chicago Stritch School of Medicine, USA (25-26 February 2019)(**Oral Presentation**).

Publications

Nalini Singh, Karan Singh Rajput and Shweta Saran. “Overexpression of calpain and its effect on autophagy in *Dictyostelium discoideum*”. (Accepted in Annals of Biology on 21-05-2019).

AGRI BIO PUBLISHER

121, Mohalla Chaudharian, Katra Ramlila, HISAR-125 001, India

E-mail: bajdass@gmail.com

Telephone: 01662-237530; Mobile 092551-26155; ISSN: 0970-0153

Ref. No. AOB/2019/14

Dated: 21.05.2019

Dear Prof. **Shweta Saran**,

The paper entitled “**Overexpression of calpain and its effect on autophagy in *Dictyostelium discoideum***” by “**Nalini Singh, Karan Singh Rajput and Shweta Saran**” has been received for publication in the Annals of Agri Bio Research

The paper has been given a MS No. 2019/74 which should be quoted while making future correspondence about the paper.

I am happy to inform you that subject to editorial corrections the above referred manuscript has been accepted for publication in Annals of Biology. Every effort will be made to accommodate it in next issue of Annals of Biology.

Yours sincerely,



(Editor)

Prof. Shweta Saran,
School of Life Sciences,
Jawaharlal Nehru University,
New Delhi 110067

Turnitin Originality Report

Processed on: 12-Jul-2019 19:39 IST

ID: 1151292932

Word Count: 32194

Submitted: 1

karan complete thesis By
Karan Rajput

Similarity by Source	
Similarity Index	
7%	
Internet Sources:	1%
Publications:	9%
Student Papers:	N/A

[include quoted](#)
[include bibliography](#)
[excluding matches < 1%](#)
[download](#)
[refresh](#)
[print](#)
mode:

2% match (publications) ✕

[Neha Gupta, Shweta Saran. "Deletion of etoposide-induced 2.4 kb transcript \(ei24\) reduced cell proliferation and aggregate-size in Dictyostelium discoideum", The International Journal of Developmental Biology, 2018](#)

2% match (publications) ✕

[Ranjana Maurya, Rakesh Kumar, Shweta Saran. " AMPKα regulates aggregate size and cell-type patterning ", Open Biology, 2017](#)

1% match (publications) ✕

[Rakesh Kumar, Ranjana Maurya, Shweta Saran. "Introducing a simple model system for binding studies of known and novel inhibitors of AMPK: a therapeutic target for prostate cancer", Journal of Biomolecular Structure and Dynamics, 2018](#)

1% match (publications) ✕

[Rakhee Lohia, Punita Jain, Mukul Jain, Himanshu Mishra, Pradeep Kumar Burma, Anju Shrivastava, Shweta Saran. "Deletion of Dictyostelium discoideum Sir2A impairs cell proliferation and inhibits autophagy", Journal of Biosciences, 2018](#)

1% match (publications) ✕

[S Rafia, S Saran. "Sestrin-like protein from Dictyostelium discoideum is involved in autophagy under starvation stress", Microbiological Research, 2018](#)

1% match (publications) ✕

["Germ Cell Development in C. elegans", Springer Nature, 2013](#)

1.1 INTRODUCTION Dictyostelium discoideum was first isolated and identified by Kenneth Raper in the year 1935 from the deciduous forest

soil and decaying leaves of North Carolina, USA. In the natural habitat, *D. discoideum* cells feed on bacteria and yeast by chemotaxis tracking and multiply mitotically (Raper, 1935). *D. discoideum* is a valuable model system to study differentiation, development, phagocytosis, chemotaxis and signal transduction. The genome of Ax4 strain of *D. discoideum* has been completely sequenced and has nearly 12, 500 protein coding genes (Eichinger et al., 2005).

1.2 Phylogenetic position of *D. discoideum*

D. discoideum, a social amoeba has a life cycle that encompass both unicellular and multicellular forms. On the basis of proteome-based studies, it has been confirmed that Dictyostelium resides in the amoeboid group (protist). It is an eukaryote, forms a separate branch from fungi, plants and animals. It occupies a strategic phylogenetic position and appeared after the divergence of plant and animal. It is present on the animal branch (Figure 1.1) (Eichinger et al., 2005). Figure 1.1: Phylogenetic tree exhibiting evolutionary relationship for *D. discoideum*. The phylogenetic analysis shows *D. discoideum* diverged after the animal-plant split and before fungi and yeast (reproduced from Eichinger et al., 2005).

1.3 Advantages of using *D. discoideum* as a model system

The social amoeba, *D. discoideum* (hereafter referred as Dictyostelium) is an attractive eukaryotic microbe having the capability of shifting from unicellular to multicellular forms. It is a simple yet powerful model organism for eukaryotic cell biology, developmental biology and molecular mechanisms of disease as it shows higher level of complexity than the yeast but simpler than animals and plants (Kreppel and Kimmel, 2002). Some of the important characteristics of this model organism are listed below:

- It has a simple and short life cycle having both vegetative (unicellular) and developmental (multicellular) stages. The unicellular stage can be maintained till there is enough of food where it can divide asexually by mitotic divisions and shows a generation time of nearly 10-12 h. Once food is depleted or starvation is set in, the unicellular amoebae comes to form multicellular structures which ultimately forms a fruiting body in approximately 24 h. The fruiting body has two terminally differentiated cells: the stalk (made up of dead vacuolated cells) and spores (viable cells). Interestingly both the forms can be maintained independent of each other.
- Dictyostelium can be grown both in rich liquid medium as well as in association with bacteria. Isolation of cellular products for further analyses using biochemical as well as proteomic approaches can be performed.
- The haploid genome of nearly 34 Mb has been completely sequenced (available online at www.dictybase.org) and is divided into 6 chromosomes. Therefore, to establish a direct link between functions and genes reverse genetic methods can be employed (Eichinger et al., 2005).
- Genetic manipulations like preparation of knockout by homologous recombination, preparation of overexpressors, knockdown by antisense RNA or RNAi are well established and relatively easy to perform (Kuhlmann et al., 2006)
- Multicellularity in this organism is initiated by a complex cAMP signaling pathway, which also acts as a chemoattractant. Thus, chemotaxis and phagocytosis are well established and can be extrapolated to study the macrophages, which share similarity with them.
- This organism shows developmental cell death, which is caspase-independent and is accompanied by autophagic cell death. It is now declared by NIH as a model system to answer questions regarding autophagy, something similar to what *C. elegans* gave for apoptosis (Roisin-Bouffay et al., 2004).
- Due to its phylogenetic position, Dictyostelium possess homologs of many eukaryotic genes which are even absent in yeast. It has emerged as a promising eukaryotic host for the ectopic expression of recombinant

eukaryotic proteins (Arya et al., 2008). • Due to the ease of handling of Dictyostelium cells and the lack of any cell wall (being transparent) helps in the utilization of enzymatic, fluorescent, antigenic protein tags and in-situ hybridization (Gerisch and Muller-Taubenberger, 2003; Maeda et al., 2003). • As these cells show controlled cell movement and cell differentiation, generation of pattern during multicellular development allows the analysis of pattern formation (Kimmel and Firtel, 2004; Williams, 2006; Weijer, 2009).

1.4 Life cycle of D. discoideum

Dictyostelium is a facultative multicellular organism having a very short life cycle and comprising of both unicellular and multicellular forms. Unicellular amoeba shows vegetative growth by feeding upon bacteria and divides mitotically by binary fission. In the absence of food, it enters multicellular developmental pathway to form spore- harboring structure called fruiting body. The life cycle can be divided into the following stages (Figure 1.2).

1.4.1 The vegetative (unicellular) phase

Dictyostelium cells exist as a unicellular haploid amoeba/ myxamoeba that via phagocytosis feed on bacteria and grow vegetatively through mitotic divisions (binary fission). Dictyostelium cells are approximately 10 to 20 microns in diameter. The cell is defined by a plasma membrane showing numerous pseudopods and food vacuoles. Cell wall and flagella are absent hence, they are non-motile in nature (Raper, 1935; Gezelius and Rånby, 1957; George et al., 1972). Presence of toxic agents cause physiological and morphological changes to the cells, which include the change in gene expression of a number of genes to increase resistance against toxins and the cells are called as aspidocytes (Serafimidis et al., 2007). Pre-starvation factor (PSF) is secreted by vegetative cells whose function is to monitor cell density in proportion to the available nutrients (Rathi et al., 1991). PSF is a glycoprotein of 87 kDa molecular mass and is sensitive to heat and proteases. Presence of bacteria as food source inhibits the accumulation of PSF. High levels of [PSF induces the expression of genes required for aggregation](#). Along with [the](#) depletion of [food supply PSF](#) production [declines and](#) the level of conditioned medium factor (CMF), another cell density sensing factor begins to increase. PSF leads to the induction of gene expression of yaka and discoidin-I.

1.4.2 The development/asexual (multicellular) phase

Starvation is the major factor that triggers the vegetative unicellular cells towards multicellular development and leads to the expression of a variety of new genes, which are responsible for chemotaxis both towards folic acid (factors from bacteria) and cAMP. Each and every amoeba can sense the cAMP, respond by releasing cAMP and leads to the signal amplification and relay. Following starvation, production of PSF declines and the accumulation of [another cell density sensing factor](#) CMF [\(conditioned medium factor\) begins](#) (Clarke and Gomer, 1995). As cell density of the starving cells is increased, accumulation of CMF regulates the cAMP signal relay to initiate cell aggregation. Under normal conditions each aggregate is formed by ~10⁵ amoebae (Yuen et al., 1995). Figure 1.2: Life cycle of Dictyostelium discoideum. (A) Starved Dictyostelium cells secrete cyclic adenosine monophosphate (cAMP) pulses. (B) These cells migrate to common collecting points via chemotactic aggregation and develop into mounds. The anterior region of the mound produces cAMP and in response to that cells move upwards (C) and form the tipped mound. At this stage, cells begin to differentiate into prespore and prestalk cells. (D) After this, the slug is formed in which further differentiation leads to the formation of prestalk A, B, AB and O cells. (E) The slug can now migrate over the surface to show a clear-cut pattern formation with [prestalk cells in the anterior and prespore cells in the posterior](#) region. (F) A massive cell movement

occurs before terminal differentiation occurs where the prespore forms spore cells to be located in the anterior end and posterior end has a stalk. (G) Finally, these cell-types culminate into fruiting body that consists of a stalk and a spore head. (H) As favourable condition arises (availability of nutrient), spores germinate which (I) divide mitotically to increase in numbers and continues the vegetative phase. (Adapted from Schaap, 2011). Another component in this signaling system involves the gene *srsA* (Sasaki et al., 2008). Within few minutes of starvation, *srsA* is induced and is repressed within 2 h. In *yakA* null cells, expression of *srsA* is not altered suggesting that it functions independent of *yakA*. Disruption or overexpression of *srsA* cause reduction in the expression of *acaA* and *carA* resulting in a delay in development along with the formation of aberrant structures, suggesting that certain critical levels of the proteins was crucial for the regulation of early development (Sasaki et al., 2008). *yakA* plays an important role in the initiation of development as *yakA* null strains fails to aggregate. In the wild type cells, induction of *carA* and *acaA* occurs within first 2 h of starvation but in case of *yakA* null cells these are not expressed. This mutant is unable to synthesize or respond to cAMP. *yakA* regulates the transition from growth-to-development (Souza et al., 1998). Aggregation Under nutrient depleted condition, vegetative cells undergo physiological changes that lead to the induction of multicellular developmental. The amoeboid cell then produces, secretes and also responds to cAMP. In response to cAMP millions (10, 000-1, 00, 000) of highly polarized chemotactic amoeba undergo head to tail streaming to a common point to form a multicellular structure called loose aggregate (Raper, 1935; Bonner and Savage, 1947; Bonner, 1952; Konijn et al., 1967). Loose aggregates are a flat, adherent mass of cells with indistinct borders (Raper, 1935; Raper, 1940). Aggregation is controlled by two important molecular mechanisms i.e. cAMP mediated signaling and chemotaxis in response to cAMP (Kimmel and Parent, 2003; Manahan et al., 2004). 5 Mostly undifferentiated cells are present in loose aggregates and very few cells start expressing cell-type specific gene markers. In loose aggregate majority of the *pstA* cells (anterior-most part of prestalk cells) appear at the periphery while other prestalk specific cells are randomly distributed. (Early et al., 1995; Early et al., 1993; Jermyn et al., 1996; Williams et al., 1989). At the loose aggregate stage, a slimy surface of polysaccharides and proteins starts forming which is completed by the late aggregation stage (Farnsworth and Loomis, 1975; Freeze and Loomis, 1977; George et al., 1972). It holds the mass of cells together in the aggregate and help in the formation of mound or tight aggregate. Cellular movements in the mound stage lead to the formation of distinct prestalk (having prestalk cells) and prespore zones (having prespore cells). Some cells at the tip- organizer secretes cAMP due to which *pstA* and *pstO* cells move towards the tip and leads to the formation of tipped-mound (Dormann and Weijer, 2001). Mainly four factors control the size of aggregates formed in *D. discoideum*: number of cells participating, cell-cell adhesion proteins (*CadA*, *CsaA*), the counting mechanism and cAMP signal strength (including proteins Adenylyl cyclase A (*AcaA*), *PdsA*, *cAR-1*, *PDI*) (Jang et al., 2002; Jang and Gomer, 2008). Counting Factor (CF) is released by the starving cells which breakup the aggregation streams into groups of ~104 cells (Tang et al., 2002). High level of CF reduces the cell-cell adhesion and lead to the formation of small-sized aggregates (Jang and Gomer, 2008). The slug stage After tipped mound stage, a finger like structure is developed called standing slug, which pulls the mass anteriorly. If the conditions are unfavourable (like cAMP release, ambient light and temperature) it

can enter the migratory phase and form migratory slug (Raper, 1940; Bonner, 1952; Newell et al., 1969). Migrating slug has been considered as the best stage to study pattern formation as the two specified prestalk and prespore cells form a typical pattern where the anterior is composed of prestalk cells and the posterior is composed of prespore (Figure 1.3A). Anterior 15 -20% of the slug is called the prestalk region having prestalk cells while the posterior 80-85% region has prespore cells is called the prespore region. The ratio of these regions remains constant regardless of the size of the slug. Prestalk region can be divided into the following zones: prestalkA region occupying the anterior-most 10% of slug, prestalkO region is at the boundary of prestalk and prespore cells and in the core region lies the prestalkAB cells (Figure 1.3A). The cells present at these regions are called pstA, pstO and pstAB cells (Williams, 2006). PstA cells express ecmA marker gene while pstO cells express low levels of ecmA gene. PstB cells express ecmB gene. PstAB cells express both ecmA and ecmB genes (Williams et al., 1989; Gaskell et al., 1992; Early et al., 1993; Early et al., 1995; Yamada et al., 2005). The "tip-organizer" is responsible for maintaining the integrity of the organism and also inhibits the development of other tips in the near vicinity. The tip-organizer directs slug movement by phototaxis and also regulates the timing of entry into culmination (Poff and Loomis Jr, 1973; Rubin and Robertson, 1975; Smith and Williams, 1980; Durston, 1976; Durston and Vork, 1979). The posterior 2/3 region of the slug is occupied by the psp cells and interspersed between them are the anterior-like cells (ALCs), which are similar to pst cells in their properties (Sternfeld and David, 1981, 1982). Rear-guard region is the posterior most region of the slug consisting of pst cells expressing ecmB gene. The culmination stage The slug stage finally culminates into the fruiting body, which is the final stage in the developmental life cycle of *D. discoideum*. It comprises of three stages: early culminant, mid culminant and late culminant (Figure 1.3B). Fruiting body has two terminally differentiated types of cells: the stalk which are made up of dead and vacuolated cells and spore which are made up of viable cells (Whittingham and Raper, 1960). In early culminant, stalk is formed of thin, translucent and central cell mass consisting of the stalk tube and has extracellular deposition by pstA and pstO cells (Raper, 1940; Raper and Fennell, 1952; Maeda and Takeuchi, 1969; Williams et al., 1989; Sternfeld, 1992). In early culminant prespore region has scattered ALC/pstB cells (ecmB expressed by anterior-like cells) which migrate downward and lead to the formation of lower cup region while a distinct subset of ALC/pstA cells which expresses ecmA from the distal part of its promoter leads to the formation of upper cup (Figure 1.3B) (Raper and Fennell, 1952; Maeda and Takeuchi, 1969; Ceccarelli et al., 1991; Jermyn and Williams, 1991; Grimson et al., 1996). Figure 1.3: Compartmentalization in the multicellular organism. (A) Finer anatomy of the migratory slug of *D. discoideum* shows the presence of prespore and prestalk regions. The localization of different sub-types of prestalk cells was identified by the use of reporter genes. (B) Cell movement during culmination. During the culmination, terminal cell differentiation occurs and is comprised of cellular movements within an early culminant. Firstly, pstB cells migrate towards the stalk tube and are replaced by pstA cells, now called as pstAB cells followed by pstO cells. This proceeds until all prestalk cells are incorporated into the stalk. (Adapted from Schaap, 2011). During the mid and late culmination stages, the pstAB cells move downwards to the stalk tube away from the prespore region. The pstA and pstO cells follow 'reverse fountain' pattern and prestalk differentiation majorly

occurs at this stage, which finally differentiate into stalk cells. The pstO cells move upward and differentiate into pstA cells, as pstA cells traverse down into stalk tube it differentiates into the pstAB cells. During late culmination, terminal differentiation of prespore into spore and prestalk into stalk occurs, which ultimately leads to the formation of a fruiting body (Williams, 1995). A basal disc is present at the bottom, which provides support and anchors the fruiting body. A mature fruiting body is made up of a long stalk and a sorus having viable spore cells. Spores are elliptical in shape protected by a rugged spore coat made up of three layer, in which the outer and inner layers are made up of GPS (galactose/N-acetylgalactosamine polysaccharide) and glycoprotein whereas cellulose forms the middle layer (Hohl and Hamamoto, 1969; Maeda and Takeuchi, 1969; West and Erdos, 1990). The length of the stalk is approximately 1.5-3 mm made up of dead vacuolated cells while sorus (viable cells) is lemon shaped and of approximately 125-300 microns in diameter. Because of the presence of spore coat, spores are resistant to the external environmental conditions and can survive for several years without nutrient. Under favourable conditions, spores germinate into amoeba and start dividing by binary fission (Murata and Ohnishi, 1980).

1.5 Cell signaling during D. discoideum development

John Bonner in 1947 first time showed that during nutritional stress conditions, Dictyostelium cells secrete a chemoattractant which was later identified as cAMP (3'-5'- cyclic adenosine monophosphate), a secondary messenger that is required for the initiation of development and differentiation (Bonner and Savage, 1947; Konijn et al., 1967). The signals and the pathways involved in Dictyostelium development are summarized in Figure 1.4. When food gets depleted, the growth-to-development transition occurs and the population density of amoeba approaches its peak. Along with cAMP, density sensing factors such as PSF (pre-starvation factor) and CMF (conditioned medium factor) comes into play to initiate development (Grabel and Loomis, 1978). High level of PSF and starvation leads to the induction of YakA expression (Souza et al., 1998) which inhibits the binding of PUFA, a translational repressor to the catalytic subunit of PKA (cAMP- dependent protein kinase) (Souza et al., 1999). Accumulation of PKA-C then mediates the expression of aggregation related genes like adenylate cyclase (*acaA*) and extracellular cAMP phosphodiesterase (*pdsA*) (Schulkes and Schaap, 1995). During growth, AprA and CfaD are secreted which forms a complex of 138 kDa that diminishes cell proliferation (Bakthavatsalam et al., 2008; Bakthavatsalam et al., 2009). Signal transduction mediated by cAR1 is required for the function of CMF which leads to the formation of polyketide MPBD (4-methyl-5- pentylbenzene-1,3-diol) that increase the early genes expression. CMF that acts as a quorum sensor, also initiates development via the activation of G proteins by cAR1 that cause ACA stimulation that leads to the synthesis of cAMP (Jain and Gomer, 1994). As cAMP bind to cAR1, activation of MAP kinase Erk2 occurs, which inhibits RegA, an internal cAMP phosphodiesterase leads to increase in cAMP concentration (Laub and Loomis, 1998). PdsA, an extracellular cAMP phosphodiesterase and protein kinase, PKA further regulate the high concentration of cAMP (Orlow et al., 1981; Franke and Kessin, 1992; Sucgang et al., 1997). Due to the cAMP pulses, GataC (transcription factor) dependent genes like for example *carA*, *acaA*, *gbfA*, *regA*, *pkaR* and the cell adhesion like *csA*, *tgrB1* and *tgrC1* are expressed, which are required during and after aggregation (Cai et al., 2014). During post-aggregation stage, differentiation of cells into particular cell-types begins. DIF-1 induces the prestalk cell-types pstA, pstO and pstB to differentiate and give rise to upper and lower cups and

mainly the basal disc of the fruiting body (Morris et al., 1987; Saito et al., 2008; Yamada et al., 2011). Another polyketide named MPBD (4-methyl-5-pentylbenzene-1,3 diol) mediates terminal differentiation, which inhibits GskA, a protein kinase that enhances the PKA activity thus blocking the release of signal peptide SDF-1 (Anjard et al., 2011). In both prestalk and prespore cells SDF-1 is responsible for terminal differentiation and block DIF-induced stalk cell differentiation via regulating the cAMP levels (Berks and Kay, 1988; Anjard et al., 1998; Anjard et al., 2011) whereas SDF-2 is responsible for terminal differentiation and sporulation induction of prespore cells (Anjard et al., 2009). Figure 1.4: Cell signaling during development of *D. discoideum*. Starving amoebae aggregate to form a mound by secreting and relaying cAMP pulses. The tip of the mound moves upwards to form the slug in which cell-type differentiation is initiated. During culmination, prestalk and prespore cells terminally differentiate into stalk and spore cells, respectively. These processes are highly regulated and summarized in above figure for better understanding. The text shown in red colour reveals the secreted and environmental signals that mediate different life cycle transition and cAMP mediated differentiation of *Dictyostelium* (highlighted yellow). Enzyme that lead to synthesis of secreted signals are highlighted by green colour whereas blue text shows the small molecules and proteins mediating the 10 signal transduction pathway. T-crosses and blue arrows represent inhibitory and stimulatory effects, respectively. Double blue arrows denote that mode of signal transduction are not known. Abbreviations: AcaA (adenylate cyclase A); AcrA (adenylate cyclase R); AcgA (adenylate cyclase G); cAMP (3'-5'-cyclic adenosine monophosphate); cdi- GMP (3',5'-cyclic diguanylic acid); CarA- cAMP receptor 1); ChIA (flavindependent halogenase Chlorination A); PKA (cAMP-dependent protein kinase); RegA (cAMP dependent phosphodiesterase); CMF (conditioned medium factor); Dhk (histidine phosphatase A); DhkB (histidine kinase B); DhkC (histidine kinase C); DgcA (diguanylate cyclase A); NH₃ (ammonia); DIF-1 (differentiation inducing factor 1); DimB (transcription factor DIF insensitive mutant A); DmtA (des-methyl-DIF-1 methyltransferase); DokA (osmosensing histidine phosphatase); GtaC (GATA-binding transcription factor C); MBPD (4- methyl-5-pentylbenzene-1,3-diol); PSF (prestarvation factor); PufA (pumilio RNA binding protein); SDF-2 (spore differentiation factor 2); StIA (polyketide synthase Steely A); StIB (polyketide synthase Steely B); YakaA (DYRK family protein kinase); Tgr (transmembrane, IPT, IG, E-set, repeat protein) (Adapted Schaap, 2016).

1.6 PUF (Pumilio and FBF)

1.6.1 Introduction

In most of the eukaryotic organisms, gene expression is regulated at the transcriptional and post-transcriptional levels. To adapt their biological functions like growth and development to the changes in environment, this type of regulation becomes an important strategy in these organisms. Reports suggest that various aspects of RNA processing like RNA splicing, capping, polyadenylation, localization, modification, translation, transport and stability are regulated by different [RNA binding proteins \(RBPs\)](#) (Wickens [et al.](#), 2002; Keene, 2007; Glisovic et al., 2008; Abbasi et al., 2010; Ray et al., 2013). Protein structure analyses and their functional characterizations have revealed that the RNA binding proteins (RBPs) have conserved motifs and domains for RNA binding like the K homology (KH) domains, RNA-recognition motifs (RRMs), zinc fingers, DEAD/DEAH boxes [highly conserved motif (Asp-Glu-Ala-Asp) in RNA helicases], pentatricopeptide-repeat (PPR) domains, Pumilio/FBF (Pumilio-fem-3 binding factor, PUF) domains (Wu et al., 2016). PUF is a large family of RNA binding family present in all

eukaryotes. Family got the name PUF from its two founding members: Pumilio from *Drosophila melanogaster* and FBF from *C. elegans* ([Murata and Wharton, 1995](#); Zhang [et al.](#), 1997). The numbers of PUF genes are variable in different model organisms. They are known to be post-transcriptional regulators where they interact with 3' UTR of their target mRNA through specific recognition sequence and regulate post-transcriptional processes like RNA decay and translational repression (Wharton and Aggarwal, 2006; Tam [et al.](#), 2010). It plays many important roles for example in cell development, stem cell maintenance and differentiation Wickens [et al.](#), 2002; Spassov and Jurecic, 2003a).

1.6.2 PUF protein structure and its RNA-binding mechanism

All the PUF proteins have an evolutionarily highly conserved domain called PUF domain or Pumilio homology domain (PUM-HD) ([Zhang \[et al.\]\(#\), 1997](#); Wharton [et al.](#), 1998) present at [the](#) C-terminal of the protein. Human PUM-HD1 crystal structure shows the configuration of an extended crescent shape in which the outer convex surface could possibly be the binding site for different proteins (Figure 1.5A) (Wang [et al.](#), 2002). The inner surface, which appears concave-like consists of 8 imperfect repeats of nearly 36 amino acids each having two flanking pseudo repeats. Each repeat consist of 3 α -helices where in the second helix at position number 12, 13 and 16 are most conserved three amino acids. The side chain of amino acid 12 and 16 interact via van der Waals contacts or base-specific hydrogen bonds with the RNA base, while the amino acid side chain present at position 13 makes stacking interactions. In each repeats, specific residues are present which dictate the base recognition (Edwards [et al.](#), 2001; Wang [et al.](#), 2001; Wang [et al.](#), 2002). In general, 8 tandem repeats that are present recognize and bind to 8 RNA bases in an antiparallel fashion i.e. N to C terminal domain of PUF and 3'-5' orientation of RNA (Figure 1.5B) (Wang [et al.](#), 2002; Jalal Kiani [et al.](#), 2017). The modular arrangement of pumilio domain (PUM-HD) coincides with the modular arrangement of Armadillo repeats of β -catenin and importin- α , suggesting folding pattern like ancestral proteins (Wang [et al.](#), 2001).

Figure 1.5: Human PUMILIO-homology domain with Hunchback NRE. (A) Domain consists of 8 repeats in which each repeat comprises of three α -helices flanked by two pseudo-repeats. Specific amino acid in the second helix of each repeat is shown in green colour dictates the base recognition. (B) Eight repeats of the PUM- HD recognize eight RNA bases specifically in an anti-parallel fashion (adapted from Jalal Kiani [et al.](#), 2017). This pattern is also detected in proteins containing penta-tricopeptide repeat (PPR) motif consisting of 2-30 repeats. Each repeats consists of \sim 35 amino acids arranged as two α -helices in hairpin form called as helix-a and helix-b (Yagi [et al.](#), 2013; Yin [et al.](#), 2013). PUF-A of human and PUF-6 of yeast shows a discrete conformation depicting a L- shaped folding having 11 repeats of PUF that binds to single and double-stranded DNA or RNA in a non-sequence specific manner (Qiu [et al.](#), 2014). N-terminal sequence of PUF protein is found not to be so conserved, as it may bear some regulatory regions which could affect the activity of the protein (Spassov and Jurecic, 2003b; Salazar [et al.](#), 2010). PUF protein binds specifically to the conserved RNA sequence UGUR, which is preset on the 3' untranslated regions (UTR) of mRNA (Zamore [et al.](#), 1997; Zamore [et al.](#), 1999; Crittenden [et al.](#), 2002; Jackson [et al.](#), 2004; Bernstein [et al.](#), 2005). If any mutation is present in these elements it can lead to disruption of protein binding and protein function ([Murata and Wharton, 1995](#); Zhang [et al.](#), 1997). An AU-rich sequence is 13 present downstream of the core UGUR sequence which specify the interaction between PUF and RNA. (Bernstein [et al.](#), 2005; Zhu [et al.](#),

2009). The consensus recognition sequence found in *Drosophila Pumilio*, *S. cerevisiae* PUF3p, and *Homo sapiens* PUM1 and PUM2 is 5'-UGUANAUA-3' an eight-nucleotide sequence where N can either be A, C or U bases (Gerber et al., 2004; Gerber et al., 2006; Galgano et al., 2008). One repeat of PUF protein recognize one RNA base, this is the general mode of recognition i.e. each Pumilio domain with its eight repeat recognize and bind to eight RNA base of the target RNA. Although there are few exception also to this rule to expand the specificity for the targets (Lu and Hall, 2011). Like in case of budding yeast, in place of 8 bases, consensus sequence of 9 and 10 bases are present in PUF4 and PUF5, respectively. To accommodate these extra bases and to flip out the extra base, PUF protein undergoes distortion from its normal RNA binding concave surface to the flat surface (Gerber et al., 2004; Miller et al., 2008). It is assumed that this extra flip out base may contribute to the interaction with some cofactor that may be responsible for ribonucleoprotein (RNP) complex function and fate of the target RNA. HsPUM1 of human proteins and [PUF-5, PUF-6, PUF-7](#), FBF of *Caenorhabditis elegans* also showed similar pattern of binding specificity (Opperman et al., 2005; Stumpf et al., 2008; Wang et al., 2009; Lu and Hall, 2011). In *Arabidopsis thaliana*, recently a ten-nucleotide binding consensus sequence has been identified for APUM23 having UUGR as core sequence in place of UGUR and has a cytosine present at position eight of nucleotide which shows its preference for PUF repeat 3 (Zhang and Muench, 2015).

1.6.3 PUF proteins and their functions in different organisms

Reports have shown that a single PUF protein can recognize a number of RNA targets, suggesting that it can regulate many processes in eukaryotic system including neuron functioning, stem cell control, biogenesis of organelles and developmental patterning. Till now most investigation has been done on *Drosophila melanogaster*, *Caenorhabditis elegans* and *Saccharomyces cerevisiae* while few studies are reported in plants. In 1987, Lehmann identified a maternal gene *Pumilio*, in the absence of which *hunchback* (*hb*) is expressed uniformly in the posterior of *Drosophila* embryo due to which no abdominal segment developed (Lehmann and Nüsslein-Volhard, 1987). Later in 1995, Murata and Wharton showed that *Pumilio* acts by binding to NRE (Nanos Response Element) like sequences present on mRNA and recruit *Nanos* (*nos*) and inhibit some translation machinery component (Murata and Wharton, 1995). Normally *Hunchback* protein is expressed at the anterior region during early development in *Drosophila* embryo. However, when *Pumilio* is mutated gradient of *Pumilio* protein is also present in the posterior region which suggest that repression of *hb* mRNA is absent in this region (Tautz, 1988; Barker et al., 1992). This finding was further supported by the fact that in *Pumilio* mutant, the mRNA isolated from the posterior region of embryo was not deadenylated [as compared to the wild type](#) suggesting [the](#) fact that [the](#) mRNA is not repressed translationally (Wreden et al., 1997). This led to the defects in abdominal segmentation (Lehmann and Nüsslein-Volhard, 1987; Barker et al., 1992). *Pumilio* also regulate some other processes like stem cell proliferation, memory formation and motor neuron functions (Weidmann and Goldstrohm, 2012). In nematode, *C. elegans*, two sexes are present, males and hermaphrodites. Hermaphrodites produce sperm initially but later on switch to produce oocyte. This switch is controlled by the 3' UTR (untranslated region) of [fem-3](#) mRNA ([Ahringer and Kimble, 1991](#)). Zheng and group (1997) identified that it was the FBF which [binds to the 3' UTR of the fem-3 mRNA](#) and was responsible [for the switch](#). To regulate [spermatogenesis to oogenesis](#) transition, there

is requirement of fem-3 repression and it is achieved post-transcriptionally via the 3' UTR region present in the regulatory region of fem-3 mRNA (Hodgkin, 1986; Barton [et al.](#), 1987; [Ahringer and Kimble, 1991](#)). When knock down of [fbf \(fbf-1 and fbf-2\)](#) was performed by RNAi it led to an increase in sperm production associated with the oogenesis inhibition and abnormal oocyte production, suggesting that this [switch from spermatogenesis to oogenesis](#) is regulated [by](#) FBF by repressing [fem-3](#) ([Zhang et al.](#), 1997). Double mutant hermaphrodites [of fbf-1- fbf-2](#), defects become even worse as all the germline stem cells undergo meiosis and start spermatogenesis ([Crittenden et al.](#), 2002). By [the](#) repression [of](#) [gld -1](#), FBF also promotes self-renewal of germline stem cell which leads to the mitosis [at the distal end of the gonad](#) ([Crittenden et al.](#), 2002). PUF-3/11 and PUF-5/6/7 are the two groups of PUF/RNA-binding proteins, which play important role in oogenesis of *C. elegans*. In oocyte formation all the PUFs are involved but PUF-3/11 inhibits growth of oocyte whereas PUF-5/6/7 is involved in the organization of oocyte and its formation ([Hubstenberger et al.](#), 2012). In *C. elegans*, Notch signaling pathway and PUF RNA binding proteins maintains the pool of Germline stem cells (GSCs) ([Wickens et al.](#), 2002; [Bray](#), 2016) . From the niche, [GLP-1/Notch signaling is](#) required for [the](#) maintenance [of](#) GSC and [FBF-1 and FBF-2 \(collectively FBF\)](#) promote GSCs self-renewal by acting as repressors of differentiation RNAs ([Crittenden et al.](#), 2002; [Kershner et al.](#), 2013). Both [sygl-1](#) and [lst-1](#) genes are identified as GSCs regulators that directly target niche signaling ([Kershner et al.](#), 2014). A single Nanos-like zinc finger is present in LST-1 which suggests its putative role in post-transcriptional regulation ([Kershner et al.](#), 2014). But how this Notch signaling regulates the activity of FBF to maintain self-renewal of stem cell is not understood. But [Shin et al.](#) (2017) reported that both SYGL-1 and LST-1 as a cytoplasmic protein present in GSC region. Both SYGL-1 and LST-1 interact with FBF physically and leads to repression of the FBF target RNA within the stem cell pool and thus maintain the stem cell pool. [Salvetti et al.](#) (2005) identified a protein called *Dugesia japonica* (DjPum), which is homologous to *Drosophila* Pumilio. It was found to be expressed in stem cells of planaria where it forms the regenerative blastema and also essential for the maintenance of neoblast. In yeast, HO is an endonuclease responsible for switching mating-types where it causes breaking of double-stranded DNA that initiate recombination. PUF protein Mpt5p removes polyA tail of HO mRNA thus leading to stability of HO mRNA ([Herskowitz](#), 1988). The PUF3 protein plays an important role in the mitochondrial functions as it binds and regulates mRNAs, which encode for more than 100 proteins that are required ([Zhu et al.](#), 2009). In *S. cerevisiae* PUF5p is a broad regulator of RNA, binds to more than thousand RNA targets, which is about 16% transcriptome of yeast. All these RNAs are important in regulation of various aspects of *S. cerevisiae* development like cell wall integrity, embryonic cell cycle, or chromatin structure ([Wilinski et al.](#), 2015). Nop9, PUF protein present in *S. cerevisiae*, is an essential small ribosomal subunit biogenesis factor. It recognizes structural features and sequences of 20S pre-rRNA present near the nuclease cleavage site (Nob1) and by inhibiting cleavage leads to the final step, to produce small ribosomal subunit 18S rRNA ([Zhang et al.](#), 2016). In *S. cerevisiae*, Mpt5p (also known as PUF5p) can promote temperature tolerance and is also responsible for replicative lifespan increase may be by the involvement of cell wall integrity (CWI) pathway. In case of Mpt5D mutant lifespan was shortened and this defect was suppressed by the activation of CWI signaling ([Stewart et al.](#), 2007). In other species also

there are available reports of PUF proteins. In *Peronophythora litchi*, PIM90 codes for a PUF protein and shows high expression during sexual and asexual development but during germination of cyst and plant infection its expression is relatively lower. Therefore, sexual and asexual differentiation of *P. litchi* is specifically regulated by PIM90 (Jiang et al., 2017). In *Plasmodium falciparum*, PfPUF1 is responsible for the differentiation and maintenance of female gametocytes. PfPUF1-disrupted lines showed a sharp decline in gametocytemia (Shrestha et al., 2016). In humans, PUM1 and PUM2 are the two Pumilio proteins, which positively regulates retinoic acid-inducible gene I (RIG-I) signaling, that plays an important role during innate immunity. PUM1 and PUM2 overexpression leads to increase in promoter activity of IFN- γ (an important factor in retinoic acid-inducible gene I, which is induced by NDV (Newcastle disease virus) (Narita et al., 2014). Mammalian Pumilio proteins play important roles in ERK signaling (Lee et al., 2007), neuronal activity (Vessey et al., 2006), stress response (Vessey et al., 2006) and also germ cell development (Moore et al., 2003). In plants, PUF proteins act as post-transcriptional repressors. In *Arabidopsis thaliana* upto 26 PUFs have been identified. *Arabidopsis* PUM5 (APUM5) plays an important role against both abiotic and biotic stress responses. Under salt and drought treatment overexpression of APUM5 showed the hypersensitive phenotypes at vegetative stage and during seedling stage. It was reported that the Pumilio homology domain of APUM5 bind to mRNA of many drought and salt stress-responsive gene at Pumilio RNA binding motif present at 3' UTR (Huh and Paek, 2014). APUM23 was found to regulate morphogenesis in leaf by the regulation of expression of KANADI (KAN) genes. GARP family member KAN genes, regulate the abaxial identity (Huang et al., 2014). Moreover, in *Arabidopsis* PUF proteins play important roles in many mechanisms like responses to light, nutrients, ABA (abscisic acid) signaling, iron deficiency and osmotic stress (Tam et al., 2010). For example, APUM23 PUF-domain protein constitutively expressed in metabolic tissues was up regulated in presence of sucrose or glucose. APUM23 loss of function in plants lead to the scrunched and serrated leaves, slow growth and also venation show abnormal pattern because of RNA processing (Abbasi et al., 2010). In *Arabidopsis*, transcriptome analysis showed that many PUF members like APUM9 and APUM11 in particular, had higher transcript levels during seed imbibition in case of reduced dormancy of mutants. These findings indicate that PUF protein may play an important role in seed dormancy in plants (Machin et al., 1995). Studies suggest that all APUM-1 to APUM-6 could be important for the growth and development of *Arabidopsis* via RNA of target genes like WUSCHEL, CLAVATA-1, PINHEAD/ZWILLE and FASCIATA-2, which regulate growth of meristem and maintenance of stem cell (Francischini and Quaggio, 2009; Reichel et al., 2016). Tissues undergoing cell division and rapid proliferations showed high expression of PUF protein APUM24. It is also essential for the rRNA by products removal for fast cell division and early embryogenesis in case of *Arabidopsis*. APUM24 loss of function mutation in plants showed defect in cell patterning (Huh et al., 2013).

1.6.4 Mechanisms of RNA repression Wickens laboratory initially described the mechanism of PUF protein mediated mRNA repression (Goldstrohm et al., 2006). Yeast PUF5 bind to Ccr4-Pop2-NOT mRNA deadenylase complex, specifically at Pop2 subunit of this complex, thereafter recruiting the deadenylase to mRNAs for its repression (Figure 1.6) (Goldstrohm et al., 2006). This PUF5 and Ccr4-Pop2-NOT mRNA deadenylase complex act as a cytoplasmic exonuclease, which cleaves the polyA tail and shortens it thus affecting both mRNA stability

and translation (Preiss et al., 1998; Amrani et al., 2008; Goldstrohm and Wickens, 2008). According to the closed loop model the 3' and 5' ends of an mRNA are present adjacent to each other (Quenault et al., 2011), which allow the binding of regulators like PUF5 at 3' UTR so that they can act on the 5' end of mRNA effectively as well (Figure 1.6). In fact, the decapping enzyme Dcp1 and the decapping activator and translational repressor Dhh1, interact with the Ccr4-Pop2- NOT complex (Coller et al., 2001; Maillet and Collart, 2002) then Pop2-Puf5 interaction lead to the recruitment of this complex to mRNAs (Goldstrohm et al., 2006). Dhh1 and Dcp1 hydrolyze of the 5' cap (decapping) further cause mRNA repression along with the function as translational repressors (Coller and Parker, 2005). When deadenylation is absent then repression by PUF protein is mediated by recruitment of different factors affecting the 5' cap (Chagnovich and Lehmann, 2001; Goldstrohm et al., 2006; Hook et al., 2007). Ccr4-Pop2-NOT recruitment is a general mechanism as *C. elegans* FBF, *Drosophila* Pumilio (Pum), yeast PUFs (PUF3 and PUF4) and human Pum1 also use this Ccr4-Pop2-NOT complex to regulate mRNA repression (Chritton and Wickens, 2010). Besides Ccr4-Pop2-NOT deadenylase recruitment mechanism, other PUF- dependent repression mechanisms have also been proposed. It includes inhibition of translation initiation factors and interaction with 5' mRNA cap, structural changes in ribonucleoprotein and effect on the elongation and termination of translation process. For instance, the translational inhibitor d4EHP through its cofactor Brain tumor (Brat) can recruit to *Drosophila* Pum mRNAs (Cho et al., 2006). d4EHP inhibits translation by binding to the cap, allowing no space for translation initiation factor eIF4E to bind (Cho et al., 2005). In *Xenopus*, binding of Pum2 to the 5' cap structure leads to the inhibition of eIF4E binding (Cao et al., 2010). In yeast PUF6, *ASH1* mRNA translation is repressed by the interaction with eIF5B/Fun12 (translation initiation factor) which inhibits its function (Deng et al., 2008).

Figure 1.6: Repression of mRNA by PUF protein. It is achieved by Ccr4-Pop2-NOT deadenylase complex recruitment. PUF5 recognize and bind to the sequence present at 3' UTR of mRNA and Ccr4-Pop2-NOT mRNA deadenylase complex through Pop2 subunit is recruited. It also recruits decapping factors Dhh1 and Dcp1. Dhh1 and Dcp1 activate the decapping process that leads to translational inhibition. PUF5 recruits different factors, which affect the polyA tail and 5' capping that leads to deadenylation and repress translation (adapted from Quenault et al., 2011). In case of yeast PUF3, changes in the ribonucleoprotein structure have been suggested as one of the mechanism. Besides Ccr4-Pop2-NOT mRNA deadenylase binding, PUF3 also affect alternative deadenylase Pan2 that causes deadenylation. Although there is no reports of interaction between Pan2 and PUF3, which suggest that PUF3 causes the structural changes in the mRNA and the polyA tail-binding protein Pab1, due to which the polyA tail is exposed to deadenylation (Lee et al., 2010).

1.7 Work done so far in *D. discoideum*

In 1999, Souza et al., identified a protein called PUFA in *D. discoideum*, which codes for a member of Pumilio RNA binding protein family of translational regulators. He showed that PUFA- cells develop precociously and overexpress cAMP dependent protein kinase (PKA-C) catalytic subunit, which is required for further development. They showed that PUFA response elements (PRE) are present in the mRNA of PKA-C and binding of PUFA to PREs regulates its translation. PUFA and PKA-C are inversely related to each other. PUFA represses the expression of genes required for the development like *acaA* and it does so by negatively regulating PKA-C via repressing the PKA-C mRNA. Function of Yaka is required to decrease the PUFA protein and mRNA

level. Figure 1.7: A model depicting the function of PUFA and YakA. Lines with bars represent negative regulation while line with arrowheads represent positive regulation. Translation inhibition of PKA-C is regulated by PUFA and this is relieved by YakA inhibition of PUFA. YakA also inhibits cell cycle either by negatively regulating promoters or by positively regulating some cell cycle inhibitor. YakA has a role during growth as it regulates the cell cycle and as nutrient is depleted and starvation begins. YakA is activated or induced which decreases the expression of vegetative genes. Subsequently repression on PKA-C mRNA by PUFA is also relieved. This leads to the activation of PKA-C, which is required for development initiation and during further development (Loomis, 1998). During the initial 4-6 h, there is around 5 fold increase in the PKA-C mRNA as well as the protein and its activity and this is an essential event for the initiation of development (Leichtling et al., 1984; Mann et al., 1992). They concluded that in response to starvation YakA is activated which represses PUFA expression and the negative control exerted on PKA-C expression is thus relieved and leads to the initiation of development. PUFA protein can also promote continued vegetative divisions. It is required at both initial and later stages of development (terminal morphogenesis into fruiting body) (Souza et al., 1999).

1.8 OBJECTIVES OF THE PRESENT STUDY

PUF proteins are the family of RNA binding proteins whose canonical function is post-transcriptional regulation. From the above literature it is clear that it plays an important role in cell division, differentiation and development. Like in case of Drosophila it is required for anterior-posterior patterning, maintenance of germline stem cells (GSCs) in C. elegans, normal development in Arabidopsis thaliana, aging, mitochondrial function and mating type switching in yeast etc. Since Dictyostelium is a very good model system to study differentiation and development and PUF proteins are also involved in the developmental processes of many organisms. PUFA in Dictyostelium plays a very important role in differentiation and development (Souza et al., 1999). Five PUF proteins in D. discoideum have been identified which may be involved in cell-type differentiation or in transition from growth to development. Since work on PUFA has already been done so we were interested to determine the role of one of other PUFs in growth, differentiation and development of this organism. Therefore, we have proposed following objectives to accomplish our study:

- To carry out in silico analysis for the identification of genes encoding PUF proteins in D. discoideum and characterization of one selected gene. It involves phylogenetic analysis, molecular modeling of PUF protein to determine its 3-D structure. Spatio-temporal expression pattern would also be analyzed.
- To carry out the functional analysis of the identified PUF protein during growth, development and differentiation of this organism. This would be accomplished by creating both overexpressor and knock out mutant strains where all the above parameters would be analyzed.
- To explore the role of PUF in cell-type differentiation, spatial patterning and cell lineage tracing. Further characterization of the identified PUF protein by finding out its interacting protein partners. Since this could not be achieved we explored the role of PUF in autophagy would also be analyzed.

2.1 INTRODUCTION

PUF proteins are the family of RNA binding proteins present in all eukaryotes, mainly involved in the regulation at post-transcriptional level of mRNA. It performs various biological functions like neurogenesis (Ye et al., 2004), morphogenesis (Wharton and Struhl, 1991; Murata and Wharton, 1995) and development of germ cell (Asaoka-Taguchi et al., 1999; Kadyrova et al., 2007) in many eukaryotic organisms. PUF proteins are characterized by

the presence of PUF domain, which comprises of 8 PUF repeats present in tandem towards the C-terminal. Each repeat recognizes and binds to specific sequence present at 3' UTR of mRNA NANOS Response Elements (NREs). Each repeat binds to single base of mRNA (Zamore et al., 1997; Zamore et al., 1999). Variable numbers of PUF proteins are present in different organisms like 6 in yeast, 2 in mammals including human, and several paralogs are present in *Arabidopsis thaliana* and *C. elegans*. Figure 2.1: Ribbon diagram of human Pumilio1 domain, HsPUM-HD. Each repeat has been represented as R1, R2, R3, R4, R5, R6, R7 and R8 comprising of 3 α -helices. Each repeat is shown in alternate blue and yellow colour. N- and C-termini has been shown (adapted from Wang et al., 2001). Wang et al. (2001) solved the crystal structure of human Pumilio1, PUM-HD at 1.9 Å resolution. They showed that 8 repeats were present in human Pumilio1 and was packed in the form of right-handed superhelix. The side chain distribution of amino acids on outer and inner surfaces of the protein explains that RNA binds to the inner surface while the outer surface interacts with cofactors to regulate mRNA post-transcriptionally (Wang et al., 2001). Genome of *Dictyostelium discoideum* harbors 5 PUF genes with id, DDB_G0279735, DDB_G0279557, DDB_G0288551, DDB_G0289987 and DDB_G0276255. Out of these DDB_G0279735 has been named as DdPUFA and we named the remaining PUF genes DDB_G0279557, DDB_G0288551, DDB_G0289987 and DDB_G0276255 as DdPUFB, DdPUFC, DdPUFD and DdPUFE respectively. All these are characterized by the presence of PUF (Pumilio) domain. *Dictyostelium* PUFA is located on Chromosome 3 on Crick strand from coordinates 2548824 to 2551966 and is about 3.14 Kb in length encompassing 4 exons interrupted with 3 introns (Figure 2.2 A and B). *Dictyostelium* PUFB is [located on Chromosome 3](#) on Crick strand [between coordinates](#) 2250584 [to](#) 2253245 and [is](#) about 2.66 Kb in length encompassing 3 exons 23 interrupted with 2 introns (Figure 2.2 C and D). *Dictyostelium* PUFC is located on Chromosome 5 on Watson strand from coordinates 1679413 to 1681553 and is about 2.14 Kb in length encompassing 2 exons interrupted with one intron (Figure 2.2 E and F). *Dictyostelium* PUFD is located on Chromosome 5 on Watson strand from coordinates 3515224 to 3518414 and is about 3.19 Kb in length encompassing 2 exons interrupted with one intron (Figure 2.2 G and H). *Dictyostelium* PUFE is located on Chromosome 2 on Crick strand from coordinates 6507776 to 6510379 and is about 2.60 Kb in length encompassing 2 exons interrupted with one intron (Figure 2.2 I and J). Figure 2.2: Genomic map and exonic positions of 5 PUF genes of *Dictyostelium discoideum*. (A) DdPUFA located on Chromosome 3 on Crick strand from coordinates 2548824 to 2551966 (B) DdPUFA comprises 4 exons and 3 introns. Exons, local and chromosomal coordinates are shown. (C) DdPUFB is located on Chromosome 3 on Crick strand from coordinates 2250584 to 2253245 and (D) DdPUFB comprises of 3 exons and 2 introns. (E) DdPUFC is located on Chromosome 5 on Waton strand from coordinates 1679413 to 1681553 and (F) DdPUFC comprises of 2 exons and 1 intron. (G) DdPUFD is located on Chromosome 5 on Waton strand from coordinates 3515224 to 3518414 and (H) DdPUFD comprises of 2 exons and 1 intron. (I) DdPUFE is located on Chromosome 2 on Crick strand from coordinates 6507776 to 6510379 and (J) DdPUFE comprises of 2 exons and 1 intron. [<http://dictybase.org/>]. Domain structure of all the 5 PUFs were predicted from the SMART (Simple Modular Architecture Research tool; <http://SMART.embl-heidelberg.de>) tool, which helps predict and classify domains that are significantly annotated with respect to functional classes, tertiary structures, phyletic distributions and functionally

important residues. Figure 2.3: Protein domains present in the 5 PUF proteins predicted from SMART program in *D. discoideum*. (A) PUFA comprises of 8 PUF repeats ranging between 539-835 amino acids. (B) 8 PUF repeats present in PUFB ranging between 410-698 amino acids. (C) PUFC comprises of 6 PUF repeats ranging between 80-188, 267-340 and 416-454 amino acids. (D) PUFD shows the presence of 8 PUF repeats ranging between 651-943 amino acids. (E) PUFE shows the presence of 6 PUF repeats ranging between 214-299, 410-482 and 582-655 amino acids (<http://smart.embl-heidelberg.de/>). The SMART profile of PUFA shows the presence of 8 PUF repeats (domain) present tandemly at the C-terminal from amino acid 539 to 835 (Figure 2.3 A). PUFA protein is 925 amino acids long with a molecular mass of 104.16 kDa. PUFB also shows the presence of 8 domains present tandemly at C-terminal from amino acid 410-698 (Figure 2.3 B). It comprises of 782 amino acids having molecular mass of 85.83 kDa. In case of PUFC, 6 repeats are present which are not arranged tandemly. 3 repeats are present at the N-terminal followed by 2 repeats, which is then followed by a single repeat (Figure 2.3 C). It comprises of 679 amino acids having molecular mass of 77.72 kDa. PUFD shows the presence of 8 domains present tandemly at the C-terminal from amino acid 651-943 (Figure 2.3 D). It comprises of 1036 amino acids having molecular mass of 118.01 kDa. While PUFE shows the presence of 6 domains, which are not present tandemly, rather they are present in a group of two (Figure 2.3 E). It comprises of 841 amino acids having molecular weight of 95.96 kDa. As discussed in the previous chapter, PUF proteins are involved in many biological processes like cell division, differentiation and development. Like in case of *Drosophila* it is required for anterior-posterior patterning, maintenance of germline stem cells (GSCs) in *C. elegans*, normal development in *Arabidopsis thaliana*, aging, mitochondrial function and mating type switching in yeast etc. PUFA in *Dictyostelium* plays a very important role in differentiation and development. So we were interested to know the role of other PUFs, in particular PUFB of *Dictyostelium*. In this chapter we have carried out bioinformatic analyses of all the 5 PUF proteins, which includes phylogenetic analysis on the basis of sequence homology of PUF proteins in different organisms. Spatial and temporal expression pattern of PUFB mRNA was analyzed through semi-quantitative RT-PCR and in situ hybridization.

2.2 OBJECTIVES OF THE PRESENT STUDY

- In silico analysis for the identification of *Dictyostelium* PUF proteins by performing homology search, sequence alignment and phylogenetic analysis.
- Structural analysis and molecular dynamics simulation of 5 PUF proteins.
- To carry out the spatio-temporal mRNA expression pattern of PUFB during development of *Dictyostelium* using semi-quantitative RT-PCR and in situ hybridization.

2.3 MATERIALS AND METHODS

2.3.1 Homology search, domain analyses and phylogenetic analyses

Protein sequences of all the 5 PUF proteins were obtained from dictyBase server (www.dictybase.org/). NCBI (National centre for biotechnology information) (<http://blast.ncbi.nlm.nih.gov/Blast.cgi>) server was used to perform protein BLAST. By using BLASTp (Basic local alignment search tool for protein sequences) (<https://blast.ncbi.nlm.nih.gov/Blast.cgi?PROGRAM=blastp>) the percentage homology of individual PUF protein from different species was analyzed. Top scoring hit sequences from various organisms obtained by BLAST were downloaded and multiple sequence alignment was performed using ClustalW 2.0 at the [EBI server](http://www.ebi.ac.uk/tools/clustalw2) (<http://www.ebi.ac.uk/tools/clustalw2>). Phylogenetic analysis was performed from the [amino acid sequences](#) from [approximately 20](#)

[organisms ranging from](#) lower [to](#) higher [eukaryotes](#) with PHYMLIP (Phylogeny Inference Package) (Felsenstein, 1993) that help construct the phylogenetic tree with maximum likelihood ([Guindon and Gascuel, 2003; Guindon et al., 2005](#)) and neighbour joining (NJ) with replication of 1000 bootstrapp. In PHYMLIP, MUSCLE (Edgar, 2004), a-log expectation software (version 3.7) was taken for multiple sequence comparison to perform multiple protein sequence alignment. Consensus tree with bootstrap values was generated using PHYMLIP program and TreeDyn was used for visualization and re-rooting of the tree (<http://www.phylogeny.fr>) (Dereeper et al., 2008).

2.3.2 in silico analysis of the promoters of 5 PUF genes

About 1000 bp upstream nucleotide sequences from the start codon of all the 5 PUF genes were extracted from the dictyBase server and uploaded in MEME (Bailey et al., 2009) suite. It predicts motifs from MEME (Multiple EM for Motif Elicitation) programme using default parameters. It represents all the motif consensus sequences as sequence logos where the height of each letter is proportional to its frequency and sorted according to the most common residue. Sequence logo is used for determining the relative frequency of the residues and information content in a particular sequence motif (Schneider and Stephens, 1990). Motif sequences were downloaded and sequences with better p-values were used for further processes.

2.3.3 Structure deduction and Molecular Dynamics (MD) simulation protocol

Protein sequences of PUFA (DDB_G0279735), PUFB (DDB_G0279557), PUFC (DDB_G0288551), PUFD (DDB_G0289987) and PUFE (DDB_G0276255) [were retrieved from dictyBase](#) (<http://dictybase.org/>).

I-TASSER (Iterative Threading/ASSEMBLY/Refinement)

program (Roy et al., 2010; Yang and Zhang, 2015) makes use of the primary sequence to predict the secondary structure and help search the PDB library ([Protein Data Bank](#)) ([Rose et al., 2010](#)) of experimental curated protein structures. Further, using the cluster of 8 threading programs suitable templates were searched. Model quality and B-factors were checked by employing the ResQ program in I-TASSER. [C- and the TM- scores](#) are [the](#) two criteria, which is used to examine the quality of generated models by I-TASSER. [Based on the significance of the threading alignments and the convergence of the I-TASSER simulations,](#) the [C-score](#) was calculated. Its value should be [in the range of -5 to 2,](#) [higher](#) value indicates [better quality](#) of model. Structural similarities between the native structure and the predicted model is then measured by the TM score. Value >0.5 indicates protein model with correct global topology. All the predicted 3D models [were optimized by](#) molecular dynamics (MD) simulation for [nearly 40 ns production run. Simulations were performed](#) in [GROMACS 5.0](#) (Groningen Machine for Chemical Simulation) (Van Der Spoel et al., 2005). Quality assurance was checked by g_rms, g_rmsf, g_gyrate modules of GROMACS. Structural validation of the protein was done by analyzing phi/psi distribution in Ramachandran plot with the help of SAVES (<http://services.mbi.ucla.edu/SAVES/>).

2.3.4 Culture of Dictyostelium cells

Fresh spores were germinated and used for all the experiments of growth, development and viability. HL5 media is a rich axenic growth medium, which was used to grow D. discoideum cells at 22°C in 90 mm petri plates. For primary culture cells were inoculated from the petri-plates into flasks and incubated at 22°C, under shaken conditions at 120 rpm until the cells reached log phase ([density of 2.5-5 x10⁶ cells mL⁻¹](#)).

2.3.5 Growth and development of D. discoideum cells

Wild type Ax2 (axenic strain) cells were grown and maintained at 22°C in HL5 media in 90 mm petri-plates. For further experiments, large scale culture was inoculated by diluting cells taken from petri-

plates into fresh HL5 media in flasks and was allowed to grow at 22 °C under shaken conditions till the log phase was reached. For development, cells were washed twice with ice-cold 1x KK2 buffer and spotted (15-20 µL) on non-nutrient agar (NNA) plates at a density of 5x10⁷ cells mL⁻¹. Plated cells were kept at 4 °C for 4-6 h for synchronization followed by incubation at 22 °C for development.

2.3.6 Temporal DdPUFB mRNA expression pattern analysis using semi-quantitative RT PCR

RNA isolation Log phase (3-5x10⁶ cells mL⁻¹) Ax2 cells were harvested, washed in 1x KK2 buffer and plated on NNA plates at a density of 5x10⁷ cells mL⁻¹. Cells were developed synchronously and different developmental stages like vegetative, loose-aggregate, mound, slug, early culminant and late culminant samples were collected at different time points. Samples were collected in chilled 1x KK2, washed twice and lysed in 1.0 mL of TRI reagent (T9424, Sigma-Aldrich) by vortexing. Then, the samples were incubated for 5-10 minutes at room temperature (RT) followed by the addition of 200 µL chloroform, mixed and further incubated for 5 minutes at room temperature. The samples were centrifuged at 12,000 g for 15 minutes at 4 °C. The aqueous phase was collected and mixed with equal volume of isopropanol and incubated for 10 minutes at room temperature. The samples were again centrifuged at 12,000 g for 15 minutes at 4 °C and the final pellet was washed with 1 mL of 75% ethanol and centrifuged at 12,000 g for 5 minutes at 4 °C. The pellet was air-dried and further dissolved in 50 µL diethylpyrocarbonate (DEPC; Sigma-Aldrich) treated water, subsequently treated with RNase free DNase (Qiagen) as per the manufacturer's instructions for 10 minutes at 22 °C to remove any traces of genomic DNA. RNA was diluted and quantified using nanodrop spectrophotometer and its purity was checked on 1.5% (w/v) agarose gel in 0.5xTBE running buffer. The RNA samples were stored at -80 °C till further use. cDNA synthesis and PCR cDNA synthesis was carried using the Verso cDNA synthesis kit (Catalog No. AB1453A, Thermofisher). Reaction mix (20 µL) was prepared with 1 µg RNA from each sample mixed with 4 µL of 5x cDNA synthesis buffer, 2 µL of dNTP mix, 1 µL of oligo dT, 1 µL of RT enhancer, 1 µL of Verso enzyme mix and nuclease free water to make up the volume to 20 µL. The reaction mixture was incubated at 42 °C for 30 minutes to synthesize the cDNA followed by deactivation step at 92 °C for 2 minutes. cDNA was then stored at -20 °C till further use. The gene specific primer combinations were used for PCR amplification from cDNA template, which also ensures the purity of the preparation. The primer combinations used for the amplification of PUFB gene and ig7 is shown below in (Table 2.1).

Table 2.1: Primer combinations used for the amplification of cDNA for PUFB and rnlA (ig7) genes. Expected amplicon sizes from cDNA and gDNA as templates are mentioned above [FP- Forward primer, RP- Reverse primer, bp- base pair] PCR amplification for PUFB was carried out by initial denaturation at 98 °C for 30 seconds followed by 24 cycles amplification of denaturation at 98 °C for 45 seconds, primer annealing at 61.5 °C for 1 minute and extension at 65 °C for 1 minute. PCR amplification for ig7 was carried out using an initial denaturation for 30 seconds at 98 °C followed by amplification which was carried for 24 cycles of denaturation at 98 °C for 15 seconds, primer annealing at 52 °C for 45 seconds and extension at 68 °C for 1 minute.

2.3.7 Spatial expression analysis of DdPUFB mRNA by in situ hybridization in multicellular structures developed

Genomic DNA isolation Genomic DNA of *D. discoideum* (Ax2 strain) was isolated according to Charette and Cosson (2004) from the log phase cultures. Cells were collected by centrifugation at 3,000 rpm for 5 minutes and washed with 1x KK2.

Cells were starved in 1x KK2 for 2 h at 22 °C under shaken conditions at a density of approximately 1 x 10⁸ cells mL⁻¹. Upon starvation, cells were centrifuged at 3, 000 rpm for 5 minutes and resuspended in DB buffer at a density of approximately 5 x 10⁷ cells mL⁻¹. Cell suspension was then carefully added drop-wise into the eppendorf tube containing 1.5 mL of RLB buffer and 31 mixed gently. Hereafter, cells were spun down at 12,000 rpm for 10 minutes at 4°C and cell pellet was resuspended in 1.5 mL of RLB buffer and centrifuged again at 12, 000 rpm for 10 minutes at 4°C. The pellet obtained was resuspended in 25 µL of RLB buffer, followed by addition of 200 µL of buffer II containing RNaseA (10 µg mL⁻¹) and incubated at 65°C for 1 h. Further, buffer I containing Proteinase K (0.2 mg mL⁻¹) was added and incubated at 37°C for 30 minutes. Hereafter, 10 µL of 5 M NaCl was added followed by phenol: chloroform (1:1) extraction step. DNA was precipitated with ethanol overnight. Next day, DNA pellet was washed with 70% ethanol, air-dried and finally dissolved in TE buffer. DNA was checked by loading 1-2 µL of it on 1% agarose gel. in situ construct preparation The spatial expression pattern of PUFB transcript was investigated using in vitro transcription of exonic region by cloning in commercially available pBSII SK+ (pBluescript II phagemid) vector. The desired exonic region of 997 bp (genomic position from 2541-3537 bp) was PCR amplified from Ax2 genomic DNA using the specific primer combination (Table 2.2) having restriction sites BamHI and XbaI. Table 2.2: Primer combinations used for the amplification of exonic region of PUFB gene. The restriction sites are underlined. The expected amplicon size is shown. The amplicon was double digested with BamHI and XbaI enzymes and cloned directly into BamHI/XbaI sites of pBSII SK+ vector at 22 °C for 16 h to give a construct as shown in Figure 2.4. Figure 2.4: Diagrammatic representation of the cloning strategy for in situ hybridization of PUFB probe in pBSII SK+ vector. Exonic region of PUFB gene (~0.997 Kb) was inserted in BamHI/XbaI sites of the multiple cloning sites (mcs) of pBluescript SK+ vector. This vector contains promoters of T3 and T7 RNA polymerases adjacent to the mcs. The construct pBSII SK+ was digested with XbaI to yield template for sense probe by T3 RNA polymerase while digestion with BamHI yield template for antisense probe synthesis by T7 RNA polymerase. The ligation products were transformed into competent E. coli DH5α cells and the clones were selected on LB-agar with 100 µg mL⁻¹ ampicillin. The positive clones were confirmed by appropriate restriction digestions of the construct pBSII SK+ (PUFB probe). Probe preparation The construct pBSII SK+ was digested with BamHI to yield template for antisense probe synthesis by T3 RNA polymerase; while digestion with XbaI yield template for sense probe synthesis by T7 RNA polymerase. For probe synthesis 1.0 µg of the linearized construct, 1x digoxigenin RNA labelling mix, 1x transcription buffer, 20U RNase inhibitor, 40U RNA polymerase and DEPC water were used per 20 µL in vitro transcription reaction. The reaction mixture was incubated for 2 h at 37 °C and further stopped by adding 0.2 M EDTA per reaction. 1.0 µL of the reaction mixture was aliquoted for checking the synthesis on 0.5% TBE agarose gel. The probes were processed for hydrolysis by using 1x carbonate buffer and incubated for 15 minutes at 65 °C. The hydrolyzed probes were precipitated using 1/10th volume of 5 M lithium chloride and 2.5 volume absolute ethanol and kept at -80 °C for overnight. Henceafter, the ethanol was washed (centrifuged at 10, 000 rpm for 20 minutes at 4 °C), pellet was air dried. The pellet was dissolved in 100 µL of DEPEC water and kept for 30 minutes at 37 °C. The probe synthesized was checked on 0.5% TBE agarose gel and stored in -80 °C until further

use. In situ hybridization In situ hybridization was done using the commercial available kit from Roche as per the manufacturer's instructions. Ax2 cells were developed ($\sim 1 \times 10^7$ cells mL⁻¹) asynchronously on dialysis membrane and collected with 1x PBS on sterile 24 well tissue culture plates. Different multicellular structures were fixed in 100% methanol and 4% paraformaldehyde. Methanol was removed and structures were kept in 4% paraformaldehyde for 2 h and 30 minutes at room temperature. Structures were washed thrice with 1x PBS and treated with proteinase K (20 μ g mL⁻¹) in PBS for 50-60 minutes at 60°C. Further, samples were fixed with 4% paraformaldehyde for 20 minutes at room temperature, washed thrice with 1x PBS and kept in prehybridization buffer for overnight at 50°C. This was followed by hybridization with 0.5 μ g mL⁻¹ sense or antisense probe for 20 h at 50°C. After washing out the excess probe with 2x SSC, 1x SSC, 0.5x SSC and 0.1x SSC subsequently for 30 minutes at 50°C, structures were treated with 0.2% blocking solution. The structures were treated with 1:1,000 diluted anti-digoxigenin antibody coupled to alkaline phosphatase in PBT containing 0.2% blocking reagent at 4°C overnight. Subsequently, the structures were washed in PBT and phosphatase buffer. Structures were then stained with 340 μ g mL⁻¹ NBT and 174 μ g mL⁻¹ BCIP in phosphatase buffer in dark at room temperature till the satisfactory colour were developed. The reaction was stopped with multiple washes of 1xPBS and multicellular structures were photographed under stereomicroscope (Olympus SZ61). Localization of antisense probes was used to determine the spatial expression of PUFB in multicellular structures. In situ hybridization reaction with sense probe act as negative control.

2.3.8 Bacterial transformation

Ligation process includes 16 h of incubation at 22°C. The ligation product was mixed with 100 μ L of DH5 α competent cells of E. coli strain, prepared by TSS method (Chung et al., 1989) by gentle tapping. The cells were then incubated for 20 minutes on ice, followed with a heat shock for 90 seconds at 42°C and then snap cooled on ice for 5 minutes. Cells were then allowed to recover from heat shock by incubation for 1 h at 37°C under shaken conditions. The cells were spread on LB agar plates using glass spreader containing appropriate selection pressure, followed by incubation for 12-16 h at 37°C. The colonies grown were picked and screened for positive transformants by various combinations of restriction digestions.

2.3.9 Statistical analyses

The statistical analyses were performed (mean, standard deviation and standard error) and values were plotted using Microsoft Excel-2013 and GraphPad Prism 6.0. Levels of significance were calculated using Student's t-test and p-values of less than 0.05 were considered as significant.

2.4 RESULTS AND DISCUSSION

2.4.1 Phylogenetic analysis of PUF proteins

Protein sequence of DdPUFA (DDB_G0279735), DdPUFB (DDB_G0279557), DdPUFC (DDB_G0288551), DdPUFD (DDB_G0289987) and DdPUFE (DDB_G0276255) were taken from dictyBase server and BLASTp tool of NCBI that uses BLOSUM62 with default parameters restricting the target sequence prediction to 1000 was used for sequence alignment of individual PUF protein. Top scoring sequences from BLAST program above a certain threshold represented as e-values (expected value) for all the organisms covering prokaryotes and eukaryotes were selected for multiple sequence alignment. For the phylogenetic analyses, amino acid sequences in fasta format were prepared and multiple sequence alignment (MSA) was performed by using MUSCLE in phylogeny.fr server. The phylogenetic tree was created in phylogeny.fr server using seqboot with 1000 bootstrapped datasets for protein sequence alignments. The distance between protein

sequences can be calculated using Protdist, which uses Jones Taylor Thornton matrix for amino acid substitution. Final tree for individual PUF was predicted from mega software as shown in Figure 2.5 to Figure 2.9

Figure 2.7: Phylogenetic tree of PUFA. A CLUSTALW2 [alignment of PUFA full-length protein sequences from different organisms was used to create a bootstrap neighbour-joining \(N-J\) tree](#). Organisms used for building the tree were Dictyostelium discoideum, Zea mays, Arabidopsis thaliana, Saccharomyces cerevisiae, Drosophila melanogaster, Caenorhabditis elegans, Plasmodium falciparum, Aedes aegypti, Gallus gallus, Danio rerio, Homo sapien , Xenopus laevis, Mus musculus and Bos Taurus. From the phylogenetic tree, PUFA of D. discoideum appears closer to plants and yeast. It shows more closeness with some PUF proteins of plants like Zea mays4, Zea mays5, Arabidopsis thaliana PUM7 and yeast PUF protein Saccharomyces cerevisiae PUF3p. It is relatively closer to Pumilio of Drosophila melanogaster than that of mammals like human, while Caenorhabditis elegans [PUF proteins, FBF-1 and FBF-2 are](#) present on a separate clade showing D. discoideum PUFA is evolutionarily farther to C. elegans PUF proteins (Figure 2.5).

Figure 2.8: Phylogenetic tree of PUFB. A CLUSTALW2 [alignment of PUFB full-length protein sequences from different organisms was used to create a bootstrap neighbour-joining \(N-J\) tree](#). Organisms used for building the tree were Dictyostelium discoideum, Zea mays, Arabidopsis thaliana, Saccharomyces cerevisiae, Drosophila melanogaster, Caenorhabditis elegans, Plasmodium falciparum, Aedes aegypti, Gallus gallus, Danio rerio, Homo sapien , Xenopus laevis, Mus musculus and Bos Taurus. Phylogenetic analysis of Dictyostelium PUFB was observed to be evolutionarily closer to the yeast PUF protein, Saccharomyces cerevisiae PUF3p, Plasmodium falciparum PUF and some PUF proteins from plants like Arabidopsis thaliana PUM5, PUM12 and Zea mays12. DdPUFB is observed to be relatively closer to C. elegans PUF [proteins, FBF-1 and FBF-2](#) rather than [the](#) animals including mammals like humans as they are present on a separate clade (Figure 2.6).

Figure 2.9: Phylogenetic tree of PUFC. A CLUSTALW2 [alignment of PUFC full-length protein sequences from different organisms was used to create a bootstrap neighbour-joining \(N-J\) tree](#). Organisms used for building the tree were Dictyostelium discoideum, Zea mays, Arabidopsis thaliana, Saccharomyces cerevisiae, Drosophila melanogaster, Caenorhabditis elegans, Plasmodium falciparum, Aedes aegypti, Gallus gallus, Danio rerio, Homo sapiens, Xenopus laevis, Mus musculus and Bos Taurus. DdPUFC protein is present on a separate clade than the PUF proteins of plants, animals including mammals, flies, nematodes and yeast. It is present as an out-group, which could be because it has 6 PUF domain/repeats as opposed to 8 PUF domain/repeats that is generally present in most of the PUF proteins (Figure 2.7).

Figure 2.10: Phylogenetic tree of PUF D. A CLUSTALW2 [alignment of PUF D full-length protein sequences from different organisms was used to create a bootstrap neighbour-joining \(N-J\) tree](#). Organisms used for building the tree were Dictyostelium discoideum, Zea mays, Arabidopsis thaliana, Saccharomyces cerevisiae, Drosophila melanogaster, Caenorhabditis elegans, Plasmodium falciparum, Aedes aegypti, Gallus gallus, Danio rerio, Homo sapiens, Xenopus laevis, Mus musculus and Bos Taurus. From the phylogenetic tree, PUF D of Dictyostelium discoideum appears closer to the plants and yeast. DdPUFD and PUF proteins of animals including mammals like human are present on separate clade. Plasmodium falciparum PUF, Arabidopsis thaliana PUM7 and PUM12, Zea mays12 and Saccharomyces cerevisiae PUF4p are observed to be relatively closer to DdPUFC (Figure2.8).

Figure 2.11: Phylogenetic tree

of PUF. A CLUSTALW2 [alignment of PUF full-length protein sequences from different organisms was used to create a bootstrap neighbour-joining \(N-J\) tree.](#) Organisms used for building the tree were *Dictyostelium discoideum*, *Zea mays*, *Arabidopsis thaliana*, *Saccharomyces cerevisiae*, *Drosophila melanogaster*, *Caenorhabditis elegans*, *Plasmodium falciparum*, *Aedes aegypti*, *Gallus gallus*, *Danio rerio*, *Homo sapiens*, *Xenopus laevis*, *Mus musculus* and *Bos Taurus*. DdPUF protein is present on a separate clade than the PUF proteins of plants, animals including mammals, flies, nematodes and yeast. It is present as an out-group, this could be because it has 6 PUF domain/repeats as opposed to 8 PUF domain/repeats which is generally present in most of the PUF proteins (Figure 2.9).

2.4.2 In silico analysis of the 5 PUF promoters

In silico analysis of promoters of all the 5 *Dictyostelium* PUFs was carried out by predicting the conserved sequence motifs using PUF sequences (1000 bp upstream of the start codon was taken). Figure 2.12: Sequence motif analysis of all the 5 PUF promoters of *D. discoideum*. Approximately 1000 bp upstream sequence from the start codon of PUFA, PUFB, PUFC, PUFD and PUFE ORF was used for predicting the conserved motifs in the MEME suite. Motifs with higher p-values were selected and sequence logos are shown as (A) motif 1, (B) motif 2 and (C) motif 3 for PUFA. (D) motif 1, (E) motif 2 and (F) motif 3 for PUFB. (G) motif 1, (H) motif 2 and (I) motif 3 for PUFC. (J) motif 1, (K) motif 2 and (L) motif 3 for PUFD. (M) motif 1, (N) motif 2 and (O) motif 3 for PUFE. We observed 3 conserved motifs for PUFA having p-values (probability value) as $3.25e-7$, $2.15e-15$ and $3.33e-8$ on sense strand. First motif was the smallest and showed high probability of consensus sequence of A (adenine) at 2nd position with good bit score (Figure 2.10 A) while the second motif was relatively large and showed the consensus sequence of A (adenine) at many positions (Figure 2.10 B). Third motif had a consensus sequence of A (adenine), A (adenine), A (adenine), T (thymine), C (cytosine), G (guanine) at positions 1st, 4th, 6th, 8th, 9th and 11th with better bit score (Figure 2.10 C). 3 conserved motifs for PUFB was observed with p-values (probability value) as $5.49e-6$, $2.02e-7$ and $1.74e-6$ on sense strand. First motif showed high probability of consensus sequence of A, C, A, C at position 3rd, 4th, 5th and 7th with good bit score (Figure 2.10 D) while the second motif showed the consensus sequence of G, T, C at positions 1st, 5th, 7th with good bit score (Figure 2.10 E). Third motif is the smallest of all and had a consensus sequence of C and A at positions 4th and 6th with better bit score (Figure 2.10 F). 3 conserved motifs for PUFC was observed with p-values (probability value) as $9.16e-17$ on sense strand, $1.23e-5$ on antisense strand and $2.69e-5$ on sense strand. First motif is very large and show high probability of consensus sequence of T, T, A, T, G, A, C, T, A, A, T and C at position 1st, 4th, 11th, 13th, 14th, 16th, 18th, 25th, 26th, 27th, 28th and 30th with good bit score (Figure 2.10 G) while the second motif showed the consensus sequence of C, C, A, A and G at positions 2nd, 3rd, 4th, 5th, 6th with good bit score (Figure 2.10 H). Third motif had a consensus sequence of G, A and G at positions 2nd, 4th and 6th with better bit score (Figure 2.10 I). We observed 3 conserved motifs for PUFD with p-values (probability value) as $3.26e-15$, $1.78e-19$ and $2.02e-5$ on sense strand. First motif is relatively large and show high probability of consensus sequence of A, C, A, T, A, A and A at position 1st, 2nd, 3rd, 5th, 7th, 11th, 15th and 21st with good bit score (Figure 2.10 J) while the second motif is the largest and show the consensus sequence of T at many positions with good bit score (Figure 2.10 K). Third motif is the smallest and had a consensus sequence of C, C, C, A, A and A bases at positions

from 1st to 6th with better bit score (Figure 2.10 L). 3 conserved motifs for PUF_E was observed having the p-values (probability value) as 1.28e-7, 1.28e-4 and 4.80e-6 on sense strand. First motif showed high probability of consensus sequence A, C, C, G and A at position 2nd, 4th, 6th, 9th and 10th with good bit score (Figure 2.10 M) while the second motif is the smallest of all and show the consensus sequence of T, C and A at positions 3rd, 5th and 6th with good bit score (Figure 2.10 N). Third motif had a consensus sequence of A, A and A at positions 2nd, 4th and 5th with good bit score (Figure 2.10 O). Sequences of the above motifs of each PUF can be used for the prediction of the transcription factor bindings to the specific motifs of the PUF promoter.

2.4.3 Structure modeling and Molecular Dynamics simulations of the 5 PUF proteins

To understand the structural property of all the 5 PUF proteins (PUFA, PUF_B, PUF_C, PUF_D and PUF_E) we took the bioinformatic approach. By using I-TASSER program, tertiary structures were predicted by providing protein sequences, which gave us 5 models, which were sorted on the basis of C-TM scores. We used domain sequences for the structure modeling. C-scores and TM-scores of PUFA were -3.0 and 0.53, respectively, which indicates better quality and correct global topology. Domains of PUFA were present at the C-terminal side from amino acid 539 to 835. Tertiary structure of PUFA domain consists mainly of α -helices (Figure 2.11 A). 3D structure of PUFA domain mainly consists of 8 repeats where each repeat comprises of 3 α -helices joined together by small loops and turns. 8 repeats are named from R1 to R8, where repeat R8 is present towards the C-terminal. It is second helix of each domain, which interacts with the RNA base. All 8 repeats together form a crescent shape structure. Figure 2.13: 3D structure and MD simulation of PUFA. (A) Tertiary structure of PUFA. (B) Root mean square deviation (RMSD) of PUFA plotted against time. (C) Root mean square fluctuation (RMSF) of protein residues for DdPUFA and (D) Radius of gyration (Rg) of DdPUFA and (E) Ramachandran plot for structural validation of optimized model of DdPUFA showing 89.2% of the residues are placed in favoured regions. To refine the tertiary structure of the predicted PUFA model, MD simulations were carried. To statistically validate the predicted model these simulations were run in triplicate. Average values of root mean square deviation (RMSD), root mean square fluctuation (RMSF) and radius of gyration ([Rg](#)) were [obtained. The RMSD plots](#) showed the convergence achieved at 0.6 nm RMSD for PUFA after 25 ns of simulation [confirming the stable behaviour and less deviation from the reference structures \(Figure 2.11 B\)](#). [The mobility of different parts of protein models was accomplished by examining the RMSF for each residue.](#) In PUFA, fluctuations occurred in the residues around 850- 870 amino acids with the average RMSF value of 0.48 nm (Figure 2.11 C). The globularity and compactness of the structure were evaluated by the radius of gyration (Rg). Radius of gyration achieved stable and steady behaviour after 20000 ps (pico second) simulation time with average value 2.95 nm (Figure 2.11 D). Overall radius of gyration for PUFA protein model was constant and stable suggesting proteins had good compactness. Stereochemical properties of the model were evaluated through Ramachandran plot. The Ramachandran plot for the optimized DdPUFA (Figure 2.11 E) model showed 89.2% of the residues are placed in favoured regions, 9.8% of the residues are placed in allowed regions and 0.9% of the residues are placed in [disallowed regions. Higher proportion of protein residues are present in favoured and allowed regions \(>90%\)](#) suggestig that the model is stereochemically stable. In case of PUF_B, [C- and TM-scores were -0.20 and 0.69, respectively,](#)

which indicates correct global topology and better quality. PUFB domains are present at the C- terminal side from amino acid 410 to 698. Tertiary structure of domain of PUFB consists mainly of α -helices (Figure 2.12 A). 3D structure of PUFB domain mainly consists of 8 repeats where each repeat comprises of 3 α -helices joined together by small loops and turns. 8 repeats are named from R1 to R8, where repeat R8 is present towards the C- terminal. All 8 repeats together form a crescent shape structure. The RMSD plots showed the convergence achieved at 0.75 nm RMSD for PUFB after 15 ns of simulation confirming the consistent behaviour and less deviation from the reference structures (Figure 2.12 B). Figure 2.14: 3D structure and MD simulation of PUFB. (A) Tertiary structure of PUFB. (B) Root mean square deviation (RMSD) of PUFB plotted against time. (C) Root mean square fluctuation (RMSF) of protein residues for DdPUFB. (D) Radius of gyration (Rg) of DdPUFA. (E) Ramachandran plot for structural validation of optimized model of DdPUFB showing 79.2% of the residues are placed in favoured regions. In PUFB, fluctuations occurred in the residues around 420-430 amino acids with the RMSF value of 1 nm (Figure 2.12 C). While radius of gyration achieved stable and steady behavior after 40000 ps simulation time with average value 3.05 nm (Figure 2.12 D). Overall radius of gyration for the model was slightly unstable. The Ramachandran plot for the optimized DdPUFB (Figure 2.12 E) model showed 79.2% of the residues are placed in favoured regions, 19% of the residues are placed in allowed regions and 1.8% of the residues are placed in [disallowed regions](#). Higher proportion of protein residues are present in favoured and allowed regions (>90%) which suggest that they are stereochemically stable. In PUFC, C- and TM-scores were -2.31 and 0.54, respectively indicating better quality with correct global topology. Domain of PUFC was present throughout the protein length starting from N-terminal side from amino acid 80 to 454. Tertiary structure of domain of PUFC mainly is composed of α -helices (Figure 2.13 A). 3D structure of PUFC domain mainly consists of 6 repeats where each repeat comprises of 3 α -helices joined together by small loops and turns. 6 repeats are named from R1 to R6, where repeat R1 is present near the N-terminal and R6 towards the C-terminal. The RMSD plots showed the convergence achieved at 1 nm RMSD for PUFC after 15 ns of simulation confirming the consistent behaviour and less deviation from the reference structures (Figure 2.13 B). In PUFC, fluctuations occurred in the residues around 40-45 and 60-65 amino acids with the RMSF value of 1.4 and 1.5 nm respectively, both of which lies outside the domain towards C-terminal (Figure 2.13 C). While radius of gyration achieved stable and steady behaviour after 35000 ps simulation time with average value 3.6 nm (Figure 2.13 D). Overall radius of gyration for the model was [stable suggesting the proteins had good compactness](#). Figure 2. 15: 3D structure and MD simulation of PUFC. (A) Tertiary structure of PUFC. (B) Root mean square deviation (RMSD) of PUFC plotted against time. (C) Root mean square fluctuation (RMSF) of protein residues for DdPUFC. (D) Radius of gyration (Rg) of DdPUFC. (E) Ramachandran plot for structural validation of optimized model of DdPUFC showing 74.4% of the residues are placed in favoured regions. The Ramachandran plot for the optimized DdPUFC (Figure 2.13 E) model showed 74.4% of the residues are placed in favoured regions, 23.5% of the residues are placed in allowed regions and 2.0% of the residues are placed in [disallowed regions](#). Higher proportion of protein residues are present in favoured and allowed regions (>90%) which suggest that they are stereochemically stable. Figure 2.16: 3D structure and MD simulation of PUFD. (A) Tertiary structure of PUFD. (B) Root mean

square deviation (RMSD) of PUFd plotted against time. (C) Root mean square fluctuation (RMSF) of protein residues for DdPUFD. (D) Radius of gyration (Rg) of DdPUFD. (E) Ramachandran plot for structural validation of optimized model of DdPUFD showing 87.2% of the residues are placed in favoured regions. In case of PUFd, [C- and TM-scores were 0.03 and 0.72, respectively](#), which indicates [better quality](#) and [correct global topology](#). Domains [of](#) PUFd are present at the C-terminal side from amino acid 651 to 943. Tertiary structure of domain of PUFd consists mainly of α -helices (Figure 2.14 A). 3D structure of PUFd domain mainly consists of 8 repeats where each repeat comprises of 3 α -helices joined together by small loops and turns. 8 repeats are named from R1 to R8, where repeat R8 is present towards the C-terminal and are clustered together. All 8 repeats together form a crescent shape structure. The RMSD plots showed the convergence achieved at 0.7 nm RMSD for PUFd after 25 ns of simulation [confirming the stable behaviour and less deviation from the reference structures \(Figure 2.14 B\)](#). In PUFd, there was no fluctuation present in the domain region but was outside the domain, near N and C-terminal which are flanking regions (Figure 2.14 D). The radius of gyration achieved stable and steady behaviour after 25000 ps [simulation time with average value 2.92 nm \(Figure 2.14 D\)](#). Overall radius of gyration for the model [was low and stable](#) indicating [the proteins](#) had better compactness. [The Ramachandran plot for the optimized DdPUFD \(Figure 2.14 E\) model](#) showed 87.2% of the residues are placed in favoured regions, 12.2% of the residues are placed in allowed regions and 0.7% of the residues are placed in [disallowed regions. Higher proportion of protein residues](#) are present [in favoured and allowed regions \(>90%\)](#) which [suggest](#) that they are [stereochemically stable](#). In case of PUF_E, [C- and TM-scores were -2.95 and 0.58, respectively](#), which indicates [better quality](#) and [correct global topology](#). 6 Domains [of](#) PUF_E are present throughout protein length from amino acid 214 to 655 in the cluster of two each separated by loops and coils (also shown in figure 2.3 E). Tertiary structure of domain of PUF_E consists mainly of α -helices. 3D structure of PUF_E domain mainly consists of 6 repeats where each repeat comprises of 3 α -helices joined together by small loops and turns. 6 repeats are named from R1 to R6 (Figure 2.15 A), where repeat R6 is present towards the C-terminal. All 6 repeats together form a crescent shape structure. The RMSD plots showed the convergence achieved at 0.8nm RMSD for PUF_E after 30ns of simulation confirming the consistent behaviour and less deviation from the reference structures 49 (Figure 2.15 B). In PUF_E, no fluctuations occurred in the domain region but only at C- terminal flanking region (Figure 2.15 C). Figure 2.17: 3D structure and MD simulation of PUF_E. (A) Tertiary structure of PUF_E. (B) Root mean square deviation (RMSD) of PUF_E plotted against time. (C) Root mean square fluctuation (RMSF) of protein residues for DdPUF_E. (D) Radius of gyration (Rg) of DdPUF_E. (E) Ramachandran plot for structural validation of optimized model of DdPUF_E showing 84.9% of the residues are placed in favoured regions. While radius of gyration achieved stable and steady behaviour after 25000 ps (picosecond) simulation time with average value 2.92 nm (Figure 2.15 D). Overall radius of gyration for the model was good indicating the proteins had better globularity. The Ramachandran plot for the optimized DdPUF_B (Figure 2.15 E) model showed 84.9% [of the residues](#) are placed [in favoured regions](#), 13.5% of the residues are placed in allowed regions and 1.6% of the residues are placed in [disallowed regions. Higher proportion of protein residues](#) are present [in favoured and allowed regions \(>90%\)](#) which [suggest](#) that they are [stereochemically stable](#).

2.4.4 Temporal mRNA expression

pattern of PUFB by RT-PCR. The temporal mRNA expression pattern of PUFB was determined by performing reverse transcriptase PCR (RT-PCR). RNA was isolated from samples collected at different time-points and various developmental stages and cDNA were prepared. The gene specific primer combinations as shown in Table 2.1 were used for the amplification of respective cDNAs. rnlA (mitochondrial large subunit rRNA, also referred as ig7), a constitutively expressing gene was used as an internal control (Hopper et al., 1993). PCR amplifications at 24 cycles were done for both PUFB and ig7 genes. The expression pattern of both the transcript was quantified by densitometry analysis using AlphaImager software from Alphainotech. The relative expression of PUFB transcript as compared to ig7 transcript was plotted at each time point and stage wise. Figure 2.18: Temporal expression pattern of PUFB transcript during development. (A) RT-PCR gel picture of PUFB and rnlA (ig7) using cDNA of different development stages; V-vegetative cells, LA-loose aggregate, M-mound, SL -Slug, EC-early culminant and FB-fruited body. (B) Relative abundance of PUFB transcript to rnlA (ig7) transcript at different stages of development. (C) Temporal expression pattern of PUFB and rnlA (ig7) by RT-PCR using cDNA samples at various time-points of development. (D) Relative abundance of PUFB to rnlA transcript at various time-points [M-DNA marker lane; n=4]. The RT-PCR analysis showed that PUFB mRNA was present throughout the growth and development (Figure 2.16). The maximum expression was observed in the early culminant while minimum expression was found in mound and slug stage. Initially 51 its expression is high in vegetative stage then its expression decreases and after slug its expression reaches maximum in early culminant thereafter expression decreases in fruited body. mRNA expression pattern suggests that it may be required both during cell proliferation (vegetative stage) as well as during the terminal differentiation.

2.4.5 Spatial mRNA expression pattern analysis of PUFB by in situ hybridization

Figure 2.18: Cloning for in situ hybridization studies. (A) PCR amplification of ~0.997 Kb genomic region for the preparation of probe. (B) Restriction digestion of PUFB PCR product (Lane 1) and pBSII SK+ vector (Lane 2) with BamHI/XbaI. (C) Confirmation of in situ positive clone by restriction digestion yielded 3.0 Kb vector backbone and a ~0.997 Kb insert. (D) The unhydrolysed (UH) and hydrolysed (H) product of sense (S) and antisense (AS) probe. [M- DNA marker, PCR-Polymerase Chain Reaction]. Spatial mRNA expression pattern of PUFB was analysed by performing whole mount in situ hybridization. The exonic region (0.997kb) of PUFB was amplified (Figure 2.17 A) followed by restriction digestion (Figure 2.17 B) and cloned in to pBSII SK+ vector (Figure 2.17 C). Linearized vector were used as a template for RNA probes synthesis for in-vitro transcription. T3 and T7 promoters were used for antisense and sense probe preparations, respectively. RNA fragments of smaller size were obtained by hydrolysing both anti-sense and sense probes (Figure 2.17 D). Antisense probe was used for hybridization in multicellular structure while sense probe was used as an internal control. To carry out the in situ hybridization wild type Ax2 cells were developed on membrane to collect the different stages of Dictyostelium. Further these structures were hybridized with probes to examine the expression pattern. Figure 2.19: Spatial expression patterns of PUFB mRNA analysed by in situ hybridization in the multicellular structures of Dictyostelium. In situ hybridization using antisense probe A (a-d) shows the presence of PUFB mRNA in the prestalk/stalk cells of multicellular structures while the in situ hybridization using sense probe B (a-d) did not show any colour and

represents the negative control (a-d) [a- Tipped mound, b-slug, c-early culminants and d-late culminant/FB; n=3]. The results showed that the expression of PUFB mRNA was found at the tip of mound (Figure 2.18 Aa). As development proceeded PUFB mRNA was clearly visible in the anterior prestalk regions of the slug (Figure 2.18 Ab). Anterior prestalk region comprised of prestalk A, prestalk O and prestalk AB cells. The prestalk A and prestalk O cells then migrate into the initial stalk tube and transform into stalk cells (Jermyn et al., 1989). In early culminant the expression was found in the initial stalk tube which are formed mainly by the pstAB cells and also present at the basal disc (Figure 2.18 Ac). In the late culminant the expression of PUFB mRNA remained only in tip and stalk tube. The prestalk specific localization of PUFB mRNA suggests it may have role in prestalk differentiation and autophagic cell death. The sense probe did not show any specific staining (Figure 2.18 B).

2.5 CONCLUSIONS

In this chapter, we have traced the phylogenetic position of all the 5 PUF proteins of Dictyostelium and found that PUFA shows more homology to plants and yeast. PUFB and PUFD also showed close homology with plants and yeast but they do not show significant similarity to mammals like human. While PUFA show relatively more closeness as compared to PUFB and PUFD protein of Dictyostelium. PUFC and PUFE both are present on separate clade of plants, animals, yeast etc rather they are present as out-group. Using bioinformatics approaches, 3 highly conserved motifs were observed in the putative promoter region of all 5 PUF genes that could act as binding site for different transcription factor. Tertiary structures of all the PUF were constructed using hybrid- modeling approaches. Structural analysis of all the PUF revealed that all the PUF have 8 repeats except PUFC and PUFE, which are having 6 repeats each. Consistent behavior of RMSD, RMSF and Rg for all the PUF models indicating models have good structural stability. Higher residues present in favoured and allowed region for all the PUF suggesting that they are stereochemically stable. Work on DdPUFA suggests its important role during growth to development transition. Out of the remaining 4 PUF proteins in Dictyostelium we choose DdPUFB to work upon further. High PUFB mRNA expression in initial stages of development suggests that it may have role in cell division and growth to development transition. Its expression is highest in later stages of development implying its role in terminal differentiation of cell types. As inferred from in situ hybridization spatial expression of PUFB mRNA is expressed in prestalk specific cells suggesting it may have role in autophagic cell death and stalk cell differentiation.

3.1 INTRODUCTION

Pumilio (Pum) of *Drosophila* and Fem-3 binding factor (FBF) of *C. elegans* are the founding members of the family of RNA binding proteins called PUF (Pumilio and FBF) (Wickens et al., 2002). A typical feature of PUF proteins is the presence of 8 repeats present at the C-terminal of the protein forming a domain called PUF domain or Pumilio homology domain (PUM-HD). Alignment of domain present at the C-terminal part of *Drosophila* Pumilio with *Xenopus* and mammalian homologs reveals the PUM- HD architecture (Figure 3.1A). The domain comprises of 8 repeats present tandemly along with N- and C-terminal flanking regions. Each repeat comprises of ~36 amino acids forming three α -helices. Most conserved three amino acids present in the second helix makes the contact with the RNA base (Wang et al., 2002). Crystal structure of Human and *Drosophila* Pumilio revealed that the domain forms an arc-like structure (Edwards et al., 2001; Wang et al., 2001). The RNA interacts with the concave surface and each repeat interact with the single base of RNA through three conserved amino acid residues present

in the second repeat (Figure 3.1B). A specific sequence is present at 3' UTR of mRNA called Nanos response element (NRE) which is recognized by the PUF protein and thus regulate the mRNA post-transcriptionally (Wang et al., 2002; Zamore et al., 1999). Figure 3.1: Schematic representation of the domain structure of *Drosophila Pumilio* and its human homolog PUM1 and PUM2. (upper panel) 8 conserved RNA binding domains present at the C-terminal while N-terminal region is of varying length and weakly conserved. (lower panel) A schematic representation showing the interaction of fly NRE present at 3'UTR of mRNA with PUM-HD domain. Each repeat interacts with a single base of mRNA in an antiparallel manner. Nos and Brat recruitment lead to the formation of a quaternary complex with Pum and hb mRNA, inhibiting the hb protein synthesis (adapted from Danislav et al., 2003). The main function of PUF protein is the post-transcriptional regulation of the target mRNA by mRNA decay or translational inhibition. Therefore, in most of the cases, it is localized primarily in the cytoplasm of cells (Archer et al., 2009; Macdonald, 1992; Zhang et al., 1997). PUF proteins can regulate various aspects of eukaryotic development like embryogenesis, gametogenesis/gamete maturation, neural development and functions. In *Drosophila*, normally Hunchback (Hb) protein is expressed at the anterior region during early development in *Drosophila* embryo. However, when *Pumilio* is mutated gradient of *Pumilio* protein is also present in the posterior region, which suggest that repression of hb mRNA is absent in this region (Barker et al., 1992; Tautz, 1988). This led to the defects in abdominal segmentation in *pumilio* mutant embryos (Barker et al., 1992; Lehmann and Nüsslein-Volhard, 1987). *Pumilio* also regulates some other processes like stem cell proliferation, memory formation and motor neuron functions (Weidmann and Goldstrohm, 2012). In case of *C. elegans*, Notch signaling pathway and PUF RNA binding proteins maintain the pool of Germline stem cells (GSCs) (Bray, 2016; Wickens et al., 2002). From the niche, [GLP-1/Notch signaling is](#) required for [the](#) maintenance [of](#) GSC and [FBF-1 and FBF-2 \(collectively FBF\)](#) promote GSCs self-renewal by acting as repressors of differentiation RNAs ([Crittenden et al., 2002](#); [Kershner et al., 2013](#)). Both *sygl-1* and *lst-1* genes are identified as GSCs regulators that directly target niche signaling (Kershner et al., 2014). But Shin et al. (2017) reported that both SYGL-1 and LST-1 as a cytoplasmic protein is present in GSC region. Both SYGL-1 and LST-1 interact with FBF physically and leads to repression of the FBF target RNA within the stem cell pool and thus maintain the stem cell pool. Also, to regulate spermatogenesis to oogenesis transition, there is a requirement of *fem-3* repression and it is achieved post-transcriptionally via the 3' UTR region present in the regulatory region of *fem-3* mRNA ([Ahringer and Kimble, 1991](#); [Barton et al., 1987](#); Hodgkin, 1986) In *Arabidopsis thaliana*, PUF proteins are involved in many cellular and developmental processes like abiotic and biotic stress responses, against many droughts and salt stress-responses, morphogenesis in leaves etc. APUM23 was found to regulate morphogenesis in leaf by the regulation of expression of KANADI (KAN) genes. GARP family member KAN genes, regulate the abaxial identity (Huang et al., 2014). APUM23 loss of function in plants leads to the scrunched and serrated leaves, slow growth and also venation show abnormal pattern because of RNA processing (Abbasi et al., 2010). In mice, two *Pumilio* genes *Pum1* and *Pum2* are present. Mice with a single knockout mutation in either of *Pum* are viable and fertile (Chen et al., 2012; Gennarino et al., 2015; Lin et al., 2018a; Xu et al., 2007). It remained unclear whether they can function redundantly to properly regulate the stem cell development

during embryogenesis. Recently it was identified that if both Pum1 and Pum2 are mutated, it causes gastrulation failure which leads to embryo lethality at E8.5 (Lin et al., 2018b). As PUF proteins play an important role during the development and morphogenesis of organisms and Dictyostelium undergoes multicellular development upon starvation, so we were interested in elucidating its role during growth and development. In this chapter, we have prepared the overexpressor and knockout strains of PUFB gene. We observed that it suppresses cell growth and cell proliferation, development of mutant strains are also affected. We have also analyzed the expression of developmentally important genes.

3.2 OBJECTIVES OF THE PRESENT STUDY

- To create PUFB mutant strains to modulate the level of PUFB in *D. discoideum*. Mutant strains developed for the present study are:
 - Ø? Construction of PUFB overexpressor (PUFBOE) [act15/PUFB-eYFP/Ax2] strain of *D. discoideum*: Full length PUFB (DDB_G0279557) was expressed as an eYFP-tagged fusion protein with the reporter enhanced yellow fluorescent protein (eYFP) at the C-terminal under the control of constitutive actin 15 promoter in wild type, Ax2 cells.
 - Ø? Construction of PUFB knockout (PUFB-) [PUFB-/Ax2] strain of *D. discoideum*: Knockout strain of PUFB was created by gene disruption by insertion of blasticidin (Bsr) cassette between the two PUFB homologous fragments followed by homologous recombination. The linearized construct having PUFB homologous fragment along with blasticidin (Bsr) resistance cassette was then transformed into Ax2 cells.
- To analyse the role of PUFB mutant strains during growth and development in their comparison with the wild type Ax2 strain. Morphological analyses of the structures formed during development by PUFB mutant strains.
- To analyse the role of PUFB in cAMP signaling and cell adhesion.

3.3 MATERIALS AND METHODS

Here we discuss the protocols which are not mentioned earlier in this thesis.

3.3.1 Materials used in the study

The cells were grown in the presence of antibiotics like Geneticin (G418) and Blasticidin S (B) when required. Oligonucleotides used for PCR were synthesized from GCC Biotech, India. For cloning purpose PCR reagents, restriction, ligation enzymes and Gel extraction kits were purchased from Fermentas Life Sciences (Thermo Scientific). Selection markers like Geneticin (G418), Blasticidin S (B) and ampicillin were procured from Sigma Aldrich, USA. The plasmids used in the study are mentioned in the appendix.

3.3.2 Transformation of *D. discoideum* Ax2 cells

Transformation of freshly grown Ax2 cells with DNA was performed according to Gaudet et al., (2007). Approximately 2.5×10^6 cells were taken and washed twice with ice-cold H50 buffer and re-suspended in 100 μ L H50 buffer. Approximately 5-10 μ g plasmid DNA is mixed with the ice-cold cell suspension and poured into the 1 mm chilled electroporation cuvette (Sigma Aldrich USA). The electroporator (Bio-Rad Gene Pulser TM) was set at 0.65-0.70 kV and 25 μ F and the cuvette containing cell suspension and plasmid DNA was pulsed twice with an interval of 10 seconds. After the second pulse, the cells were immediately kept on ice for 5 minutes and then transferred to 90 mm culture plate containing HL5 medium for recovery from the electric pulse. Only after 24 h of incubation at 22°C, appropriate selection marker (antibiotics) was added for the selection of the transformants. Maximum concentration of G418 used was 100 μ g mL⁻¹ and blasticidin S was 10 μ g mL⁻¹.

3.3.3 Construct preparation and confirmation of PUFB overexpressing strain

Full length PUFB (DDB_G0279557) gene was PCR amplified from the Ax2 genomic DNA (Genomic position 1004-2662) using gene-specific primer set (Table 3.1) having restriction sites SacI at the 5' end and XhoI at the 3' end for directional cloning [into](#)

[act15/acg-eYFP vector](#) (appendix). [The act15/acg-eYFP vector](#) contains an [actin15 promoter, reporter enhanced yellow fluorescent protein \(eYFP\) at the C-terminus](#), an ampicillin [resistance marker for selection in](#) bacteria [and](#) a G418 [resistance marker for selection in](#) Dictyostelium. Plasmids from approximately 6-8 positive colonies were checked by double digestion with SacI/XhoI. The positive colonies were then cultured in Luria Broth media and plasmid DNA was isolated using the alkaline lysis method (Bimboim and Doly, 1979). Plasmid DNA (5-10 µg) was then transformed into Ax2 cells by using the electroporation method. They were sequentially selected from 10 µg mL⁻¹ and grown till 100 µg mL⁻¹ of G418. Single clones of overexpressing cells were isolated and developed on NNA plates to form fruiting bodies. The spores were stored for long-term use in -80°C. Table 3.1: Primer combination used for the amplifying PUFB for making overexpressing strain. The restriction sites are underlined and the expected amplicon size is shown. Figure 3.2: Schematic representation of the PUFB^{OE} construct. PUFB ORF was introduced in act15/acg-eYFP vector having an eYFP-tagged [gene at the C-terminus and a 6X His tag at the N-terminus](#). PUFB replaced acg. The restriction sites used for cloning the PUFB gene downstream of actin15 are shown.

3.3.4 Subcellular localization of the PUFB-eYFP fusion protein by confocal microscopy

PUFBOE cells were grown on a sterile coverslip and placed inside 6 well petri- plates containing HL5 media. The PUFBOE cells have an eYFP reporter for direct visualization under a fluorescent microscope (excitation wavelength of 514 nm and an emission wavelength of 527 nm). Cells were stained with different cellular markers and incubated for 5-10 minutes, washed with 1x KK2 and visualized under Nikon confocal microscope. For subcellular localization studies, 1 µg mL⁻¹ of 4', 6-diamidino-2- phenylindole (DAPI) and 1 µM mL⁻¹ of 3, 6-Bis(diethylamino)-9-[2-(4-methylcoumarin- 7-yloxycarbonyl)phenyl] xanthylum chloride Mitored (Rhodamine based dye) were used to stain the cells. DAPI (excitation wavelength of 358 nm; emission wavelength of 461 nm) was used for nuclear staining and cell membrane permeable Rhodamine-based dye, Mitored (excitation of 569 nm; emission of 594 nm) was used for mitochondrial staining. For colocalization studies, cells were then visualized under Nikon confocal microscope at 100X/0.16 objective and subcellular localization was revealed by merging of the images of PUFBOE (green) with DAPI (blue), Mitored (red) using Nikon software (NIS- elements).

3.3.5 Construct preparation and confirmation of PUFB knockout (PUFB-) strain

PUFB- (knockout) strain was created by gene disruption method followed by standard homologous recombination. Two knockout fragments (KF1 and KF2) from the 5' and 3' end regions of the gene were PCR amplified from the Ax2 genomic DNA using specific primer sets (Table 3.2) [and introduced into the flanking side of the Blastidicin resistance \(Bsr\) cassette](#) in pDrive vector by restriction digestion (Figure 3.3). The ligated construct was then transformed in competent E. coli DH5α cells and incubated at 37°C in LB agar plates supplemented with 100 µg mL⁻¹ ampicillin. Plasmids from approximately 5-10 positive colonies were checked by double digestion. Linearized plasmid containing KF1-Bsr-KF2 fragment was transformed [into Ax2 cells by electroporation. The transformed cells were selected at 10 µg mL⁻¹ Blastidicin-S \(Invitrogen\)](#). The validation of the [PUFB-/Ax2] knockout strain was carried by PCR amplification using different primer combinations (Figure 3.4). Table 3.2: Primer combinations used for PUFB knockout construct preparation. Primer pairs with restriction sites (underlined) were used for the amplification of first and second fragments (KF1 and KF2) required for creating the

knockout construct. The genomic positions of primers and the expected amplicon sizes are mentioned. Figure 3.3: Gene disruption strategy for the creation of PUFB knockout strain. Transformation of the linearized vector containing 5' and 3' targeting regions (KF1 and KF2) interrupted by the Bsr cassette undergo homologous recombination with the wild type (Ax2) PUFB gene to create the disruption strain. The sizes and the restriction sites of the fragments in the construct are also shown.

Figure 3.4: Schematic representation for the validation of [PUFB-/Ax2] knockout strain using various primer combinations. Primer combinations used for the confirmation of the knockout strain and their expected genomic sizes are mentioned. Upper panel shows the primer sequences and the lower panel shows the primer combinations and the expected amplicon sizes for the validation of knockout strain.

3.3.6 Confirmation of PUFB mutant strains through mRNA level measurement

Approximately 1×10^6 vegetative cells from wild type Ax2, PUFBOE and PUFB- were harvested and washed twice with chilled 1x KK2 buffer. Cells were lysed in 1.0 mL TRI reagent (T9424, Sigma-Aldrich) and incubated for 20 minutes at room temperature. RNA was isolated, quantified and 1.0 μ g RNA from each sample was used to synthesize the respective cDNA. The gene-specific primer combinations (Table 3.3) were used for PCR amplification from cDNA template, which also ensures the purity of the preparation. PCR amplification for PUFB was carried out by initial denaturation at 98°C for 30 seconds followed by 24 cycles amplification of denaturation at 98°C for 45 seconds, primer annealing at 59.1°C for 1 minute and extension at 65°C for 1 minute. PCR amplification for ig7 was carried out using an initial denaturation for 30 seconds at 98°C followed by amplification which was carried for 24 cycles of denaturation at 98°C for 15 seconds, primer annealing at 52°C for 45 seconds and extension at 68°C for 1 minute. PCR amplified DNA samples were run on 1.5% agarose gel and AlphaImager 3400 was used to calculate the IDV values of each DNA band along with blank. The relative abundance of PUFB in each sample was calculated with respect to ig7 levels. Table 3.3: Primer combinations used for the amplification of cDNA for PUFB and rnlA/ig7 genes for RT analyses. Expected amplicon sizes from cDNA and gDNA as templates are mentioned above [FP- Forward primer, RP- Reverse primer, bp- base pair].

3.3.7 Cell proliferation analysis

Ax2, PUFBOE and PUFB- cells were grown in axenic HL5 media from fresh spores at 22°C. For growth analysis, logarithmic phase cells ($3-5 \times 10^6$ cells mL⁻¹) were diluted into fresh media at a seeding density of 5×10^5 cells mL⁻¹ and counted every 12 h up to 96 h as a measure of cell proliferation. Cell densities were measured by counting cells in a hemocytometer after appropriate dilutions in triplicates and were plotted as a function of time. Generation time was calculated as follows: $T_d = (t_2 - t_1) \times \log_2 / \log (q_2/q_1)$ 62 Where: t_1 - initial time t_2 - final time q_1 -growth at t_1 q_2 -growth at t_2

3.3.8 Analysis of development

For development analyses, the logarithmic phase ($3-5 \times 10^6$ cells mL⁻¹) cells from wild type Ax2 and PUFB mutants were harvested, washed in 1xKK2 buffer and spotted (10-20 μ L) as droplets at a density of 5×10^7 cells mL⁻¹ on 1.5% NNA plates. The plated cells were kept at 4°C for 4-6 h to bring synchronization in development, followed by incubation at 22°C for comparison of developmental timings and morphologies between different strains. Developing structures were photographed every 4 h using Nikon SMZ1500 stereomicroscope and analyzed using NIS Elements AR v. 4.0.

3.3.9 Morphological analyses of multicellular structures formed during development

Upon starvation, cAMP signaling is triggered which leads to multicellular development. Cells tend to move towards each other in response to cAMP gradient forming

aggregates. To analyze the effect of PUFB mutation in development we measured the [size and number of the aggregates formed by](#) the wild type [Ax2 cells](#) and the PUFB mutants using Nikon software (NIS Elements ARv.4.0). As the development proceeded to culmination PUFB mutants formed fruiting bodies showing different morphology than the wild type Ax2 cells. We measured the number of fruiting bodies formed in all the three strains and also measured the length of stalk and sorus and calculated the stalk: sorus ratio for each strains using NIS elements. Approximately 200 fruiting bodies from three individual experiments were analyzed.

3.3.10 Spore viability assay [Spore viability assay was performed](#) as described in [Maurya et al. \(2017\)](#). Logarithmic phase ($3-5 \times 10^6$ cells mL⁻¹) cells from wild type Ax2 and PUFB mutants were harvested in 1x KK2 buffer and plated on 1.5% NNA and allowed to develop at 22°C. Spores were collected from fruiting bodies in spore buffer (40 mM KH₂PO₄, 20 mM KCl, 2.5 mM MgCl₂), centrifuged at 12,000g for 2 minutes at 22°C and washed with spore storage buffer. Upon appropriate dilutions, spores were [counted in a haemocytometer](#) and [aliquots of 100 spores](#) from each strain [were](#) then [mixed with](#) heat-killed *Klebsiella aerogenes* bacterial suspension and grown on NNA plates for 5-6 days. [Clear plaques formed on the bacterial](#) lawn were counted. The percent spore viability [was measured by counting the number of clear plaques divided by total spores plated followed by multiplication of 100](#). All [experiments](#) were performed [in](#) triplicates.

3.3.11 Cell cycle and cell size analysis To analyze the cell size and cell cycle of different PUFB mutant strain and wild type Ax2, BD FACS Aria with BD FACS DIVA software were used. For this purpose 1×10^7 cells mL⁻¹ were harvested and washed with 1xKK2 buffer followed by resuspending in [1.5 mL buffer \(0.9% NaCl, 5 mM EDTA, 2% sucrose in KK2 buffer\)](#). Fixing of the cells was done by using 75% ethanol dropwise then incubated at 22°C for 30 minutes and stored at 4°C. Just before analysis cells were washed and resuspended in 1 mL 1xKK2 buffer then 10 µg mL⁻¹ RNase A (Sigma-Aldrich, USA) was added and incubated for 30 minutes at 37°C. After this, 50 µg mL⁻¹ propidium iodide (Sigma-Aldrich, USA) was added and further incubated at room temperature for 30 minutes. Cells were washed with 1xKK2 buffer and resuspended in an appropriate volume of 1xKK2 buffer.

3.3.12 Pinocytosis and exocytosis assay Endocytosis and exocytosis assay was performed according to Rivero and Maniak (2006). We inoculated 3×10^6 cells mL⁻¹ of Ax2, PUFB- and PUFBOE and kept it for 15 minutes under shaken condition then 2 mg mL⁻¹ of FITC dextran (Sigma Aldrich) was added and the samples were collected at different time points (0, 15, 30, 45, 60, 90, 120 and 180 minutes) and 1.5 mL of ice-cold Sorenson buffer (see Appendix) was added to it followed by washing (twice) with Sorenson buffer. After that cells were lysed with 500 µL of lysis buffer and then the fluorescence was measured in multiplate Reader (Thermoscientific Varioskan Flash) at $\lambda_{Ex} = 470$ nm and $\lambda_{Em} = 515$ nm. For exocytosis, 3×10^6 cells mL⁻¹ cells of different strains were subjected to incubation in FITC-dextran for 3 h followed by washing then cells were resuspended in the growth medium again. Samples were collected at different time points (0, 15, 30, 45, 60, 90, 120 and 180 minutes) and 1.5 mL of ice-cold Sorenson buffer (see Appendix) was added to it followed by washing twice with Sorenson buffer. After that cells were lysed with 500 µL of lysis buffer then measured the fluorescence in multiplate Reader (Thermoscientific Varioskan Flash) at $\lambda_{Ex} = 470$ nm and $\lambda_{Em} = 515$ nm

3.3.13 Measurement of mRNA levels for developmental genes Logarithmic phase wild type Ax2, PUFBOE, and PUFB- cells were harvested and developed on 1.5% NNA plates [at a](#)

[density of 5x10⁷ cells mL⁻¹](#) 1. [Various developmental](#) stages like vegetative, loose aggregate, mound, slug, early culminant and late culminant were collected and RNA was extracted. cDNA was prepared and RT-PCR was performed for various genes involved in early development like *cadA*, *csaA*, *ctnA*, *acaA*, *carA1*, *pdsA*, *cotA* and *cotB* using the specific primer combinations as shown in Table 3.4. Table 3.4: Primer combinations used for RT analyses of genes involved in the development of *Dictyostelium*. Expected amplicon sizes of genomic DNA and cDNA are mentioned.

3.3.14 cAMP level measurement The [total cAMP levels were measured using](#) commercially available [cAMP Enzyme Immunoassay Kit \(CA200, Sigma Aldrich\)](#) as per the manufacturer's instructions. [1x10⁶ cells from logarithmic phase](#) cultures [of Ax2 and PUFB mutants were](#) harvested and washed twice in 1x KK2 buffer. Cells [were starved in 1xKK2 buffer for 0, 4 and 6 h. Cells were harvested and treated with 0.1 M HCl.](#) cAMP levels of each sample were calculated according to the kit manual.

3.4 RESULTS AND DISCUSSION

3.4.1 Preparation of PUFB overexpressing strain [act15/PUFB-eYFP/Ax2]

PCR amplification of PUFB gene (~2.66 Kb) using genomic DNA as the template was performed (Figure 3.5A) and the amplified product was eluted using the gel elution [kit available from](#) Genetix [as per the manufacturer's instructions](#) and double digested with SacI/XhoI and further purified by gel elution kit. Similarly, pB17S vector (6.1 Kb) was double digested with SacI/XhoI and ligated with the digested 2.66 Kb amplicon (Figure 3.5B). The ligated product was transformed into competent bacteria for amplification. Plasmid DNA of 5-6 colonies was isolated using alkaline lysis method (Sambrook and Russel, 2007) and confirmed for the presence of positive construct by restriction digestion with SacI/XhoI yielding 6.1 Kb fragment of vector and 2.66 Kb fragment of insert (Figure 3.5C). The construct was also confirmed by sequencing. Plasmid DNA (2-10 µg) was then transformed by electroporation into *D. discoideum*, Ax2 cells (Gaudet et al., 2007). The [transformed cells were](#) sequentially [selected on](#) 10 µg [mL⁻¹](#) of [G418 and](#) grown till 100 µg mL⁻¹. The transformed cells were cloned out on the bacterial lawn and the *Dictyostelium* cells overexpressing PUFB were now called as PUFBOE strain. Figure 3.5: Construct preparation for the PUFB overexpressor (PUFBOE). (A) PCR amplification of the full length PUFB (2.66 Kb) using gene-specific primers. (B) Restriction digestion of the PUFB amplified product (2.66 Kb) (Lane1) and pB17S vector (6.1 Kb) (Lane2) using SacI/XhoI. (C) Confirmation of clone; Lane 3- Digested vector (6.8 Kb); Lane 4: Restriction digestion of the plasmid with SacI/XhoI yields the vector fragment of 6.8 Kb and the insert of 2.66 Kb [M-DNA marker].

3.4.2 Subcellular localization of PUFB-eYFP fusion protein

To analyze the subcellular localization of PUFB expression of the fusion protein with the available PUFBOE (*Dictyostelium* PUFB gene fused to eYFP as a reporter) cells. The cells were grown on coverslip overnight and then incubated in DAPI and Mitored. DAPI is a fluorescent stain that binds to AT-rich regions in DNA whereas Mito-Red binds to the mitochondria in live cells. Figure 3.6: Subcellular colocalization studies in PUFBOE cells. (A) The PUFBOE cells expressing PUFB gene fused to eYFP as a reporter were stained with nuclear stain, DAPI (blue) and (B) Mitochondrial stain, Mitored (red) for 10 minutes and images were captured in confocal microscope. The PUFB fusion protein (green) showed cytosolic localization and did not colocalize with mitochondria. [Scale bar=10 µm]. Through confocal microscopy analysis, we found that the eYFP fluorescence of PUFB-eYFP fusion protein was expressed in the cytosol (Figure 3.6A). As reported in other organisms also, PUF protein is predominantly localized in the cytosol (Miller and Olivas, 2011). Except

for PUF6p of *S. cerevisiae* which is localized in both cytoplasm and nucleus (Gu et al., 2004) and PUF7 of *T. brucei* which is present in the nucleolus (Droll et al., 2010). Microscopic examination showed that PUFB-eYFP fluorescence did not colocalize with the Mitored (Figure 3.6B), a mitochondrial marker. Colocalization was determined through the analysis of merged images using NIS elements software.

3.4.3 Preparation of the PUFB knockout construct

PUFB knockout strain was created by gene disruption followed by homologous recombination. 5' and 3' targeting region (KF1 and KF2 respectively) of PUFB is cloned in such a way that it flanked the Blasticidin resistance cassette (Bsr) of the pDrive vector, which was transformed into Ax2 cells to create the knockout strain. Both 5' and 3' end of the gene (KF1 and KF2 respectively) were PCR amplified from the genomic DNA using the forward and reverse primer combination giving amplicon sizes of 1.05 Kb and 0.951 Kb respectively (Figure 3.7A). The fragment 1 (KF1 from the 5' end) was digested with the restriction enzymes NotI/XbaI and ligated with the similarly digested vector. Also, fragment 2 (KF2 from the 3' end) was digested with the restriction enzymes KpnI/MluI and ligated with the similarly digested vector for directional cloning. The ligation product was then transformed in *E. coli* competent cells and grown on LB agar plates supplemented with 100 µg mL⁻¹ ampicillin and incubated at 37°C.

Figure 3.7: Cloning of PUFB knockout construct and validation of knockout construct via PCR amplification and restriction digestions. (A) PCR amplification of 5' targeting region Fragment 1 (KF1) and 3' targeting region Fragments 2 (KF2) from the genomic DNA yields a 1.05 Kb and 0.951 Kb products respectively. (B) Confirmation of PUFB knockout construct and Bsr cassette by restriction digestions. The restriction enzymes used along with the respective sizes of the release are as mentioned; Lane 3: NotI /XbaI (6.75 Kb vector backbone + 1.05 Kb insert); Lane 4: KpnI/MluI (6.85 Kb vector backbone + 0.951 Kb insert). (C) Lane 5: KpnI/NotI (~3.8 Kb vector backbone + ~4 Kb linearized product); (D) Confirmation of construct by PCR amplification. Lane 6 & 7: fragment 1 & 2 of size 1.5 & 0.95 Kb, respectively. (E) Lane 8: PCR amplification of linearized construct of ~4 Kb. All band sizes are approximate [M= DNA ladder]. Various combinations of restriction enzymes were used to confirm the positive clone. The plasmid was digested with KpnI/NotI enzymes to get the linearized construct (fragment 1 + bsr cassette + fragment 2) of ~4 Kb (Figure 3.7C). Digestion of plasmid with NotI/XbaI yield the fragments of size 6.75 Kb and 1.05 Kb (Fragment 1) while digestion with KpnI/MluI yield the fragments of size 6.85 Kb and 0.95 Kb (Fragment 1) respectively (Figure 3.7B). They were further confirmed by PCR using different primer combinations. Fragment 1 (1.05 Kb), fragment 2 (0.95 Kb) (Figure 3.7D) and linearized construct (~4 Kb) (Figure 3.7E) were successfully amplified from the plasmid further confirmed the construct preparation.

3.4.4 Preparation and validation knockout (PUFB-) strain by PCR

The knockout construct was linearized using KpnI/NotI restriction digestion (~4 Kb), eluted by gel extraction protocol and 2-10 µg of the linearized plasmid was transformed into Ax2 cells by electroporation method. Homologous recombination resulted in disruption of 2.62 Kb PUFB gene with the Blasticidin resistance (bsr) cassette. Following transformation, cells were selected on 2 µg mL⁻¹ of Blasticidin S and selected until 10 µg mL⁻¹. After 10-15 days clear plaques were picked and transferred to 1mL of HL5 media (containing 10 µg mL⁻¹ of Blasticidin S) in 24-well culture plates. Around 500 independent resistant clones were isolated and their cell lysate was used as a template to screen for positional integrants by PCR amplification. Figure

3.8: Schematic representation of various primers and a list of primer combinations used for the validation of positional integrant. Product size of the various PCR amplifications are mentioned in the table. 69 The schematic representation of various primers used for screening and the expected amplicon sizes are mentioned in Figure 3.8. Primer combinations to validate PUFB⁻ strain by PCR amplification were mentioned in figure 3.4. Reverse complement primers of the blasticidin cassette were denoted as P4 and P5, respectively. P1 and P8 are primers upstream to fragment 1 and downstream to fragment 2 in the genomic DNA, respectively. Positional integrants (PI) were screened by the primer combinations P1/P4 and P5/P8 to yield amplicon sizes of 2.2 Kb and 3.2 Kb, respectively (Figure 3.9). Four positive clones were obtained from the screening that showed almost similar growth and development phenotype. One of these clones was chosen and designated as PUFB⁻ for further studies. Figure 3.9: Screening of PUFB⁻ knockout strain by PCR amplifications. Confirmation of PUFB⁻ knockout strain by PCR from PUFB⁻ gDNA using various primer combinations; C: PUFB⁻ construct plasmid is used as control for the amplification of fragment 1+ Bsr and fragment 2+ Bsr (random integrants); Lane 1: Primer combination 2 and 4, amplicon size ~1.5 Kb; Lane 2: Primer combination 5 and 7, amplicon size ~2.4 Kb; Lane 3: Primer combination 1 and 4, amplicon size ~2.2 Kb; Lane 4: Primer combination 5 and 8, amplicon size ~3.2 Kb. [expected sizes are marked; M-DNA marker].

3.4.5 Confirmation of PUFB overexpressor (PUFBOE) and knockout strain (PUFB⁻) by mRNA levels Figure 3.10: mRNA levels of PUFB in different strains. Semi-quantitative RT-PCR of PUFB mRNA in the vegetative stage of Ax2, PUF⁻ and PUFBOE. (A) Gel picture showing PUFB mRNA levels and ig7 mRNA levels (internal control) in Ax2, PUF⁻ and PUFBOE cells. (B) Relative expression of PUFB mRNA in graphical form. [The values represent mean ± standard deviation; n=3]. mRNA expression pattern of PUFB in the vegetative stage of Ax2, PUFB⁻ and PUFBOE confirmed the creation of both knockout and overexpressor strains. There was negligible mRNA in PUFB⁻ strain while PUFBOE showed nearly 2-fold increase of PUFB mRNA (Figure 3.10).

3.4.6 Comparative cell proliferation and growth profile studies of Ax2, PUFB⁻ and PUFBOE strains To measure the cell proliferation rate in Ax2, PUFB⁻ and PUFBOE cells, fresh spores of these strains were inoculated in 90 mm petri-plates. A primary culture was inoculated from the cells of different strains. Log phase cells of all three strains were then diluted into a fresh medium at an equal density of ~5x10⁵ cells mL⁻¹ and monitored for 4- 5 days. Figure 3.11: Effect of overexpression and deletion of PUFB on cell proliferation as compared to the wild type cells. The graph represents comparative cell proliferation of wild type Ax2, PUFBOE, and PUFB⁻ cells. All strains were seeded at a density of 5x10⁵ cells mL⁻¹ and monitored over 5-6 days; doubling time was calculated at logarithmic phase. The PUFBOE cells showed slower cell proliferation as compared to other strains. [The values represent mean ± standard deviation; n=5). Ax2 and PUFB⁻ cells attained maximum cell density at 72 h while PUFBOE attained maximum cell density at 84 h. Wild type Ax2 cells acquired stationary phase at ~10.2x10⁶ cell density, PUFB⁻ acquired stationary phase at ~10.9x10⁶ cell density while PUFBOE acquired stationary phase at ~8.79x10⁶ cell density. We observed a slightly higher cell proliferation rate in PUFB⁻ cells as compared to the other strains, it reached a maximum cell density of ~10.9x10⁶ and thereafter decline phase was observed. PUFBOE showed slower proliferation rate throughout and reached a maximum cell density of ~8.79x10⁶ at 84 h, 12 h later than the Ax2

and PUFB- (Figure 3.11). Doubling time for Ax2, PUFB- and PUFBOE was found to be 12.66 ± 0.7 , 11.10 ± 0.35 , 18.34 ± 0.91 h, respectively. It shows that overexpression or knockout of PUFB gene leads to aberration in cell proliferation rate. Next, we wanted to know whether this aberration in cell proliferation was due to alteration in cell cycle or defect in pinocytosis and exocytosis.

3.4.7 Cell cycle analysis of PUFB mutants

To know if the aberration observed in the cell proliferation of PUFB- and PUFBOE was due to changes in the cell cycle, we checked for the percentage of cells in each phase of the cell cycle. To investigate the effect of PUFB mutation on the phases of cell cycle flow cytometry was used. For this, cells were fixed with 75% ethanol at a different time point (0-96 h) during cell cycle progression. Cells were then stained with PI (Propidium iodide) and subjected to analysis in flow cytometer. Figure 3.12: Cell cycle analyses in PUFB mutants. Cell cycle analyses were performed using FACS in wild type Ax2, PUFB^{OE}, and PUFB- cells at different time points. The bar graph represents the percentage of cells in G1, S and G2/M phases of the cell cycle at 0 h, 24 h, 48 h, 72 h and 96 h (The values represent mean \pm S.E.; n=3; Student t-test). We observed that the percentage of PUFB- cells present in the G1 phase of the cell cycle are significantly less when compared to wild type while in case of PUFBOE no significant difference was observed. During S-phase, PUFB- at the time point t24 and t48 showed a significant increase in the percentage of cells as compared to the wild type (Figure 3.12). This suggests that knockout of PUFB leads to an increase in cell proliferation possibly by suppressing G1 arrest and initiating the G1-S transition.

3.4.8 Endocytosis and exocytosis studies in PUFB mutants

Dictyostelium internalize particles and fluid by the process of endocytosis (also called macropinocytosis or cell drinking) that involves the function of the actin cytoskeleton. This is then surrounded by plasma membrane to form endosome which fuses with lysosome where internalized material is acted upon by various enzymes to digest it and undigested remnants are released outside by exocytosis (Hacker et al., 1997; Maniak et al., 1995). Thus we measure the pinocytosis rate of FITC dextran, which is a fluid phase marker. We inoculated 3×10^6 cells mL⁻¹ of Ax2, PUFB- and PUFBOE and kept it for 15 minutes under shaken condition then 2mg mL⁻¹ of FITC dextran was added and the samples were collected at different time points (0, 15, 30, 45, 60, 90, 120 and 180 minutes) to measure the intracellular fluorescence. The intracellular fluorescence was normalized with protein content to account for any differences in cell size. The maximum value of intracellular fluorescence was taken as 100 percent (for pinocytosis) and values at different time points were compared to it. We observed no significant difference in the pinocytosis rate of Ax2, PUFB- and PUFBOE cells. Figure 3.13: Pinocytosis and exocytosis analysis in Ax2 and PUFB mutants by using FITC- labeled dextran (A) For pinocytosis analysis, Ax2 and PUFB mutants strain at a cell density of 3×10^6 cells mL⁻¹ were incubated with FITC-dextran (2 mg mL⁻¹) and intracellular fluorescence of internalized fluorescent marker was measured at various time points using a spectrofluorimeter (excitation at 544 nm and emission at 574 nm). (B) Exocytosis analysis was done in all three strains by incubation of 3×10^6 cells mL⁻¹ with FITC-dextran for 3 h, washed and cell suspension was used to measure the fluorescence from the marker that remained in the cell at various time points (The values represents the average \pm standard deviation; n=3; experiments were carried out in triplicate). For exocytosis, 3×10^6 cells mL⁻¹ cells of different strains were subjected to incubation in FITC-dextran for 3 h followed by washing then cells were resuspended in the growth medium again. Samples were collected at different time points

(0, 15, 30, 45, 60, 90, 120 and 180 minutes) to measure the intracellular fluorescence. Percent fluorescence was determined by taking maximum fluorescence as 100% and the values at each time points were compared. PUFBOE cells showed an increase in intracellular fluorescence representing reduced exocytosis as compared to the wild type Ax2 while fluorescence in PUFB- appeared to be comparable to wild type cells. This result suggests that in PUFBOE pinocytosis is normally operating inside the cells i.e. there is no defect in the uptake of food but there is a defect in exocytosis process as the rate is slower [as compared to the wild type](#). Due to defects [in](#) exocytosis process, undigested remnants or other excretory products may not be released outside at a proper rate and accumulate inside the cells that could be toxic to the cells and this may lead to the decreased cell proliferation and growth. This could be the reason that the PUFBOE cells are slow proliferating. Cell proliferation and cell growth [are regulated independently](#) in Dictyostelium. [To determine the role of PUFB in regulating growth](#) (increase in [cell mass](#) or size) [we measured the cell mass of Ax2](#), PUFB- and PUFBOE. Increase in cell mass represents the increase in growth of cell over time due to which protein content of cell increases. The [average cell mass of Ax2 was](#) found to be 10.3 ± 0.33 mg while the PUFBOE showed a significant decrease in cell mass having 7.6 ± 0.33 mg. The average cell mass of PUFB- was observed to be 11 ± 0.57 mg (Figure 3.14A). The [average cell mass of PUFB- cells was insignificant as compared to Ax2 cells](#). In other words, this result suggests that PUFBOE cells accumulate less mass because of decreased cell growth while the non- significant increase in growth of PUFB- cells was observed. Figure 3.14: Cell dry weight and cell size analysis of PUFB- and Ax2, PUFBOE cells. (A) 5×10^7 cells of Ax2, PUFB- and PUFBOE were harvested for dry weight analysis. (B) Cell size analysis of Ax2, PUFB- and PUFBOE cells were done using BD FACS Calibur flow cytometer. [The values represent mean \pm standard deviation; **p < 0.01, ns- non-significant (Student's t-test); n=3]. Further to know whether PUFB- cells affect cell size, we performed flow cytometry analysis (Figure 3.14B). No significant difference between cell sizes of Ax2, PUFB- and PUFBOE was observed.

3.4.9 Comparative developmental profile study of Ax2, PUFB- and PUFBOE

To understand the role of PUFB in multicellular development, cells of mutant strains of PUFB i.e. PUFB- and PUFBOE [along with wild type were developed on NNA plates at a final density of](#) 5×10^7 cells mL⁻¹. After synchronization at 4°C for 4-6 h, the cells were allowed to develop at 22°C and pictures were taken at different time interval as shown in figure 3.15. Figure 3.15: Developmental profile of PUFB- and PUFBOE as compared to the wild type Ax2 cells. All the strain were grown till log phase ($\sim 3-5 \times 10^6$ cells mL⁻¹), washed and spotted on NNA [plates at a density of](#) $\sim 5 \times 10^7$ cell mL⁻¹ [and kept for synchronization](#) of development. Different developmental stages were photographed using Nikon- SMZ1500 microscope. The timings after starvation is also indicated. scale bar; 500 μ m [n=3]. Wild type Ax2 develop synchronously and start streaming at 4 h while in case of PUFB- and PUFBOE streaming did not occur till 4 h, suggesting a delay in the initiation of development of both the mutant strain. After 8 h of development wild type Ax2 cells formed tight aggregates while PUFB- and PUFBOE cells formed loose aggregate. The number of loose aggregates formed by the overexpressing strain was much less (~ 2.5 fold decrease) as compared to wild type and also in PUFB null strain number of loose aggregates formed were significantly lower (~ 1.5 fold decrease) (Figure 3.16B). Also, the size of loose aggregate formed by the PUFBOE cells are smaller (~ 4.5 fold decrease) [as compared to the](#)

wild type while in case of PUFB- cells, relatively larger aggregates (~1.3 fold increase) are formed (Figure 3.16A and C). Figure 3.16: Analysis of aggregate size in Ax2, PUFB- and PUFBOE strains (A) The image shows the complete spot of cells plated for development on NNA plate. (B) The graph shows the number of aggregates formed by each strain. (C) The graph representing the area of mounds in Ax2 PUFB- and PUFBOE cells. [The values represent mean \pm standard deviation; ***p < 0.001, **p < 0.01 (Student's t-test); n=3]. At 12 h in Ax2, the formation of slug began but in case of PUFB- and PUFBOE strains they were still in the mound stage suggesting the delayed development of the mutant strains during the initial part of the developmental life cycle. But as time progressed the mutant strain matched up to the developmental timing and formed slug at 16 h, comparable to the slug formed by wild type cells. The slugs formed by the overexpressor strain are smaller in size as compared to wild type Ax2 and PUFB- strain. Finally, they all culminated into the fruiting body at 24 h.

3.4.10 Morphological analysis of the fruiting bodies in Ax2 and PUFB mutants

Fruiting bodies formed by the overexpressing strain are smaller in size having relatively large sorus while PUFB null cells formed large fruiting bodies as compared to the wild type (Figure 3.17A). Figure 3.17: Morphological analyses of the fruiting bodies formed by PUFB mutants and its comparison with wild type cells. (A) Images showing the fruiting body of Ax2, PUFB- and PUFBOE strains. (B) The graph represents the stalk: sorus ratio of fruiting bodies formed by each strain (C) The graph represents the number of fruiting bodies formed by each strain. [The values representing mean \pm standard error (S.E.); the number of structures analyzed \sim 200; n = 3; Student t-test, p-value \leq 0.05, \leq 0.01 and \leq 0.001 has been represented as *, ** and ***, respectively]. Stalk /spore ratio of PUFB- was found to be 1.25 fold more than the wild type suggesting that PUFB- formed stalky fruiting body while in case of PUFBOE the ratio was found to be \sim 1.6 fold less than the wild type suggesting that the fruiting body formed by the PUFBOE had small stalk and relatively large sori (Figure 3.17B). The numbers of fruiting bodies formed by PUFB- (\sim 1.3 fold decrease) and PUFBOE (\sim 2.2 fold decrease) are lower in number as compared to the wild type (Figure 3.17C). Both PUFB- and PUFBOE mutant strains showed asynchronous development as all the structures formed during the intermediate stage of development did not culminate into fruiting bodies.

3.4.11 mRNA expression of genes involved in aggregate formation

Defects observed in the aggregation of PUFB mutants could be due to the number of cells that participate in the formation of multicellular structure, any alteration in cell adhesion, the counting mechanism that is responsible for controlling the aggregation size in Dictyostelium and intracellular as well as extracellular cAMP level (Jang et al., 2002; Jang and Gomer, 2008). Counting factor (CF), a 450 kDa complex is composed of about five polypeptides including Countin and CF50 that plays a major role in regulating the number of cells within the mounds. It regulates group size by down-regulating cell-cell adhesion proteins Gp24 (CadA) (Roisin-Bouffay et al., 2000). A gene called smlA which regulates the expression of CF as in the absence of smlA gene the level of CF increases, resulting in the formation of smaller aggregates and fruiting body than wild type (Brock et al., 1996; Brock and Gomer, 1999). Countin, a 40 kDa hydrophilic protein negatively regulates the aggregates size and cell adhesion. By regulating the number of cells that participates in the aggregate formation Countin regulates the size of aggregates. Elevated Countin levels cause breaking of aggregates that eventually results in small-sized fruiting bodies with less number of

spores per sorus (Spratt Jr and Haas, 1961). The mRNA level of *ctnA* was found to be high during early stages development in case of PUFBOE which contribute to the formation of small-sized aggregates and thus small sized fruiting bodies as well. In the case of PUFB- an expression of *ctnA* was low during the early stages of development, which leads to the formation of relatively large-sized aggregates as compared to Ax2 (Figure 3.18A). Figure 3.18: mRNA expression of genes involved in early development. The relative abundance of the various transcripts involved in the formation of aggregates during early development in wild type Ax2. PUFBOE and PUFB- were analyzed. (A) The relative abundance of *ctnA* in Ax2, PUFB- and PUFBOE cells (B) Relative abundance of *cadA* in Ax2, PUFB- and PUFBOE cells. (C) The relative abundance of *csA* in Ax2, PUFB- and PUFBOE [*ctnA*- CounTiN; *csA*- Contact Site A protein and *cadA*- Calcium-dependent Adhesion molecule A (V- Vegetative stage, LA- Loose aggregate, M- Mound, S- Slug, EC- Early Culminant, FB- Fruiting body). The values represent mean \pm standard deviation; *** $p < 0.001$, ** $p < 0.01$, * $p < 0.05$ (Student's t-test); n=4]. Two cell adhesion protein namely Gp24 (*CadA*) and Gp80 (*CsA*) that play an important role in regulating the size of the aggregates are expressed during early development. *CadA*, like Cadherins is calcium-dependent cell adhesion molecule. In *Dictyostelium* *CadA* gene codes for DdCAD-1, a calcium-dependent cell adhesion molecule. If *cadA* is deleted, it leads to a reduction in EDTA-sensitive cell adhesion, cell- type proportioning and pattern formation (Wong et al., 2002). The contact site A (*CsA*) glycoprotein is a Ca^{2+} -independent cell adhesion protein in *Dictyostelium discoideum*. Both *CadA* and *CsA* mediate EDTA-sensitive cell adhesion. It had been reported that the overexpression of *CsA* leads to the fragmentation of aggregates i.e. it causes aggregation stream to break up leads to the formation of small size aggregates (Faix et al., 1992). The expression of *CadA* mRNA in PUFB- was found to be significantly high in early developmental stages i.e. in loose aggregate and mound resulting in increased cell-cell adhesion and thus form the relatively large size aggregate while in case of PUFBOE the expression was significantly low as compared to wild type Ax2 (Figure 3.18B) suggesting that the cell-cell adhesion is low and thus form small-sized aggregates. The level of *CsA* in PUFB- was found to be significantly low in loose aggregate stage and leads to the formation of large sized aggregate along with the activity of *CadA*. While in other stages the decrease in *CsA* level was not significant. In PUFBOE the expression of *CsA* was observed to be high (Figure 18C) in the loose aggregate, mound resulting in the formation of small-sized aggregates.

3.4.12 Expression levels of spore coat proteins and spore viability in PUFB mutants As we observed that very less number of fruiting bodies formed by PUFB- and PUFBOE strains, we were interested to check the viability of spores formed by these mutants. Figure 3.19: Spore viability and mRNA expression of genes involved in development. (A) Spore viability of Ax2, PUFB- and PUFBOE strains. (B) RT-PCR analyses of spore coat gene (*cotA*) (C) RT-PCR analyses of spore coat gene *cotB* during the development of Ax2, PUFB- and PUFBOE using *ig7* as an internal control. [V- Vegetative, LA-Loose aggregate, M- Mound, S- Slug, EC-Early Culminant, FB- Fruiting body; n=3; Student t-test, p-value ≤ 0.05 , ≤ 0.01 and ≤ 0.001 has been represented as *, ** and ***, respectively]. The average spore viability of Ax2 was $88.25 \pm 3.025\%$ (Brock and Gomer, 2005; Myre et al., 2011). While the average spore viability of PUFB- and PUFBOE were significantly reduced to $70.25 \pm 1.7\%$ and $51.5 \pm 2.8\%$, respectively (Figure 3.19A). Therefore, it suggests that PUFB protein should be present in optimal concentration

for spore germination as very high or very low concentration of this protein reduces the efficiency of spores to germinate properly. This led us to investigate the expression of two proteins that are present specifically in spores, SP96 and SP70. *cotA* and *cotB* genes encode spore coat proteins SP96 and SP70, respectively that are expressed throughout the post-aggregation stages of development in *Dictyostelium* and are required for maintaining the integrity of spore coat. *cotA* expression is dependent on extracellular cAMP while cAMP-dependent protein kinase regulates the expression of *cotB* (Hopper et al., 1995). Deletion of *cotA* and *cotB* leads to reduced spore viability due to increased porosity of the spore coat (Fosnaugh et al., 1994). We analyzed the expression of *cotA* and *cotB* mRNA during the development of PUFB- and PUFBOE along with wild type Ax2. We found the expression of both *cotA* and *cotB* were significantly decreased in PUFB- and PUFBOE as compared to the wild type Ax2 cells (Figure 3.19B and C).

3.4.13 PUFB mutants show reduced cAMP signaling

As we observed that the development was delayed in both PUFB- and PUFBOE strains as compared to the wild type, it led us to investigate whether it involves any change in cAMP level. It is well known that cAMP and cell adhesion molecules are essentially required during the early development in *Dictyostelium discoideum*. The cAMP-mediated cell signaling and chemotaxis to cAMP (chemoattractant) are two important mechanisms that control aggregation in *Dictyostelium* (Manahan et al., 2004). Defects observed in the aggregation of PUFB- and PUFBOE may involve the alteration in cAMP signaling. For this, we measured cAMP levels in wild type Ax2 and both PUFB mutant strains. Cells from the logarithmic phase culture of Ax2, PUFB- and PUFBOE were starved for 0, 4 and 6 h and the levels of cAMP were measured by using cAMP Enzyme Immunoassay Kit. For the quantitative estimation of cAMP, this kit uses polyclonal 82 antibody specific to cAMP that binds to cAMP in a competitive manner. We harvested the samples and treated them with 0.1 M HCl and incubated at room temperature in 96 well plate coated with a secondary antibody. Thereafter, the substrate was added which gives a yellow colour that represents an inversely proportional relationship with the concentration of cAMP in the samples. Reading was taken at 405 nm and cAMP concentration (pmol mL⁻¹) was calculated as per the manufacturer's instructions. Optical density obtained from the standard and samples were used to plot the graph. Figure 3.20: cAMP level measurements in Ax2, PUFB- and PUFBOE cells. The graph shows intracellular cAMP levels in various strains. cAMP concentrations in PUFB- and PUFBOE cells upon starvation was reduced when compared to the wild type cells. [The values representing mean \pm standard error (S.E.); n = 3; Student t- test, p-value ≤ 0.05 , ≤ 0.01 and ≤ 0.001 has been represented as *, ** and ***, respectively; ns: non-significant]. It revealed that both the PUFB mutant strains showed a significant decrease in the cAMP level under starved condition. PUFB- showed ~ 1.3 fold decrease in cAMP level while PUFBOE showed ~ 1.5 fold decrease in cAMP level as compared to Ax2. Low levels of cAMP in both the PUFB mutant strains could be the possible reason for the delayed development. Low levels of cAMP slow down the chemotactic movement of cells and that could also be one of the possible reasons for the small-sized aggregates formed by the PUFBOE cells (Figure 3.20). Interestingly the levels reached to near normal by 6 h, suggesting that normal development may proceed thereafter.

3.4.14 Expression level of genes involved in the cAMP signaling

We further analyzed the expression of genes involved in cAMP signaling. In response to starvation, cells undergo cAMP-mediated chemotaxis in *Dictyostelium*.

83 cAMP signaling plays a very important role in the expression of genes required for aggregation and in the induction of post-aggregative differentiation in *Dictyostelium discoideum* (Kay, 1982; Schaap and van Driel, 1985). Under starvation condition conversion of ATP to cAMP by aggregation stage adenylyl cyclase (AcaA) leads to the release of extracellular cAMP that functions as a chemoattractant by binding to the high-affinity cAMP receptor (CarA) on the surface of neighboring cells that triggers chemotaxis, streaming and aggregation (Huber et al., 2017). To understand the cAMP signaling in PUFB mutant strains, we analyzed the mRNA expression pattern of *acaA* (adenylyl cyclase), *carA1* (cyclic AMP receptor1) and *pdsA* (extracellular cAMP phosphodiesterase) genes. Figure 3.21: mRNA expression of genes involved in cAMP signaling. (A) The relative abundance of *acaA* in Ax2, PUFB- and PUFBOE cells. (B) The relative abundance of *carA1* in Ax2, PUFB- and PUFBOE - cells and (C) Relative abundance of *pdsA* in Ax2 PUFB- and PUFBOE cells. [V- Vegetative, LA-Loose aggregate, M-Mound, S- Slug, EC-Early Culminant, FB- Fruiting body. The values represent mean \pm standard deviation; *** $p < 0.001$, ** $p < 0.01$, * $p < 0.05$; (Student's t-test); n=4]. The mRNA expression of *acaA* and *carA* was found to be significantly low during the initial stages of development in both PUFB- and PUFBOE mutant strains responsible for the delay in development and also less number of aggregate formation 84 (Figure 3.21A and B). Low levels of *acaA* and *carA* cause low cAMP levels during culmination stage, which results in the reduced viability of spores formed by PUFB- and PUFBOE mutant strains. The cAMP level is further regulated by a cAMP phosphodiesterase (PdsA) which is responsible for the degradation of extracellular cAMP (Darmon et al., 1978). We checked the expression pattern of PdsA in both PUFB mutant strains. We found the expression was significantly high only in loose aggregates while in other stages its expression is non-significantly high in PUFB-. While in case of PUFBOE no significant difference was observed (Figure 3.21C) when compared to wild type, which could be because the level of cAMP is already less so it further does not need to be down regulated so that a certain level of cAMP is maintained to complete the development process.

3.5 CONCLUSIONS

As discussed earlier, PUFB is expressed in both growth and development. So it is expected to have a role in both cell proliferation and development of *Dictyostelium discoideum*. In this chapter, we have characterized the PUFB by successfully creating overexpressor and knockout strains. The PUFBOE strain was successfully created by expressing full length PUFB gene under constitutive actin15 promoter fused with an eYFP reporter gene. This was confirmed by mRNA expression and microscopy studies. PUFB fusion protein showed localization in the cytosol. On the other hand knockout of PUFB was also successfully made by gene disruption method, which was confirmed by various PCR and mRNA expression studies. Both PUFBOE and PUFB- strains were further used to study the growth and development in *Dictyostelium discoideum*. Cell proliferation and cell growth studies were performed and found that PUFB- strain showed an increased proliferation rate as compared to wild type and cell cycle analysis showed that it could be possibly by suppressing G1 arrest and initiating the G1-S transition. While PUFBOE strain showed decreased proliferation rate as compared to the wild type. Any significant difference was not observed during the cell cycle but showed defects in exocytosis rate, which was found to be reduced as compared to wild type suggesting that reduced exocytosis leads to increased accumulation of undigested remnants which may cause toxicity to the cells affecting both cell proliferation and cell growth of PUFBOE cells. We

also showed cell growth analysis in which the cell mass of PUFBOE was found to be significantly low as compared to Ax2 and PUFB- strain suggesting decreased cell growth of PUFBOE cells. We showed that mutation of PUFB leads to defects in the multicellular development of Dictyostelium. We observed that there was a defect in the aggregation size determination mechanism as PUFBOE strain formed very less number of [small-sized aggregates as compared to the wild type](#) while PUFB- strain formed less number of relatively large size aggregates. And this defect was found to be because of misregulation of certain genes involved in aggregation. In PUFBOE less number of [small-sized aggregates](#) formation was [due to](#) increased expression of [Countin](#) and csA, [a cell adhesion molecule and](#) lower [expression of](#) cadA another cell adhesion molecules. While in case of PUFB-, countin and csA expression was found to be low and lower expression of cadA leads to relatively large-sized aggregates. Because of the mutation of PUFB, defect in cAMP signaling was observed as the levels of cAMP was low in both the mutant strains and also there was misregulation of cAMP signaling mRNA of acaA, carA was observed. Due to this development of both the strains are delayed and also contribute to defects in aggregation size and number. Formation of the fruiting body is one of the important aspects in the life cycle of Dictyostelium to maintain their generation. We found an alteration in the morphology of fruiting body as PUFB- forms large fruiting bodies while PUFBOE forms a smaller fruiting body having a small stalk and relatively large sorus. Also, the spore viability of both the mutant strains was found to be significantly low because of the reduced expression of cotA and cotB. It suggests that an optimum level of PUFB protein is required for the efficient spore formation. Thus, our study suggests the important role of PUFB during growth and development by regulating the expression of genes important in [growth and development of Dictyostelium discoideum](#).

4.1 INTRODUCTION

[Dictyostelium cells](#) exist as a unicellular haploid amoeba/myxamoeba that via phagocytosis feed on bacteria and grow vegetatively through mitotic division (binary fission). Starvation is the major factor that triggers the vegetative unicellular cells towards multicellular development and leads to the expression of a variety of new genes, which are responsible for chemotaxis both towards folic acid (factors from bacteria) and cAMP. Each and every amoeba can sense the cAMP, respond by releasing cAMP and leads to the signal amplification and relay. In response to cAMP, millions (10, 000-1, 00, 000) of highly polarized chemotactic amoeba undergo head to tail streaming to a common point to form a multicellular structure called loose aggregate (Kimmel and Firtel, 1991). From this very stage onwards differentiation of cell into prestalk and prespore cells starts in response to cAMP signaling and cell-specific gene expression can be observed (Araki et al., 1997). Cellular movements in the mound stage lead to the formation of distinct prestalk (having prestalk cells) and prespore zones (having prespore cells). Some cells at the tip-organizer secretes cAMP due to which pstA and pstO cells move towards the tip and leads to the formation of tipped-mound (Dormann and Weijer, 2001). Reports suggest that deletion of Disintegrin family proteins that are crucial for differential cell adhesion and movement of prestalk cells leads to defects in cell sorting and cell-type specific patterning (Varney et al., 2002). Migrating slug has been considered as the best stage to study pattern formation as the two specified prestalk and prespore forms a typical pattern [where the anterior is composed of prestalk cells and the posterior is composed of prespore](#). Prestalk [cells](#) show expression of specific marker genes, ecmA and ecmB. PstB cells express ecmB gene.

PstAB cells express both *ecmA* and *ecmB* genes (Jermyn et al., 1987). Prestalk cells expressing both *ecmA* and *ecmB* are present in the core of anterior region called pstAB cells (Gaskell et al., 1992). During culmination, it moves to the posterior position of the fruiting body forming the stalk region that makes the basal disc (Ceccarelli et al., 1991). Prespore cells express *cotB* gene (Fosnaugh and Loomis, 1993), the prespore region consists of *pstA*, *pstB* and ALCs (anterior-like cells).

Figure 4.1: Diagrammatic representation of morphogenesis and cell differentiation in Dictyostelium. Spatial expression pattern of different prestalk and prespore cell- types in the slug, early culminant and fruiting body. Different cells are shown as blocks of colour. The fate of different cells in various multicellular structures are shown (adapted from Jermyn et al., 1996) Various studies suggest the important role of PUF protein in the differentiation and patterning of organisms. In *Drosophila*, PUF protein is responsible for maintaining the anterior-posterior patterning of embryo where mutation of this gene leads to the abnormal segmentation of the early embryo (Barker et al., 1992; Lehmann and Nüsslein-Volhard, 1987). In *C. elegans*, PUF protein is responsible for maintaining spermatogenesis to oogenesis transition (Zhang et al., 1997) and also for maintaining the pool of Germline stem cell (Shin et al., 2017). In *Arabidopsis thaliana*, it plays a role in the growth and development, morphogenesis of leaves (Huang et al., 2014; Reichel et al., 2016). In Dictyostelium, patterning and cell-type differentiation plays a crucial role in the multicellular development and terminal differentiation into the fruiting body and as discussed above the role of PUF in cell differentiation and patterning. So in this chapter, we would explore the functions of PUF in cell-type differentiation and patterning of this organism. As discussed in the previous chapter that mutation in PUF leads to aberrant development and multicellular structures formed, thus we hypothesized that this defect would be due to the improper proportioning of the cells or alteration in the prestalk to the prespore ratio of cells.

4.1.1 Cell death and autophagy in Dictyostelium

In the life cycle of Dictyostelium, starvation-induced multicellular development leads to the formation of the fruiting body which is composed of [dead vacuolated stalk cells and](#) live [spore cells](#) (Schaap et al., 1981; Whittingham and Raper, 1960). Since in Dictyostelium cell death by apoptosis does not occur because of the absence of caspases or metacaspases (Eichinger and Noegel, 2003), thus cell death by means of developmental programmed cell death is the only process that leads to the formation of stalk cells (Laporte et al., 2007). Dictyostelium can undergo either autophagic or necrotic cell death depending upon the environmental conditions (Kosta et al., 2004; Laporte et al., 2007; Levraud et al., 2003). *D. discoideum* has been considered as a good model system for caspase-independent cell death or developmental autophagic cell death (ACD) which occurs in the absence of apoptosis. Starvation induces the Atg1 required for autophagosome formation (De Chastellier and Ryter, 1977; Tresse et al., 2007) and DIF promotes the stalk cell differentiation (Town et al., 1976; Town and Stanford, 1979) are the two mechanisms in Dictyostelium on which ACD depends. Figure 4.2: Autophagy signaling pathways of Dictyostelium. Phagophore engulfs the cytoplasmic materials, which then fuse with the lysosome, to degrade the cytoplasmic materials and then recycled for later utilization. Role of Dictyostelium autophagy proteins in this signaling process hypothesized (Calvo- Garrido et al., 2010). TOR (target of rapamycin) regulates autophagy in Dictyostelium. It belongs to the serine/threonine kinase family made up of TOR, Kog1 (Raptor) and Lst8. It functions upstream of Atg1 complex and regulates

cell metabolism and cell growth (Mizushima, 2010; Schmelzle and Hall, 2000). TORC1 And TORC2 are the two complexes formed by TOR after interacting with different proteins and it is TORC1, which is involved in autophagy. It regulates autophagy via the phosphorylation of Atg13 and Atg1 or through a signal transduction pathway with other proteins (Figure 4.2) (He and Klionsky, 2009). Autophagic mutants in Dictyostelium show aberrant development as it does not aggregate normally and forms defective fruiting bodies (Otto et al., 2004). In mammalian cells, Atg8 (known as LC3 in mammals) is present in phagophore membrane in cytosolic form and on autophagosome present in the lipidated form. The conversion of LC1 to LC3 is used to study the process of autophagic flux while in Dictyostelium it is difficult to interpret autophagic induction as Atg8 can be observed in one form only. Dictyostelium Atg1 [is a serine/threonine protein kinase](#) having a conserved kinase [domain and](#) conserved [C- terminal domain that is essential for the](#) induction and development of autophagosome. DdAtg1 and DdAtg8 colocalize on the autophagosome and recruit other proteins to the assembly site, which is required for the induction and maturation of autophagosomes (Tekinay et al., 2006). DdAtg8 is an ubiquitin-like protein used as an autophagosome marker to study autophagic induction as it is attached to the autophagosome membrane upon lipidation by phosphatidylethanolamine (PE) (Mizushima et al., 2010). Autophagy can be monitored using GFP-Atg8 as a marker where GFP-Atg8 puncta represent the autophagosome formation and autophagy defect can be studied by monitoring variation in the GFP-Atg8 puncta formation (Klionsky et al., 2008). In Dictyostelium ubiquitin-like protein conjugation system is formed by Atg5, Atg12 and Atg16 along with Atg8 and is required for the expansion of phagosome membrane into autophagosome (Webber et al., 2007; Calvo-Garrido et al., 2010). Interaction between Atg18 and Atg2 is mediated by phosphatidylinositol 3- phosphate, which is essential for the recruitment of other autophagic proteins to the assembly site and for autophagy to proceed. 90 Since Dictyostelium is a good model system to study autophagy and there are no reports of autophagy related to PUF proteins so we were interested to know its role in the autophagy process. Based on the above information we laid down the following objectives for this chapter.

4.2 OBJECTIVES

Ø? To explore the role of PUFB in cell-type differentiation and patterning. Following strains were prepared in Ax2 and PUFB-cells:

- Ax2 cells: ecmA-lacZ/Ax2, ecmB-lacZ/Ax2, ecmO-lacZ/Ax2, ecmAO-lacZ/Ax2 and pspA-lacZ/Ax2.
- PUFB- cells: ecmA-lacZ/PUFB-, ecmB-lacZ/PUFB-, ecmO-lacZ/PUFB-, ecmAO-lacZ/ PUFB- and pspA-lacZ/PUFB-.

Ø? Exploring the role of PUFB in cell-lineage tracing in Dictyostelium by making chimeras. To perform this study act15-GFP/Ax2 and act15-RFP/ PUFB- strains were prepared.

Ø? To purify the PUFB protein from Dictyostelium via nickel affinity column and look for its interacting partners. Since we could not purify the protein next objective was proposed.

Ø? To explore the role of PUFB in the autophagy process by performing the autophagic flux study and expression level of different genes involved in the autophagy. To achieve this objective Ax2 and PUFB- cells were transformed with RFP-GFP- Atg8 to study autophagic flux.

4.3 MATERIAL AND METHODS

4.3.1 Storage of Dictyostelium spores

Dictyostelium Ax2 cells were grown in HL5 medium at 22 °C and developed on SM agar plates to form fruiting bodies. Spores from sorus of fruiting bodies were collected in spore storage solution (pre-chilled) having 0.45 mL H-50 buffer, 0.1 mL DMSO and 0.45 mL horse serum. Aliquots of spore suspension were stored in eppendorf tubes, slow freeze at -20°C for 1-2 h and finally stored in

-80°C until further use. 4.3.2 mRNA expression analysis of cell-type specific marker using semi-quantitative RT-PCR Log phase Ax2 and PUFB- cells were developed on NNA plates at an equal cell density of 5×10^7 cells mL⁻¹. Various multicellular structures at different stages/timings were collected and RNA isolation was done as mentioned in chapter 3. cDNA was prepared using Verso cDNA synthesis kit and further used for semi-quantitative RT-PCR of the cell-type specific marker genes. Expression analyses of mRNA levels of the cell-type specific marker genes ecmA, ecmB and d19 were done using specific primer combinations as mentioned in Table 4.1 Table 4.1: List of primer combinations used for the semi-quantitative RT-PCR expression analyses of cell-type specific markers. It shows the genomic positions of primers used for expression analysis of ExtraCellular Matrix protein (ecmA), ExtraCellular Matrix protein (ecmB), PreSpore-specific gene A (pspA); expected amplicons sizes in bp from cDNA and gDNA are mentioned.

4.3.3 β - galactosidase staining in multicellular structure for cell type patterning studies Cell-type patterning using β - galactosidase staining was performed as mentioned by Gosain et al. (2012) with slight modifications from the protocol described by Escalante and Sastre (2006). The log phase cells of wild type Ax2 and PUFB- cells were transformed with cell-type specific prestalk marker genes like ecmA, ecmB, ecmO and ecmA0 and fused to LacZ reporter. Also, transformed with cell-type specific prespore marker gene pspA (d19) fused to LacZ reporter. Log phase cells (3- 5×10^6 cells mL⁻¹) expressing ecmA, ecmB, ecmO, ecmAO and pspA (d19) fused to LacZ reporter from Ax2 and PUFB- were collected and washed with 1xKK2 buffer (ice cold) and resuspended in 1xKK2 at an equal cell density of 5×10^7 cells mL⁻¹. Cell suspension of Ax2 and PUFB- were spotted (15-20 μ L) on dialysis membrane placed on 1.5% non-nutrient agar plates. Cells were kept at 22°C to develop and form various multicellular structures that were 92 collected in 24 well plates. Various developmental structures collected on dialysis membrane were fixed with methanol at room temperature for 30 minutes. Structures were then washed twice with Z buffer to remove the methanol completely and incubated for 1 h in permeabilization buffer containing 0.1% NP40 in Z-buffer. This was followed by washing the structures with Z-buffer for 2-3 times and staining the structure using staining solution containing X-gal (20 mg mL⁻¹), potassium ferrocyanide (133 mM) and potassium ferricyanide (133 mM). Colour reaction was stopped after evident staining was observed in structures by washing the structures with Z buffer for 2-3 times. Images of stained structures of Ax2 and PUFB- were captured using Nikon AZ100 microscope.

4.3.4 Development of chimeras of Ax2 cells tagged with GFP and PUFB- cells tagged with RFP Log phase Ax2 cells tagged with GFP and PUFB- tagged with RFP were collected, washed with ice-cold 1xKK2 buffer twice and resuspended in 1xKK2 buffer at a cell density of 1×10^6 cells mL⁻¹. Cells from each strain were then mixed in various proportions (10% to 100%), collected by centrifugation at 3000 rpm for 2-3 minutes, washed with ice-cold 1xKK2 and resuspended in 1xKK2 to a final dilution of 5×10^7 cells mL⁻¹. Cell suspensions in various proportions were then spotted (15-20 μ L) on 1.5% NNA plates and kept at 22°C to develop. Developmental structures formed by mixing of tagged Ax2 and PUFB- cells in various proportions were observed at different developmental timings and photographed (both DIC and fluorescent images) using Nikon SMZ1500 microscope.

4.3.5 Spore count from fruiting bodies developed from the chimeras Fruiting bodies formed from chimeras of Ax2 cells tagged with GFP and PUFB- tagged with RFP in various proportion from 10% to

100% were used for spore count by picking spore-heads from the individual fruiting body on a glass slide. Spores were visualized under Nikon eclipse 80i fluorescence microscope and photographed using DIC, TRITC and FITC filter to count the number of red and green fluorescent spore. 10– 15 fruiting bodies from each proportion per experiment were counted.

4.3.6 mRNA levels of autophagy-related genes in wild type Ax2 and PUFB- cells cDNA was prepared using Verso cDNA synthesis kit (Thermo Scientific) as mentioned earlier and semi-qualitative RT-PCR was carried for various genes that are involved in autophagy like atg1, atg5, atg18, and atg8. The specific primer combinations used are mentioned in Table 4.2 Oligo Name Primer Sequence (5'.....3') Genomic Position Expected amplicon cDNA size(bp) Expected amplicon gDNA size(bp)

Oligo Name	Primer Sequence (5'.....3')	Genomic Position	Expected amplicon cDNA size(bp)	Expected amplicon gDNA size(bp)
atg1 RT	FP: ATGAAACGAGTAGGAGAT	1001-1018	1768-1788	661 788
atg8 RT	FP:ATGTATCAAGCTTTAAAAACGACCAC			
atg5 RT	FP:ATGTCATTTGACGAA RP:GGGTATGATTGGAAATGAAC	1001-1018	1599-1618	494 618
atg16 RT	FP: ATGTTTTTCATCACAAAATAA			
atg18 RT	FP:ATGAATGTTGGAGGTAAATT RP:TACTATGAATGATTGCAGGT	1001-1020	1901-1920	685 920

Table 4.2: List of primer combinations used for semi-quantitative RT-PCR analyses of autophagy-related genes. Expected amplicon sizes of cDNA and gDNA are mentioned.

4.3.7 Analysis of autophagic flux using RFP-GFP-Atg8 assay Autophagic flux was measured in both wild type Ax2 cells and PUFB- cells that were transformed with plasmid containing tandemly fused RFP-GFP-Atg8, selected on antibiotic (G418) ([Calvo-Garrido et al., 2011](#); [Lohia et al., 2017](#)). Autophagic flux was analysed by confocal microscopy under different stimuli like control, starvation for 4 h and treatment with 100 mM NH₄Cl (lysosomotropic agent) for 4 h in both wild type Ax2 cells and PUFB- cells. Autophagic flux was calculated by counting the number of fluorescent puncta formed per cell in both the samples. For preparation of starvation sample, log phase cells from both wild type Ax2 cells and PUFB- cells were collected by centrifugation at 3, 000 rpm for 3 minutes in 1x KK2 at 22°C and incubated for 4 h at 22°C under shaken conditions (120 rpm). For preparation of NH₄Cl treated sample, harvested wild type Ax2 cells and PUFB- cells were resuspended in HL5 media at a cell density of 1x10⁶ cells mL⁻¹ and 1 mL of cell suspensions were placed in a sterile 6-well plate. 100 mM NH₄Cl was added twice to the cells at an interval of 2 h and incubated at 94 22°C. The NH₄Cl treated cells from each well were collected by centrifuged at 3, 000 rpm for 3 minutes. Treated as well as control samples were placed on thin layer of 1% agarose slides for visualization under Nikon confocal microscope using Andor iQ 2.7.1 software. The fluorescent puncta (Red or Green)/cell were analyzed by NIS Elements AR version 4.0.

4.4 RESULTS AND DISCUSSION 4.4.1 Cell-type differentiation and patterning in PUFB- Till there is surplus food, Dictyostelium cells grow and divide mitotically but as food becomes limited they initiate multicellular developmental. In response to cAMP, Dictyostelium cells move towards each other to form aggregates (Kay, 1982; Loomis, 1993). During multicellular development cell differentiation in Dictyostelium occurs forming prestalk and prespore cells which finally forms terminally differentiated stalk and spore cells, respectively. Thus, during development, cAMP signaling plays a crucial role in cellular differentiation and pattern formation (Bretschneider et al., 1997; Louis et al., 1994; Williams, 1995). The differentiated cell-types show characteristic expression patterns of specific marker genes and during

development, the ratio of prestalk and prespore cells remain constant regardless of the size of the slug and any alteration in this leads to the aberrant differentiation (Chung et al., 1998; Jaffer et al., 2001). Prestalk cells are distinguished by the expression of two specific markers, ecmA and ecmB (extracellular matrix) (Jermyn et al., 1987). PstA (ecmA-expressing prestalk cells) cells are scattered in the aggregate but during mound stage, it migrates upwards forming the tip. PstB (ecmB-expressing cells) cells are present in the basal region of the mound while the prespore cells are present in the posterior region of slug except at the base and the tip region (Williams et al., 1989). To elucidate the role of PUFB in cell-type differentiation and patterning, cell-type specific marker expression studies were performed by RT-PCR and lacZ reporter assay during the development of Ax2 and PUFB- cells. We analyzed the mRNA levels of prestalk specific marker (ecmA and ecmB) and prespore specific marker (pspA or d19) using specific primer combinations (Table 4.1). The mRNA expression level of prestalk-specific gene ecmA in PUFB- shows a significant increase from the mound stage to the fruiting body as compared to the wild type Ax2. The mRNA expression level of the prespore marker, pspA was significantly reduced during later stages of development but in mound stage, it showed an insignificant decrease in PUFB- cells as compared to wild type Ax2 cells (Figure 4.3). To substantiate our results, we examined the spatial cell-type patterning in both Ax2 and PUFB- cells by using cell-type specific promoters fused to LacZ reporter. Figure 4.3: mRNA expression analysis of cell-type-specific marker genes during the development of Ax2 and PUFB- cells. Relative abundance of cell-type specific genes (A) ecmA (ExtraCellular Matrix protein A), (B) ecmB (ExtraCellular Matrix protein B) and (C) d19 (pspA; PreSPore- specific gene during developmental stages of Ax2 and PUFB- was analyzed using RT-PCR after normalization to ig7. [V: vegetative; LA: loose aggregate; M: mound; EC: early culminant; FB: fruiting body. The values represent Two way ANOVA, p-value ≤ 0.05 , ≤ 0.01 and ≤ 0.001 has been symbolized as *, ** and ***, respectively; n=3]. Spatial expression pattern study of ecmA/lacZ The wild type Ax2 cells were transformed with prestalk-specific ecmA promoter fused to LacZ reporter gene and selected at 40 $\mu\text{g mL}^{-1}$ of G418 and the PUFB- cells were transformed with the same and selected at 40 $\mu\text{g mL}^{-1}$ of G418 and 10 $\mu\text{g mL}^{-1}$ of Blasticidin S. Various multicellular structures formed during development were collected in 24 well culture plates and fixed in methanol. Structures were permeabilized and stained with X-gal to analyze the staining pattern in both strains (Figure 4.4). In case of Ax2, the expression in slug was found to be at the tip, which is formed by the prestalk cells and also in the fruiting body the expression was present in the anterior prestalk region (Figure 4.4 a & a'). In PUFB- the staining region in slug was found expanded as compared to Ax2 while in case of the fruiting body the staining was present in the anterior prestalk region which is found to be expanded. Staining was also present in the lower cup, stalk and basal disc as compared to wild type (Figure 4.4). In all the structures developed staining was found to be more pronounced than the wild type as is also revealed by RT-PCR. Figure 4.4: Expression pattern of prestalk specific marker ecmA/lacZ in wild type Ax2 and PUFB- multicellular structures. Wild type Ax2 cells and PUFB- were transformed with ecmA/lacZ and developed on dialysis membrane placed on NNA plates. Structures were collected, fixed with methanol and X-gal staining of ecmA/lacZ in wild type Ax2 and (a and b) and PUFB- (a' and b') in the multicellular structure was performed. Structures were visualized and photographed under Nikon AZ100

microscope. [slug (a-a'), Fruiting body(b-b'); Scale bar- 50 μ m; n=3]. Spatial expression pattern study of ecmB/lacZ The wild type Ax2 cells were transformed with prestalk-specific ecmB promoter fused to LacZ reporter gene and selected at 40 μ g mL⁻¹ of G418 and the PUFB- cells were transformed with the same and selected at 40 μ g mL⁻¹ of G418 and 10 μ g mL⁻¹ of Blasticidin S. Various multicellular structures formed during development were collected in 24 well culture plates and fixed in methanol. Structures were permeabilized and stained with X-gal to analyze the staining pattern in both strains (Figure 4.4). Figure 4.5: Expression pattern of prestalk specific marker ecmB/lacZ in wild type Ax2 and PUFB- multicellular structures. Wild type Ax2 cells and PUFB- were transformed with ecmB/lacZ and developed on dialysis membrane placed on NNA plates. Structures were collected, fixed with methanol and X-gal staining of ecmB/lacZ in wild type Ax2 (a-c) and PUFB- (a'-c') in the multicellular structure was performed. Structures were visualized and photographed under Nikon AZ100 microscope. [Slug (a-a'), Early culminants (b-b'), Fruiting bodies (c-c'); Scale bar- 50 μ m; n=3]. We observed that in Ax2 the expression of ecmB was present at the anterior region of the slug while in the early culminant and culminant there was staining in the upper and lower cups and was also present throughout the stalk and base (Figure 4.5 a-c). In case of PUFB-, no noticeable difference in the spatial localization of ecmB was observed as was also observed in RT-PCR analysis (Figure 4.4 a'-c'). Spatial expression pattern study of ecmO/lacZ The wild type Ax2 cells were transformed with prestalk-specific ecmO promoter fused to lacZ reporter gene and selected at 40 μ g mL⁻¹ of G418 and the PUFB- cells transformed with the same were selected at 40 μ g mL⁻¹ of G418 and 10 μ g mL⁻¹ of Blasticidin S. Various multicellular structures formed during development were collected in 24 well culture plates and fixed with methanol. Structures were permeabilized and stained with X-gal to analyze the staining pattern. Figure 4.6: Expression pattern of prestalk specific marker ecmO/lacZ in wild type Ax2 and PUFB- multicellular structures. Wild type Ax2 cells and PUFB- were transformed with ecmO/lacZ and developed on dialysis membrane placed on NNA plates. Structures were collected, fixed with methanol and X-gal staining of ecmO/lacZ in wild type Ax2 (a and b) and PUFB- (a' and b') in the multicellular structure was performed. Structures were visualized and photographed under Nikon AZ100 microscope. [Slug (a-a'), Fruiting body (b-b'); Scale bar- 50 μ m; n=3]. We observed that the ecmO/lacZ expression in wild type Ax2 slug was present at the neck region in the anterior prestalk region while expression is also present at towards the posterior basal region. In PUFB- an expression of ecmO/lacZ in the slug stage was expanded more towards the prespore region while the expression was absent at the base in the posterior region. In Ax2, the fruiting body shows the expression of ecmO in the anterior region and also in the stalk region. While in PUFB- the staining was present at the anterior prestalk region extending towards the tip while in the stalk region staining was present as comparable to the wild type (Figure 4.6). Spatial expression pattern study of ecmAO/lacZ The wild type Ax2 cells were transformed with prestalk-specific ecmAO promoter fused to lacZ reporter gene and selected at 40 μ g mL⁻¹ of G418 and the PUFB- cells transformed with the same were selected at 40 μ g mL⁻¹ of G418 and 10 μ g mL⁻¹ of Blasticidin S. Various multicellular structures formed during development were collected in 24 well culture plates and fixed with methanol. Structures were permeabilized and stained with X-gal to analyze the staining pattern in both Ax2 and PUFB- cells. The ecmAO/lacZ expression was present in the anterior prestalk region

covering the tip [and](#) neck region of slug in Ax2 while in case of PUFB- this region was further 99 extended. Expression was also found in the rear-guard region of PUFB- slug as compared to Ax2 slug. Fruiting body shows the expression of ecmAO in the anterior region, lower cup and stalk region in Ax2 while PUFB- shows a similar type of expression (Figure 4.7). Figure 4.7: Expression pattern of prestalk specific marker ecmAO/lacZ in wild type Ax2 and PUFB- multicellular structures. [Wild type Ax2 cells](#) and PUFB- [were transformed with](#) ecmAO/lacZ [and](#) developed on dialysis membrane placed on NNA plates. Structures were collected, fixed with methanol and X-gal staining of ecmAO/lacZ in wild type Ax2 (a and b), and PUFB- (a' and d') in the multicellular structure was performed. Structures were visualized and photographed under Nikon AZ100 microscope. [Slug (a-a'), Fruiting body (b-b'); Scale bar- 50 μ m; n=3]. Spatial expression pattern study of pspA/lacZ The [wild type Ax2 cells were transformed with](#) prespore-specific pspA promoter fused to lacZ reporter gene and selected at 40 μ g mL⁻¹ of G418 and the PUFB- cells transformed with the same were selected at 40 μ g mL⁻¹ of [G418 and 10 \$\mu\$ g mL⁻¹ of Blasticidin S](#). Various [multicellular structures](#) formed during development [were collected](#) in 24 well culture plates and fixed with methanol. Structures were permeabilized and stained with X-gal to analyze the staining pattern in both Ax2 and PUFB- cells Figure 4.8: Expression pattern of prestalk specific marker pspA/lacZ in wild type Ax2 and PUFB- multicellular structures. [Wild type Ax2 cells](#) and PUFB- [were transformed with](#) pspA/lacZ [and](#) developed on dialysis membrane placed on NNA plates. Structures were collected, fixed with methanol and X-gal staining of pspA/lacZ in wild type Ax2 and (a and b), and PUFB- (a' and b') in the multicellular structure was performed. Structures were visualized and photographed under Nikon AZ100 microscope. [Slug (a-a'), Fruiting body (b-b'); Scale bar- 50 μ m; n=3]. In Ax2, the lacZ staining of pspA showed the expression of pspA primarily localized in the prespore region of slug while in the fruiting body it is located in the sorus. In case of PUFB- the expression of pspA [was present in the prespore/spore region of](#) both slug and fruiting body but the expression was less than the wild type (Figure 4.8), also suggested by the RT-PCR analysis in figure 4.1. The staining was observed only in the posterior region of prespore suggesting that the boundary between the prestalk and prespore was lost in the slugs developed. Our results suggest the important role of PUFB- in maintaining distinct boundaries between the two cell-type during development and differentiation of Dictyostelium. PUFB mutant showed misregulation of some of the prestalk marker suggesting that there is a defect in the normal prestalk cell-type patterning and this is due to the disturbed prestalk/prespore ratio that leads to loss of clear boundaries in PUFB- structures. As we observed that in PUFB- the multicellular structures formed showed the aberration in the prespore region and prestalk region which resulted in the [fruiting bodies](#) formed [with small sori and long](#) stalk due to reduced prespore region suggesting the role of PUFB- in cell-type differentiation, proper proportioning of prestalk/prespore ratio and patterning during multicellular development in Dictyostelium.

4.4.2 Cell lineage tracing by chimera formation of GFP marked Ax2 cells and RFP marked PUFB- cells

In order to have a better understating of cell lineage tracing and the fate of PUFB- cells in the chimeras cell-mixing experiments were performed. Structures formed by mixing two or more types of cells from different genetic backgrounds are called chimeras. Wild type Ax2 cells tagged with GFP and PUFB- cells tagged with RFP in different proportions to form chimeras. Chimera study in various organisms revealed that under the influence of various

factors and differential gene expression, cells show 101 differential preferences in cell patterning resulting in aberrant development and mislocalization during cell differentiation. Figure 4.9: GFP tagged Ax2 cells and RFP tagged PUFB- cells in the pure populations (100%) in slugs and fruiting bodies. Wild-type, Ax2 cells expressing GFP and PUFB- cells expressing RFP were used as controls. (A) Multicellular structures formed by Ax2 cells expressing GFP in pure population. (B) Multicellular structures formed by PUFB- cells expressing RFP in pure population. [DIC image – (a`-d`), TRITC image (c and d) and images capture in FITC image (a-b); Slug stage (a-a` and c-c`); and Fruiting body (b-b` and d-d`); Scale bar- 50 μ m; n=3]. For the chimera studies, multicellular structures formed by 100% GFP marked Ax2 cells and 100% RFP marked PUFB- cells were used as controls (Figure 4.9 A, B). RFP tagged PUFB- cells and GFP tagged Ax2 cells were mixed in various ratios (10 to 90%) and cell suspensions of equal densities (5×10^7) were prepared in 1xKK2 buffer, spotted on NNA plates and allowed to develop at 22°C. The various developmental structures formed by the chimeras were visualized under SMZ1500 fluorescence microscope. Figure 4.10: Cell fate of PUFB- cells in chimeric structures. (A) 10% GFP-tagged wild type Ax2 cells and 90% RFP- tagged PUFB- cells, (B) 20% GFP-tagged wild type cells and 80% RFP tagged PUFB- cells were mixed and developed on NNA plates. Position of Ax2 cells and PUFB- cells in the chimaeric structure was monitored using Nikon SMZ1500 fluorescence microscope. Multicellular structures (slug and fruiting body) were imaged under DIC, FITC and TRITC filter [Scale bar- 50 μ m; n=3]. When cells were mixed in the ratio of 10% GFP tagged Ax2 (Green) and 90% RFP tagged PUFB- (Red) Ax2 cells distribute themselves at the tip and posterior part of the slug while PUFB- cells are present throughout the structure while in early culminants Ax2 is primarily localized in the upper, lower cups and in the stalk while prespore region is occupied by PUFB- cells (Figure 4.8A). When 20% Ax2 and 80% PUFB- cells were mixed then also wild type Ax2 is present at the tip and rear-guard cell of the prestalk region while the prespore region is once again occupied mainly by the PUFB- cells (Figure 4.8B). Figure 4.11: Cell fate of PUFB- cells in chimeric structures. (A) 50% GFP-tagged wild-type Ax2 cells and 50% RFP- tagged PUFB- cells, (B) 80% GFP-tagged wild type cells and 20% RFP tagged PUFB- cells were mixed and developed on NNA plates. Position of Ax2 cells and PUFB-cells in the chimeric structure was monitored using Nikon SMZ1500 fluorescence microscope. Multicellular structures (slug and fruiting body) were imaged under DIC, FITC and TRITC filter [Scale bar- 50 μ m; n=3]. The distribution pattern of PUFB-cells appeared more pronounced as the percentage of PUFB- cells become less and the percentage of Ax2 increases. In 1:1 ratio i.e. when an equal number of cells were taken, PUFB- cells distribute itself in the prespore region while the wild type cells occupy the anterior prestalk region in both the slug and early culminants. But as the percentage of PUFB- cells decreases further in the ratio to 20% (Figure 4.11B) and 10% (Figure 4.12B) the picture becomes clearer as PUFB- cells occupy the prespore region in slug and early culminants despite such low percentage. Figure 4.12: Cell fate of PUFB- cells in chimeras. 90% GFP-tagged wild type cells and 10% RFP tagged PUFB- cells were mixed and developed on NNA plates. DIC, TRITC and FRITC images of multicellular structure (migratory slugs and fruiting body) were captured using Nikon SMZ1500 fluorescence microscope. [Scale bar- 50 μ m; n=3]. Our results showed that the PUFB- cells have the tendency to distribute itself in the prespore region in different chimeric multicellular structures formed with wild type Ax2 cells. 4.4.3 Contribution of PUFB- cells in

spore formation in the chimeras developed GFP marked Ax2 cells and RFP marked PUFB- cells were mixed in different proportions and allowed to develop on NNA plates at 22 °C to form fruiting bodies. Fruiting bodies formed by the chimeras in all the ratios, 10%, 20%, 50%, 80%, 90 and 100% PUFB- cells were mixed with wild type. Fruiting bodies were analyzed for the spore-forming tendencies of PUFB- cells in the chimeric mixtures. Approximately, 10-15 spore heads from the chimeric fruiting bodies from all ratios were counted for each experiment. Figure 4.13: Percentage (%) spore count of PUFB- in chimeric fruiting bodies. RFP tagged PUFB- cells were mixed in various proportions from 10%, 20%, 50% and 80% with GFP-tagged wild-type cells and cell suspensions were allowed to co-develop till the culminant formation. About 10-15 fruiting bodies per ratio per experiment were scored. The values represent mean \pm standard deviation; ***p < 0.001, **p < 0.01, *p < 0.05 (Student's t-test); n=4]. We found that PUFB- cells contributed 34.6 \pm 2.06%, 40.8 \pm 4.85%, 78.3 \pm 3.6%, 89.2 \pm 3.6%, 95.2 \pm 2.39% spores from 10%, 20%, 50%, 80%, 90 and 100% PUFB- cells, respectively in chimeric mixtures with wild type (Figure 4.12). This suggests that in the chimeric mixtures PUFB- cells show more spore-forming tendency as compared to the wild type. Cell lineage study with chimeric mixtures of PUFB- and Ax2 cells in various proportions showed the tendency of Ax2 and PUFB- cells to occupy the different regions in the multicellular structure formed. We found that the distribution of PUFB- cells was found to be more in the prespore region in the multicellular structures as compared to the wild type. Also, the spore-forming tendency of PUFB- cells was found to be more as compared to the wild type.

4.4.4 Expression of autophagy-related genes in Ax2 and PUFB- cells

Autophagy is a degradative process which maintains the cellular homeostasis of the cell such as stress or DNA damage. It eliminates long-lived misfolded or unfolded proteins or even entire organelle (via lysosomal degradation) that the ubiquitin- proteasome system cannot degrade (Decuyper, 2011). In Dictyostelium, during multicellular development under starvation condition autophagy is required. Figure 4.14: mRNA expression of autophagy-related genes in Ax2 and PUFB- cells. Semi- quantitative RT-PCR analysis in wild type Ax2 and PUFB-cells. mRNA expression of autophagy-related genes atg1, atg5, atg8, atg16 and atg18 with ig7 as internal control are shown in the graph (Two way ANOVA, p-value \leq 0.05, \leq 0.01 and \leq 0.001 has been symbolized as *, ** and *** respectively; n=3). We found a significant decrease in the mRNA expression of atg5, atg8 and atg16 and atg18 in PUFB- cells in the vegetative stage as compared to the wild type Ax2 cells. This could be the reason for the reduced autophagic flux observed. Thus, we conclude that in Dictyostelium PUFB affects the process of autophagy by regulating the autophagy-related genes that are important in the formation of autophagosome, membrane trafficking and ultimately autolysosome formation.

4.4.5 PUFB knockout leads to suppression of autophagy and autophagic flux in Dictyostelium

To determine whether deletion of PUFB has any effect on autophagic process Ax2 cells and PUFB- cells were transfected with a tandemly tagged mRFP-GFP-Atg8 plasmid. Atg8 is an autophagic marker used for monitoring autophagic flux in Dictyostelium. On autophagy induction, Atg8 (known as LC3 in mammals) becomes lipidated and become integrated to cytosolic side of the autophagosome and remain attached to the autophagosome membrane until cleaved from phosphatidylethanolamine (PE) by Atg4 and recycled (Mesquita et al., 2013). The process of autophagosome formation to fusion of autophagosome to lysosome can be monitored using RFP-GFP-Atg8

autophagic marker with NH₄Cl treatment that facilitates autophagic flux assessment by measuring the number of fluorescent puncta under confocal microscopy (Calvo-Garrido et al., 2011). GFP fluorescence is rapidly quenched in acidic environment of lysosome but the RFP fluorescence is more resistant to the acidic and protease-rich conditions of the lysosome. So the formation of red- green puncta is indicative to early autophagosome whereas presence of red puncta in absence of green puncta suggest the fusion of autophagosomes with lysosome (Kimura et al., 2007). When the cells were treated with NH₄Cl, a lysosomotropic agent that increases lysosomal pH leads to inhibition of autophagosome- lysosome fusion.

act15: (RFP-GFP-Atg8)/Ax2 Control Control +NH₄Cl Starvation Starvation +NH₄Cl

Figure 4.15: Analysis of autophagic flux measurement in wild type Ax2 cells using confocal microscopy. Ax2 cells expressing RFP-GFP-Atg8 marker were diluted at a cell density of 1×10⁶ cells mL⁻¹ and the cell suspension was placed in a 6 well plate having HL5 and in 1xKK2 buffer to induce starvation. 100 mM NH₄Cl was added to the cell for 2 h and incubated at 22 °C. After 2 hours cells were washed and again 100 mM NH₄Cl was added and incubated at 22 °C for another 2 h. After incubation cells were visualized under confocal microscopes and photographs were captured in DIC, FITC and TRITC filters. [Scale bar- 5 μm; n=3]. Quantitative analysis of autophagic puncta formed per cell using confocal microscopy revealed that Ax2 cells expressing RFP-GFP-Atg8 in HL5 media showed a typical green/red puncta formation although very few cells showed red/not green puncta indicating basal autophagy (Figure 4.16 and 4.18). However, starvation induces autophagy in Dictyostelium as the Ax2 cells starved for 4 h showed increased number of red puncta that indicates autolysosomes over yellow puncta that indicates autophagosomes, thus increased autophagic flux than the basal level was observed. Upon NH₄Cl treatment, Ax2 cells expressing RFP-GFP-Atg8 marker showed a significant 108 increase in number of red puncta that indicates a rapid increase in autophagy flux (Figure 4.16 and 4.18).

act15: (RFP-GFP-Atg8)/PUFB- Control Control +NH₄Cl Starvation Starvation +NH₄Cl

Figure 4.16: Analysis of autophagic flux measurement in PUFB- cells using confocal microscopy. PUFB- cells expressing RFP-GFP-Atg8 marker were diluted at a cell density of 1×10⁶ cells mL⁻¹ and the cell suspension was placed in a 6 well plate having HL5 and in 1xKK2 buffer to induce starvation. 100 mM NH₄Cl was added to the cell for 2 h and incubated at 22 °C. After 2 h cells were washed and again 100 mM NH₄Cl was added and incubate at 22 °C for another 2 h. After incubation cells were visualized under confocal microscopes and photographs were captured in DIC, FITC and TRITC filters. [Scale bar- 5 μm; n=3]. In PUFB- cells expressing RFP-GFP-Atg8, number of yellow or red puncta per cell were very low but starvation and/or NH₄Cl treatment lead to an increase in the number of yellow or red puncta per cell which still is significantly less when compared to the Ax2 cells under starvation and NH₄Cl treatment (Figure 4.17 and 4.18). Reduced autophagy flux suggests that PUFB play a regulatory role during basal and starvation-induced autophagy in Dictyostelium. Therefore, we postulate that PUFB is required during autophagy in Dictyostelium.

Figure 4.17: Quantitative measurement of yellow and red puncta formed in Ax2 and PUFB- cells. Wild type and PUFB- cells expressing the RFP-GFP-Atg8 marker were starved for 4 h and treated with 100 mM NH₄Cl in HL5 for 2+2 h. Both treated and control samples were visualized under confocal microscope. Graph represents the score of yellow and red puncta. Nearly 30-40 cells per experiment for each condition were scored (The values represent mean, ±standard deviation; Two way ANOVA, p-value ≤0.05, ≤0.01 and

